Author:
Pridgeon, Ashley J

Title:
Investigating Stomatal Responses to Darkness

INVESTIGATING STOMATAL RESPONSES TO DARKNESS

Ashley J. Pridgeon

A dissertation submitted to the UNIVERSITY OF BRISTOL in accordance with the requirements for award of the degree of DOCTOR OF PHILOSOPHY in the FACULTY OF LIFE SCIENCES.

SCHOOL OF BIOLOGICAL SCIENCES

March 2021

Word count: 43463

ABSTRACT

Stomata are microscopic pores composed of two guard cells that open and close to regulate the movement of gasses, mainly H_2O vapour and CO_2, into and out of leaf tissue. They allow plants to regulate transpirational water loss and photosynthetic carbon assimilation in response to changes to their environment. As well as playing an important role for plants on an individual level, the function of stomata affects global hydrological and carbon cycles. Stomata are sensitive to many signals including water availability, temperature, CO_2 and light, and have developed complex signalling networks that allow for the integration of these signals. This thesis investigates the signalling mechanisms behind stomatal responses to darkness. The mechanisms underlying dark-induced stomatal closure are poorly understood in comparison to other closure inducing signals such as the phytohormone abscisic acid (ABA), known for its role in plant drought responses. This thesis examines the role of ABA signalling in stomatal responses to darkness. ABA signalling has previously been linked to stomatal responses to darkness, however its exact role is unclear. This thesis shows that ABA signalling is not essential for dark-induced stomatal closure, however mutations within ABA metabolic and signalling machinery do affect stomatal response speeds to darkness and light. Additionally, this thesis investigates the longer-term effects of darkness on ABA signalling and metabolism transcript dynamics. Here, darkness is found to specifically upregulate a subset of ABA receptor transcripts. Exploring a physiological role for dark induced ABA receptor upregulation, the effect of daylength on the stomatal development of various ABA signalling and metabolism mutants is analysed. This thesis also explores the roles of a plant cGMP activated kinase (protein kinase G/PKG) in regulating stomatal movements. Here, evidence is provided showing a role for PKG in dark-induced stomatal closure, furthermore, suggesting a role for cGMP signalling in this process.

ACKNOWLEDGEMENTS

First and foremost, I would like to thank my supervisor Prof. Alistair Hetherington for his support and mentorship, giving me the freedom to go in my own direction whilst making sure I stayed on track. I would also like to thank all past and present members of the Bristol Guard Cell Group (especially Aude, Peng and Deirdre) who were also integral in introducing me to plant and particularly stomatal biology and taught me many techniques. Additionally, I am grateful to the SWBioDTP and BBSRC for funding my studies over the past years.

Throughout my studies, I have been immensely lucky to meet many supportive colleagues and friends. Although at the time of writing the pandemic has restricted social gatherings for the last 12 months, I fondly recall the many occasions of meeting new people after work on a Friday, or the spur of the moment trips to a gig or the pub. I'd like to thank all of the lab 324 members who took me in and gave me wise words advice when I was just starting out (especially Donald, Dora, Fiona, Mike and Katie), and helped and supported me throughout my PhD (especially Ashutosh, Alice, Bhavana, Emily, and Vicky). I would also like to acknowledge the many undergraduate students who I demonstrated for or supervised. They made teaching a pleasure and constantly reminded me why I enjoy what I do. Another person I must mention is Lucia the lab manager. From the moment Lucia arrived in 324 she made everything 100% easier, her friendliness and wisdom have been of great help to me and all other members of lab 324.

My fellow PhD students Zoe, Chiara, Beth and Gilda have been a source of constant friendship throughout my studies, without a doubt they have made my time in Bristol immeasurably more enjoyable. My friends elsewhere (Jonnie, Naomi, Abi, Rob) have also continually provided much appreciated support.

Finally, I would like to also acknowledge my family for their continued belief and support, without which this thesis would not be possible.

AUTHORS DECLARATION

I declare that the work in this dissertation was carried out in accordance with the requirements of the University's Regulations and Code of Practice for Research Degree Programmes and that it has not been submitted for any other academic award. Except where indicated by specific reference in the text, the work is the candidate's own work. Work done in collaboration with, or with the assistance of, others, is indicated as such. Any views expressed in the dissertation are those of the author.

SIGNED _____ DATE 16.3.2021

CONTENTS

LIST OF FIGURES

LIST OF TABLES

NOMENCLATURE

ABA	Abscisic acid
ABA-GE	Abscisic acid conjugated to glucose ester
ABF	ABRE BINDING FACTOR
ABI	ABSCISIC INSENSITIVE
ALMT	ALUMINIUM ACTIVATED MALATE TRANSPORTER
AREB	ABA RESPONSIVE ELEMENT BINDING PROTEIN
BG1/2	β GLUCOSIDASE1/2
bHLH	Basic helix loop helix
BLUS 1	BLUE LIGHT SIGNALLING 1
BRI1	BRASSINOSTEROID INSENSITIVE 1
βCA	β CARBONIC ANHYDRASE
CaM	CALMODULIN
CAP	CATABOLITE ACTIVATOR PROTEIN
CBC	CONVERGENCE OF BLUE LIGHT AND CO_2
CBL	CALNEURIN-B-LIKE PROTEINS
CDPK	CALCIUM DEPENDENT PROTEIN KINASE
C_i	Leaf intercellular CO_2 concentration
CIPK	CBL INTERACTING PROTEIN KINASE
CLC	CHLORIDE CHANNEL
CLE	CLAVATA3/ESR-RELATED
CNGC	CYCLIC NUCLEOTIDE GATED CHANNEL
COP1	CONSTITUTIVE PHOTOMORPHOGENIC 1
CRSP	CO_2 RESPONSE SECRETED PROTEASE
CRY	CRYPTOCHROME
CYP707A1/3	CYTOCHROME P707 A1/A3
EPF	EPIDERMAL PATTERNING FACTOR
EPFL	EPIDERMAL PATTERNING FACTOR LIKE
ER	ERECTA
ERL	ERECTA LIKE
EtOH	Ethanol
EXPA1	EXPANSIN A1

FLS2	FLAGELLIN SENSITIVE 2
GC	GUANYLYL CYCLASE
GFP	GREEN FLUORESCENT PROTEIN
GHR1	GUARD CELL HYDROGEN PEROXIDE RESISTANT
GMC	Guard mother cell
GORK	GATED OUTWARDLY RECTIFYING K^+ CHANNEL
GPA1	G PROTEIN ALPHA SUBUNIT 1
GUN5	GENOME UNCOUPLED 5
Gs	Stomatal conductance
HT1	HIGH LEAF TEMPERATURE 1
KAT1	K^+ CHANNEL
LHY	LATE ELONGATED HYPOCOTYL
LRR-RLK	Leucine rich repeat – receptor like kinase
MAMP	Microbial associated molecular pattern
MAPK	MITOGEN ACTIVATED PROTEIN KINASE
MAPKKK	MITOGEN ACTIVATED PROTEIN KINASE KINASE KINASE
MEK	MAP KINASE/ERK KINASE 1
MKK	MAP KINASE KINASE
MMC	Meristemoid mother cell
MYB	MYB INTERACTING PROTEIN
NCBI	National Center for Biotenchnology Information
NCED	9-CIS-EPOXYCAROTENOID DEOXYGENASE
NHX	Na^+/H^+ EXCHANGER
NO	Nitric oxide
OST1	OPEN STOMATA 1
PA	Phosphatic acid
PDE1	PHOSPHODIESTERASE 1
PHOT	PHOTOTROPIN
PHY	PHYTOCHROME
PIF	PHYTOCHROME INTERACTING FACTOR
PKG	PROTEIN KINASE G
PLC	PHOSPHOLIPASE C
PLD	PHOSPHOLIPASE D
PP1	TYPE 1 PROTEIN PHOSPHATASE

PP2C	PROTEIN PHOSPHATASE 2C
PRR9	PSEUDO RESPONSE REGULATOR 9
PSKR	PHYTOSULFOKINE RECEPTOR 1
PYL	PYRABACTIN-LIKE
RBOH	RESPIRATORY BURST OXIDASE HOMOLOGUE
RCAR	REGULATORY COMPONENT OF ABA RECEPTOR
RHC1	RESISTANT TO HIGH CO_2 1
ROS	REACTIVE OXYGEN SPECIES
SLAC	SLOW ANION CHANNEL ASSOCIATED
SLGC	Stomatal lineage ground cell
SNRK2	SNF1-RELATED PROTEIN KINASE
SPCH	SPEECHLESS
SWC	Soil water content
TMM	TOO MANY MOUTHS
TOC1	TIMING OF CAB EXPRESSION 1
TPC1	TWO PORE CHANNEL 1
TPK1	TWO PORE K^+ CHANNEL 1
WT	Wild type
YDA	YODA

CHAPTER 1: INTRODUCTION

Stomata are microscopic pores found mainly on the leaves of plants. They consist of two guard cells that are able to swell and deflate, changing the aperture of the pore. Plants open and close their stomata in response to internal and external stimuli, allowing them to control the flow of H_2O vapour and CO_2 into and out of the internal leaf tissue (gas exchange), which in turn impacts photosynthetic carbon assimilation and water use efficiency. The action of stomata also affects global processes such as the global carbon and water ecosystems [1,2].

As well as changing the aperture of the stomatal pore, plants alter the size and density of stomata on newly developing leaves. Whereas stomatal movement allows for immediate responses to changes within a plant's surrounding environment, the regulation of stomatal size and density allow for longer term adaptions. All three traits (movement, size, and density) have been shown to be key for regulating transpiration (ie the loss of water vapour from the plant) and subsequently water use efficiency and stress tolerance [3]. Although nearly all stomata contain two guard cells surrounding a central pore (other than plants that have one partially divided guard cell), there is some variation in the morphology/function of the surrounding cells. In grasses there has been considerable specialisation of the adjacent cells, which have evolved to be tightly incorporated into the stomatal complex. Here they are known as subsidiary cells and have led to large increases in the speed of stomatal movements [4].

1.1 How stomatal movement is mediated

The opening and closing of stomata is predominantly mediated through changes in guard cell turgor pressure, which is in turn controlled by changes within guard cell solute concentrations (first suggested in 1856 [5]). Stomata open due to a build-up of solutes within the cell. This leads to a decrease in the water potential between the guard cell and the extracellular environment, causing water to enter the cell, increasing the cellular turgor pressure. This in turn leads to the opening of the stomatal pore. When stomata close, the opposite occurs. A decrease in solutes within the guard cells lead to the movement of water out of the cell, a decrease in turgor pressure

and the closing of the stomatal pore [6]. As mature guard cells contain no plasmodesmata connecting them with surrounding cells [7], the changes in solute concentrations must arise from guard cell metabolic processes and the movement of solutes/ions across guard cell membranes.

1.1.1 Guard cell solutes

Prior to the 1940s, it was widely believed that changes in guard cell solute concentrations arose from sugar generated by starch breakdown. This was termed the starch sugar hypothesis [8]. However after the 1940s, studies began to show that guard cells contained high concentrations of K^+ ions [9], K^+ concentration was higher in open guard cells, and that addition of K^+ to could stimulate stomatal opening in epidermal peels of *Commelina communis* [10]. Further work confirmed a major role for K^+ as the primary guard cell osmolyte, however this study also suggested that other organic or inorganic ions acted to counter the positive charge of the K^+ ions [11], such as $malate^{2-}$ [12,13]. Later, studies suggested that the changes in K^+ and $malate^{2-}$ concentrations observed in guard cells were too small to account for the forces required to power stomatal opening [14] (the history of guard cell osmolyte research is reviewed in further detail here [15]). Currently it is thought that the cation K^+, the anions Cl^- [16], $malate^{2-}$, and NO_3^- [17], and the organic solute sucrose all act as guard cell osmolytes, where changes in their concentrations mediate changes in guard cell turgor pressure. Studies suggest that the time of day may have an effect on which solute is playing a key role in driving changes in turgor pressure. The accumulation of K+ ions may play a key role in stomatal opening during the first half of the day, before sucrose takes over as the main solute in the latter half [18,19].

Whereas concentrations of K^+ and Cl^- are predominantly altered through ion transport, metabolic pathways can also contribute to the guard cell levels of malate and sucrose. In plant cells malate can be generated from glucose entering the TCA cycle (situated in the mitochondria) [20,21] and via acetate entering the glyoxylate cycle (situated in the peroxisome) [22]. In both processes malate represents a metabolic intermediate, however it could potentially be transported out of the respective cellular compartment and mobilised to mediate guard cell solute concentrations. It has been shown that acetate derived malate was important in stomatal opening in response to light [22]. Recently the breakdown of starch in guard cells (in response to light) has been shown to be important for stomatal movements, however instead of producing osmolytes this breakdown provides glucose that is used to maintain cellular sugar pools and doesn't appear to directly affect

ion transport or malate accumulation [23]. The role of sucrose as an osmolyte is under debate, as recently multiple studies have suggested, similar to starch breakdown, it is more likely playing a role in energetic processes [24,25]. The breakdown of triacylglycerols has also been shown to play a key role in fuelling stomatal opening [26].

1.1.2 Guard cell ion movement during stomatal opening

Guard cell plasma membrane H^+ATPases play a key role in stomatal opening [27] (fig. 1.1a). Fuelled by ATP derived from photosynthetic activity, the breakdown of lipid droplets, and the breakdown of starch [25,26], the action of these proton pumps increases the electrochemical gradient across the guard cell plasma membrane and activates voltage gated inward rectifying K^+ channels [28]. During stomatal opening the majority of K^+ entering the guard cell passes through the voltage gated K^+ channel KAT1 [29–31]. However, there are various H^+ coupled symport channels that have been shown to also transport K^+, Cl^-, $malate^{2-}$, and other solutes into guard cells (reviewed here [6]). Once transported across the plasma membrane and into the cytoplasm, ions are stored in the vacuole/tonoplast [32,33]. The tonoplast takes up the majority of intracellular space in guard cells and shows large changes in size during stomatal movements [34]. Less is known regarding the mechanisms of ion transport across the tonoplast membrane. However, H^+ coupled antiporters, such as CHLORIDE CHANNEL (CLC), NA+/H+ EXCHANGER (NHX), ALUMINIUM-ACTIVATED MALATE TRANSPORTER (ALMT) family members play a role in the transport of solutes/ions into the tonoplast during stomatal opening [32].

1.1.3 Guard cell ion movement during stomatal closure

Stomatal closure has been best characterised in response to the plant phytohormone ABA, however, different closure signals appear to converge on a similar collection of downstream targets [6] (fig. 1.1b). The earliest observed closure events are changes within the voltage sensitivities of Ca^{2+} channels, leading to an influx of Ca^{2+} from extracellular and endomembrane stores [35]. Together, activated signalling cascades and increases in cytoplasmic Ca^{2+} concentrations act to inhibit the activity of plasma membrane H^+ATPases [36] and inward facing K^+ channels (KAT1) [37,38]. Additionally, they activate outward facing anion channels such as SLOW ANION CHANNEL-ASSOCIATED (SLAC) and ALMT family members leading to the efflux of anions [39–42]. The activity of the outward facing anion channels depolarises the guard cell membrane and

activates the outward facing K^+ channel GATED OUTWARDLY RECTIFYING K+ CHANNEL (GORK) [43–45]. In addition to these events on the plasma membrane, again less is known about the events on the tonoplast membrane. It is unclear how Ca^{2+} efflux from the tonoplast occurs, only one channel with the ability to transport Ca^{2+} into the cytoplasm has been identified, TWO PORE CHANNEL 1 (TPC1) [46], however the only stomatal closing phenotype recorded is an inability to close in response to extracellular Ca^{2+} [47,48]. During closure, the tonoplast shows acidification, mediated by the activities of ATP and PPi proton pumps on the tonoplast membrane [33,49]. TWO PORE K^+ CHANNEL 1 (TPK1) has been shown to be activated by increased cytoplasmic Ca^{2+} concentrations and signalling cascades [50,51] and is involved in tonoplast K^+ release during stomatal closure [52]. Additionally, CLC, NHX, ALMT channels on the tonoplast membrane have been linked to the release of ions from the tonoplast (reviewed here [32]).

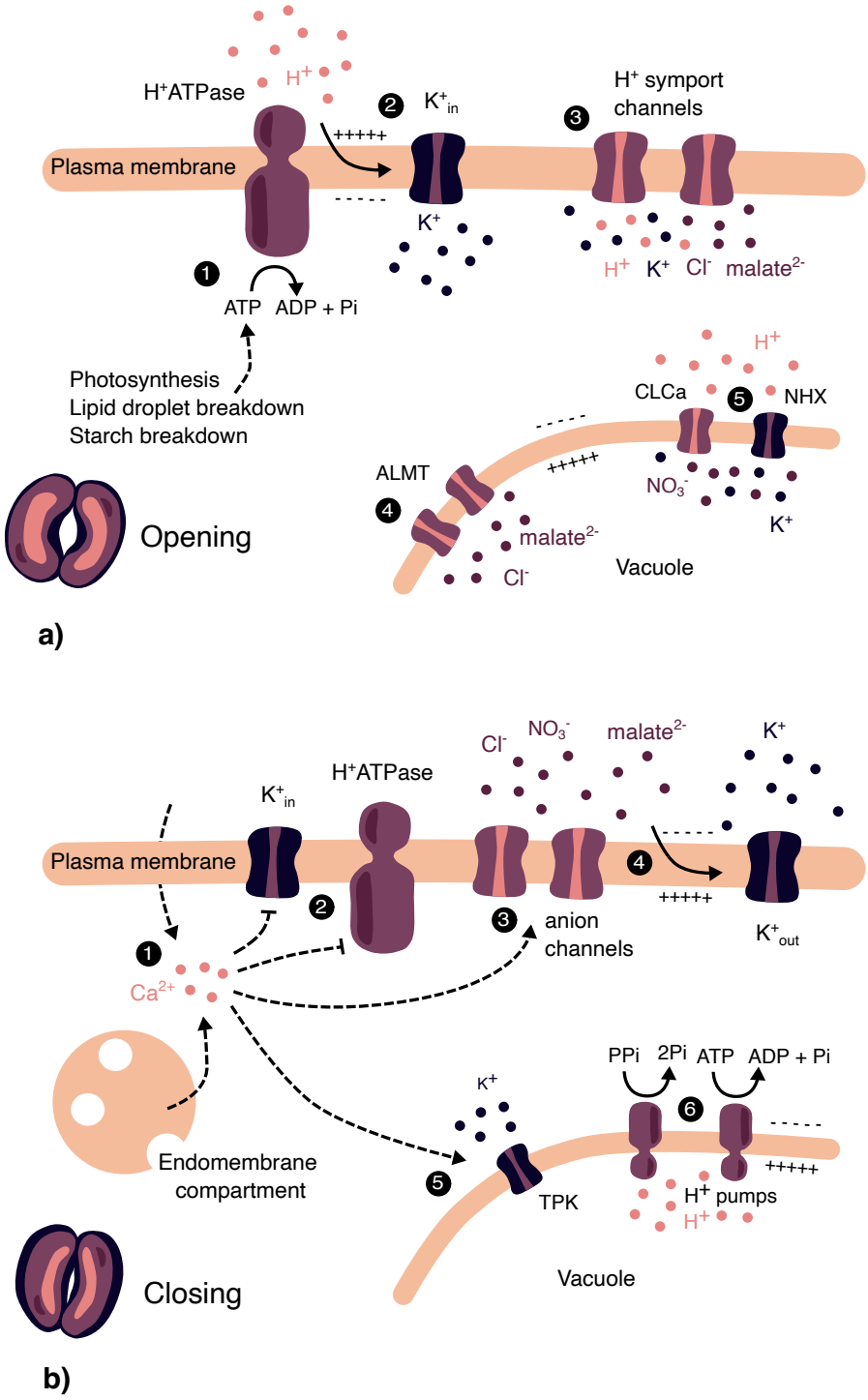

Figure 1.1 Ion movements during stomatal opening and closing

a) 1. During stomatal opening ATP generated from metabolic processes such as photosynthesis, lipid droplet breakdown, and starch breakdown fuel plasma membrane H^+ATPases and hyperpolarise the plasma membrane. 2. The hyperpolarisation of the membrane activates inward facing K^+ channels. 3. Additionally H^+ coupled symport channels transport further ions into the guard cell cytoplasm. Ions within guard cell cytoplasm are transported into the vacuole by 4.

ALMT and 5. H^+ antiport channels (CLCa, NHX) on the tonoplast membrane. This leads to net movement of ions into guard cells, and ultimately stomatal opening. b) During stomatal closure among the earliest recorded events is 1. an influx of Ca^{2+} from apoplastic and endomembrane stores into the cytoplasm. Ca^{2+} coupled with signalling pathways lead to 2. the inhibition of K^+_{in} channels and H^+ATPases. 3. Outward facing anion channels are activated and 4. depolarise the plasma membrane, which in turn activates K^+_{out} channels. 5. Ca^{2+} and further signalling pathways activate ion channels on the tonoplast that transport ions into the cytoplasm. 6. Additionally, ATP and PPi proton pumps acidify the vacuole. This leads to a net movement of ions out of guard cells and ultimately stomatal closure.

1.1.4 Other important processes involved in stomatal movements

In addition to the control of ion transport, stomatal movements also rely upon changes in cell cytoskeleton, membrane transport, and cell wall dynamics. Actin is a highly conserved protein found across eukaryotic organisms. It plays a key role in the formation of the cell cytoskeleton. The reorganisation of actin filaments has been observed in guard cells in response to multiple signals [53–56]. During stomatal closure, guard cell actin filaments undergo changes. Initially, as the stomatal pore begins to close the filaments change from an organised radial distribution, to a random distribution. Once the stomatal pore has closed, actin filaments reorganise into longitudinal distribution. When actin filament reorganisation is blocked (via phalloidin treatment) [57] or the machinery involved in regulating actin reorganisation is defective, stomatal movements are affected. Guard cell responses to darkness appear to be particularly sensitive to defects within actin reorganisation machinery [56].

During stomatal movements, guard cells also show vast changes to their surface area. This requires large scale membrane trafficking, either to or from the plasma membrane, in order to permit these changes in membrane surface area [58,59]. In addition to providing membrane, trafficking also allows regulation of protein subcellular location, that can be further used to regulate signalling responses (such as the FLAGGELIN SENSITIVE 2 -FLS2 - immune receptor and ABA receptors) [60–62] and the action of ion channels (such as in the case of the KAT1 K^+ channel) [63,64]. Endomembrane trafficking compartments may also act as sources of intracellular Ca^{2+} which could be mobilised during the calcium oscillations observed during various stomatal signalling responses [65].

The guard cell wall plays key roles in determining the structure and shape of stomata, as well as the mechanics behind stomatal movements [66,67]. Analysis of the guard cell wall has shown that it is compositionally different from other epidermal cell walls [68,69]. During stomatal development, different amounts of cell wall are synthesised at different locations leading to thicker cell walls at certain regions of the stomata, however, the molecular mechanisms underlying this process are not well understood. Distinctive patterns of cell wall component modification (such as pectin de-methylesterification) allow for regions of altered stiffness, which in turn optimises aperture changes in response to alterations in cell turgor pressure. Additionally, reorganisation of cellulose (one of the polymers that composes the plant cell wall providing tensile strength) is thought to

facilitate stomatal movements [70]. In lines where cell wall properties of stomata are altered, such as *pectin methylesterase 6* (*pme6*) and an EXPANSIN A1 (EXPA1) overexpression line (expansin is involved in cell wall loosening and expanding), stomatal movements are affected [68,71].

1.1.5 Adaption of stomata in grass species

The majority of plant species that possess stomata have kidney shaped guard cells, however, in grasses (Poaceae) guard cells have evolved a dumbbell shape and interact with two adjacent specialised subsidiary cells (forming a complex of 4 cells – 2 guard cells and 2 subsidiary cells – referred to as the stomatal complex) [72]. In grass species the altered dumbbell shape of guard cells and the addition of specialised subsidiary cells into the stomatal complex have resulted in increases in the speed of stomatal movements. The distinctive dumbbell shape of guard cells reduces the volume to surface area ratio of the cell, allowing turgor pressure changes in response to smaller amounts of ions and water transport. The increase in the length to width ratio of the pore also allows for greater changes in pore area when guard cell turgor pressure changes [73,74]. Additionally, subsidiary cells are able to act as solute/ion reservoirs, providing a ready source of solutes for when stomata need to open, and an available sink when stomata need to close. It has been shown that upon genetic removal of subsidiary cells (through mutations within development machinery), grass stomatal complexes show vastly reduced stomatal response speeds [75]. It is thought that the development of this specialised stomatal complex has contributed to the success of grass species which are found across the globe in many ecosystems and whose crops account for 2/3 of the calories consumed by humans every day [76]. Further information regarding the features of grass stomata can be found in a recent review [4].

1.2 Molecular signalling underlying stomatal movements

Stomata move in response to a number of stimuli, including light, drought, changing CO_2 concentrations, relative humidity, temperature, and microbial associated molecular patterns (MAMPs). This allows a plant to best adapt gas exchange to suit its immediate surroundings, or in the case of responses against microbes provide a barrier to prevent infection.

1.2.1 Role of ABA in drought responses

Perhaps the best characterised stomatal signalling pathway is the abscisic acid (ABA) signalling pathway, integral to the plant drought response. When a plant experiences drought stress ABA biosynthesis is triggered and causes a number of physiological changes in the plant including stomatal closure [77–79]. There was much debate over the source of drought stress induced ABA [80]. Although traditionally ABA biosynthesis was thought to occur in roots before travelling to the aerial portion of the plant and promoting stomatal closure, reciprocal grafting experiments using ABA deficient mutants have shown that stomatal responses depend on the aerial tissue genotype [81,82]. Additionally the majority of ABA biosynthesis occurs within the aerial tissue [83–87]. Recently, a root derived peptide, CLAVATA3/ESR-RELATED 25 (CLE25), was shown to act as a drought induced root to shoot signal promoting ABA biosynthesis and stomatal closure in leaf tissue [88,89], supporting the idea that root derived ABA is not the main cause of aerial plant responses to drought.

The ABA signalling pathway has also been linked to other plant processes, including CO_2 signalling, seed dormancy and germination, plant pathogen interactions, high light responses and hypocotyl development [90–94].

1.2.2 ABA biosynthesis and conjugation

ABA is an isoprenoid hormone that in most plants is derived from β-carotene. The majority of the *de novo* biosynthesis pathway occurs within the plastid and the final steps within the cytoplasm [95]. The enzyme 9-CIS-EXPOXYCAROTENOID DEOXYGENASE (NCED) catalyses the rate limiting step of the pathway and has been shown to be a major point of

regulation when a plant experiences abiotic stress [96]. However, additional ABA biosynthesis enzymes also show regulation at the transcriptional level [97]. Plants can also store inactive pools of ABA by conjugation to a glucose ester (ABA-GE). β-glucosidase enzymes can rapidly generate active pools of ABA by removal of the glucose ester, providing another method of generating ABA which has shown to be important in the plant drought response [98,99].

1.2.3 General overview of ABA signalling

The identity of the ABA receptors was uncovered relatively recently, where it was shown that members from a family of 14 cytoplasmic proteins (the PYRABACTIN LIKE - PYL or REGULATORY COMPONENT OF ABA RECEPTOR - RCAR protein family) were involved in ABA sensing [100–102]. The basic properties of the ABA signalling pathway are as follows). Upon binding to ABA, the PYL/RCAR receptors are able to change conformation and bind a family of phosphatases, known as the PROTEIN PHOSPHATASE 2C (PP2C) phosphatase family. This prevents PP2C phosphatase activity, which in turn prevents them from inhibiting a group of kinases, known as SNF1-RELATED PROTEIN KINASE 2 (SnRK2) kinases (including SnRK2.6/OPEN STOMATA 1/OST1) [103]. Recently instead of SnRK2 autophosphorylation, it was shown that, as well as PP2C inhibition, a group of Raf-like MITOGEN ACTIVATED PROTEIN KINASE KINASE KINASEs (MAPKKKs) are required to phosphorylate SnRK2 kinases in order to activate downstream ABA signalling [104]. In any case, upon activation, SnRK2 kinases phosphorylate downstream targets such as SLAC1, which in guard cells is involved in anion efflux, that decreases guard cell turgor and promotes stomatal closure [41,105,106]. In addition to ion channels, it was shown SnRK2 kinases also target transcription factors (mainly the ABA INSENSITIVE 5 - ABI5/ABA RESPONSIVE ELEMENT BINDING PROTEIN - AREB/ABRE BINDING FACTOR - ABF family of transcription factors) to alter gene expression [107,108].

1.2.4 The use of second messengers in amplifying the ABA signal

In addition to the core ABA pathway, ABA signalling is known to also involve numerous second messengers; including H_2O_2, Ca^{2+}, $InsP_3$, and NO [109,110] that activate many parallel downstream signalling pathways (fig. 1.2).

Reactive Oxygen Species (ROS)

One of the key second messengers involved in ABA responses are reactive oxygen species (ROS). Reactive oxygen species (ROS) are a group of short-lived (oxygen containing) metabolites found within all aerobic organisms. ROS include hydrogen peroxide (H_2O_2), superoxide ($O_2^{\bullet-}$), hydroxyl radicals ($HO^{\bullet}$), and singlet oxygen ($^1O_2$) [111]. In plants there are various metabolic processes that lead to ROS production; including photosynthesis within the chloroplasts, carbon metabolism in the peroxisome, and respiration (the electron transport chain) in mitochondria [112].

The role of ROS in regulating stomatal movement was confirmed when it was shown that H_2O_2 production is required to activate guard cell Ca^{2+} channels in the ABA signalling pathway, leading to stomatal closure [113]. H_2O_2 production in response to ABA is predominantly mediated by the action of two members of the RESPIRATORY BURST OXIDASE HOMOLOGUE family (RBOH), RBOHD and RBOHF. These enzymes were discovered to be one of the main targets of OST1 [114]. Upon activation by OST1, RBOHD and F generate H_2O_2 in the apoplastic space. The production of H_2O_2 leads to inhibition of the ABA INSENSITIVE 1 and 2 (ABI1 and ABI2) PP2C phosphatases, the activation of Ca^{2+} channels, and the activation of mitogen activated protein kinases (MAPKs) 9 and 12. The pseudokinase GUARD CELL HYDROGEN PEROXIDE RESISTANT1 (GHR1) is required downstream of ROS production for the activation of guard cell calcium channels. Additionally GHR1 has been proposed regulate the activity of SLAC1 by acting as a scaffold protein, bringing SLAC1 and regulatory proteins such as CALCIUM DEPENDENT PROTEIN KINASE3 (CDPK3) within close proximity [115].

Ca^{2+}

Ca^{2+} also plays a key role in ABA signalling. High cytoplasmic concentrations of Ca^{2+} are cytotoxic to cells, therefore under resting conditions cells keep cytoplasmic concentrations in the

range of 150 nM. Low cytoplasmic concentrations are achieved through Ca^{2+} export out of the cytoplasm into the apoplast or internal stores though the action of Ca^{2+}ATPases and Ca^{2+}/H^{+} ion exchangers. Although, generally kept at low levels, when analysed, a small subset of guard cells show spontaneous transient increases in Ca^{2+} concentration (Ca^{2+} transients) [35,116–118]. However, upon application of a stimulus (eg ABA, cold, Ca^{2+}_{ext}), guard cell Ca^{2+} transients are usually observed in the majority of guard cells and are thought to play role in mediating stomatal closure [119–121]. Different stimuli cause different patterns of Ca^{2+} transients, some showing a single increase, others showing oscillations with different amplitudes and frequencies [122]. Additionally, in response to some stimuli (eg ABA) subsets of guard cells show different responses. The variability in guard cell responses may be partly due to microenvironments over the leaf, and experimental and growth condition differences between studies [121].

Upon an increase in Ca^{2+}_{cyt} concentration, the activity of multiple targets can be affected. Ca^{2+} affects target proteins through binding to a conserved EF-hand domain, causing conformational changes, and as a result changes in protein activity/behaviour. There are around 250 proteins thought to contain EF-hand domains including CALCIUM DEPENDENT PROTEIN KINASES (CPKs) [123,124], CALNEURIN-B LIKE PROTEINS (CBLs), which further regulate CBL INTERACTING PROTEIN KINASES (CIPKs) [125,126], CALMODULINS (CaMs) [127], ion channels, and small GTPases [128]. This indicates the wide possibility of potential targets ABA induced Ca^{2+} increases may be affecting. CPK and CIPKs have been observed to share targets with the core ABA signalling machinery (SnRK2 kinases and PP2C phosphatases) including RBOHs, ion channels (SLAC1/SLAC1 HOMOLOGUE 3 (SLAH3) – OST1, K^{+}TRANSPORTER1 (AKT1)/AKT2 – PP2C), and transcription factors (ABI5/ABF1/ABF4). Overall, this points to a highly complex situation where ABA, Ca^{2+}, and ROS signalling are intertwined, sharing common targets and also interacting with one another (fig. 1.2).

Other second messengers

In an addition to ROS and Ca^{2+}, the secondary messenger NO, a gaseous signalling molecule implicated in many plant developmental and physiological processes [129], has been linked to ABA signalling and stomatal closure [130,131]. Guard cells have been shown to produce NO via nitrate reductase in response to ABA in a H_2O_2 dependent manner [132,133]. The increase in NO is thought to promote Ca^{2+} release into the cytoplasm which then further regulates K^{+} and Cl^{-} ion channels

inducing stomatal closure. NO has been suggested to promote Ca^{2+} through the production of further secondary messenger molecules cGMP and cADPR [134]. Additionally, NO induced stomatal closure has been shown to require the production of phosphatic acid (PA) via phospholipase D (PLD), which in turn binds to rbohD to stimulate ROS production [135,136]. As well as through the production of further second messengers, NO has been shown to directly affect ABA signalling through S-nitrosylation of OST1. However, in this case the S-nitrosylation inhibits OST1 activity after a delay acting as negative feedback preventing an overresponse to ABA [137].

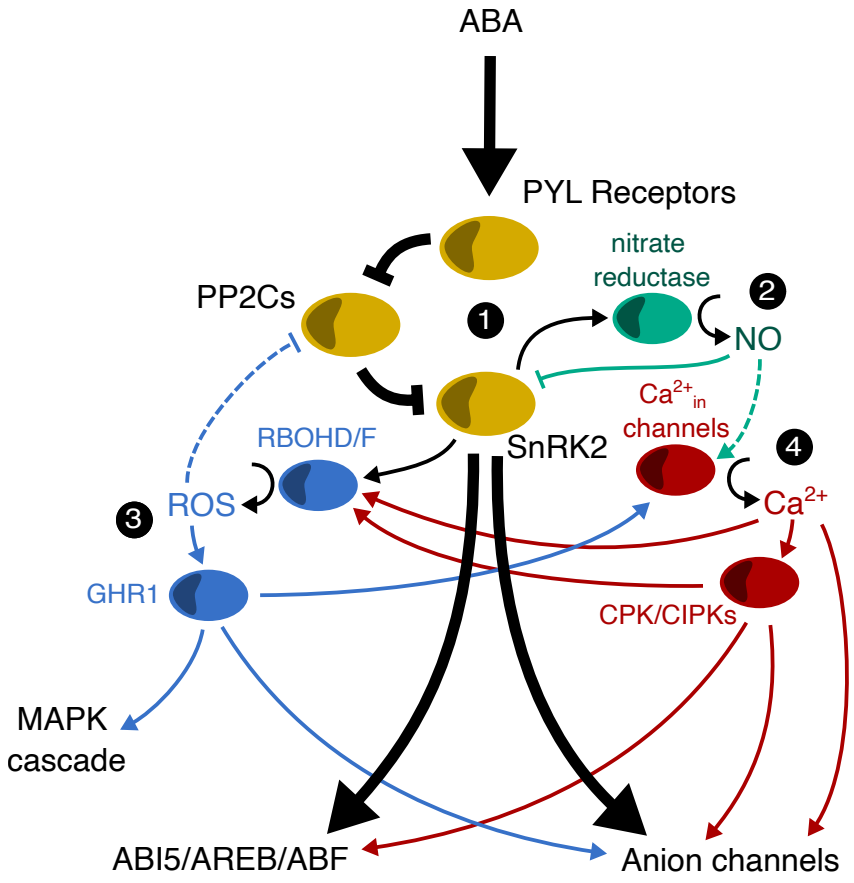

Figure 1.2 Key components of ABA signalling

1. ABA signalling consists of a core pathway. The PYR-like (PYL) receptor family binds to ABA. Upon binding the PYL receptors can bind and inhibit a family of PP2C phosphatases. This in turn lifts members of a family of SnRK2 kinases from inhibition and allows them to activate downstream targets including ABI5/AREB/ABF transcription factors and anion channels. ABA signalling also recruits various secondary messenger molecules to amplify the signal, interact with downstream targets, and ultimately promote stomatal closure. 2. ABA signalling produces NO via nitrate reductase. NO leads to the activation of Ca^{2+}_{in} channels through a pathway that involves cGMP and cADPR. Additionally, NO can modify OST1 (a SnRK2) in the presence of ROS to inhibit its activity and prevent an ABA overresponse. 3. SnRK2 kinases target enzymes RBOHD/F in order to produce ROS. ROS interacts with GHR1 which leads to the activation of Ca^{2+}_{in} channels, anion channels, and a MAPK cascade involving MPK6 and MPK12. ROS signalling also inhibits PP2C phosphatases. 4. One of the earliest events in ABA signalling is the occurrence of Ca^{2+} influxes into the cytoplasm. Ca^{2+} is able to bind to many targets including anion channels, the kinases CPK and CIPKs, and RBOHD/F. CPK and CIPKs are also able to target further downstream components, including the RBOHs, anion channels and ABI5/AREB/ABF transcription factors. It is clear that there is a high degree of interaction between the core and secondary messenger signalling pathways and overlap between the targets of these pathways.

1.2.5 Regulation of ABA signalling

Feedback inhibition of ABA signalling, such as that observed for NO mediated S-nitrosylation [137], allows cells to prevent overresponses to ABA. Recently work has shown there are extensive mechanisms in place to negatively regulate ABA signalling. At the guard cell vacuole, the early ABA-induced increase in cytoplasmic Ca^{2+}, which is known to promote the efflux of K^+ from the vacuole and induce stomatal closure, also promotes the activity of a CBL/CIPK signalling complex which is thought to limit vacuolar K^+ efflux by promoting vacuolar K^+ uptake through NHX K^+/H^+ antiporter channels. Loss of the CBL/CIPK complexes leads to increased Ca^{2+} influx and elevation, causing hypersensitivity to ABA, suggesting these function to negatively regulate ABA signalling [138]. A number of E3 ubiquitin ligases that function to target proteins for degradation have been shown to target various ABA signalling components including the PYL ABA receptor family, the PP2C phosphatase family, SnRK2 kinases, and ABI5/AREB/ABF transcription factor [139]. The ABA receptors particularly appear to be under the regulation of multiple types of E3 ligases, which suggests they represent an important point of regulation in ABA signalling and perhaps suggests diverse range of functions and/or subcellular locations of the ABA receptors.

1.2.6 Guard cell CO_2 signalling

Elevated CO_2 levels also promote stomatal closure. ß carbonic anyhdrases (ßCAs), that catalyse the production of bicarbonate ions (HCO_3^-), play a role in the early stages of CO_2 signalling [140]. When CO_2 levels are high ßCAs produce HCO_3^-, which is then believed to be sensed by a MATE-type transporter RESISTANT TO HIGH CO2 1 (RHC1). This induces a conformational change in RHC1, which allows it to interact with and inhibit HIGH LEAF TEMPERATURE 1 (HT1) kinase [141]. MAP KINASE 4 and 12 (MPK4 and MPK12) are also thought to inhibit HT1 under elevated CO_2 conditions [142]. HT1 kinase acts as a negative regulator of elevated CO_2 signalling. Under low CO_2 concentrations HT1 phosphorylates and inhibits OST1 kinase and GHR1, leading to open stomata. Under high CO_2 conditions HT1 inhibition releases OST1 and GHR1 from inhibition and promotes stomatal closure via the activation of SLAC1 and ALUMINIUM-ACTIVATED MALATE TRANSPORTER 12 (ALMT12 ion channels) [42,143,144]. Similar to ABA induced stomatal closure, Ca^{2+} has also been implicated in playing a key role in CO_2 induced stomatal movements [145]. Mutations within high

order calcium dependent protein kinases (CPKs) have been shown to affect the speed of both elevated CO_2 induced closure and low CO_2 induced opening, suggesting functionally redundant roles for CPKs in CO_2 induced stomatal movements [146].

As well as through RHC1 mediated inhibition of HT1, some studies have observed that ABA signalling upstream of OST1 is required for elevated CO_2-induced stomatal closure. Mutants within ABA biosynthesis genes (*nced3/5*), aba receptor genes (*pyr1pyl1pyl2pyl4*), PP2C phosphatase genes (*abi1, abi2*), and genes involved in ROS production (*rbohd/f*) show defective stomatal closure in response to elevated CO_2 [90,147]. Additionally, the ABA degradation mutant *cytochrome p450 family 707 a1/3* (*cyp707a1/3*) show a hypersensitive response to CO_2 induced stomatal closure [148]. Recently, it was shown that expression of the ABA receptor PYL4 or PYL5 is sufficient to rescue elevated CO2 induced stomatal closure in higher order ABA receptor mutants (*pyr1pyl2pyl4pyl5pyl8*) [149] (although why the *pyr1pyl1pyl2pyl4* mutant, with a functional PYL5 gene, presents an elevated CO_2 unresponsive phenotype [90] is unclear).

However, there is some disagreement about the role of ABA signalling in CO_2 induced stomatal closure. Some studies have observed elevated CO_2 responses in *nced3/5* and various ABA receptor mutants (*pyr1pyl1pyl2pyl4, pyr1pyl1pyl4pyl5pyl8, pyr1pyl2pyl4pyl5pyl8*, and *pyr1pyl1pyl2pyl4pyl5pyl8*). Here these mutants are able to reduce stomatal conductance in response to elevated CO_2, but show altered conductance response kinetics [150–152]. It has been proposed that SLAC1 ion channels are activated via an ABA independent signalling pathway in response to elevated CO_2, potentially via a direct binding of HCO_3^- to specific residues of SLAC1 [153,154].

1.2.7 Guard cell responses to light

Stomatal opening can be induced by both red and blue light treatment; however, they activate opening via separate signalling pathways (fig. 1.3). Blue light mainly acts upon the PHOTOTROPIN 1 and 2 (PHOT1 and 2) photoreceptors to induce stomatal opening [155] (although the cryptochrome photoreceptors CRYPTOCHROME 1 and 2 (CRY1 and 2) have also been shown to play a role [156]). Upon activation PHOT1 phosphorylates the downstream kinases BLUE LIGHT SIGNALLING 1 (BLUS1) and CONVERGENCE OF BLUE LIGHT AND CO2 1 (CBC1). Phosphorylation of BLUS1 stimulates a signalling pathway involving a type 1 protein phosphatase (PP1) that leads to the activation of H^+ATPases [157,158].

Phosphorylation of CBC1 leads to the activation of its homologue CBC2 and the inhibition of SLAC1 anion channels [159]. Together the activation of H^+ATPases and inhibition of anion efflux channels leads to the opening of stomata. However, recently the CBC kinases were implicated in the negative regulation of H^+ATPases, suggesting a more complex signalling situation [160].

The mechanisms behind red light induced opening are less clear. Some studies have implicated the red light photoreceptor PHYTOCHROME B (PHYB) in the stomatal opening process [161]. However, it is thought that red light-induced stomatal opening is reliant upon photosynthetic activity as it can be inhibited using the photosynthetic electron transport chain inhibitor DCMU [162,163]. There is debate as to whether stomata respond to changes within the leaf intercellular CO_2 concentration (C_i) or other photosynthetic signals. C_i usually correlates with the photosynthetic capacity of a plant, therefore when photosynthetic carbon fixation decreases, the C_i increases, and vice versa [164]. However, stomatal responses to red light are observed when C_i is kept constant, suggesting another signal/s may be responsible for coordinating stomatal movements with photosynthetic activity [165,166]. HT1 has been shown to be involved in the red light response, suggesting there is a link between red light and CO_2 signalling [167]. Regardless, similarly to blue light induced stomatal opening, red light induced stomatal opening culminates in the activation of guard cell plasma membrane H^+ATPases [168], which predominantly mediates stomatal opening.

Regulation of stomatal opening

As well as promoting stomatal closure both ABA and elevated CO_2 signalling can inhibit the opening of stomata (fig. 1.3). ABA signalling is known to achieve this by inhibiting the blue light induced phosphorylation of the plasma membrane H^+ATPase via a mechanism that involves the ABI1 and ABI2 phosphatases and OST1 [169–171]. While there is considerable overlap in the ABA signalling components involved in stomatal closure and inhibition of stomatal opening (including the secondary messengers Ca^{2+}, H_2O_2, and NO [172,173]), there are some differences, including the reported involvement of the G protein G PROTEIN ALPHA SUBUNIT 1 (GPA1) [174], PI-phospholipase C [175], and a sphingosine kinase [176] in inhibition of stomatal opening and not ABA-induced stomatal closure. Also, experiments using the *pyr1pyl1pyl2pyl4* ABA receptor mutant show that the mutant is still sensitive to ABA inhibition of stomatal opening in comparison to ABA-induced stomatal closure that is severely limited. This suggests that additional ABA receptors may be selectively involved in the inhibition of opening response [177].

Similarly, the components behind elevated CO_2-mediated inhibition of stomatal opening show differences to that of elevated CO_2-induced stomatal closure. A large protein that may act as a scaffold, BIG, has been shown to function only in CO_2 mediated inhibition of stomatal opening (not in elevated CO_2 promotion of closure or ABA signalling), however its mode of operation is unknown [178]. Further components in the elevated CO_2 inhibition of opening pathway are unclear, however similarly to the promotion of closure, it is thought CO_2 and ABA signalling pathways converge [147].

In addition to light, low levels of CO_2 are also able to promote stomatal opening. The HT1 kinase functions in this pathway in addition to functioning in the red light induced opening and as a negative regulator in the elevated CO_2 promotion of stomatal closure pathway [143,167,179]. Under low CO_2 conditions HT1 has been shown to phosphorylate the CBC1 and CBC2 kinases (providing a link between blue light induced opening, red light induced opening and low CO_2 induced opening). The CBC1 and CBC2 kinases in turn inhibit downstream anion channels (SLAC1) preventing stomatal closure [159]. Additionally, CPKs have been implicated in regulating low CO_2 induced stomatal opening [146].

1.2.7.2 Guard cell dark-induced closure

In the absence of light, stomatal closure occurs. The mechanisms behind this process are unclear. Few mutants have been isolated that show strong defects within dark-induced stomatal closure and those that do are mostly involved in regulating stomatal opening. Such as COP1 (involved in photoreceptor signalling) [156] and *ost2-2D* (a dominant mutant in the AHA1 H^+ATPase that leads to constitutive activity) [180]. Additionally, mutations that affect actin dynamics show defects within dark-induced closure [56,181]. Recently, GHR1, RBOHD, RBOHF, and a signalling cascade involving MAP KINASE/ERK KINASE 1 (MEK1), MPK6, and NO production were shown to be required for dark induced closure [115,182]. ABA signalling has also been implicated in regulating stomatal closure, this is discussed further in chapter 3.

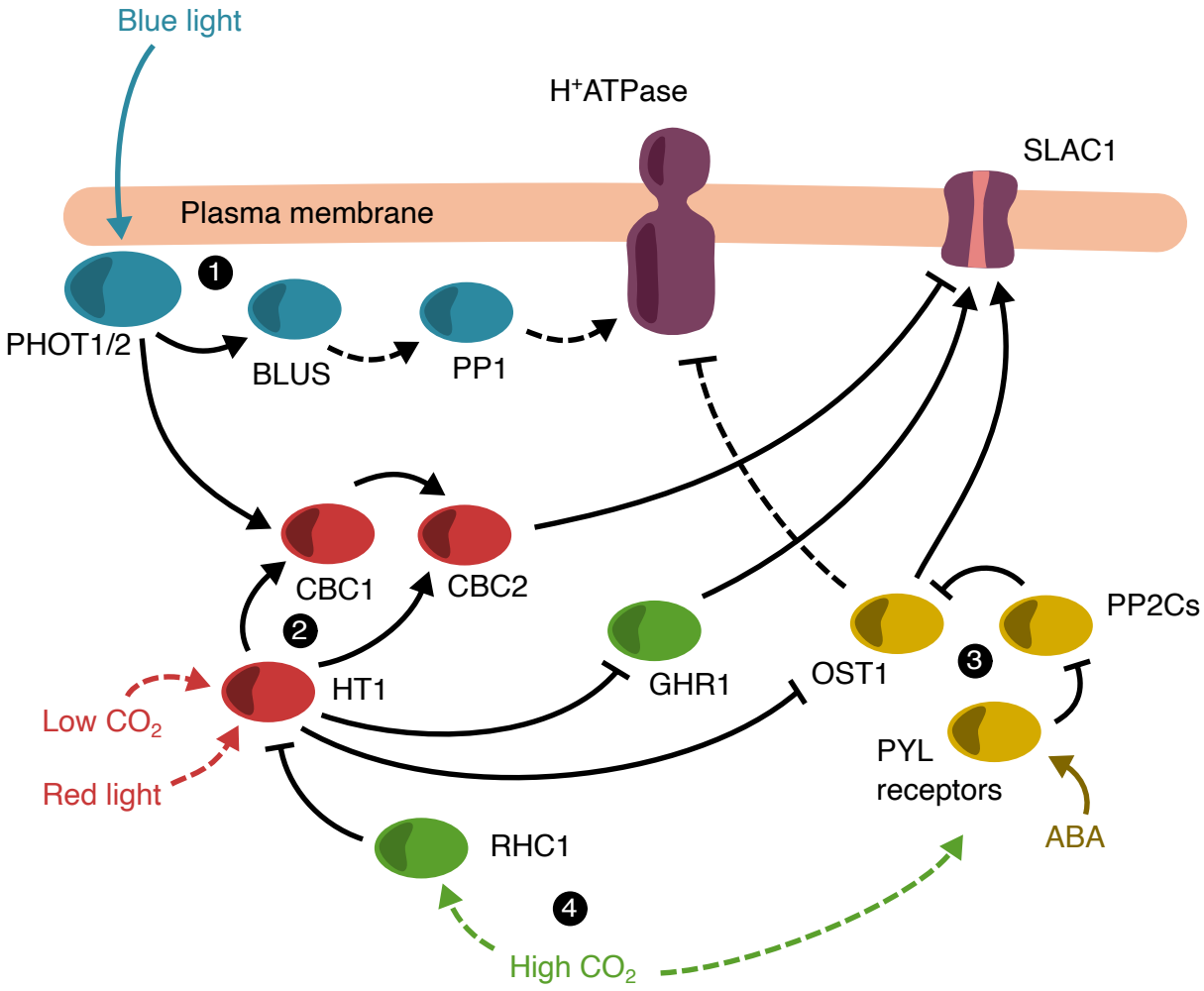

Figure 1.3 Environmental signals affecting stomatal opening

1. Blue light promotes stomatal opening through activation of the PHOT1 and 2 photoreceptors. These receptors activate plasma membrane H^+ATPases through a signalling pathway involving BLUS kinase and PP1 phosphatase. They also activate the CBC1 and 2 kinases to inhibit the SLAC1 anion channel. 2. Low CO_2 levels and red light are thought to promote the activity of the HT1 kinase that in turn activates CBC1 and CBC2 leading to the inhibition of SLAC1. Additionally, HT1 inhibits GHR1 and OST1. 3. ABA inhibits stomatal opening through the inhibition of plasma membrane H+ATPases and the activation of SLAC1 anion channels. 4. High CO_2 levels inhibit stomatal opening, however the process behind this unknown. It could involve the RHC1 mediated inhibition of HT1 (known to play a role in high CO_2-induced closure) and activation of the ABA signalling pathway.

1.3 Molecular signalling underlying stomatal development

Plants are also able to manipulate gas exchange through the regulation of stomatal density (ie the number of stomata per leaf surface area) [183]. Unlike, the regulation of stomatal movements that allow almost immediate responses to changes within the environment, regulation of stomatal density allows plants to regulate gas exchange over a longer timescale. Ultimately, the regulation of stomatal density restricts the maximum theoretical amount of gas exchange that can occur [184]. The regulation of stomatal density primarily occurs through modulation of stomatal development (controlling the number of cells that differentiate into mature functional stomata).

1.3.1 Regulation of stomatal development

In Arabidopsis the mechanisms underlying stomatal development are relatively well known. Stomata are formed from protodermal cells on the epidermis. The protodermal cells have stem cell-like qualities that allow them to differentiate into either trichomes, pavement cells or stomata. In order to differentiate into stomata, protodermal cells have to undergo a number of developmental stages. First, they must transition into a meristemoid mother cell (MMC). The MMC can asymmetrically divide forming a stomatal lineage ground cell (SLGC) and a meristemoid cell. Here, both the SLGC and meristemoid cell can undergo further divisions. If the SLGC divides it will produce a further meristemoid cell separated from the 1st meristemoid cell by a pavement cell (known as a spacing division). If the meristemoid cell divides it will produce another meristemoid cell and a further SLGC (known as an amplifying division). Meristemoid cells can also transition into guard mother cells (GMCs) or exit the stomatal lineage and form pavement cells. GMCs can symmetrically divide to form 2 guard cells or exit the stomatal lineage. Correct functioning of this process ensures stomata are never directly adjacent to one another and are separated by at least one pavement cell[185].

Differentiation of epidermal cells into stomata is primarily controlled by a trio of basic helix-loop-helix (bHLH) transcription factors; SPEECHLESS (SPCH), MUTE, and FAMA. Expression of SPCH is required for protodermal cells to transition into MMC cells [186,187], MUTE expression is required for the transition of meristemoid cells into GMCs [187,188], and FAMA

expression is required for the final transition of GMCs into guard cells [189]. Underlying the expression of these bHLH transcription factors is a complex network involving hormone and peptide signals that allow the integration of endogenous and exogenous signals to modulate stomatal development [185,190]. In grasses, MUTE orthologues have been shown to play roles in subsidiary cell recruitment as well as stomatal differentiation [75,191].

A family of secreted peptides, known as the epidermal patterning factors (EPFs), are involved in regulating the expression of SPCH, MUTE and FAMA, and act as a key point of entry for endogenous and exogenous signalling to regulate stomatal development [185,190]. Three EPF peptides have been studied in detail, EPF1, EPF2, and EPFL9 (also known as STOMAGEN). EPF1 and EPF2 function to inhibit entry into the stomatal lineage whereas EPL9 functions to promote stomatal lineage entry. These peptides are recognised by the ERECTA and ERECTA-LIKE 1 and 2 (ER/ERL1/ERL2) leucine rich repeat receptor like kinases (LRR-RLKs) and the leucine rich receptor TOO MANY MOUTHS (TMM) [192–194] which activate a downstream signalling pathway involving a MAPK cascade involving YODA (YDA), MAP KINASE KINASE 4/5 (MKK4/5), and MPK3/6 which culminate in repressing of the bHLH transcription factors [195–197]. EPF1 is expressed by late meristemoid, GMC, and young stomatal cells [198] and is thought to be involved in ensuring that asymmetric division of meristemoid cells leads to spacing of stomata [199]. Additionally, EPF1 functions in an autocrine manner in transitioning meristemoid to GMC cells to inhibit MUTE activity and allow FAMA mediated differentiation into stomata to occur at the correct time [200]. EPF2 is expressed in MMCs and early meristemoid cells [201,202] and functions to inhibit SPCH activity (via promoting SPCH degradation). This prevents cells nearby from entering the stomatal lineage [195]. EPFL9 is expressed in the mesophyll and competes with EPF1 and EPF2 to bind to ER/ERL1/ERL2 and blocks them from initiating downstream signalling [203,204].

1.3.2 The effect of light on stomatal development

Increased light intensity is known to increase stomatal density. Both the CRY1 and CRY2 blue light cryptochrome and PHYA and PHYB phytochrome photoreceptors (far red and red light respectively) play a role in this process in conjunction with the E3 ubiquitin ligase COP1 [205]. COP1 is involved in the negative regulation of stomatal development. It is thought to act upstream of the YDA MAPK cascade [205], and additionally thought to target the interaction

partners of the SPCH, MUTE, and FAMA transcription factors [206]. Upon activation the CRY1, CRY2, PHYA, and PHYB photoreceptors inhibit the activity of CONSTITUTIVE PHOTOMORPHOGENIC 1 (COP1), thereby promoting stomatal development and increasing stomatal density [205]. Light intensity has also been shown to regulate stomatal development on the hypocotyl through a separate mechanism involving a group of transcription factors known as the B-GATA transcription factors. The B-GATA transcription factors are thought to promote stomatal development upstream of the bHLH transcription factors and are inhibited by the phytochrome interacting factors (PIFs). Upon red light induced PHYB activation, PHYB promotes the degradation of the PIFs thereby releasing B-GATA transcription factors from inhibition, allowing the promotion of stomatal development [207].

1.3.3 The effect of ABA on stomatal development

ABA plays an opposite role to light with respect to the regulation of stomatal development. Application of ABA has been observed to decrease stomatal density in wheat [208], mutants within ABA signalling and biosynthesis show increased stomatal densities, and mutants within ABA degradation show decreased stomatal densities [90,209]. However, in some cases ABA has been shown to increase the stomatal density in water submerged leaves, but this is likely a specialised function [210]. Overall ABA functions to decrease stomatal density. This is achieved through limiting entry into the stomatal lineage via restricting SPCH and MUTE expression as well as promoting the expansion of pavement cells [209]. The opposing role of ABA and light is highlighted in the fact that mutations within the ABA deconjugating enzyme *β-glucosidase 1* (*bg1*) can partially rescue the decreased stomatal density phenotype of a *phyb* mutant [211].

1.3.4 The effect of CO_2 on stomatal development

As CO_2 concentrations increase stomatal density in most species decreases [212]. This process is regulated by components of the CO_2 signalling pathway. Mutants within the carbonic anhydrases (which convert CO_2 into HCO_3^- and function early in CO_2 signalling) show increased stomatal density under elevated CO_2 conditions [140]. A mechanism was uncovered that suggests under elevated CO_2 the EPF2 peptide is upregulated in a carbonic anhydrase dependent manner. In addition, a protease, CO2 RESPONSE SECRETED PROTEASE (CRSP), that cleaves the EPF2 pro-peptide producing the active EPF2 peptide is also upregulated in elevated CO_2

conditions and functions in this response [213]. Similarly to CO_2 induced stomatal movements, components of ABA signalling and metabolic pathways are also involved in stomatal density responses to elevated CO_2. The quadruple receptor mutant *pyr1pyl1pyl2pyl4*, the ABA biosynthesis mutants *aba3* and *nced3/5*, and the ABA degradation mutant *cyp707a1/2* all show insensitivity to elevated CO_2 with respect to stomatal development [90,148].

1.4 Aims

The broad aim of this project was to explore the role of ABA metabolism and signalling in stomatal responses to darkness. Previous work has suggested roles for ABA signalling components in dark-induced stomatal closure, however, there is confusion over the exact role of ABA signalling in this process [180,214]. Using the model plant *Arabidopsis thaliana* this study measures the stomatal physiology of various ABA signalling and metabolism mutants in response to darkness and light in combination with other techniques to address this question. Furthermore, as well as immediate stomatal responses to darkness, the longer-term transcriptional responses of ABA signalling components to darkness are investigated along with the physiological relevance of these changes. Finally, this study also aimed to identify new stomatal signalling components involved in regulating stomatal movements. Overall, using a genetic and physiological approach this project aims to further the understanding of the mechanisms behind stomatal signalling pathways and how these affect stomatal behaviour.

CHAPTER 2: GENERAL METHODS

2.1 Plant Physiology

2.1.1 Plant material

All plants used in this study were *Arabidopsis thaliana*. All mutants were in the Col-0 ecotype unless otherwise stated. Table 2.1 contains information regarding all Arabidopsis lines used.

2.1.2 Plant standard growth conditions

Plants were grown in Snjider Labs Micro Clima-Series High Specs Plant Growth Chambers. Standard conditions were set to short day (10 hours light, 14 hours darkness), 22 ˚C in light and 20 ˚C in darkness. Relative humidity was set to 70 % humidity and light concentration was set to 120 ± 10 μmol m^{-2} s^{-1}. Temperature and light were set to gradually change over a 15 minute period during the dusk and dawn transition periods.

Plant seeds were sterilised in 70% ethanol for 10 mins and sown onto trays containing a soil mixture (3:1 all purpose compost (Sinclair): silver sand (Melcourt). Soil was prepared and oven baked for 48 hours at 60 ˚C prior to use). Seeds were stratified in darkness at 4 ˚C for 2-3 days before placement of tray into growth cabinet. Trays were fitted with clear humidity lids for 1st week of growth. Plants were watered every 2-3 days.

Line name	Description	Accession no	Ref.
q1124	Quadruple ABA receptor mutant. EMS induced point mutation within *PYR1*. T-DNA insertions within *PYL1, PYL2,* and *PYL4*.	*pyr1:* Q169* (nonsense) *pyl1*: SALK_054640 *pyl2*: CSHL_GT2864 *pyl4*: SAIL_517_C08	[100,215]
s112458	Sextuple ABA receptor mutant. Additional T-DNA insertions in *PYL5* and *PYL8* crossed into *q1124*.	*pyl5*: SM_3_3493 *pyl8*: SAIL_1269_A02	[216]
nced3/5	Double mutant containing T-DNA insertions within *NCED3* and *NCED5*.	*nced3*: GABI_129B08 *nced5*: GABI_328D05	[217]
cyp707a1	T-DNA insertion within *CYP707A1*.	SALK_069127	[218]
cyp707a3	T-DNA insertion within *CYP707A3*	SALK_078173	[219]
bg1	T-DNA insertion within *BG1*	SALK_024344	[220]
bglu18-1	T-DNA insertion within *BG1*	SALK_075731	[220,221]
pOST1::OST1-GFP	*ost1-3* mutant complemented with OST1-GFP under control of the OST1 promoter		[137]
pkg-1	T-DNA insertion within *PKG*	SALK 108016	
pkg-2	T-DNA insertion within *PKG*	SALK 000828	

Table 2.1 Lines used in this study

A list of *Arabidopsis thaliana* lines that were used in this study. A short description, T-DNA accession codes, and references to where lines have previously been described are provided.

2.1.3 Stomatal aperture bioassays

Stomatal apertures were measured in both leaf discs or epidermal peels using the following protocol. For each timepoint/treatment per genotype, a total of 9 leaf discs/epidermal peels each from individual plants were analysed over 3 independent experiments. From each leaf disc/epidermal peel 10 stomata were measured. In total this accounts for 90 stomatal aperture measurements for each timepoint/treatment per genotype. Further information regarding specific timecourses/treatments can be found in the specific methods sections of the various data chapters.

Leaf disc harvesting

Leaf discs were harvested from leaves of 5 week old plants using a 4 mm biopsy punch (KAI). A single leaf (the largest leaf) was removed from a plant using a clean razor blade and a leaf biopsy was rapidly taken from the same region of each leaf, halfway between the midvein and the leaf edge 2/3rds of the way up the length of the leaf where width is generally at its largest. After the biopsy was taken the leaf disc was rapidly transferred to 50 mm single vented petri dish containing 10 ml of 10/50 buffer (10 mM MES, 50 mM KCl, pH 6.2 with KOH) preheated to 22 ˚C. Leaf discs were floated abaxial face down.

Epidermal peel harvesting

Epidermal peels were harvested from leaves of 5 week old plants using a clean razor blade and forceps. A single leaf (the largest leaf) was removed from the plant. A razorblade was used to cut away leaf edges, leaving clean straight edged leaf. A small nick was made on the straight edge and forceps were used to carefully remove the abaxial epidermis. Surgical scissors were used to aid in the epidermis removal and subsequent removal of any attached mesophyll. The epidermis was transferred to 50 mm single vented petri dishes containing 10 ml of 10/50 buffer. Epidermal peels were floated with the abaxial face up.

Leaf disc/epidermal peel incubation

After harvesting, petri dishes containing leaf discs/epidermal peels were transferred to a tank. The tank was filled with water and contained a pump and heater to ensure that ensure water temperature is maintained at 22 ˚C. Cool water was pumped through metal tubes at the far side of the tank from the heater to generate a current enabling more consistent heating. The tank had

clear sides that allow light to pass through. Tube lamps (Crompton Lamps 13 W white) placed underneath the tank illuminate pots placed on the surface of the water with 120 μmol m^{-2} s^{-1}.

Depending on whether stomatal opening or closing was being measured leaf discs/epidermal peels were incubated in darkness (to ensure closed stomata) or light (to ensure open stomata) for 2 hours respectively. Darkness was achieved by covering 50 mm petri dishes with black electrical tape to prevent light reaching inside the petri dish. After 2 hours of incubation, using clean forceps, leaf discs/epidermal peels were transferred to petri dishes containing the desired treatment, or were placed on microscope slides to be measured.

Stomatal aperture measurements

Upon measurement leaf discs/epidermal peels were transferred to microscope slides in a small pool of 10/50 buffer. A coverslip was placed on top of the leaf discs/epidermal peels and the microscope slide was rapidly imaged using a Leica DMI6000 B microscope fitted with a Leica DFC360FX monochrome camera. The microscope was set to brightfield settings and image stacks were taken using a 40x lens. For each leaf disc/epidermal peel 3 image stacks were taken. Over these image stacks 10 stomata were measured per leaf disc/epidermal peel using ImageJ.

2.1.4 Gas exchange measurements

6-8 week old plants were used when measuring stomatal conductance. A GFS3000 gas analyser machine (Walz) set up in a growth cabinet with a standard measuring head fitted with an Arabidopsis leaf adaptor was used to measure conductance. Flow was set to 750 μmol s^{-1}, impeller speed was set to 7, T_{cuv} was set to 22 ˚C, H_2O was set to 16000 ppm and $CO_2$was set to 400 ppm. Before measurements the GFS3000 was run for at least 30 mins with an empty cuvette. Once stomatal conductance (G_s) stabilised and was set to 0, a large mature leaf was clamped into the cuvette (still attached to the plant). Measurements then began. After measurements an image of the leaf within the cuvette was taken and if not all the cuvette was filled, the area taken up by the leaf was determined using imageJ. The leaf area was then used to determine absolute transpiration values.

2.2 Molecular Biology

2.2.1 Genotyping

DNA was extracted from Arabidopsis leaf tissue using the Wizard® Genomic DNA Purification kit following the manufacturers instructions. Thermofisher DreamTaq Green PCR mastermix (2x) was used to amplify DNA from plants being genotyped following the manufacturers instructions. Plants were genotyped individually by amplifying a gene specific and T-DNA specific amplicon, therefore allowing the verification of whether a mutant was homo or heterozygous. Primers were designed using the iSect primer design tool from the Salk Institute Genomic Analysis Laboratory website (http://signal.salk.edu/cgi-bin/tdnaexpress). Amplified DNA was visualised via gel electrophoresis. Primers are listed in table 2.2

2.2.2 QPCR

RNA was extracted from leaf material using the Machery Nagel Nucleospin RNA plant and fungi kit, following the manufacturers instructions. Flash frozen leaf tissue was ground to a powder using a TissueLyser II (Qiagen) and 5 mm steel beads. cDNA was generated from RNA samples diluted to 1.5 μg/μl using the Applied Biosystem High Capacity cDNA synthesis kit with RNase inhibitor, following manufacturers instructions. QPCR was performed using the Agilent Brilliant III Ultra-Fast SYBR Green QPCR master mix and the Agilent Mx3000P thermocycler machine. Primers were designed manually with the help of the NCBI primer design tool. Primers were ordered from Eurofins Genomics and suspended in RNAse free H_2O. All primers were tested prior to use by plotting a standard curve using serially diluted cDNA samples. For each sample at least 2 technical replicates were run and all samples within the same analysis were run at the same time. Unless otherwise stated transcript abundances were determined with the ΔΔCt method using geometric mean of *EF1a* and *PP2A* as a reference. For all treatments it was tested whether *EF1a* or *PP2A* transcript abundance remained stable before their use as reference genes. Primers are listed in table 2.3.

Primer name	Sequence (5' – 3')
pyl1 SALK_054640 FP	TGCCAATTTTCAGACATTAAGC
pyl1 SALK_054640 RP	AACCATGCCTTCCGATTTAAC
pyl2 CSHL_GT2864 FP	ACCGGCAAGATTTCTTGACTC
pyl2 CSHL_GT2864 RP	CAGAAAGGGATAAATCCGTCC
pyl4 SAIL_517_C08 FP	TTCCAATCGTTCCAAATATCG
pyl4 SAIL_517_C08 RP	TAAGACTCGACAACGACGGTC
pyl5 SM_3_3493 FP	AAACACAAAGCCTTCACATCC
pyl5 SM_3_3493 RP	AAGTTTTGTGAATCCCCCAAC
pyl8 SAIL_1269_A02 FP	AGAGAGTGGAACCCCATGATC
pyl8 SAIL_1269_A02 RP	TTCTTCTTCTTCCTTCATGCG
nced3 GABI_129B08 FP	ACAGAGGCTCTCCTCCGTAAC
nced3 GABI_129B08 RP	GTCAGCCACGAGAAGCTACAC
nced5 GABI_328D05 FP	TAACACCAAACCCAACCAAAC
nced5 GABI_328D05 RP	TGACTCAACCCAAACCATCTC
bg1 SALK_024344 FP	TTTGGCTCCAACAACTTATGG
bg1 SALK_024344 RP	ACCGGTAGATGAAAACGATCC
bglu18-1 SALK_075731 FP	TTTGGCTCCAACAACTTATGG
bglu18-1 SALK_075731 RP	ACCGGTAGATGAAAACGATCC
bg2 SALK_047384 FP	ACGCAGTCGGATGTTTACATC
bg2 SALK_047384 RP	AGGGGGTGAAGTTCTACAACG
cyp707a1 SALK_069127 FP	CATGAACGTATTGGGTTTTGG
cyp707a1 SALK_069127 RP	TCCTGATATTGAATCCATCGC
cyp707a3 SALK_078173 FP	GTTCCTGGAAGATTAATCGGC
cyp707a3 SALK_078173 RP	ACGTGCTCTCGTCACTCTCTC
SALK LBb1.3	ATTTTGCCGATTTCGGAAC
SAIL LB1	TAGCATCTGAATTTCATAACCAATCTCGATACAC
CSHL DS5	GTTCGAAATCGATCGGGATAAAAC
GABI LB	ATATTGACCATCATACTCATTGC
Spm3	ACCGTCGACTACCTTTTTTCTTGTAGTG
pkg-1 SALK_108016 FP	CTGGATAACATACAGGCCCTG
pkg-1 SALK_108016 RP	GCTTACAGGTTCGGAATCTCC
pkg-2 SALK_000828 FP	TTCGCAGAATTATGCCGTTAC
pkg-2 SALK_000828 RP	TAATCTCGCGAATTCATCACC

Table 2.2 Genotyping primers

Primers used for genotyping the *Arabidopsis thaliana* lines used in this study. Primers were designed using the iSect primer tool on the Salk Institute Genomic Analysis Laboratory website.

Primer name	Sequence (5' – 3')
PYR1 FP	ACCAACTCGATCCAGGAAGC
PYR1 RP	GTTTTGTTCGACGGAGCAGG
PYL1 FP	AGAGTCCTCCTCCTCACCAG
PYL1 RP	TCGGCGATTGATTGGGAGAG
PYL2 FP	GGCCTAACCGATGAAGAGCA
PYL2 RP	TAAGAGGCCAAACCACGGAG
PYL4 FP	GTGACCACCGGCTCTCTAAC
PYL4 RP	GCCTGGAGGAACATCAACGA
PYL5 FP	ATCGGTGACGACACTACACG
PYL5 RP	AGCCAGAGACTGAAGGTTGC
PYL6 FP	TATCGGAGACGGTCGAGAGG
PYL6 RP	CACCAACGACGCTGAAACTG
PYL7 FP	GTACGGAGCTCTAGTGACGG
PYL7 RP	ACCAAACAAGATGAACAGGAGC
PYL8 FP	ACGGGATTGAGAACTTGACGA
PYL8 RP	ACCACACAATATGAACAGGAGC
PYL9 FP	TCAAAGCTCCTCTTCATCTCGTTT
PYL9 RP	CTCTAAGACTGCCGATTTCAGGA
SLAC1 FP	CAACGCTCAGCAAACAAAAGTC
SLAC1 RP	CTTCATTGTCCTTGACTTCATCCAA
OST1 FP	ATCAACCGGGCCAAAGCATA
OST1 RP	ATGTCCAAGCTTCCTGTGAGG
PHYA FP	CGGTTGATGAAGCAATCGGG
PHYA RP	TCCTCAGTTCCTTCTAATGCGT
PHYB FP	CTCGTGCTTTGAGAGGGGAC
PHYB RP	CGCCGACAATGTTGTTCAAGT
PHOT1 FP	TCATCCCAAACTCATTCCTCAGT
PHOT1 RP	CCATCTTTGAGCTCTCTCTTGC
PHOT2 FP	CTATCAAGGACGACCAGGGC
PHOT2 RP	CTCCTTCTGGCGAGCATCAT
CRY1 FP	TGCTGCGTTTTGGGAGAGAT
CRY1 RP	ACACATTTAGACACATCCCCTGA
CRY2 FP	CTGCGAAAAGGGCAAACCTT
CRY2 RP	TTCAGCCGCTGCAGTTATTG
EF1α FP	TGTGCTGTTCTTATCATTGACTCC
EF1α RP	TGGCATCCATCTTGTTACAACAG
PP2A FP	TAACGTGGCCAAAATGATGC
PP2A RP	GTTCTCCACAACCGCTTGGT

Table 2.3 QPCR primers

A table of QPCR primers used in this study. Primer names and sequences are provided. QPCR primer efficiencies and R^2 values were calculated for each primer pair prior to use. Primers were only used if R^2 was above 0.98 and efficiencies were within 100 ± 10 %.

2.3 Data Analysis

Data was analysed using the R statistical programming language (version: 4.0.2, url: https://www.r-project.org/). Unless otherwise stated normally distributed data were analysed using 1 or 2 way ANOVAs to test for significance with post-hoc TukeyHSD tests for multiple comparisons, while non normally distributed data was analysed using Kruskal Wallis tests for significance with post hoc Dunn tests for multiple comparisons. Data was visualised using the R package ggplot2 [222].

CHAPTER 3: MUTATIONS WITHIN CORE ABA SIGNALLING AND BIOSYNTHESIS MACHINERY LEAD TO SLOWED STOMATAL RESPONSES TO DARKNESS AND LIGHT

3.1 Introduction

Plants rapidly respond to environmental stimuli by regulating gas exchange through changes in the aperture of stomata on leaf surfaces. Stomata are composed of two guard cells surrounding a central pore. Changes in guard cell turgor bring about changes in the aperture of the stomatal pore. The regulation of gas exchange allows plants to balance the uptake of carbon dioxide with the loss of water [3]. Much work has focused on the underlying mechanisms of stomatal movements, especially on how ion transport across guard cell membranes helps to mediate changes in guard cell turgor pressure, the mechanisms behind blue and red light induced stomatal opening, and how the drought hormone abscisic acid (ABA) leads to stomatal closure

and the inhibition of stomatal opening [6]. However, the process underlying dark-induced stomatal closure is unclear. It is unknown whether darkness actively accesses stomatal closure machinery or whether it is a passive response to the absence of light. In addition, as there is an increase in leaf intercellular CO_2 concentration (Ci) during dark treatment it is possible that CO_2 also has a contribution to make towards dark-induced closure. However, the contribution of Ci to dark-induced closure has not been investigated in the present study.

Few mutants have been identified that show strongly defective dark-induced stomatal closure responses. Those that do are often involved in regulating stomatal opening; such as mutants in COP1, an E3 ubiquitin ligase that functions downstream of the cryptochrome and phototropin photoreceptors[156], or the dominant mutation, *ost2-2D,* causing constitutive activation of the H^+ ATPase AHA1 (a proton pump that hyperpolarises guard cell membranes, inducing ion transport and ultimately stomatal opening) [180]. Additionally, reorganisation of the actin cytoskeleton has been shown to be crucial for stomatal dark-induced closure, as mutations within the ACTIN RELATED PROTEIN 2 and 3 (Arp2/3) and SUPPRESSOR OF CAMP RECEPTOR/WASP FAMILY VERPROLIN-HOMOLOGOUS (SCAR/WAVE) complexes that control actin cytoskeleton dynamics show lack of dark-induced closure [56,181]. Weaker phenotypes have also been observed, such as in the *myb domain protein 61* (*myb61*) transcription factor mutant, where stomatal apertures are increased in dark conditions, however here, stomatal apertures are also increased in light conditions and there is a noticeable but reduced response to darkness [223]. More recently additional signalling components required for dark-induced closure have been identified. The pseudokinase GHR1, involved in activating the downstream ion channel SLAC1, has been demonstrated to be required for stomatal closure in response to a number of signals, including darkness [115]. A MEK1/MPK6 signalling cascade activated by H_2O_2 (produced by RBOHD and RBOHF) and culminating in the production of NO by NITRATE REDUCTASE 1 (NIA1) has also been shown to be required for dark-induced closure [182].

Studies have linked ABA signalling to dark-induced closure, but the precise way in which it is involved in regulating dark-induced closure is unclear. Microarray data have shown components of the ABA signalling pathway undergo transcriptional regulation in response to darkness, however these changes are likely to reflect longer term adaptation rather than the short term closure. [149]. Additionally, another study has shown that a selection of ABA receptor mutants

(*pyr1pyl1pyl2pyl4, pyr1pyl4pyl5pyl8, pyr1pyl2pyl4pyl5pyl8, pyr1pyl1pyl2pyl4pyl5pyl8*) all show increased stomatal conductance under light and dark conditions. However, when comparing the change in stomatal conductance from light to dark conditions all of the previously mentioned ABA receptor mutants (except the strongest mutant, *pyr1pyl1pyl2pyl4pyl5pyl8*) show changes in stomatal conductance similar to wild type. Similarly, mutations within PP2C phosphatases (downstream negative regulators of ABA signalling) and ABA degradation mutants, affect stomatal conductance without preventing responses to darkness. In the ABA biosynthesis mutants, *aba1-1* and *aba3-1,* stomatal conductance is also increased, however both mutants still respond to a dark (although this appears weakened in *aba3-1*) [214]. In addition, stomatal aperture changes in the PP2C mutants *abi1* and *abi2* show reduced responses to darkness [224]. This suggests a situation where ABA signalling may make a contribution to dark-induced stomatal closure, however, it also suggests that ABA has more general effects on stomatal apertures regardless of light or dark conditions.

In this chapter the effect of defects in ABA signalling and metabolism on stomatal responses to darkness and light were investigated. The movement of stomata was analysed through direct measurements on leaf discs and through monitoring changes in stomatal conductance. A list of mutants used in this chapter are shown in Table 3.1. Evidence was found showing that ABA signalling is not essential for dark-induced closure. However, additional evidence that defects in ABA signalling and metabolism affect the timing of stomatal responses to both light and darkness is provided. Overall, this chapter concludes that ABA signalling does not play a major role in mediating dark-induced stomatal closure but does play a role in modulating the speed of closure.

Mutant name	Genes affected	Function
q1124	*pyr1, pyl1, pyl2, pyl4*	ABA receptor mutant
s112458	*pyr1, pyl1, pyl2, pyl4, pyl,5, pyl8*	ABA receptor mutant
nced3/5	*nced3, nced5*	ABA biosynthesis mutant
cyp707a1	*cyp707a1*	ABA degradation mutant
cyp707a3	*cyp707a3*	ABA degradation mutant
bg1	*bg1*	ABA activation mutant
bg2	*bg2*	ABA activation mutant

Table 3.1 List of ABA signalling and metabolism mutants used in Chapter 3

A list of the ABA signalling and metabolism mutants used in chapter 3 with a brief description of the genes affected and the gene function.

3.2 Specific Methods

3.2.1 Leaf disc aperture measurements

Dark induced closure: Leaf discs were harvested from 5 week old plants grown under standard conditions 2 hours post dawn. Leaf discs were incubated under light for 2 hours before transfer to darkness or measurement. Stomatal apertures were recorded after the initial 2 hours (0 mins), then 30, 60, and 120 mins of dark treatment. Additionally, one group of leaf discs were left in light for a further 2 hours acting as a light control (120 mins L).

Light induced opening: Leaf discs were harvested from 5 week old plants grown under standard conditions before the onset of dawn under green light. Leaf discs were incubated in darkness for 2 hours, before transfer to light or measurement. Stomatal apertures were recorded after 2 hours of dark treatment (0 mins), then 30, 60, and 120 mins of light treatment. Additionally one group of leaf discs were left in dark coated petri dishes for a further 2 hours acting as a dark control (120 mins D).

ABA induced closure: Leaf discs were harvested from 5 week old plants grown under standard conditions 2 hours post dawn. Leaf discs were incubated under light for 2 hours before transfer or aperture measurement. Leaf discs were transferred to a 50 mm petri dishes containing 10/50 buffer supplemented with 10 μM ABA (0.05% EtOH). Apertures were measured after 10, 20, and 30 mins ABA treatment. Additionally, one set of leaf discs were transferred to pots containing 10/50 buffer supplemented with 0.05% EtOH (acting as a light control – 30 mins C).

3.2.2 Transpiration measurements

Midday darkness 6-8 week old plants were grown under standard conditions. Plants were placed into the gas analyser cuvette at midday and left for 2 hours to equilibrate, before either the whole plant was placed into darkness (fig. 3.5) or the leaf within the cuvette was placed in darkness (fig. 3.2). Plants were left in darkness for 60 (fig. 3.5) or 120 mins (fig. 3.2) before being reintroduced to light.

Dusk/Dawn measurements 6-8 week old plants were grown under standard conditions. Plants were placed into the gas analyser cuvette at least 2 hours prior to dusk. The plants were left in the gas analysers until 2 hours after dawn the following day.

3.2.3 OST1-GFP intensity measurement

Leaf discs from 5 week old *pOST1::OST1-GFP* plants were harvested 2 hours post dawn. They were incubated under 120 μmol m^{-2} s^{-1} light for 2 hours before transfer to darkness or 10/50 buffer supplemented with 10 μM ABA, or light. Leaf discs were incubated in their respective treatment for 2 hours before fluorescence measurements. A Leica SP5-AOBS confocal laser scanning microscope attached to a Leica DMI6000 inverted epifluorescence microscope was used to capture z stacks of leaf disc epidermises. Leaf disc treatments were staggered to allow for sufficient time for fluorescent measurements. GFP was excited using a 488 nm argon laser and fluorescence was captured at 500-600 nm (GFP), 650-800 nm (chlorophyll autofluorescence). Z stacks were analysed in FIJI. The image within the stack dissecting the centre of a pair of guard cells was used in order to avoid autofluorescence from the inner stomatal ridges. Cross sections were drawn across individual guard cell pairs. One cross section bisecting the 2 perinuclear regions, one avoiding the perinuclear regions. Maximum intensity from the plasma membrane and perinuclear region was recorded for each guard cell pair. The ratio of perinuclear/membrane intensity was calculated by dividing the perinuclear intensity by the plasma membrane intensity. Due to non-parametric nature of the data, it was statistically analysed using a Kruskal Wallis test followed by Dunn's multiple comparison test.

3.3 Results

3.3.1 ABA signalling and metabolism leaf disc responses to the onset of darkness

To explore whether mutations in ABA biosynthesis, degradation or signalling genes affect stomatal responses to darkness, stomatal movements were measured in leaf discs from ABA metabolism and signalling mutants. Of the 14 member ABA receptor family, quadruple and sextuple ABA receptor mutants (*pyr1pyl1pyl2pyl4* [225] – *q1124* and *pyr1pyl1pyl2pyl4pyl5pyl8* [216] – *s112458*) were used. The ABA biosynthesis double mutant *nced3nced5* [217] (*nced3/5* – a double mutant in the *NCED3* and *5* genes which catalyse the first committal step in ABA biosynthesis, thought to be the rate limiting step under drought conditions [217,226,227]) and mutants within 2 genes involved in rapid ABA activation from inactive glucose esters (*bg1* and *bg2* [99]) were used. Additionally mutants in ABA hydroxylation genes (*cyp707a1* and *cyp707a3* [219]) involved in ABA catabolism were used (exact mutant accession codes are shown in the methods section and a list of mutants analysed in this chapter is shown in table 3.1).

Delays in stomatal closure following dark treatment were observed for the ABA receptor mutants *q1124* and *s112458*, the ABA biosynthesis mutant *nced3/5*, and the ABA activation mutant *bg1,* which all showed no significant change in stomatal aperture, as opposed to wild type, after 30 minutes dark treatment (fig. 3.1a, b, and c). No delays in dark-induced stomatal closure were observed in the ABA activation mutant *bg2* or the ABA catabolism mutants *cyp707a1* or *cyp707a3* (fig. 3.1c and d). The absence of a delay phenotype in the *bg2* mutant could be due to the difference in subcellular location and/or reduced activity of the BG2 protein compared with BG1 [99]. Additionally, mutations in *CYP707A1 and 3* genes lead to increased levels of ABA [219,228] and increased ABA signalling activity (the opposite of what occurs in ABA biosynthesis and signalling mutants), explaining the lower starting apertures (as observed previously [219]) and potentially the absence of delay.

In addition to delays in dark-induced stomatal closure, changes to stomatal apertures regardless of treatment are observed for many of the mutants analysed. The ABA receptor and biosynthesis mutants (*q1124*, *s112458* and *nced3/5*) show significantly increased stomatal apertures before (*q1124* – $p = 0.00003$, *s112458* – $p < 0.00001$, *nced3/5* – $p < 0.00001$; Tukey multiple

comparison tests) and after two hours of dark treatment compared with Col-0 (*q1124* – $p < 0.00001$, *s112458* – $p < 0.00001$, *nced3/5* – $p < 0.00001$; TukeyHSD). Conversely, the ABA catabolism mutants (*cyp707a1* and *cyp707a3*) show reduced stomatal apertures prior to dark treatment (*cyp707a1* – $p = 0.00268$, *cyp707a3* – $p = 0.02927$; TukeyHSD) and similar apertures after two hours dark treatment. The ABA biosynthesis mutants *bg1* and *bg2* show no difference when compared with Col-0 before or two hours after dark treatment.

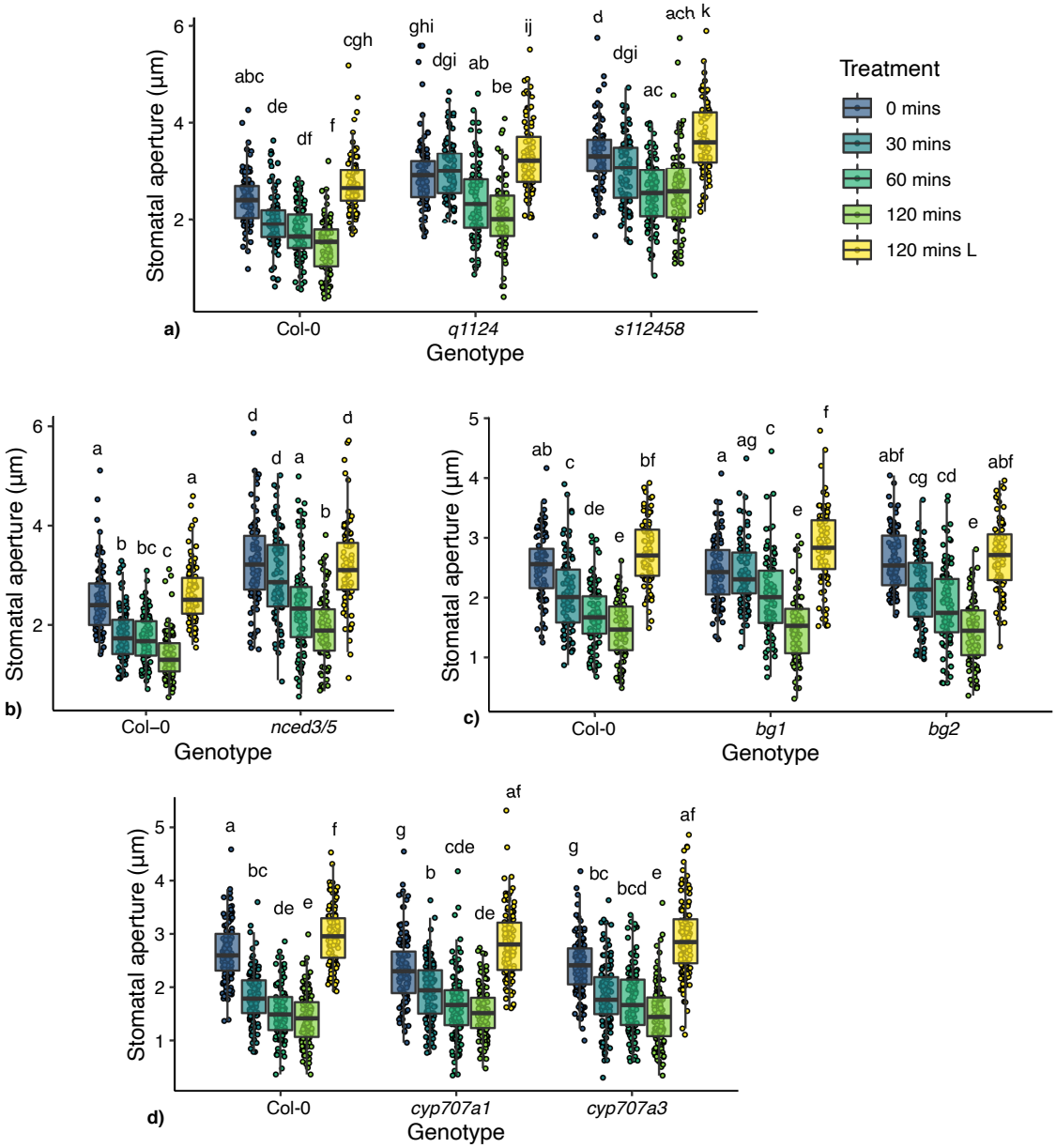

Figure 3.1 ABA signalling, biosynthesis, and degradation mutants show a delay in dark induced stomatal closure.

Stomatal responses to darkness over a 120 min time course were tracked in leaf discs harvested from a) ABA receptor mutants (*q1124* and *s112458*), b) *nced3/5*, c) ABA activation mutants (*bg1* and *bg2*) and d) ABA degradation mutants (*cyp707a1* and *cyp707a3*). Leaf discs were incubated under light for 120 mins before transfer to darkness. 120 mins L represent aperture data from leaf discs left under light for 120 mins. N = 90 from 9 individual plants over 3 independent experiments. Data is presented in boxplots showing the median and interquartile range of each group. The upper and lower whiskers represent data within 1.5 * the interquartile range. All data values are represented by points. Data statistically analysed using 2-way ANOVA with Tukey multiple comparison tests, samples indicated with the same letter cannot be distinguished at $p < 0.05$.

3.3.2 Gas exchange responses of ABA signalling and metabolism mutants to darkness

A number of key gas exchange parameters were tracked in response to darkness for the following mutant genotypes; Col-0, *q1124*, *bg1*, *cyp707a1*, and *cyp707a3*. Due to the smaller leaf phenotype of the *s112458* and *nced3/5* mutants, measurements could not be recorded. Here, a single leaf still attached to the plant was incubated in leaf cuvette chamber until stomatal conductance had stabilised (approximately 2 hours), then the chamber was covered preventing light from reaching the leaf for 2 hours, before uncovering for a further 2 hours.

Initially focusing on dark induced decreases in stomatal conductance, it is evident this response occurs much faster than dark induced closure in leaf discs (fig. 3.1). The absolute and relative stomatal conductance values are shown for the mutants in fig. 3.2. All mutants appear to respond by decreasing their transpiration values by ~ 50 % in response to darkness. Delayed responses are only noticeable for the *q1124* receptor mutant (fig. 3.3a and b). *q1124* shows increased half response times (the time taken for stomatal conductance to reach 50% of its maximum response) to light and darkness (fig. 3.3a and b respectively). A 1-way Welch ANOVA (due to unequal variances of the closing half times) shows there is a significant effect of genotype on the dark induced closing half times ($F_{4,4.8} = 6.059$, $p = 0.040$). Similarly, a Kruskal Wallis test on the light induced opening half times shows a significant effect of genotype (chi square = 9.70, df = 4, p = 0.045).

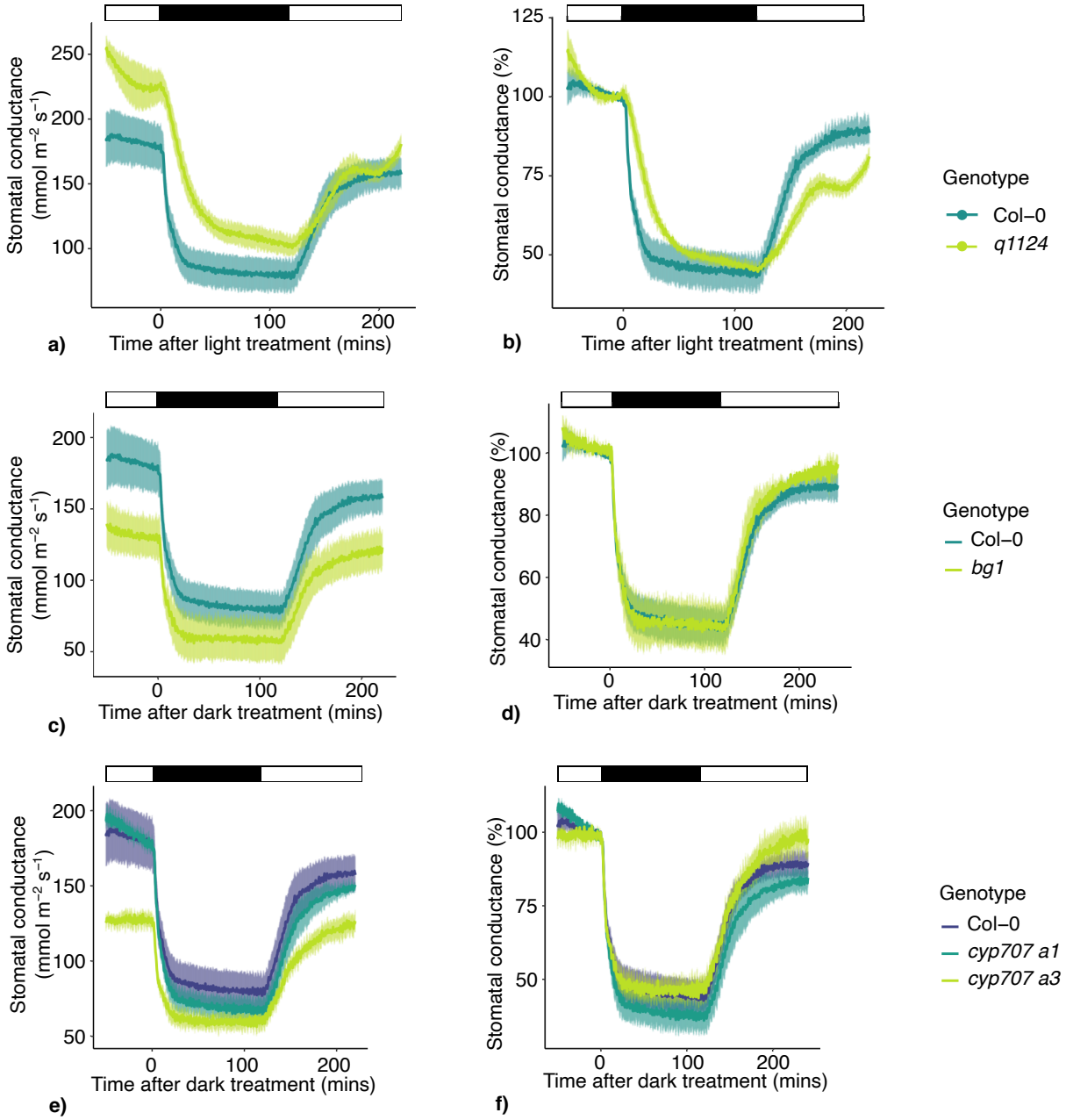

Figure 3.2 Stomatal conductance responses to darkness for ABA signalling, activation, and degradation mutants

Stomatal conductance of ABA signalling and metabolism mutants were measured in response to 120 mins darkness, followed by a further 120 mins light. Absolute and relative stomatal conductance values for **a)**, **b)** *q1124*, **c)**, **d)** *bg1* and **e)**, **f)** *cyp707a1* and *cyp707a3* are shown. Lines represent the mean ± s.e.m. 3-4 plants were measured per genotype. Light treatment is represented above each plot, with black boxes representing darkness and white boxes representing light.

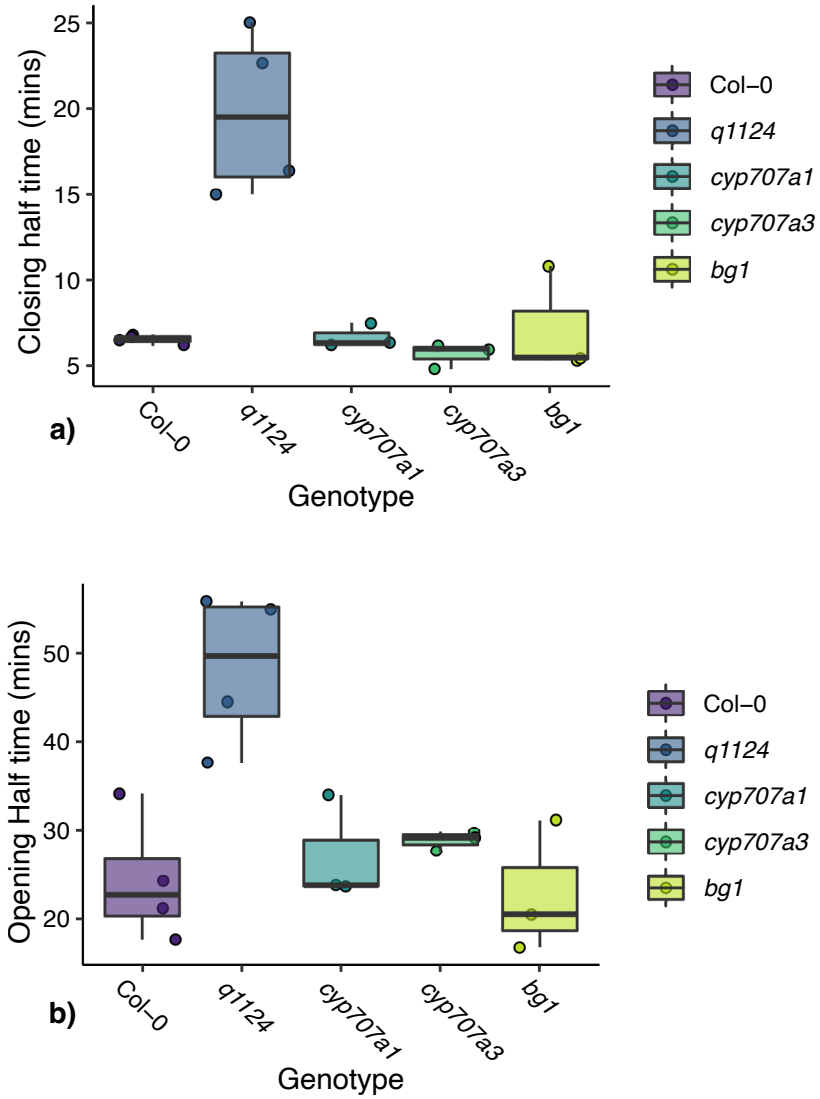

Figure 3.3 Stomatal conductance response half times to 120 mins darkness and 120 mins light

Stomatal conductance response half times of ABA signalling and metabolism mutants for **a)** 120 mins of darkness and **b)** 120 mins of light. Data is presented in boxplots showing the median and interquartile range (IQR). The whiskers represent data points within 1.5 * IQR. All data are shown as points on the plot. N =3-4 per genotype.

The transpiration and photosynthetic capacity were also analysed for the ABA signalling and metabolism mutants over the time-course (fig. 3.4 and 3.5 respectively). Transpiration rates closely follow the trend of stomatal conductance. Similarly to stomatal conductance in fig 3.2, *q1124* shows an altered transpiration response to darkness and light. The total amount of water lost during the dark (0 to 120 mins) and light (120 to 240 mins) is shown in fig. 4d. A 2-way ANOVA analysing the effect of treatment and genotype shows that both factors have a significant effect on waterloss (treatment – $F_{1,24} = 34.863$, $p < 0.0001$, genotype – $F_{4,24} = 8.898$, $p = 0.0001$).

Unlike stomatal conductance and transpiration, photosynthetic assimilation (A) does not appear to be largely affected by mutations within ABA signalling and metabolism components (fig. 3.5). However, it does show a rapid response, much faster than stomatal conductance and transpiration, to both dark and light treatment.

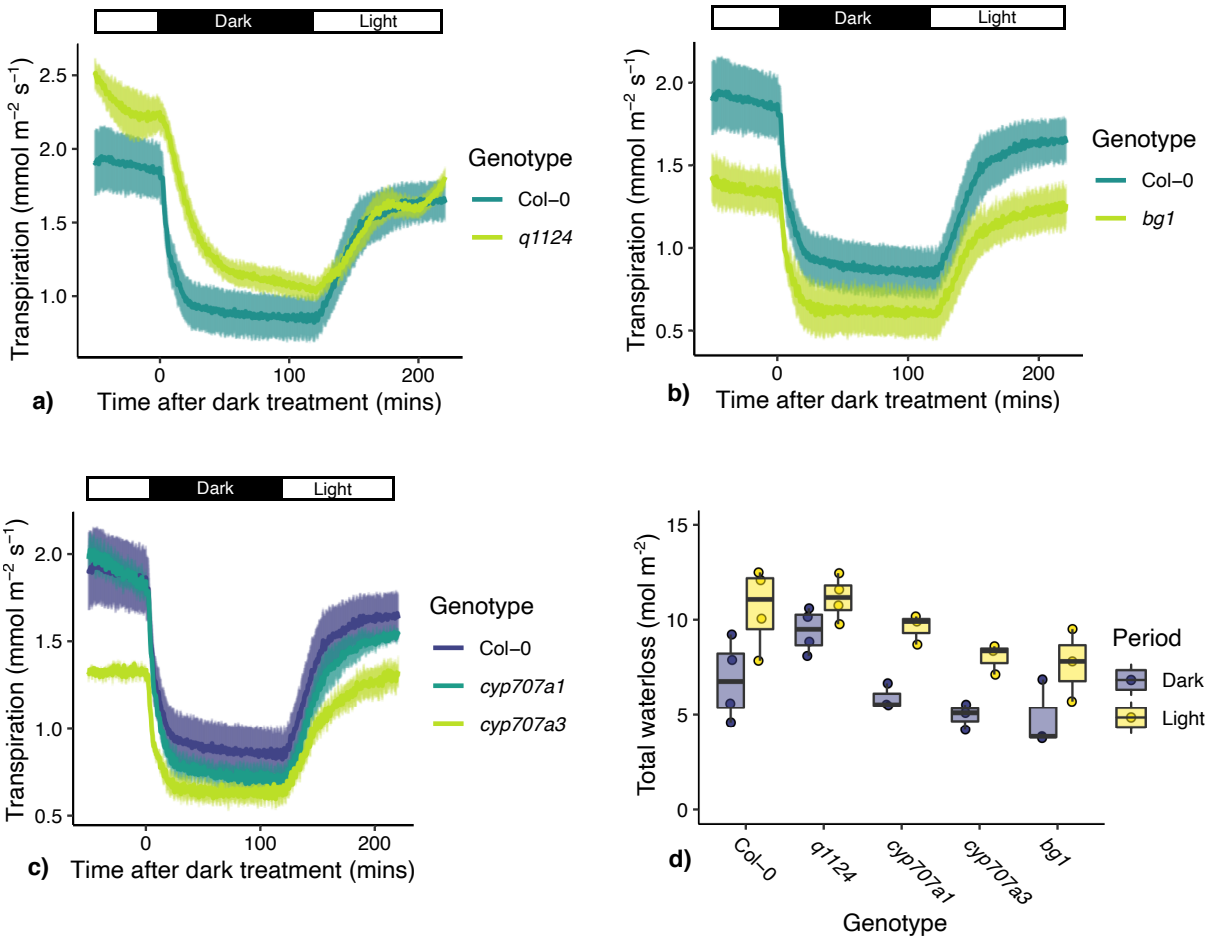

Figure 3.4 Transpiration responses to darkness for ABA signalling, activation, and degradation mutants

Transpiration rates in response to 120 mins darkness, followed by 120 mins of light for **a)** *q1124,* **b)** *bg1*, and **c)** *cyp707a1* and *cyp707a3*. The mean ± s.e.m. of transpiration is presented for each genotype. n = 3-4 for each genotype. **d)** Total waterloss via transpiration during the 120 mins of darkness and 120 mins of light for Col-0, *q1124*, *cyp707a1*, *cyp707a3*, and *bg1*. Data is presented in boxplots showing the median and interquartile range (IQR). The whiskers represent data points within 1.5 * IQR. All data are shown as points on the plot. Light treatment is represented above each transpiration plot, with black boxes representing darkness and white boxes representing light.

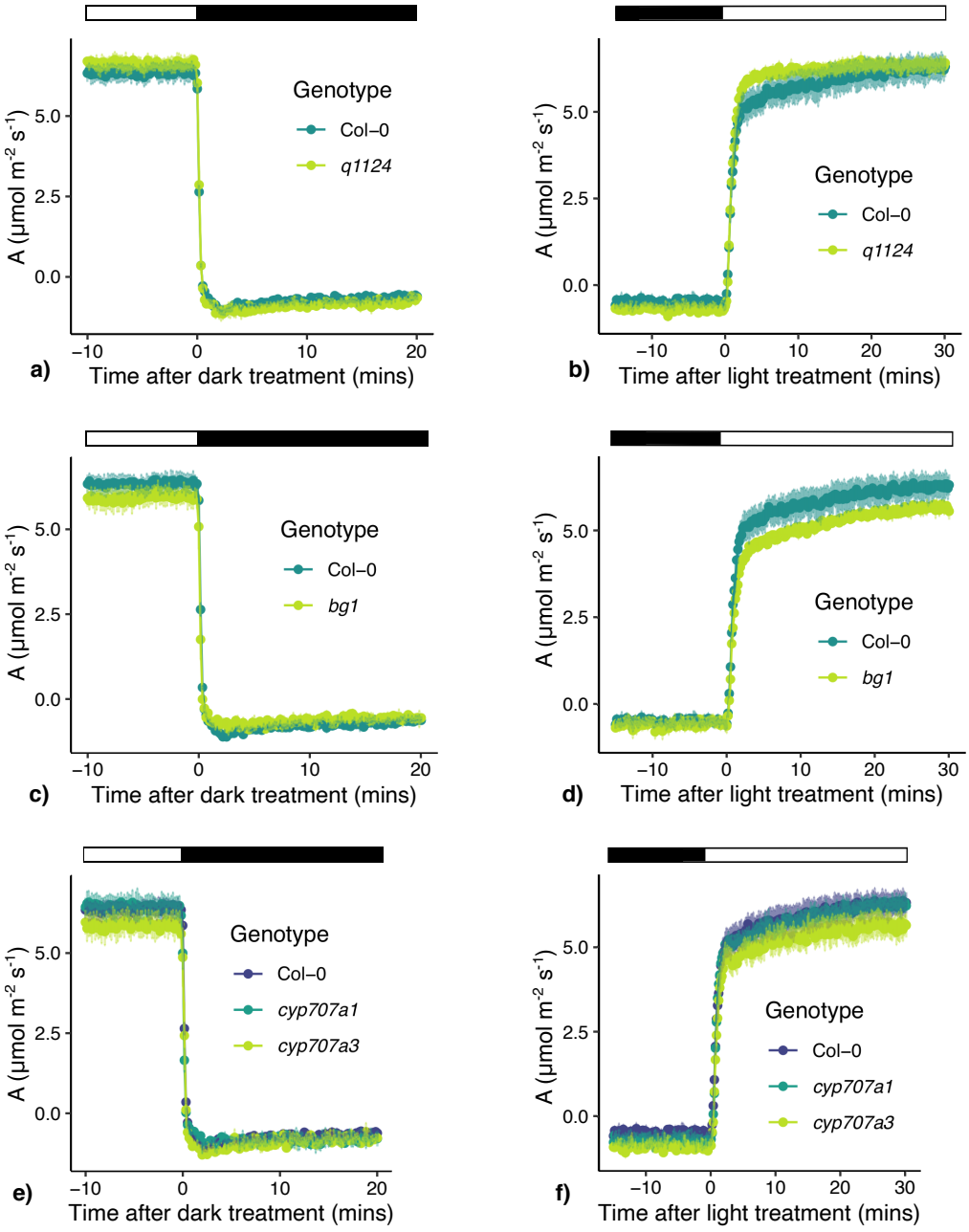

Figure 3.5 Photosynthetic assimilation rate responses to darkness for ABA signalling, activation, and degradation mutants

Photosynthetic assimilation rates (A) in response to **a)**, **c)**, **e)** 120 mins darkness (only the first 20 mins of the response is shown), followed by **b)**, **d)**, **f)** 120 mins light (only the first 30 mins of the response is shown). *q1124* is shown in **a)** and **b)**, *bg1* in **c)** and **d)**, *cyp707a1* and *cyp707a3* in **e)** and **f)**. Data is presented as mean photosynthetic assimilation rate ± s.e.m. . Light treatment is represented above each plot, with black boxes representing darkness and white boxes representing light.

3.3.3 Further analysis of *q1124* stomatal conductance responses to darkness

For Col-0 and *q1124*, the stomatal conductance responses were measured when whole plants were placed in darkness 4-5 hours after dawn. Leaves were clamped into the gas analyser leaf cuvette, 2 hours prior to the onset of darkness. After 1 hour of darkness plants were reintroduced to light for a further hour. *q1124* shows higher stomatal conductance (at time 0 – p = 0.0023) and stomatal conductance is reduced to a lesser extent than wild type in darkness. This is true in absolute (fig. 3.6a) and relative (fig. 3.6b) terms. The time taken for *q1124* to reach half of its total stomatal conductance response to darkness (darkness half response time - Fig. 3.6c) and to light (light half response time - Fig. 3.6d) shows greater variability when compared with Col-0. The *q1124* half response time to darkness is significantly increased ($F_{1,3.16}$ = 18.361, p = 0.021; Welch ANOVA), whereas the half response time to light is not ($F_{1,3.21}$ = 5.676, p =0.092; Welch ANOVA). Additionally, there do appear to be differences in the response of *q1124* to darkness when comparing Fig. 3.2a, b and Fig. 3.6a, b suggesting a degree of biological variation in the *q1124* dark response phenotype.

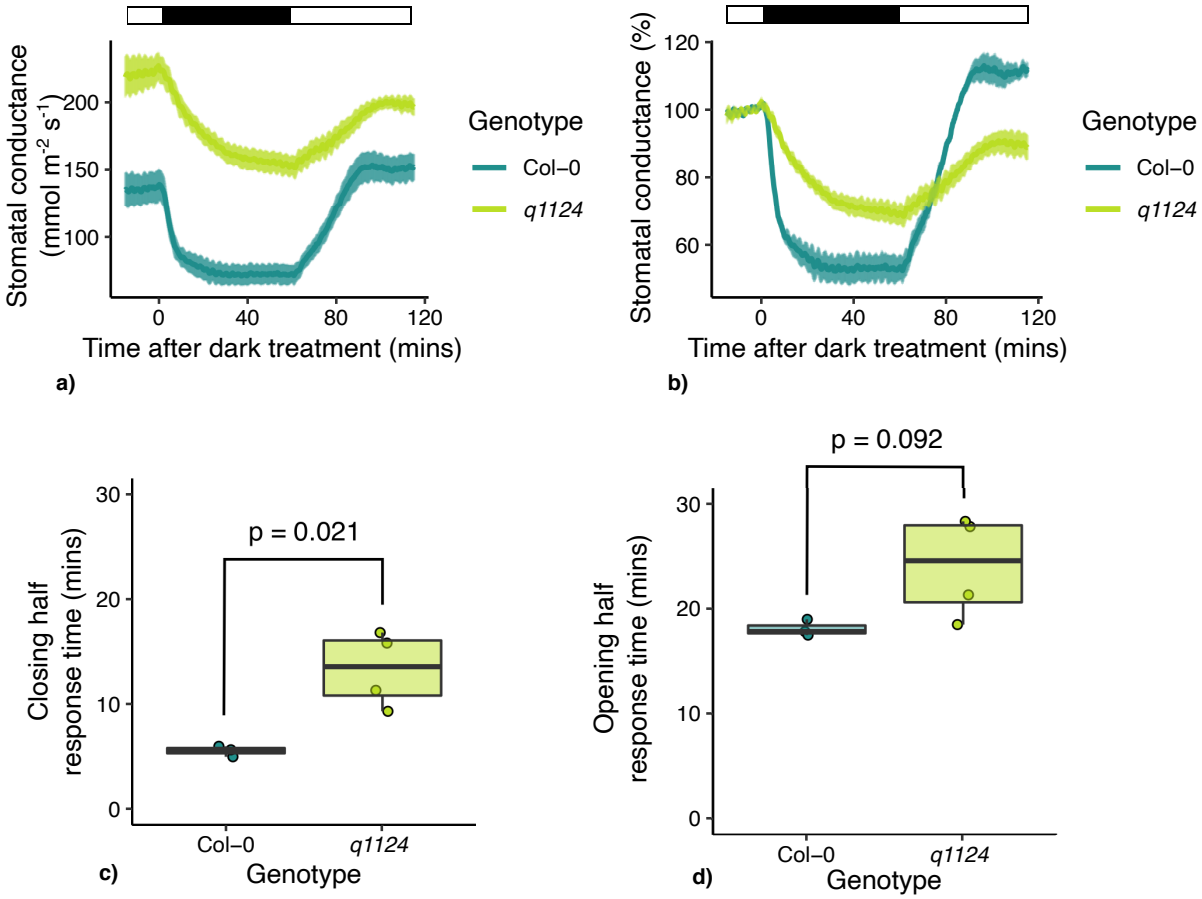

Figure 3.6 *q1124* stomatal conductance responses to immediate darkness at midday

Stomatal conductance of *q1124* ABA quadruple receptor mutant was measured in response to darkness applied 4-5 hours post dawn. **a)** Absolute and **b)** relative stomatal conductance values are presented as the mean ± s.e.m. The time taken to reach half of the maximum stomatal conductance change (half response times) in response to **c)** darkness and **d)** light are presented in boxplots showing the median and interquartile ranges. 3-4 plants measured per genotype. Light treatment is represented above each stomatal conductance plot, with black boxes representing darkness and white boxes representing light.

The stomatal conductance responses of Col-0 and *q1124* were also measured at dusk. Unlike the response to darkness at midday, where plants were suddenly plunged into darkness, the onset of dusk was marked with a 15 minute transition from light to dark. The absolute stomatal conductance of Col-0 and *q1124* is shown in fig. 3.7a. It is clear both genotypes respond to dusk but due to the difference in absolute stomatal conductance it is difficult to make comparisons. However, relative stomatal conductance (shown in fig. 3.7b) show the response of the *q1124* ABA quadruple receptor mutant is not as rapid as Col-0. The data in fig. 3.7b suggest that the speed of stomatal conductance change in the *q1124* ABA quadruple receptor mutant is reduced compared with Col-0. The difference between Col-0 and *q1124* is less pronounced than that observed in fig. 3.6, yet measurement of dusk half response times supports a slower stomatal conductance response of *q1124* to darkness ($F_{1,7} = 15.03$, $p = 0.00607$; 1-way ANOVA).

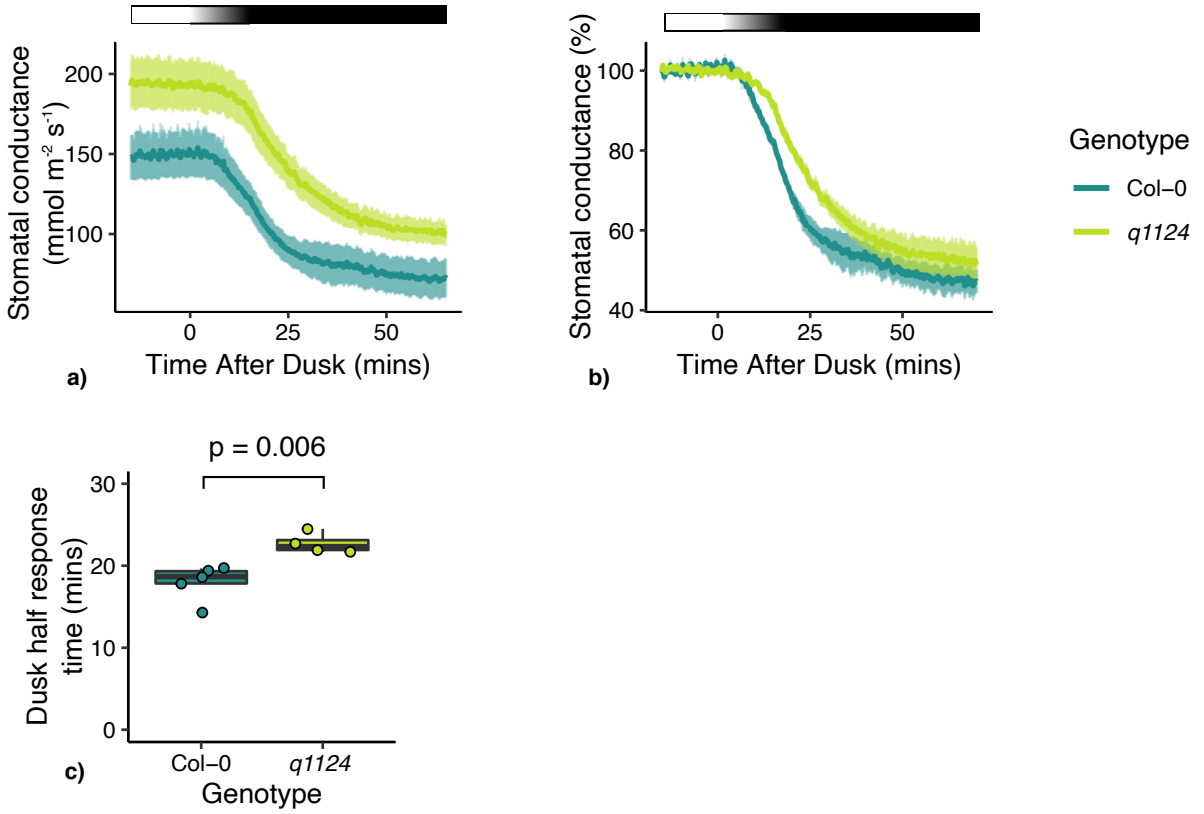

Figure 3.7 *q1124* stomatal conductance response at dusk

Stomatal conductance of the *q1124* quadruple ABA receptor over the dusk transition period. On the onset of dusk, the lights were dimmed over a 15 min period until completely turned off. **a)** absolute and **b)** relative stomatal conductance values are presented as the mean ± s.e.m. **c)** The time taken to reach half of the maximum stomatal conductance change (half response times) upon dusk are presented in boxplots showing the median and interquartile ranges. 4-5 plants measured per genotype. Light treatment is represented above each stomatal conductance plot, with black boxes representing darkness and white boxes representing light. A gradient represents the 15 minute transition from light to darkness.

3.3.4 The effect of mutations within ABA biosynthesis, signalling and activation upon stomatal responses to light

In addition to the delay in dark-induced stomatal closure and slower stomatal conductance responses observed in *q1124*, the data in Fig. 3.2 and Fig. 3.6 suggest that there might also be defects in the light-induced opening response of the quadruple receptor mutant. Stomatal conductance of *q1124* was measured over the dawn period. Here, similarly to dusk, the onset of dawn was marked with a 15 minute transition period from dark to light. Absolute and relative stomatal conductance values are presented in Fig. 3.8a and b respectively. Similar to the response observed at dusk, in comparison to wild type, the *q1124* mutant shows increased absolute stomatal conductance values and an increased half stomatal conductance response time, suggesting this response also occurs at a slower rate (Fig. 3.7c) ($F_{1,7} = 47.1$, $p = 0.000239$; 1-way ANOVA).

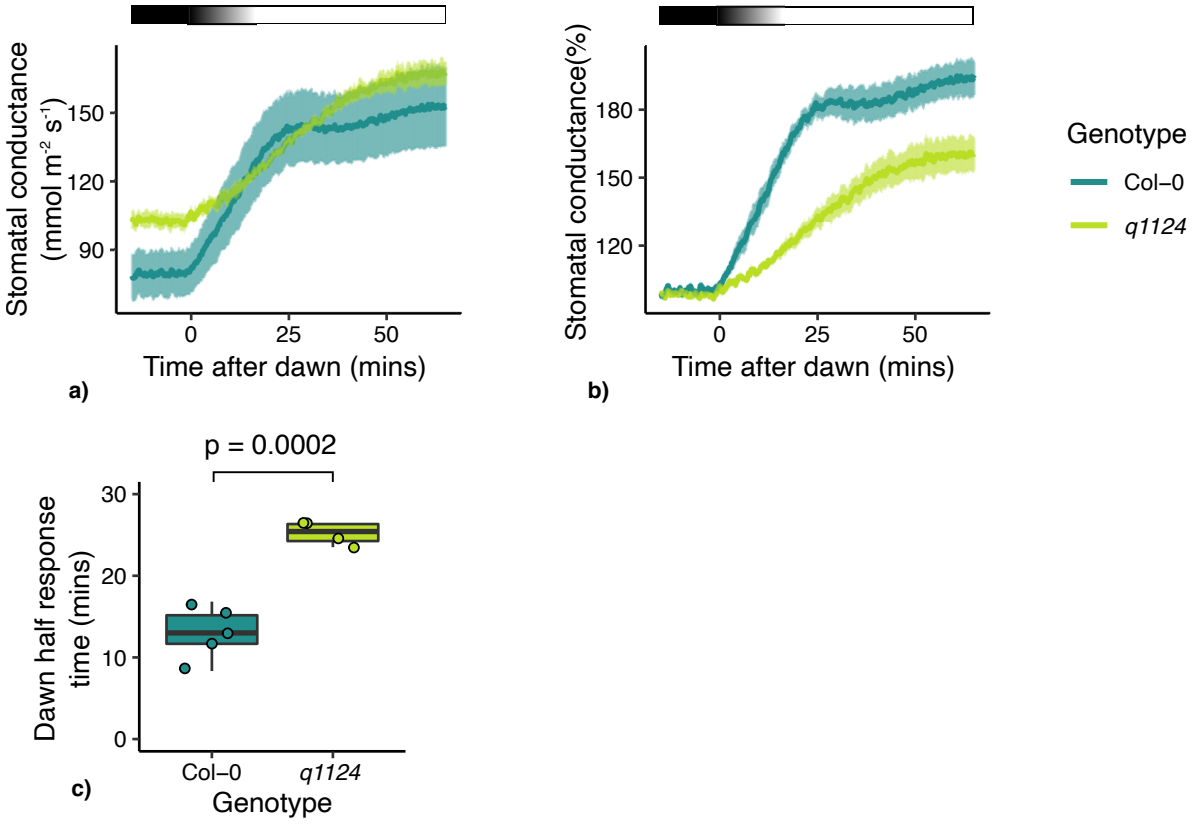

Figure 3.8 *q1124* stomatal conductance responses at dawn

Stomatal conductance of the *q1124* quadruple ABA receptor over the dawn transition period. On the onset of dawn, the lights were turned on over a 15 min period until reaching full brightness. **a)** absolute and **b)** relative stomatal conductance values are presented as the mean ± s.e.m. **c)** The time taken to reach half of the maximum stomatal conductance change (half response times) upon dusk are presented in boxplots showing the median and interquartile ranges. 4-5 plants measured per genotype. Light treatment is represented above each plot, with black boxes representing darkness and white boxes representing light. A gradient represents the 15 minute transition from darkness to light.

The stomatal movements of *q1124*, *nced3/5* and *bg1* mutants were also analysed in leaf discs. Here, leaf discs were harvested pre-dawn under green light, incubated in the dark for two hours, before being transferred to light. The apertures were monitored over a two hour time course. Fig. 3.9 shows both the absolute and absolute change in stomatal aperture for the three mutants. It is evident that both *q1124* and *nced3/5* have significantly increased stomatal apertures at 0 mins ($p < 0.0001$, $p < 0.0001$ respectively, TukeyHSD), whereas *bg1* is similar to Col-0. This makes comparisons between the absolute stomatal apertures of Col-0, *q1124* and *nced3/5* more difficult to interpret. However, when analysing the absolute change in stomatal aperture for both *q1124* and *nced3/5* there are no initial significant differences at 30 mins, but by 120 mins there are significantly smaller responses ($p < 0.005$, $p < 0.0001$ respectively, TukeyHSD).

Unlike *q1124* and *nced3/5*, the *bg1* mutant shows a response analogous to that observed when plants are placed in darkness (except instead of an initial delay in dark induced stomatal closure, here a delay in light induced stomatal opening is observed). *bg1* shows a significantly weakened response at 30 mins ($p < 0.0005$, TukeyHSD), before the *bg1* mutant eventually catches up by 60 and 120 mins.

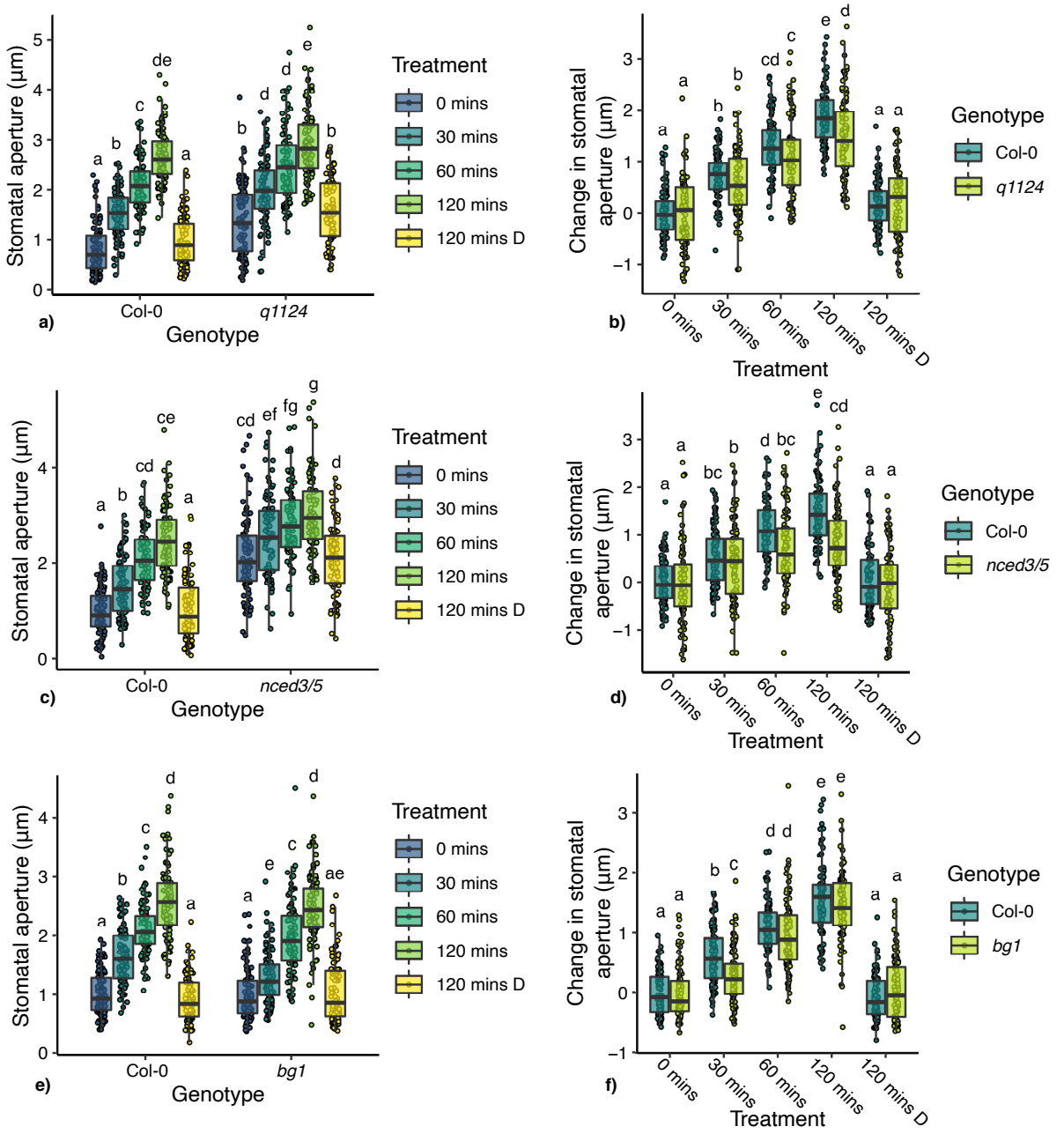

Figure 3.9 ABA biosynthesis and signalling mutants show aberrant response to light

a), **c)**, and **e)** show absolute stomatal apertures and **b)**, **d)**, and **f)** show change in stomatal aperture for *q1124*, *nced 3/5*, and *bg1* respectively. Leaf discs were harvested under green light before dawn and incubated in darkness for 2 hours. Treatment times refer to time in light (other than 120 mins D - which refers to 120 mins in darkness). Each bar represents mean ± se from 90 apertures over 3 independent experiments. Data statistically analysed using 2-way ANOVA with Tukey multiple comparison tests, samples indicated with the same letter cannot be distinguished at $p < 0.05$.

3.3.5 The *nced3/5* ABA biosynthesis mutant shows rapid stomatal responses to ABA

The stomatal response of the *nced3/5* ABA biosynthesis mutant to ABA was analysed to determine whether there were situations in which the stomatal aperture of the mutant could change rapidly. In fig. 3.10, *nced3/5* shows a rapid response to 10 μM ABA, showing a significant change in aperture over a period of 10 mins. This provides support that the dark-induced closure delays observed in *nced3/5* leaf disc responses are not found in response to all stomatal movement inducing signals. This supports the notion that the dark-induced closure delays observed in *nced3/5* are more likely due to defects within molecular signalling rather than mechanical or structural defects, as mutants previously shown to exhibit mechanical defects are generally defective to multiple stomatal movement inducing signals [68,229]. However, it cannot be ruled out that there are mechanical or structural defects within *nced3/5* stomata, and that darkness and ABA induced closure utilise different components that produce different mechanicals strains on the stomatal closure machinery, or that due to the defect within *de novo* ABA biosynthesis *nced3/5* stomata are particularly sensitive to ABA signals.

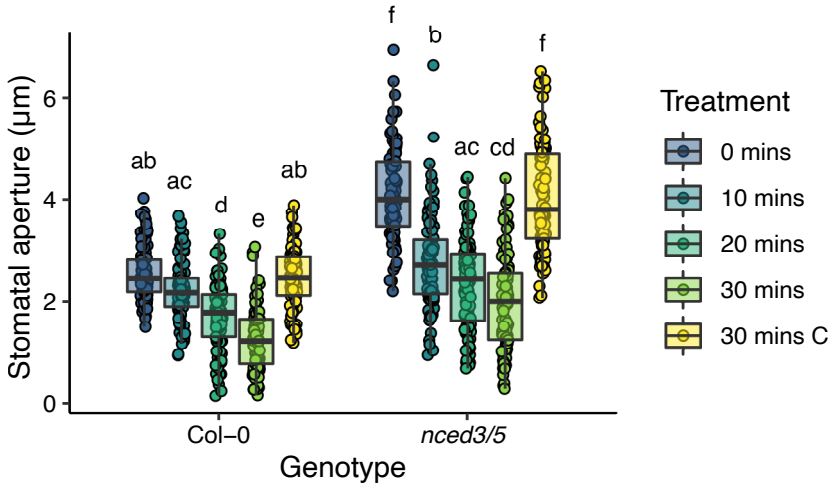

Figure 3.10 *nced3/5* stomata respond rapidly to ABA treatment

Leaf discs harvested from Col-0 and *nced3/5* were incubated in white light for 2 hours before treatment with 10 µM ABA. Stomatal apertures were measured over a 30 min timecourse. A no ABA control was measured after 30 mins (30 mins C). Both genotypes respond rapidly to ABA treatment. Each violin plot represents the spread of data for 90 stomatal apertures (10 per individual plant). The median is shown by a horizontal line. Three independent repeats were carried out and pooled for analysis. Data statistically analysed using 2-way ANOVA with Tukey multiple comparison tests, samples indicated with the same letter cannot be distinguished at $p < 0.05$.

3.3.6 There are no differences in the steady state transcript levels of photoreceptors in ABA biosynthesis and signalling mutants

The cryptochrome, phototropin, and phytochrome photoreceptors have all been shown to play roles in regulating stomatal aperture in response various light treatments [155,156,161]. Although none have been linked to defects in dark induced closure, it was thought altered photoreceptor activities may lead to delays in responses to dark and light treatment. In order to explore whether photoreceptor activities are altered in ABA signalling and metabolism mutants, the transcript levels of phytochrome (*PHYA*, *PHYB*), cryptochrome (*CRY1,* CRY2) and phototropin (*PHOT1*, *PHOT2*) photoreceptors were analysed. Analysis of transcript levels was performed on leaf tissue sampled midday from 5-week old plants. Fig. 3.11 shows for all 6 photoreceptors tested, no significant differences were found in *q1124*, *s112458*, or *bg1* mutants. This suggests that observed delayed stomatal responses are not due to altered photoreceptor transcript levels. However, this doesn't rule out differences in photoreceptor post-transcriptional regulation in ABA signalling and biosynthesis mutants.

Additionally, the transcript levels of two key components of the ABA signalling pathway, OST1 and SLAC1, were analysed in the *nced3/5* double mutant to investigate whether altered levels of *OST1* or *SLAC1* would lead to changes in stomatal dynamics. However, similarly to that observed for the photoreceptor transcripts, no significant differences in transcript abundance were observed (Fig. 3.12).

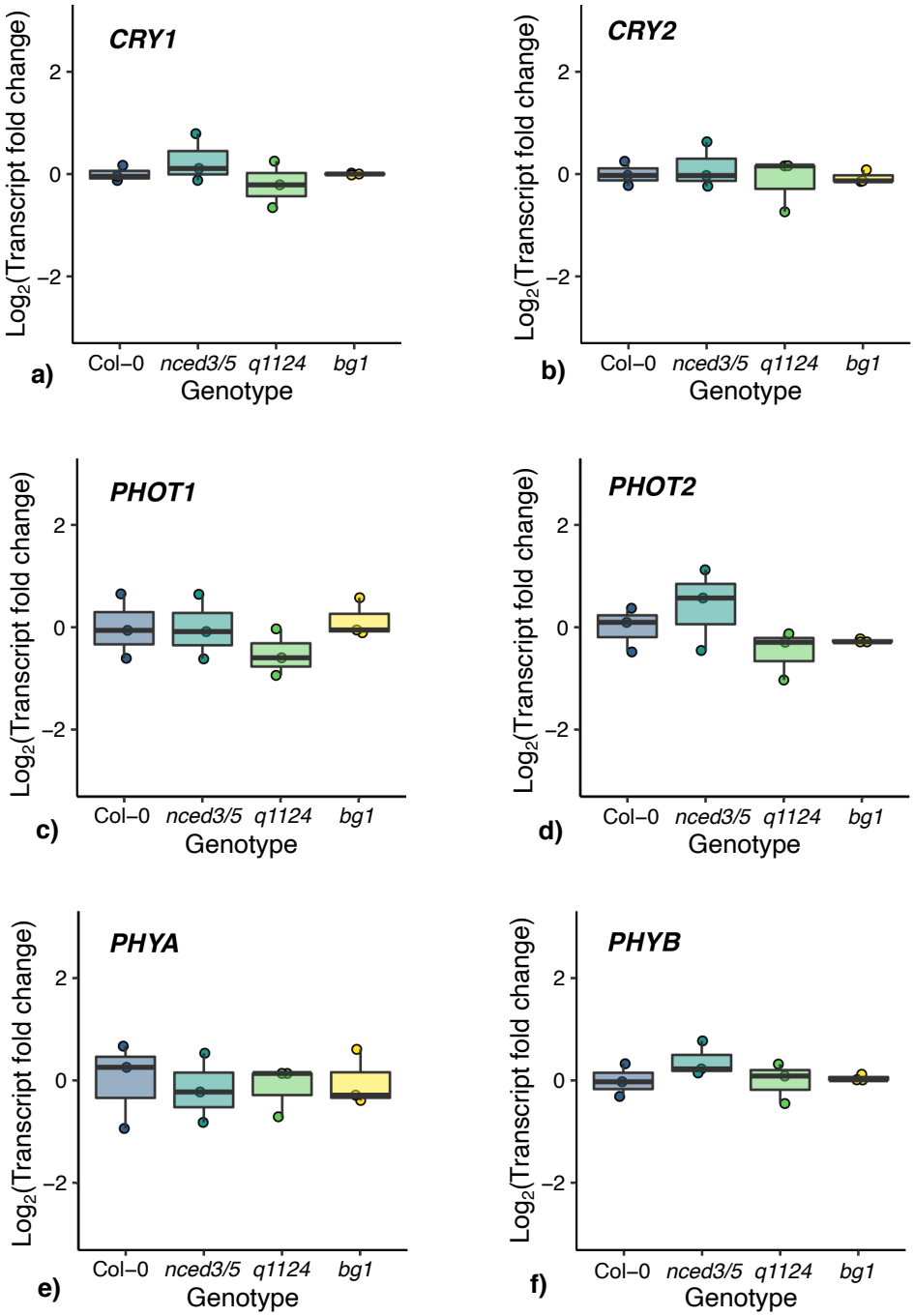

Figure 3.11 Photoreceptor transcript levels in ABA biosynthesis and signalling mutants

Relative transcript abundance of photoreceptors **a)** *CRY1,* **b)** *CRY2*, **c)** *PHOT1*, **d)** *PHOT2*, **e)** *PHYA*, and **f)** *PHYB* in Col-0, *nced3/5, q1124,* and *bg1*. Leaf tissue was harvested at midday. Relative transcript abundances were determined using the ΔΔCt with *EF1a* and *PP2A* as reference genes. 3 samples were analysed per genotype.

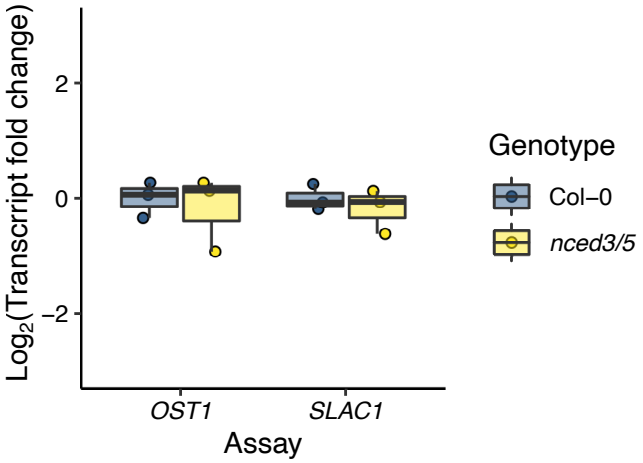

Figure 3.12 *OST1* and *SLAC1* transcript abundances in the *nced3/5* mutant

Relative transcript abundance of *OST1* and *SLAC1* in Col-0 and *nced3/5*. Leaf tissue was harvested at midday. Relative transcript abundances were determined using the ΔΔCt with *PP2A* as a reference gene. 3 samples were analysed per genotype.

3.3.7 Darkness may lead to increased levels of OST1 near/on the guard cell plasma membrane

A stable Arabidopsis line expressing *OST1-GFP* (one of the key ABA signalling pathway SnRK2 kinases, OST1 [230]) under the native *OST1* promoter (*pOST1::OST1-GFP*), described previously [137], was used to analyse OST1 protein dynamics. As this transgenic line is a complemented *ost1-3* mutant, before analysis of protein dynamics, the stomatal aperture in response to darkness was analysed and compared with Col-0 (Fig. 3.13a). A 2-way ANOVA suggests both dark treatment ($F_{4,890} = 186.083$, $p < 0.0001$) and genotype ($F_{1,890} = 28.524$, $p < 0.0001$) have significant effects on stomatal aperture. Post hoc Tukey multiple comparison tests show the *pOST1::OST1-GFP* line shows no visible delays in dark induced closure within the first hour of treatment. At 120 mins dark and light treatment *pOST1::OST1-GFP* the stomata were slightly but significantly more open. However, as these differences were slight and the initial closing response was similar to Col-0, protein dynamics were analysed in this reporter line.

The levels of OST1-GFP in guard cells was measured using leaf discs. Leaf discs were harvested midday, incubated under light for 2 hours before being transferred to darkness, 10 μM ABA, or left under light. After two further hours the intensity of GFP fluorescence was measured using a confocal microscope. Intensity was measured over stomatal cross sections either bisecting two guard cell nuclei or avoiding them. Max intensity was recorded at the plasma membrane and at the perinuclear region. Fig. 3.13b, c and d show the distribution of intensity results for the different treatments. The results suggest there are no significant differences in the intensities at the perinuclear region and membrane region. However, analysis of the guard cell ratio of perinuclear/membrane intensity shows there is a significant effect of treatment (chi squared = 8.17, df = 2, p = 0.017; Kruskal Wallis test). Multiple comparison testing shows in dark treatment shows the ratio is significantly reduced when comparing dark to light treatment (p = 0.041; Dunn multiple comparison test). This suggests in darkness OST1 has an increased presence at the membrane relative to the perinuclear region. However, this reduction is slight and further repeats are required to verify this result.

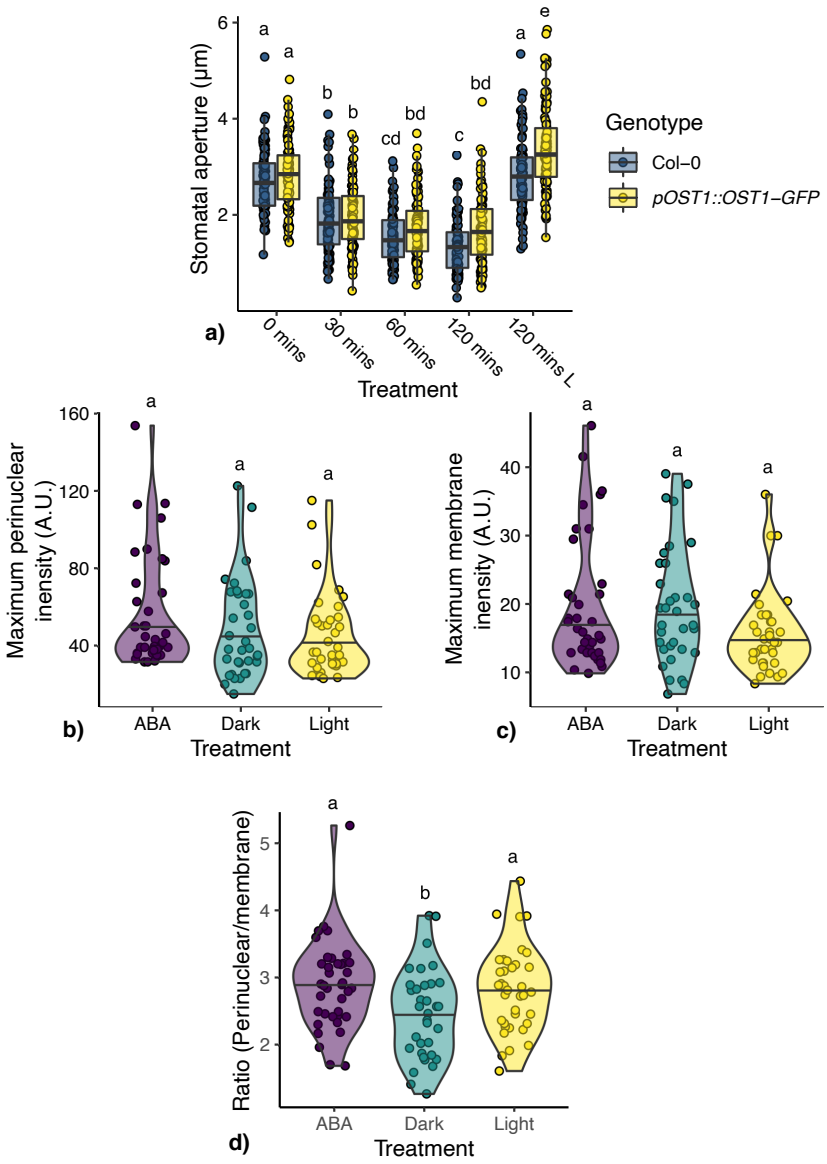

Figure 3.13 The response of *pOST1::OST1-GFP* to darkness

a) Stomatal response to darkness applied midday. Leaf discs were transferred from 120 µmol m^{-2} s^{-1} light to darkness, and the stomatal apertures were tracked over a 120 min time course. Each boxplot represents the median and interquartile range (IQR). Whiskers represent data within 1.5 * IQR. All data are represented as points on the plot. n = 80-90 stomatal apertures (10 per individual plant) from 8-9 individual plants over 3 independent experiments. Data was statistically analysed using 2-way ANOVA and TukeyHSD multiple comparison test. **b)** and **c)** show maximum fluorescence intensity at the perinuclear region and plasma membrane region of guard cells from *pOST1::OST1-GFP* leaf discs treated with light, darkness, or 10 µM ABA. **d)** shows the ratio of perinuclear/plasma membrane fluorescence intensity. Each violin plot represents the spread of data for 34-38 measurements (10 – 15 per individual plant) from 3 individual plants per treatment. The median is shown by a horizontal line. Data was statistically analysed using Kruskal-Wallis test followed by Dunn multiple comparison test. Samples indicated with the same letter cannot be distinguished at $p < 0.05$.

3.4 Discussion

ABA is well known as a regulator of seed dormancy and plant responses to drought including reductions in stomatal aperture and inhibition of light-induced opening [231]. Additionally, evidence is emerging supporting roles for basal ABA signalling under non-stress situations [232]. On a molecular level, a subset of ABA receptor family members (subfamily 1) are known to activate downstream signalling under basal amounts of ABA [233] and mutation of ABA signalling and metabolism components alters plant growth and development under non stress conditions [234,235]. Here we explore the role of ABA and ABA signalling in stomatal responses to the onset of light and darkness.

The mechanisms behind light-induced stomatal opening are relatively well understood. Stomatal opening in response to light is driven by the activity of plasma membrane H^+ATPases. This generates a proton gradient across the guard cell plasma membranes, resulting in membrane hyperpolarization leading to the influx of cations and anions, changes in guard cell turgor pressure, and ultimately the opening of stomata. Blue and red light promote stomatal opening via independent pathways. Blue light-induced opening is predominantly initiated via activation of phototropin photoreceptors within the guard cell [236], whereas red light-induced opening is dependent on photosynthetic electron transport [165,237]. When Arabidopsis plants are moved from light to dark their stomata close, however, the mechanisms behind dark-induced stomatal closure are less clear [238]. Studies have linked ABA signalling to dark-induced closure, but it is unclear to what extent ABA signalling is required for this process [149,180,214,224,239].

3.4.1 ABA signalling and metabolism mutants showed delayed responses to darkness in leaf discs

Here, evidence is presented that supports a non-central role for ABA metabolism and ABA signalling in dark-induced stomatal closure. In leaf discs we observe that all ABA signalling, and metabolism mutants analysed were able to respond to darkness (Fig. 3.1). Compared with wild type, ABA receptor mutants (*q1124* and *s112458*) and the ABA biosynthesis mutant (*nced3/5*) showed increased stomatal apertures before treatment whereas ABA degradation mutants (*cyp707a1* and *cyp707a3*) showed decreased stomatal apertures. This is in line with previous reports, namely that, defects in ABA signalling and production lead to increases in steady state

stomatal apertures and transpiration, whereas defects in ABA degradation lead to the opposite [214,216,217,228]. This shows links between ABA, ABA signalling and the regulation of stomatal apertures under non stress conditions. However, following dark treatment *cyp707a1* and *cyp707a3* mutants close to the same extent as wild type. On the other hand, the stomata of *q1124, s112458,* and *nced3/5* mutants all remain more open than wild type. These results are similar to those observed for stomatal conductance in ABA receptor mutants (*q1124/pyr1pyl1pyl2pyl4, pyr1pyl4pyl5pyl8, pyr1pyl2pyl4pyl5pyl8*) in Merilo *et al* 2013 with one exception. Whereas Merilo *et al* 2013 report no response to darkness, here we report that the stomata of *s112458* mutant are still able to respond to darkness, but to a lesser extent than wild type. The strong ABA biosynthesis mutant *nced3/5* also behaves similarly to the *aba1-1* and *aba3-1* biosynthesis mutants in Merilo *et a*l 2013. *nced3/5* shows significantly more open stomata throughout the experiment and responds to darkness, although to a lesser extent than wild type. Additionally, we report ABA signalling (*q1124* and *s112458*) and biosynthesis mutants (*nced3/5* and *bg1*) show a delay in closure, with no significant change in stomatal aperture following 30 mins of dark treatment, when measured in leaf discs. In Merilo *et al* 2013, T-DNA insertion mutants in the downstream ABA signalling component OST1 (*ost1-3*) and the ion channel SLAC1 (*slac1-3*) show similar dark-induced transpiration changes to those of ABA biosynthesis mutants (*aba1-1* and *aba3-1*), where stomatal conductances are increased but still show responses to darkness. This suggests a non-central role for ABA and ABA signalling in dark-induced closure.

3.4.2 Dark-induced stomatal conductance responses are altered in *q1124*

Exploring this further it was found that the time taken for the *q1124* mutant to reach its maximum stomatal conductance response is increased compared to Col-0 (fig. 3.2, 3.3, 3.6, 3.7). This is observed when darkness and light are applied during the middle of the day and also at the dawn and dusk transition periods. This suggests that although ABA signalling is not essential for dark-induced closure, it appears to be involved in increasing the speed of stomatal responses to darkness and light. It should be noted there is a difference between the time taken for stomatal apertures to show maximum responses (fig. 3.1) and stomatal conductance responses to reach their maximum (Fig 3.2, 3.6, 3.7), with stomatal movement on leaf discs appearing slower than that of changes in conductance. The reasons for this are unclear but likely due to differences between the systems of a leaf disc and an attached leaf. Regardless, manipulating the speed of stomatal responses has been shown to increase biomass accumulation [240] and may improve key

plant processes such as photosynthetic carbon assimilation and water use efficiency [241], suggesting it could be a key target for plant breeders. How defects within ABA metabolism and signalling are affecting the speed of stomatal responses is currently unclear but may stem from altered amounts or activities of further signalling components and/or ion channels within plant cells. Additionally, exogenous ABA application has been reported to alter stomatal kinetic responses to changes in light conditions in gymnosperms, suggesting roles for ABA in modulating stomatal kinetics across taxa [242].

3.4.3 *nced3/5* mutants can respond rapidly to ABA treatment

Recently more attention has been given to the mechanical processes behind stomatal movements [66]. Mutations within genes affecting cell wall structure, such as the pectinase *PGX3*, and the pectin methylesterase *PME6*, have been shown to affect the speeds of stomatal movement [68,229]. As delays were observed in ABA signalling and biosynthesis mutants to both darkness and light, the response to a further signal, ABA, was investigated in *nced3/5* to assess whether there were situations in which the stomata could respond rapidly. Here, *nced3/5* displayed very fast changes in stomatal aperture in response to ABA (fig. 3.10). Although this doesn't definitively address whether the defective stomatal movements in response to light and dark are due to structural/mechanical cell wall defects, it does provide evidence that shows the mutant possesses the ability to change its stomatal aperture very fast and may suggest it is more likely the delayed movements observed in ABA signalling and metabolism mutants stem from defective signalling. However, it is not possible to rule out the prospect that darkness and light act on different structural components and may induce mechanical stresses that act on different components, or the possibility that due to ABA synthesis *nced3/5* stomata are hypersensitive to ABA.

3.4.4 Photoreceptor transcript levels are not altered in a selection of ABA signalling and metabolism mutants

It was hypothesised that delayed responses to light could be caused by decreased levels or activity of photoreceptors. The phytochrome, cryptochrome, and phototropin photoreceptors have all been linked to regulating stomatal movements in response to light [155,156,161]. Additionally, crosstalk between the phytochrome and ABA signalling pathway has been observed in seedling

germination and hypocotyl elongation, often via interactions of ABA signalling components with PIFs (phytochrome interacting factors) [243–246]. Therefore the transcript levels of a these photoreceptors were analysed in *q1124, nced3/5,* and *bg1*. Here, no differences were observed in transcript levels (fig. 3.11), suggesting that at least on a transcriptional level, photoreceptor dynamics were not drastically altered. However, it is unknown whether the activity of the photoreceptors had been changed. Additionally, the levels or activity of downstream components of photoreceptor signalling pathways may be altered in ABA signalling and metabolism mutants.

3.4.5 Are the delays in stomatal movements due to post-transcriptional regulation of ABA signalling components?

Similarly to the photoreceptor transcripts, the transcript abundances of *OST1* (a key kinase in the ABA signalling pathway) and *SLAC1* (a key anion channel involved in stomatal closure) are not affected by the *nced3/5* mutation (fig. 3.12). As no alterations in the abundances of photoreceptors or key downstream components of ABA signalling had been observed thus far on a transcriptional level, an OST1-GFP fusion protein under the control of its native promoter [137] was obtained in order to investigate potential post-transcriptional regulation of OST1. Previously, intracellular localisation of specific ABA signalling components has been shown to be a point of regulation, such as membrane nano-domains containing the ABA activated CIPK21 kinase and its target ion channel SLAH3 [247], and the ALIX mediated trafficking of active ABA receptors on the membrane to the vacuole for degradation [248]. Here, the intensity of OST1-GFP fluorescence at the plasma membrane and perinuclear regions of guard cells was measured in plants in response to 2 hours ABA, dark, and light treatment (fig. 3.13). A slight decrease in the perinuclear/membrane ratio of OST1-GFP was observed in dark treatment suggesting there may be trafficking of OST1 to the membrane or degradation of perinuclear localised OST1 in response to darkness. However, further experiments would be needed to confirm this. Additionally, the OST1-GFP reporter would need to be introduced into various ABA signalling and biosynthesis mutants to investigate whether OST1 protein localisation is altered in these mutants.

3.5 Conclusion

The results presented in this chapter, using ABA signalling and metabolism mutants show that stomatal conductance and stomatal apertures decrease in response to darkness. The differences between the mutants and the wild type were reflected in the slower rates of closure and stomatal conductance changes found in the mutants. While these results do not support a primary role for ABA in the events underlying dark-induced stomatal closure, the data in this chapter does support a role for ABA in modulating the speed of reaction. This highlights the role of ABA in regulating stomatal aperture/transpiration under non-stress conditions. Investigating potential causes of the altered stomatal response speed, no evidence was found for differences in transcriptional regulation of photoreceptors and key ABA signalling components.

3.6 Note

Data from this chapter has been published as

Pridgeon, A. J. & Hetherington. A. M. ABA signalling and metabolism are not essential for dark-induced stomatal closure but affect response speed. *Sci. Rep.* **11,** 5751 (2021).

A copy of the paper is presented in the appendix.

CHAPTER 4: EFFECT OF DARKNESS ON ABA SIGNALLING AND METABOLISM TRANSCRIPTION DYNAMICS

4.1 Introduction

As plants generate their energy via photosynthesis, altering their physiological and developmental processes to best suit the light quality and quantity of their environment is paramount to their survival. Throughout the majority of a plant's life cycle, it will most commonly experience darkness (or the absence of light) during the night-time. Due to the predictable nature of day and night conditions (eg length, light, temperature) plants have evolved complex circadian rhythm machinery to anticipate day/night and regulate many physiological and developmental processes [249]. However, such as in the case of hypocotyl growth, where darkness promotes hypocotyl growth and circadian regulation restricts this promotion to the night period [250], the existence of circadian regulation does not remove a role for environmental light conditions (as well as endogenous circadian rhythms) in the regulation of physiological and developmental processes [251].

Light acts as a regulator for many processes throughout the life cycle of a plant, including germination, hypocotyl growth, phototropism, stomatal movements, stomatal development, and

flowering times [252]. Often plant responses to darkness are presented as passive responses to lack of photoreceptor activation. However, some claim that although darkness may not activate photoreceptors the fact that photoreceptor signalling leads to the activation and inhibition of downstream components suggests that in both active and inactive states photoreceptors transmit information, and therefore darkness should be considered a signal in its own right [251].

One rapid physiological response to darkness is dark-induced stomatal closure (see previous chapter). There has been debate as to whether dark induced stomatal closure is an active response (activating closure machinery) or a passive response to the absence of light induced stomatal opening [180]. Recently with the finding that GHR1 [115] and a MEK1/MPK6 signalling cascade [182] are required for dark induced closure, the support for an active stomatal response to darkness is growing. However, in addition to the rapid triggering of stomatal closure, a recent study looking at the functional specificity of ABA receptor proteins, found that in guard cell enriched RNA samples dark treatment significantly affected the transcript abundance of core parts of the ABA signalling machinery [149], suggesting that as well as the rapidly induced stomatal closure darkness may be affecting ABA signalling on a longer term scale as well.

Links have been found between ABA signalling and light/dark signalling previously in both seed germination [243–245,253] and hypocotyl elongation [246,254]. In both of these cases PIFs appear to be a point of connection between ABA signalling and light (phytochrome) signalling. Here, both PIF-mediated regulation of ABA signalling and metabolism components and ABA signalling mediated regulation of PIF expression have been observed. Interestingly, in seedlings the PYL8 and PYL9 ABA receptors were shown to interact with certain PIFs to mediate PIF upregulation of ABI5 (a key transcription factor within the ABA signalling pathway) expression in the dark [246]. Taken together these suggest a complex interaction between ABA and light signalling.

Similar to germination and hypocotyl development, light and ABA have both been found to play roles in the regulation of stomatal development. Increasing light intensity has been shown to promote stomatal development through phytochrome and cryptochrome signalling [205,255,256], whereas ABA signalling inhibits the entry of cells in to the stomatal lineage and inhibits the expansion of pavement cells [209]. Additionally ABA has also been linked to mediating stomatal development responses to CO2, where Arabidopsis reduces stomatal density under high CO2

conditions in an ABA signalling dependent manner [90]. The opposing roles of light and ABA signalling in stomatal development have been highlighted in the fact that the addition of *phyB* mutations into a *bg1* (ABA activation enzyme) mutant can rescue the increased stomatal density phenotype of *bg1* [211].

This chapter focuses on dark induced changes in the transcription of ABA signalling and metabolism genes. A specific subset of ABA receptors are found to be upregulated under dark conditions. Focusing on the upregulation of the *PYL5* receptor, it was found that defects within ABA signalling and metabolism increase receptor transcript abundance under light conditions, while under dark conditions the receptor transcript abundance remains the same as wild type. This suggests a role for ABA signalling in maintaining low levels of ABA receptors under light conditions which is lifted upon dark treatment. Physiological relevance for dark induced ABA receptor upregulation is explored with respect to stomatal development using a number of ABA signalling and metabolism mutants shown in table 4.1.

Mutant name	Genes affected	Function
q1124	*pyr1, pyl1, pyl2, pyl4*	ABA receptor mutant
s112458	*pyr1, pyl1, pyl2, pyl4, pyl,5, pyl8*	ABA receptor mutant
nced3/5	*nced3, nced5*	ABA biosynthesis mutant
cyp707a1	*cyp707a1*	ABA degradation mutant
cyp707a3	*cyp707a3*	ABA degradation mutant
bglu18-1	*bg1*	ABA activation mutant

Table 4.1 List of ABA signalling and metabolism mutants used in Chapter 4

A list of the ABA signalling and metabolism mutants used in this chapter with a brief description of the genes affected and the gene function.

4.2 Specific Methods

4.2.1 Diurnal microarray expression data growth conditions

Plant growth conditions and sampling time are shown in table 4.2. Information was gathered from http://diurnal.mocklerlab.org/. The LL_LDHC and LL23_LDHH samples were moved to continuous light following growth at 12/12 hour light/dark (L/D) cycles when sampling began. The LL12_LDHH sample was moved to continuous light for 2 days after growth at 12/12 hour L/D cycles. After 2 days in constant light conditions sampling began.

Sample name	Ecotype	Plant age (days)	Media	Tissue	Light conc. (μmol m^{-2} s^{-1})	Day length (L/D hours)	Temp. (˚C)	Ref.
COL_LDHH	Col-0	7	Agar 3% sucrose	Seedling	120	12/12	22	[257]
COL_SD	Col-0	7	Agar	Seedling	100	8/16	22	[258]
LDHH_SM	Col-0	29	Soil	Leaf	180	12/12	20	[259]
LDHH_ST	Col-0	35	Soil	Leaf	130	12/12	22	[260]
LL_LDHC	Col-0	7	Agar	Seedling	100	12/12	22	[258]
LL12_LDHH	Col-1	7	Agar 3% sucrose	Seedling	60	12/12	22	[261]
LL23_LDHH	Col-0	7	Agar 3% sucrose	Seedling	60	12/12	22	[262]

Table 4.2 Diurnal growth conditions

The growth conditions and experimental details for the microarray datasets analysed in this study from the diurnal expression tool dataset are described in the above table. Further information can be found either at http://diurnal.mocklerlab.org/ or in the references for each study.

4.2.2 Dittrich, et al. 2019 plant growth conditions and tissue harvesting

Full details are described in the original study [149]. Plants were grown under 12/12 hour light/dark cycles. 125 μmol m^{-2} s^{-1} and 22 ˚C during light, 16 ˚C during dark, at 60 % RH. Plants were treated with light or dark at 6/7 weeks. Here, plants were placed in cabinets set to 22 ˚C with 100 μmol m^{-2} s^{-1} light with a constant air stream of 400 ppm CO2, 50 ± 5 % RH for 2 hours (light treatment) and then sampled or placed in darkness for a further 2 hours (dark treatment). RNA was extracted from epidermal peels (containing intact guard cells) prepared via blending as described previously [263].

4.2.3 Microarray analysis

Raw microarray data from Dittrich, et al. 2019 was retrieved from the NCBI GEO database (series GSE118520). Specifically, 4 light samples (GSM3331440 - GSM3331443) and 3 dark samples (GSM333144 – GSM3331446) were re-analysed. Microarray data was analysed using the R package limma [264]. The background from each array was corrected using the normexp method, and data was normalised between arrays using the quantile method. Probes were filtered out of the microarray datasets if they showed no expression above background rates. Differential expression was determined by fitting the data to a linear model using the lmfit function and statistical analysis of this modelling was carried out using the eBayes function. Quality assessment of the microarray datasets was carried out by observing the distribution of raw background intensities for each microarray run, and principle component analysis of the filtered microarray datasets was performed to observe the repeatability of the dark and light treatments.

4.2.4 PYL Receptor responses to light, darkness, or dehydration

Whole leaves were detached from 5 week old Arabidopsis Col-0 plants grown under standard 10/14 hour light/dark conditions at 2 hours post dawn. The leaves were floated on 10/50 buffer under 120 μmol m^{-2} s^{-1} light at 22 ˚C for 2 hours in 50 mm single vented petri dishes (pots). Leaves were transferred to dark covered pots containing 10/50 buffer at 22 ˚C (dark treatment), clear empty pots (dehydration treatment) under 120 μmol m^{-2} s^{-1} light, or kept floating on buffer under light (light treatment) for a further 2.5 hours. Leaves were flash frozen in liquid nitrogen and subsequent RNA extraction and QPCR analysis was performed as described in the general methods section.

4.2.5 Whole plant light or dark treatment

Whole plant light and dark treatment was applied to 5 week old plants. Here plants were transferred to cabinets set to standard growth conditions. At 2 hours post dawn plants were either kept under normal conditions with lights remaining on (light treatment) or with lights off (dark treatment). The plants remained in light or dark for 2 hours before tissue harvesting as described in general methods.

4.2.6 Short and long day growth conditions

Plants were grown under standard short day 10/14 hours light dark conditions (120 μmol m^{-2} s^{-1}, light 22 ˚C, 70 % RH), as outlined in the general methods (section 2.1.2). Plants under long day conditions were grown in 16/8 hour light/dark cycles. Light was set to 120 μmol m^{-2} s^{-1}, relative humidity set to 70 %, and temperature set to 22 ˚C in light and 20 ˚C in darkness. Plants were grown until bolting, which was after 7-8 weeks under short day conditions, and 3 weeks under long day conditions.

4.2.7 Stomatal and pavement cell density and index measurements

Leaf imprints were taken from the largest fully expanded leaf. The leaf was detached from the rosette and firmly pressed into dental putty (The Dental Directory, PRESIDENT The Original Light Body). Leaves were left in dental putty for at least 30 mins. Once the dental putty had solidified the leaf tissue was removed from the dental putty imprint. A thin layer of clear nail polish was used to coat the imprint and left to dry for at least 30 mins. After 30 mins, transparent tape was used to transfer the dried nail varnish imprint mould onto a microscope slide. Epidermis imprints were imaged on a Leica DMI6000 B microscope fitted with a Leica DFC360FX monochrome camera. The microscope was set to brightfield settings and image stacks were taken using a 40x lens. One image stack was taken per leaf, midway between the leaf edge and the midrib, 2/3 of the way up the leaf. Epidermal cells were counted within a 0.16 mm^2 region of the image stack. Epidermal cells (both stomata and other cells) were included in the count if they did not overlap with 2 sides of the image. Stomatal density was determined by multiplying the stomatal cell count by 6.25 to determine density per mm^2. Stomatal index was calculated by dividing the stomatal cell count by the total epidermal cell count.

4.3 Results

4.3.1 A list of core ABA signalling and metabolism genes

A list of core ABA signalling and metabolism genes were compiled (shown in table 4.3 and 4.4 respectively). The core signalling genes include members of the *PYL* ABA receptor family [100,102], the subgroup A PP2C phosphatase family [265], three members of the SnRK2 family that have been linked to ABA signalling [234], the ABI5/ABF/AREB bZIP transcription factor family (known to mediate ABA signalling by binding to ABA RESPONSIVE ELEMENT – ABRE - targets in gene regulatory sequences [266]) and ABI3 (B3 domain containing transcription factor [267]) and ABI4 (DEHYDRATION RESPONSE ELEMENT BINDING – DREB - transcription factor family [268]). In addition, 3 genes that contain ABRE regulatory regions within their promoters are also included [269,270]. The core metabolism genes include members of the NCED enzyme family (which are thought to be key to determining rate of ABA biosynthesis in response to drought stress [217,226]), ß-glucosidases 1 and 2 (involved in ABA activation [99]), the CYP707A family (involved in ABA hydroxylation, marking it for degradation [219,228]), and members of the UDP-glycosyltransferase family (UGT family - linked to ABA glucosylation/ABA inactivation [271–274]).

Gene Name	Gene AT number	Gene Function
PYR1	AT4G17870	ABA Receptor
PYL1	AT5G46790	ABA Receptor
PYL2	AT2G26040	ABA Receptor
PYL3	AT1G73000	ABA Receptor
PYL4	AT2G38310	ABA Receptor
PYL5	AT5G05440	ABA Receptor
PYL6	AT2G40330	ABA Receptor
PYL7	AT4G01026	ABA Receptor
PYL8	AT5G53160	ABA Receptor
PYL9	AT1G01360	ABA Receptor
PYL10	AT4G27920	ABA Receptor
PYL11	AT5G45860	ABA Receptor
PYL12	AT5G45870	ABA Receptor
PYL13	AT4G18620	ABA Receptor
ABI1	AT4G26080	PP2C Phosphatase
ABI2	AT5G57050	PP2C Phosphatase
HAB1	AT1G72770	PP2C Phosphatase
HAB2	AT1G17550	PP2C Phosphatase
HAI1	AT5G59220	PP2C Phosphatase
HAI2	AT1G07430	PP2C Phosphatase
HAI3	AT2G29380	PP2C Phosphatase
AHG1	AT5G51760	PP2C Phosphatase
PP2CA	AT3G11410	PP2C Phosphatase
SNRK2.2	AT3G50500	SnRK2 Kinase
SNRK2.3	AT5G66880	SnRK2 Kinase
SNRK2.6	AT4G33950	SnRK2 Kinase
ABF1	AT1G49720	ABI5/ABF/AREB Transcription Factor
ABF2	AT1G45249	ABI5/ABF/AREB Transcription Factor
ABF3	AT4G34000	ABI5/ABF/AREB Transcription Factor
ABF4	AT3G19290	ABI5/ABF/AREB Transcription Factor
AREB3	AT3G56850	ABI5/ABF/AREB Transcription Factor
ABI5	AT2G36270	ABI5/ABF/AREB Transcription Factor
ABI3	AT3G24650	B3 domain Transcription Factor
ABI4	AT2G40220	DREB Transcription Factor
RD29B	AT5G52300	ABRE Targets
EM1	AT3G51810	ABRE Targets
EM6	AT2G40170	ABRE Targets

Table 4.3 Core ABA signalling Machinery

A list of genes designated as core ABA signalling machinery. This list includes all members of the PYL gene family of ABA receptors and the group A PP2C phosphatases. Three members of the SnRK2 gene family linked to ABA signalling. Members of the ABI5/ABF/AREB transcription factor family, ABI3, and ABI4. Three genes containing ABA Responsive Elements (ABREs) in their regulatory regions are also included.

Gene Name	Gene AT number	Gene Function
NCED2	AT4G18350	Biosynthesis
NCED3	AT3G14440	Biosynthesis
NCED5	AT1G30100	Biosynthesis
NCED6	AT3G24220	Biosynthesis
NCED9	AT1G78390	Biosynthesis
CYP707A1	AT4G19230	Degradation
CYP707A2	AT2G29090	Degradation
CYP707A3	AT5G45340	Degradation
CYP707A4	AT3G19270	Degradation
BG1	AT1G52400	Activation
BG2	AT2G32860	Activation
UGT87A2	AT2G30140	Deactivation
UGT75D1	AT4G15550	Deactivation
UGT71B6	AT3G21780	Deactivation
UGT71B7	AT3G21790	Deactivation
UGT71B8	AT3G21800	Deactivation
UGT71C5	AT1G07240	Deactivation

Table 4.4 Core ABA metabolic machinery

A list of genes designated as core ABA metabolism machinery. This list includes members of the NCED gene family shown to be involved in ABA biosynthesis, all members of the CYP707A family, BG1 and BG2, and members of the UGT gene family that have been linked to ABA deactivation.

4.3.2 Diurnal expression patterns of ABA signalling and ABA metabolic genes

The expression of the core ABA signalling and metabolism genes (shown in table 2 and 3) over a 48 hour diurnal period was analysed using the data from the web based tool 'diurnal' [275]. Here, 4 diurnal micro-array time course experiments were analysed. Two experiments involved 7 day old seedlings in 12/12 hours light/dark growth conditions and 8/16 hours light/dark growth conditions (COL_LDHH and COL_SD respectively), the other two experiments involved 4 or 5 week old plants in 12/12 hours light/dark conditions (LDHH_SM and LDHH_ST). Full details of these experiments can be found in the chapter specific method section. Initially the expression of all core ABA signalling and metabolism genes were analysed. Genes that showed little expression compared to others in the same family were dropped from further analysis. The relative expression of the remaining genes over a 48-hour time course are shown in fig. 4.1 and fig. 4.2.

ABA signalling

Expression patterns are first described for 7 day old seedlings. Here, ABA receptors show clear diurnal expression patterns with low expression in light conditions and high expression under dark conditions. The pattern of PP2C phosphatases generally shows the opposite. Here, all but *HYPERSENSITIVE TO ABA 1* (*HAB1*) show peak expression under light conditions and low expression in the dark. *HAB1* expression appears to peak at dawn (before lights have turned on) before rapidly lowering expression levels midway through the day. *SNRK2.2* also shows clear diurnal expression patterns where its expression peaks 4 hours into the dark period. Unlike the receptors and phosphatases, there appears to be no clear consensus in the diurnal expression patterns of the *ABI5*/*ARF*/*AREB* transcription factors. *ABF1* expression peaks in the latter parts of the day, *ABF3* expression peaks in the earlier half of the day, and *AREB3* peaks at dawn under 12/12 hours light/dark conditions or in the latter part of the night in 8/16 hours light/dark conditions. Similarly, although the ABRE containing targets show diurnal expression there is no consensus between experiment. In 12/12 hours light/dark conditions their expression peaks at dawn or in the first part of the day, and in 8/16 hours light/dark conditions their expression consistently peaks at dusk.

In 4/5 week old leaf tissue, fewer genes show clear diurnal expression patterns. However, all ABA receptors show the same pattern observed in 7 day old seedlings, where expression is low in the daytime and high at night. Only the *ABI1* and *HAB1* phosphatases show diurnal expression patterns in mature leaf tissue. Both of these patterns are similar to that observed in seedlings, where *ABI1* peaks in the latter half of the day and *HAB1* peaks at dawn. *SNRK2.2* shows a clear diurnal pattern, however, this differs from seedlings as it peaks earlier, in the latter half of the day. Only the *ABF1* and *ABF3* transcription factors show diurnal expression patterns consistent to what was observed in seedlings. Additionally, unlike in seedlings none of the ABRE containing target genes show consistent diurnal expression patterns.

ABA metabolism

Similarly to genes involved in ABA signalling, ABA metabolism genes show stronger diurnal expression patterns in seedlings. Here, the ABA biosynthesis gene *NCED3*, the ABA activation gene *BG1*, and the ABA degradation genes *CYP707A1-A3* show diurnal expression patterns, where peak transcript abundance is found during the daytime. In seedlings all of the ABA deactivation genes show diurnal expression patterns, however there is no clear pattern among them. In 4/5 week old leaf tissue there are no clear, consistent diurnal expression patterns other than for *CYP707A2-3*, *UGT71B7*, and *UGT75D1*. These diurnal expression patterns are consistent with that observed in seedlings.

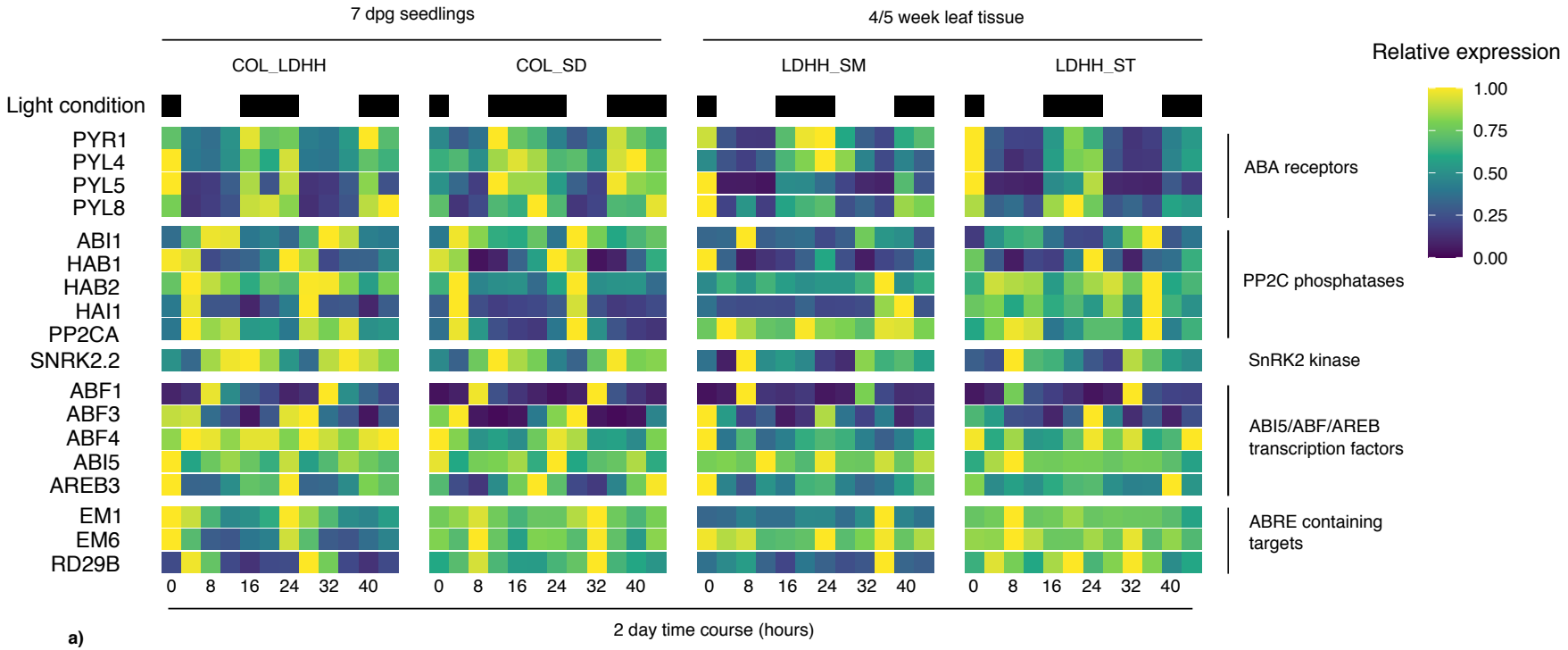

Figure 4.1 Diurnal expression pattern of core ABA signalling genes

Tiles show the relative expression of core ABA signalling genes over a 48 hour time course. Tile colour corresponds to relative gene expression. 4 microarray experiments are presented in 4 parallel vertical columns. ABA signalling genes (named on the left hand side) are grouped based on their gene/function (displayed on the right hand side). Light condition is shown by black and white tiles, representing dark and light respectively. Time is displayed at the bottom of the figure, 0 corresponds to dawn. Relative expression was determined for each gene by dividing normalised microarray expression values by the maximum expression value over the 2 day time course. See Table 4.2 for full details of growth conditions and age of material.

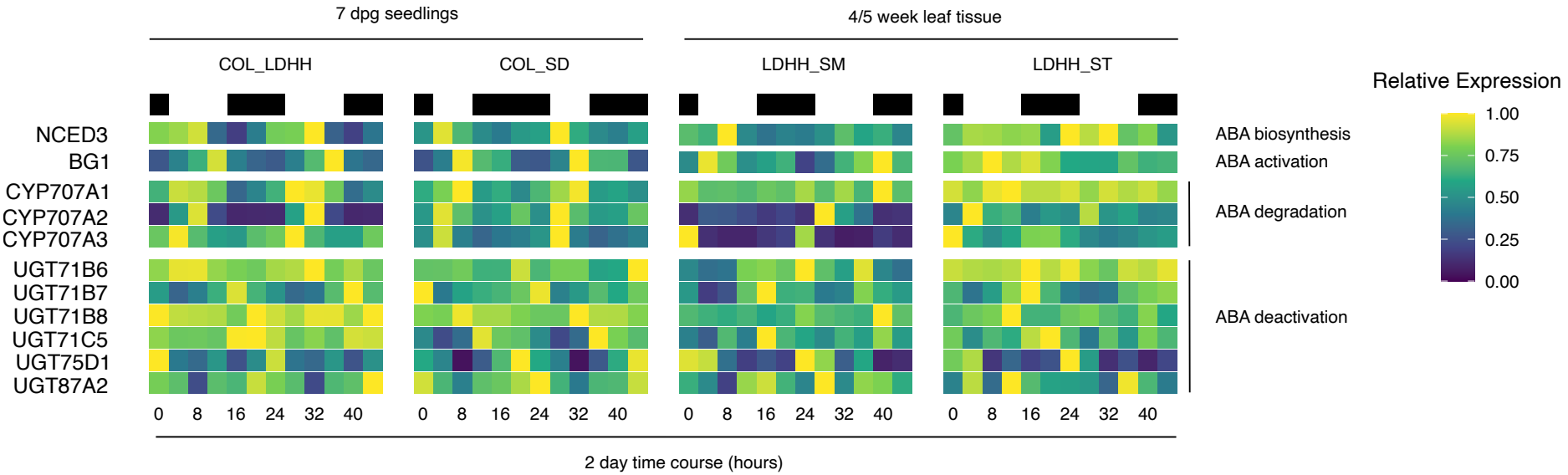

Figure 4.2 Diurnal expression pattern of core ABA metabolism genes

Tiles showing the relative expression of core ABA metabolism genes over a 48 hour time course. Tile colour corresponds to relative gene expression. 4 microarray experiments are presented in 4 parallel vertical columns. ABA metabolism genes (named on the left hand side) are grouped based on their gene/function (displayed on the right hand side). Light condition is shown by black and white tiles, representing dark and light respectively. Time is displayed at the bottom of the figure, 0 corresponds to dawn. Relative expression was determined for each gene by dividing normalised microarray expression values by the maximum expression value over the 2 day time course. See Table 4.2 for full details of growth conditions and age of material.

4.3.3 Circadian expression patterns of ABA signalling and ABA metabolic genes

As there were clear diurnal expression patterns observed for both ABA signalling and metabolism genes (fig. 4.1 and fig. 4.2 respectively), further analysis was performed to assess whether these expression patterns occurred in the absence of day/night transitions. This would provide evidence for circadian regulation. Using the online diurnal tool the expression pattern of the ABA signalling and metabolic genes were analysed from three microarray experiments (LL_LDHC, LL12_LDHH, LL23_LDHH) that investigated the circadian regulation of gene expression. All three experiments involved seedlings grown under 12/12 hours light/dark conditions for 7 days, transferred to constant light, and then sampled every 4 hours for 48 hours. Full details of the experimental conditions can be found in the methods section.

ABA signalling

Fig. 4.3 shows the expression pattern of ABA signalling genes and a selection of key circadian oscillating genes. Over all experiments the known circadian oscillating genes show clear circadian rhythms except for *PSEUDO RESPONSE REGULATOR 9* (*PRR9*) in LL_LDHC. However, whereas clear light/dark patterns could be observed for ABA receptor transcripts under diurnal conditions (fig. 4.1), no consistent pattern is observed for plants under constant light (fig. 4.3). The *PP2C* phosphatase genes *ABI1* and *HAB1* show signs of periodic oscillations in 2/3 experiments analysed. Additionally, *SNRK2.2*, *ABF1*, and *ABF3* show clear oscillating expression patterns similar to that observed under normal 12/12 hours light/dark conditions. This suggests a role for circadian regulation of some *PP2C* phosphatase, *SNRK2* kinase, and *ABI5*/*ABF*/*AREB* transcription factor genes over day night cycles. It also suggests that the expression patterns of the ABA receptors observed in fig. 4.1 may not be due to circadian regulation.

ABA metabolism

In 7 day old seedlings *NCED3, BG1*, and *CYP707A1-A3* presented clear diurnal expression patterns (fig. 4.2), when transferred to constant light conditions their gene expression shows weak/little patterns of oscillation (fig. 4.4). The ABA deactivation enzymes *UGT71C5*, *UGT75D1*, and *UGT87A2* show oscillating patterns of expression, with *UGT71C5* generally showing higher expression in the daytime, and *UGT75D1* and *UGT87A2* showing higher expression at night. The expression of selected circadian oscillator genes is also presented in fig. 4.4 to show circadian rhythms are still occurring under these constant light conditions.

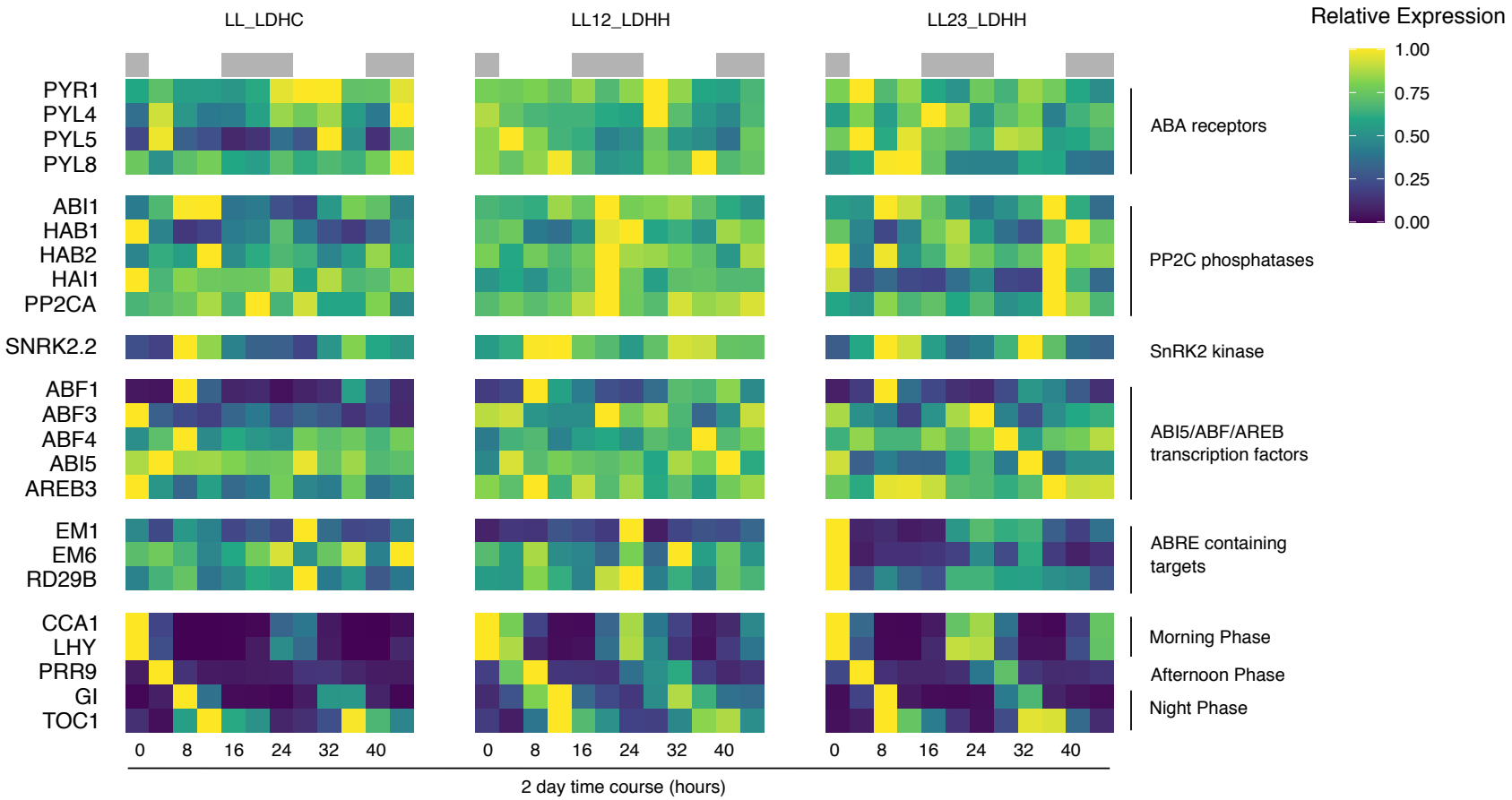

Figure 4.3 Circadian expression of ABA signalling genes

Tiles show relative expression of ABA signalling genes over a 48 hour circadian time course. Tile colour corresponds to relative gene expression. 3 microarray experiments are presented in 3 parallel vertical columns. ABA signalling genes (named on the left hand side) are grouped based on their gene/function (displayed on the right hand side). The expected light condition is shown by grey and white tiles, representing expected dark and light respectively. Time is displayed at the bottom of the figure, 0 corresponds to dawn. Relative expression was determined for each gene by dividing normalised microarray expression values by the maximum expression value over the 2 day time course. See Table 4.2 for full details of growth conditions and age of material.

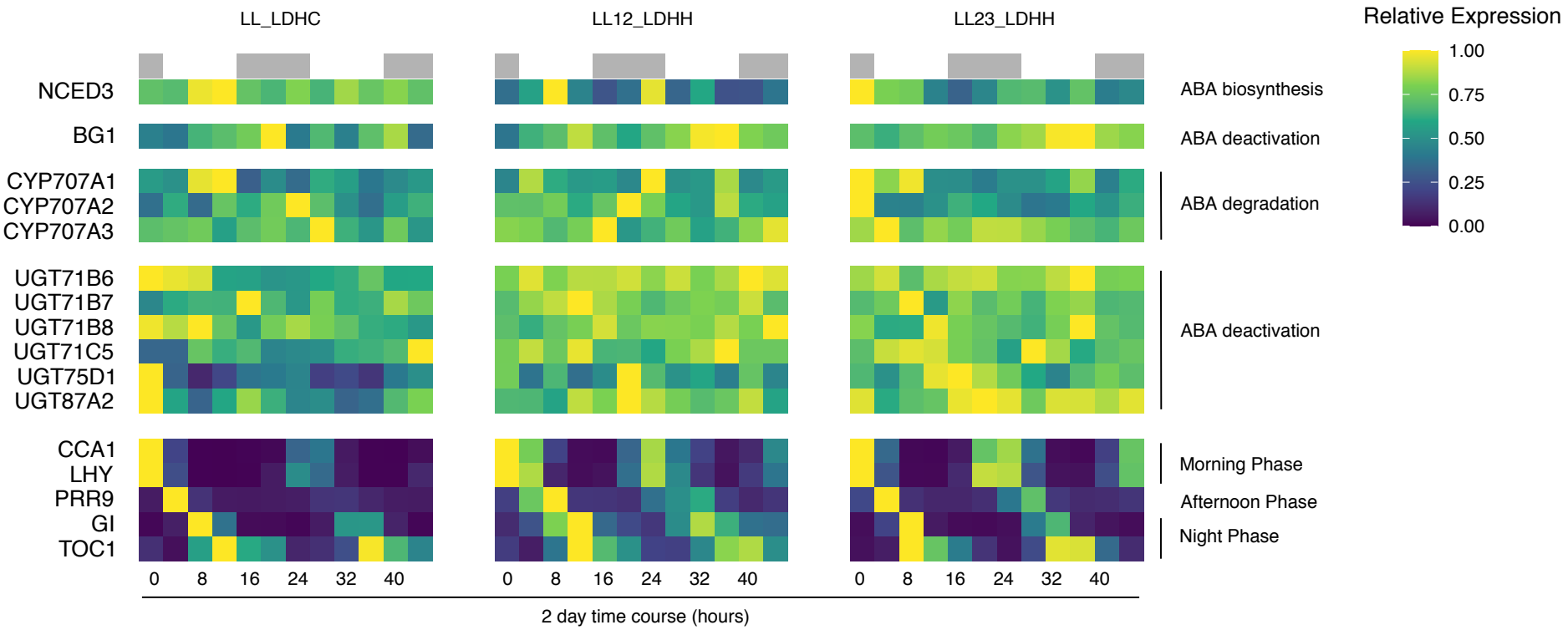

Figure 4.4 Circadian expression of ABA metabolism genes

Tiles show relative expression of ABA metabolism genes over a 48 hour circadian time course. Tile colour corresponds to relative gene expression. 3 microarray experiments are presented in 3 parallel vertical columns. ABA metabolism genes (named on the left hand side) are grouped based on their gene/function (displayed on the right hand side). The expected light condition is shown by grey and white tiles, representing expected dark and light respectively. Time is displayed at the bottom of the figure, 0 corresponds to dawn. Relative expression was determined for each gene by dividing normalised microarray expression values by the maximum expression value over the 2 day time course. See Table 4.2 for full details of growth conditions and age of material.

4.3.4 Guard cell gene expression responses to darkness

To investigate the effects of darkness on guard cell transcriptional changes in Arabidopsis, microarray data from collaborators was analysed. In this experiment 6-7 week old plants grown under 12/12 hours light/dark conditions were exposed to darkness or a control light treatment of 100 μmol m^{-2} s^{-1} for 2 hours. RNA was extracted from epidermal peels (containing intact guard cells) prepared via blending [263]. The microarray data has been re-analysed here as the original study looked at guard cell responses to multiple different stimuli, whereas this study is focused on dark/light transitions.

In order to assess whether dark treatment is affecting the expression of the ABA signalling and biosynthesis machinery, the expression of the genes listed in table 4.2 and 4.3 were analysed. Fig. 4.5 and fig. 4.6 show the $\log_2$ (fold change) of all probes associated with the genes of interest when plants are transferred from light conditions to dark. For the signalling machinery (fig. 4.5) the highest upregulation is seen for the ABA receptors, in particular *PYL5* and *PYL6*. Additionally, the *PYR1*, and *PYL8* ABA receptors also show upregulation in darkness. Conversely, certain PP2C phosphatases (*ABI1, ABI2, PP2CA*), SnRK2 kinases (*SNRK2.6*), and ABA activated transcription factors (*ABF2* and *ABF3*) show downregulation upon dark treatment. There appears to be no major changes to the expression of ABRE containing target genes. Unlike the ABA signalling machinery, the ABA metabolism machinery show no clear trends among gene classes in response to darkness. *BG1, UGT75D1, UGT87A2, CYP707A2,* and *CYP707A4* appear to show slight downregulation. *UGT71B6*, *UGT71B7*, *UGT71C5*, and *CYP707A3* show slight upregulation. *BG2,* the ABA biosynthesis genes (*NCED3* and *NCED5*), *UGT71B8,* and *CYP707A1* show no major changes.

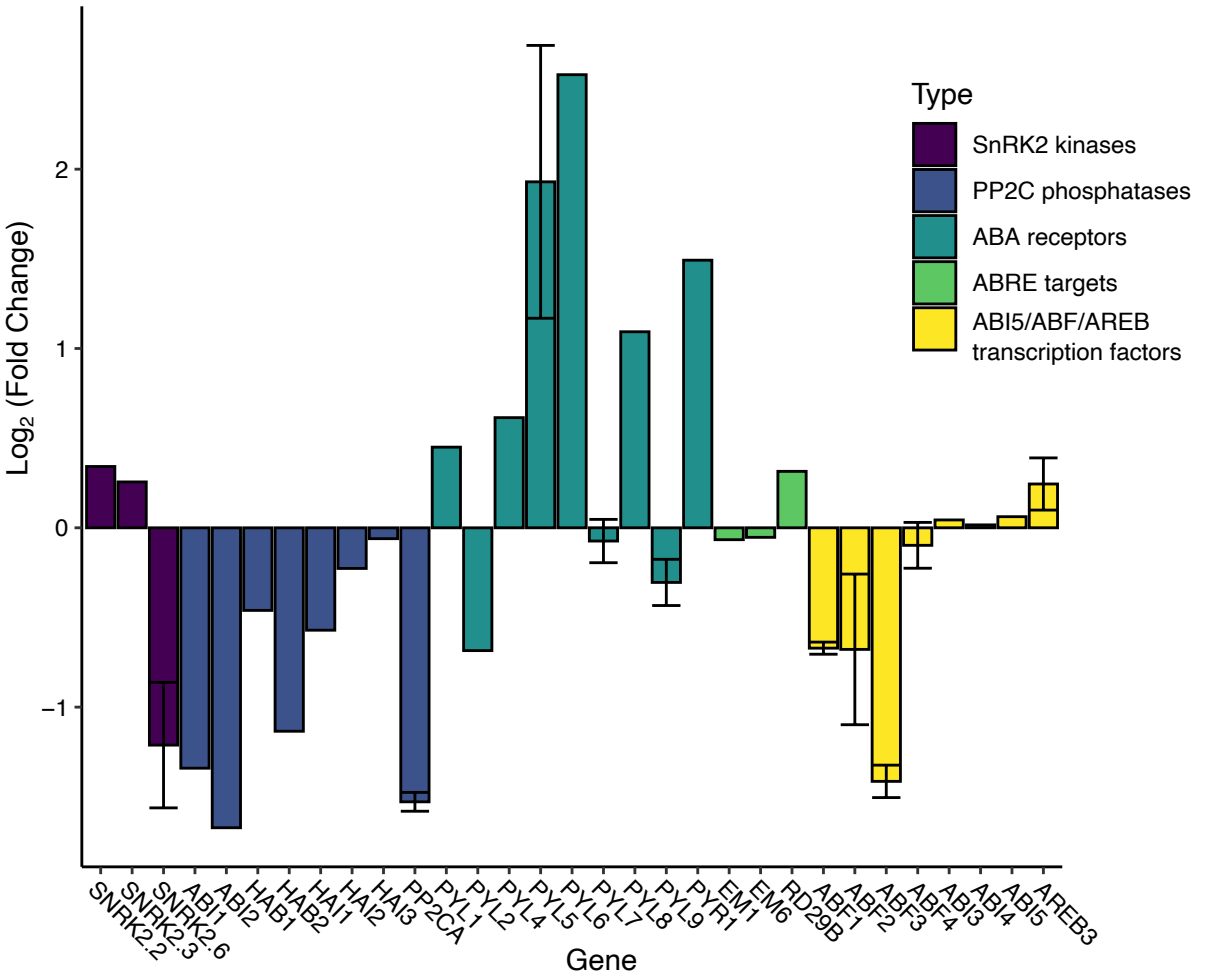

Figure 4.5 Core ABA signalling gene expression changes in guard cell responses to darkness

Log_2 (fold change) for ABA core signalling machinery genes from a guard cell enriched microarray study comparing dark and light treated samples. Positive values represent upregulation in darkness, negative values represent downregulation in darkness. Data is represented as mean ± s.e.m. of probes for the same gene. n = 1-3 probes per gene.

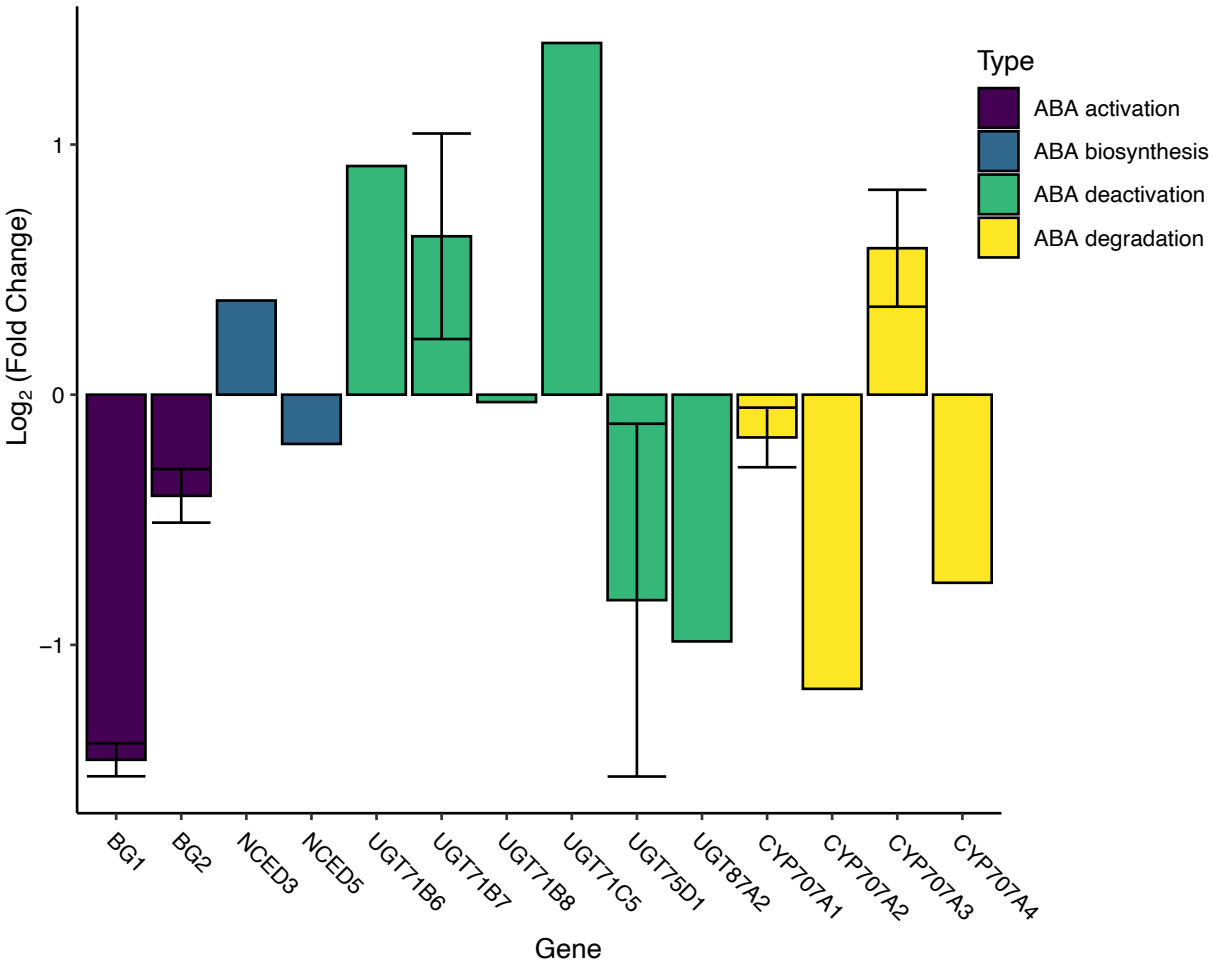

Figure 4.6 Core ABA metabolism gene expression changes in guard cell responses to darkness

Log_2 (fold change) for ABA core metabolism machinery genes from a guard cell enriched microarray study comparing dark and light treated samples. Positive values represent upregulation in darkness, negative values represent downregulation in darkness. Data is represented as mean ± s.e.m. of probes for the same gene. n = 1-3 probes per gene.

4.3.5 Validation of the ABA receptor transcript responses to darkness

QPCR was performed in order to verify the upregulation of specific ABA receptors in response to darkness. Here, leaves were detached from plants grown under standard 10/14 hours light/dark conditions, floated on 10/50 buffer kept at 22 °C and treated with 120 μmol m^{-2} s^{-1} light for 2 hours. Then leaves were transferred either to buffer in darkness, or removed from buffer and left to wilt in the light for a further 2.5 hours. Leaf tissue was flash frozen, RNA extracted, and QPCR was performed to analyse the transcript dynamics of the PYL ABA receptor family. ABA receptors *PYR1*, *PYL1-2*, and *PYL4-9* were analysed, as either detection could not be detected or efficient QPCR primers could not be obtained for *PYL3*, *PYL10-13*.

The QPCR results verify that the *PYL5* transcript is significantly upregulated in response to darkness (fig. 4.7, $p < 0.0001$) to a similar extent in leaf tissue as to which was observed for guard cell specific microarray samples (fig. 4.5) [149]. It is also evident that there are distinct differences in the transcriptional dynamics for different groups of PYL receptors. The ABA receptors *PYL4*, *PYL5,* and *PYL6* all show similar transcriptional responses to light, darkness, and dehydration, where darkness increases, and dehydration decreases transcript abundance (although not significantly for *PYL6*). Conversely, darkness has little effect upon *PYL7* and *PYL9* transcript abundance, however they are strongly upregulated in response to dehydration ($p < 0.0001$ for both).

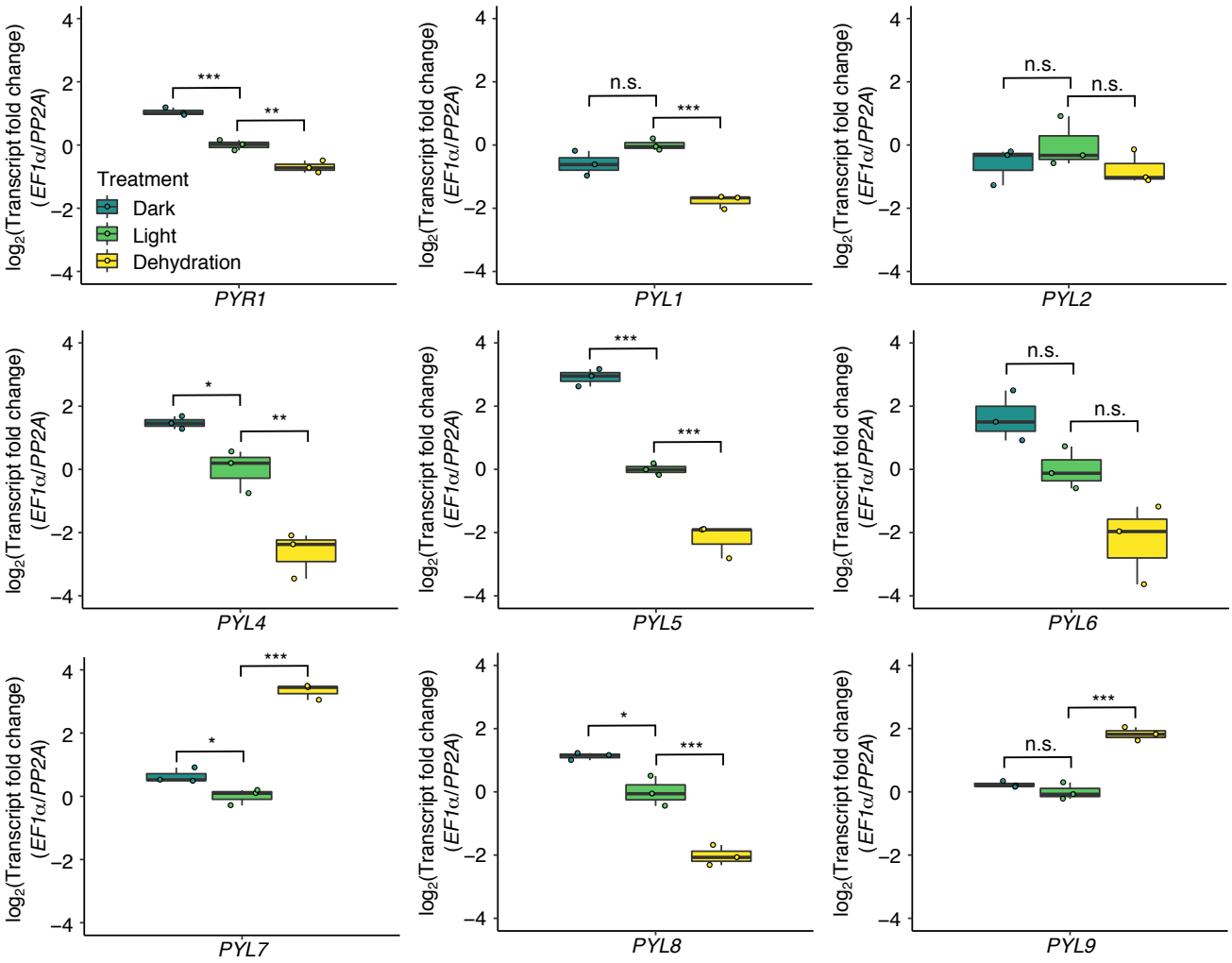

Figure 4.7 *PYL* receptor expression patterns in responses to light, darkness, and dehydration

Log_2 (fold change) of ABA receptor transcripts from detached leaves floated on buffer incubated in light, darkness, or removed from buffer and left to wilt (dehydration). Log_2 (fold changes) were determined via QPCR using the ΔΔCt method. *EF1a* and *PP2A* were used as reference genes. n = 3 per ABA receptor transcript per condition. Data was statistically analysed using 1-way ANOVAs and TukeyHSD post hoc tests. *, **, *** represent $p < 0.05$, $p < 0.01$, and $p < 0.001$ respectively. n. s. represents non significant comparisons.

4.3.6 The effect of ABA mutations on *PYL5* receptor gene expression

To investigate whether mutations within ABA signalling components affect the transcriptional dynamics of *PYL5* upregulation, and to additionally confirm that *PYL5* upregulation occurs in whole plants as well as detached leaves, a number of ABA signalling and metabolism mutants were either subjected to 2 hours of light or darkness during midday. These mutants include the quadruple receptor mutant *q1124,* the biosynthesis double mutant *nced3/5*, and the ABA hydroxylation mutants *cyp707a1* and *cyp707a3*. Following treatment RNA was extracted from leaf tissue and receptor dynamics were analysed via QPCR (fig. 4.8).

There is a significant upregulation of *PYL5* in response to darkness for all genotypes analysed other than *nced3/5*. For both *q1124* and *nced3/5* mutants increased *PYL5* levels are observed under light treatment relative to Col-0, however, in darkness a significant increase is not observed. Interestingly in the ABA catabolism mutants, although post hoc tests do not show any significant differences between groups, 2-way ANOVAs show for *cyp707a1* and *cyp707a3* that treatment ($F_{1,8} = 91.258$, $p < 0.0001$ and $F_{1,8} = 79.541$, $p < 0.0001$ respectively) and genotype ($F_{1,8} = 13.546$, $p = 0.006$ and $F_{1,8} = 7.627$, $p = 0.025$ respectively) have significant effects on *PYL5* transcript abundance. This likely reflects that the *PYL5* transcript abundance is slightly decreased across both treatments in *cyp707a1* and *cyp707a3* when compared to Col-0.

This suggests that ABA signalling is playing a role in regulating *PYL5* transcript abundance. This likely occurs through the ABA signalling mediated repression of *PYL5* transcription under light conditions, which is lifted upon dark treatment. This is supported by the observations that *PYL5* transcript abundances are increased under light but not dark conditions in ABA signalling and biosynthesis mutants. However, in mutants where ABA levels are elevated (*cyp707a1* and *cyp707a3*), decreased *PYL5* transcript abundances are observed in both light and darkness.

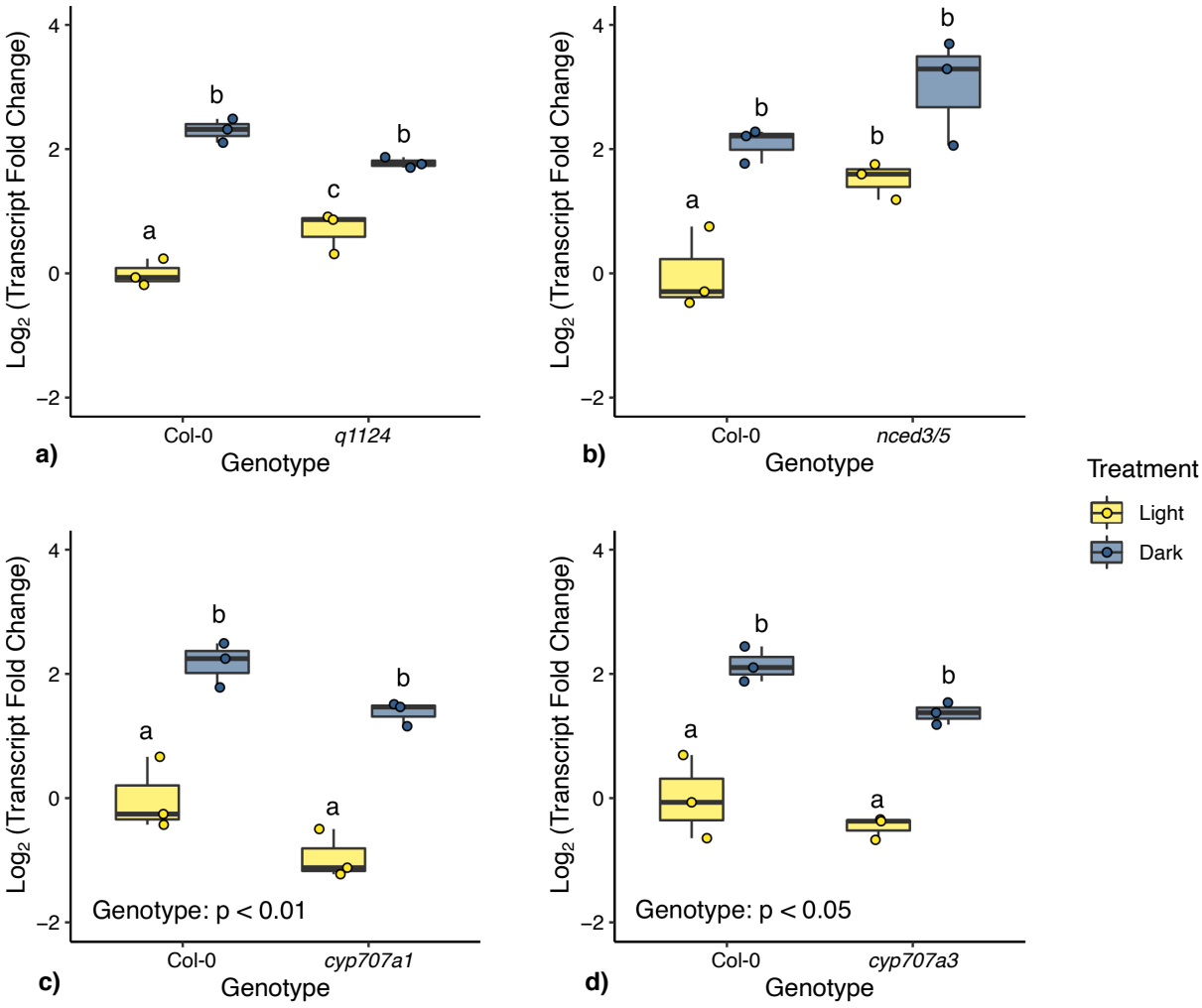

Figure 4.8 *PYL5* expression in response to darkness in ABA signalling and metabolism mutants

Log_2 (fold change) of *PYL5* in response to darkness for **a)** *q1124,* **b)** *nced3/5,* **c)** *cyp707a1*, and **d)** *cyp707a3*. Log_2(fold change) was determined using the ΔΔCt method with *EF1a* and *PP2A* as reference genes. n =3 per genotype and treatment. Data was statistically analysed using 2-way ANOVA with TukeyHSD post hoc tests, samples indicated with the same letter cannot be distinguished at $p < 0.05$.

4.3.7 Mutations in ABA signalling genes affect epidermal cell development

Due to the time taken for darkness to upregulate *PYL5* transcripts it is unlikely that this will regulate immediate physiological responses to darkness such as stomatal movements. Instead, it was hypothesised that this regulation of *PYL5* is affecting longer term responses such as the sensitivity of stomata to future signals and/or plant development. In order to investigate a developmental role for the light and dark mediated regulation of *PYL5,* the stomatal development traits of ABA signalling and metabolism mutants were analysed in short (10 hour light, 14 hour darkness) and long (16 hour light, 8 hour darkness) day conditions. The ABA signalling and metabolism mutants analysed include the ABA hydroxylation mutant *cyp707a1*, the ABA activation mutant *bglu18-1,* the ABA receptor mutants *q1124* and *s112458,* and the ABA biosynthesis double mutant *nced3/5*. In order to analyse plants at the same developmental stage epidermal cell densities were analysed upon plant bolting.

In fig. 4.9 the stomatal density, stomatal index, and pavement cell density are presented for the ABA signalling and metabolism mutants. Focusing on stomatal density, analysis using a 2-way ANOVA looking at the effect of genotype and day length on stomatal density shows there is a strong significant effect of genotype ($F_{5,278} = 50.794$, $p < 0.0001$) and weaker effect of day length on stomatal density ($F_{1,278} = 5.352$, $p = 0.021$). However, post-hoc tests show no significant differences between day lengths within genotypes. These results reflect the fact that the strong ABA receptor and biosynthesis mutants *s112458,* and *nced3/5*, have drastically increased stomatal densities regardless of day length. Under short day conditions there may be a slight increase in stomatal density, but this effect appears to be very weak.

Similarly to stomatal density, analysis of pavement cell density shows a strong effect of genotype ($F_{5, 278} = 46.400$, $p < 0.0001$). However, a strong effect of day length is also observed ($F_{1,278} = 31.051$, $p < 0.0001$). The ABA receptor mutants *q1124, s112458* and the biosynthesis mutant *nced3/5* all show significantly increased stomatal densities in long and short day conditions compared to Col-0. For all genotypes there is a trend of increased pavement cell densities under short day conditions, however post hoc analysis shows no significant differences within genotypes.

Analysis of stomatal index shows both genotype ($F_{5,278} = 5.071$, $p = 0.0002$) and day length ($F_{1,278} = 27.647$, $p < 0.0001$) have significant effects on stomatal density. Additionally, there is a

significant interaction between the two factors ($F_{5,278} = 2.889$, $p = 0.0146$), suggesting genotypes respond differently to day length. Here, day length appears to significantly reduce stomatal index in Col-0, and dramatically in *q1124*. All other genotypes analysed show no significant differences between short and long days, however all but *bglu18-1* trend towards decreased stomatal indices.

These results suggest that the increased stomatal densities observed in the *s112458* receptor mutant and *nced3/5* biosynthesis mutant are not due to an increase in number of cells differentiating into mature stomata but more likely due to decreased epidermal cell sizes. Similarly, day length is likely similarly influencing epidermal cell sizes, with plants grown under short day conditions showing slight increases in both pavement cell and stomatal density suggesting smaller cell sizes. However, shorter day length appears to also reduce the number of cells differentiating into mature stomata due to the decrease in stomatal index. Interestingly compared to Col-0 under short day conditions the *q1124* receptor mutant shows a significantly reduced stomatal index, suggesting even fewer cells differentiating into mature stomata. This phenotype appears to be rescued by growth in long day conditions and the mutation of *PYL5* and/or *PYL8*. This suggests certain ABA receptors may show opposing roles under short day conditions. Some functioning to promote the number of cells differentiating into mature stomata (some or all of *PYR1*, *PYL1*, *PYL2*, and *PYL4*) and some functioning to restrict the number of cells differentiating into mature stomata (*PYL5* and/or *PYL8*)

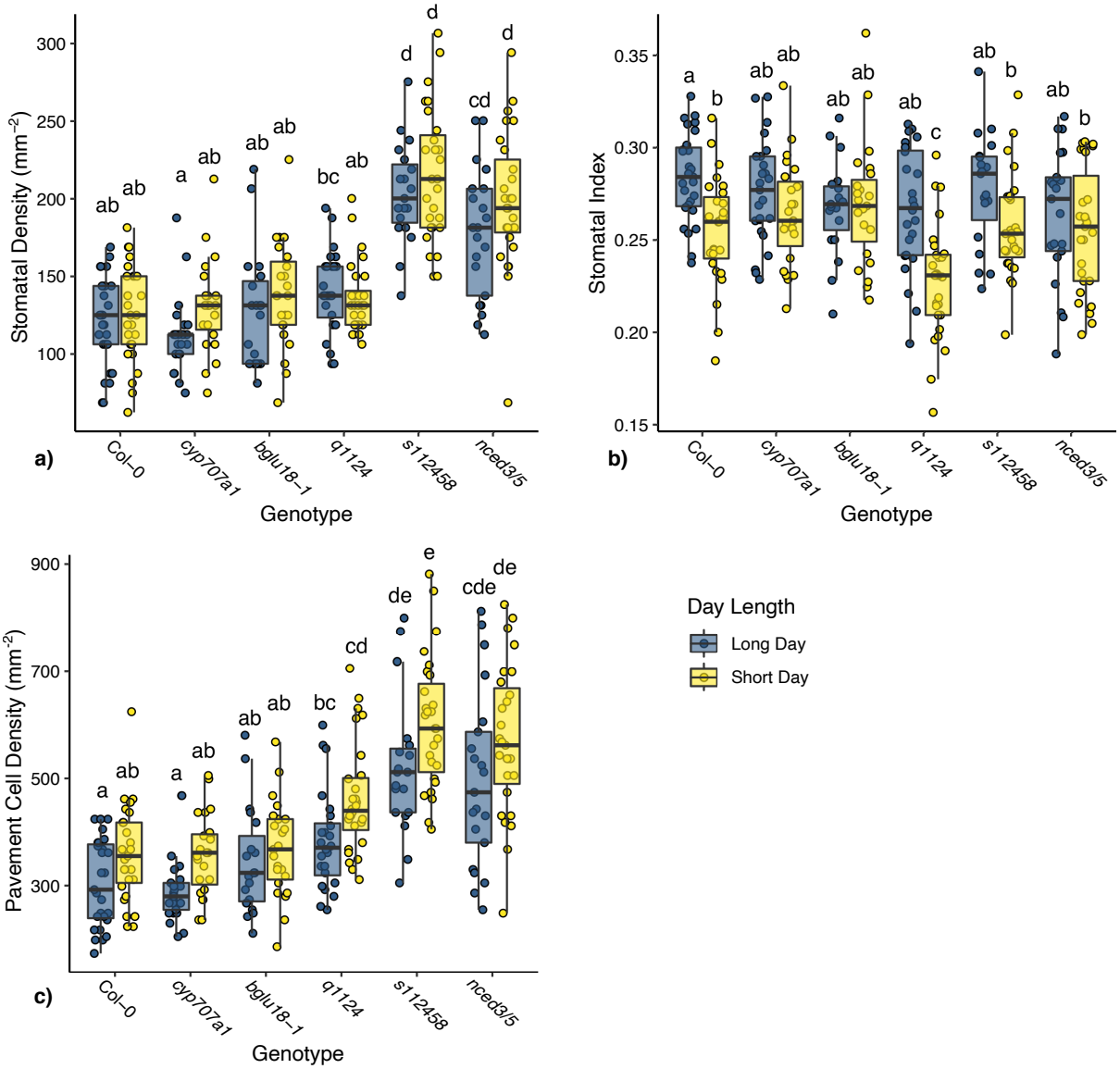

Figure 4.9 The effect of day length on stomatal development in ABA signalling and metabolism mutants

a) Stomatal density, **b)** stomatal index, and **c)** pavement cell density for ABA signalling and metabolism mutants in long and short day conditions. Data is presented in boxplots showing the median and interquartile range (IQR). Whiskers show the maximum and minimum data within 1.5 * IQR. All data is plotted as points. n = 19-27 over 2 independent experiments. Data was analysed using 2-way ANOVAs with TukeyHSD post hoc tests, samples indicated with the same letter cannot be distinguished at $p < 0.05$.

4.4 Discussion

4.4.1 The expression patterns of ABA signalling and metabolism genes

This chapter initially investigates the expression patterns of key ABA signalling and metabolism genes using publicly available expression data. It is observed that in seedlings many core ABA signalling and metabolism genes show diurnal patterns of expression. However, the studies in mature 4/5 week old plants show much less rhythmicity in ABA signalling and metabolism gene expression (fig. 4.1 and 4.2). Further analysis of transcript levels under constant light conditions (circadian time course experiments) suggests that the subset of genes that retain rhythmicity are likely under circadian regulation (fig. 4.3 and 4.4). This may also contribute to why there is a difference in the diurnal expression patterns of seedlings and 4/5 week old plants as age and tissue have been shown to feature differences in circadian regulation in Arabidopsis [276,277]. The increased rhythmicity of ABA signalling and metabolism genes observed in seedlings may reflect a greater need for time of day specific ABA signalling in young plants or seedling tissue types. This could be due to the role of ABA in regulating hypocotyl elongation [246,254], a process that occurs at specific times of day and is under circadian regulation [278]. Alternatively, it may reflect the cellular composition of seedling tissue and leaf tissue. The most prominent cell types in these tissues may mask the expression patterns of less prominent cell types. Eg. Strong rhythmic expression patterns in guard cells may be masked by non-rhythmic expression patterns in mesophyll cells in whole leaf RNA extractions.

There is a complex interaction between circadian rhythms and ABA signalling [279]. Studies have previously shown that various aspects of ABA signalling and metabolism show circadian regulation. A key circadian clock component *LATE ELONGATED HYPOCOTYL* (*LHY*) has been shown to directly target the *NCED3* promoter, regulating the rhythm of ABA accumulation under drought conditions. Additionally, *LHY* was shown to bind to the promoters of several ABA signalling components including ABA receptors, PP2C phosphatases, SnRK2 kinases, and ABA responsive transcription factors [280]. Additionally ABA treatment has been shown to modulate circadian rhythms, where exogenous ABA treatment reduced the circadian period [281,282]. Another key clock component TIMING OF CAB2 EXPRESSION 1(TOC1) was shown to inhibit GENOME UNCOUPLED 5 (GUN5) expression which was thought to lead to suppression of ABA signalling [283]. GUN5 was thought to be an ABA receptor [284], however subsequent research cast doubt upon this claim and the role of GUN5 in ABA perception is

now disputed [285,286]. The effect TOC1 has on ABA signalling is now thought to be due to its regulation of LHY [280].

4.4.2 A subset of ABA receptors show upregulation in darkness

A selection of the ABA receptor genes show distinct diurnal expression patterns in both seedlings and 4/5 week old plants (fig. 4.1), that are not observed under constant light conditions (fig. 4.3). This suggests that the ABA receptor upregulation seen during periods of darkness may not be directly due to circadian regulation and instead may be due to a darkness/absence of light signal. This is further supported by the finding that even in the middle of the photoperiod darkness upregulates ABA receptor transcripts in guard cell enriched RNA samples (fig. 4.5) detached leaf samples (fig. 4.7) and in whole plants (fig. 4.8). Upon analysing the transcript abundance of ABA receptors PYR1, PYL1-2, PYL4-9, it was found that different ABA receptors show different responses to darkness, with PYL5 showing the strongest response to darkness (fig. 4.7).

ABA receptor expression in response to leaf dehydration as well as darkness was analysed (fig. 4.7). Here, *PYL7* and *PYL9* show upregulation in response to leaf dehydration whereas all other ABA receptors analysed either show downregulation or no change. Interestingly, the difference in response behaviours observed here broadly follows the phylogenetic history of the ABA receptors. The family of ABA receptors has been categorised into major 3 clades, clade A/III (containing *PYR1, PYL1-3*), clade B/II (*PYL4-6*), and clade C/I (*PYL7-10*). Some studies additionally include *PYL11-13* in clade B [102].

Two members of clade C (*PYL7* and *PYL9)* have previously been shown to oppose the behaviour of the majority of ABA receptors, similar to what is observed in fig. 4.7 [287,288]. The majority of ABA receptors are downregulated in response to ABA treatment, however, *PYL7* and *PYL9* are upregulated. The general downregulation of ABA receptors coupled with the upregulation of PP2C phosphatases has been proposed to favour ABA signalling by increasing the ratio of bound PP2C:PYL complexes to unbound PYL receptors [288], opposingly, this could be a mode of negative feedback reducing ABA signalling over time. Multiple mechanisms for the negative regulation of ABA signalling components have been observed [139]. Clade C ABA receptors are thought to possess additional functions as well as canonical PP2C inhibition, and it is thought this has arisen through evolution via the positive selection of domains that enable

these receptors to bind to other factors [287], as has been observed for *PYL8* and *PYL9* and their interactions with MYB [289,290] and PIF transcription factors [246]. These additional interaction partners of clade C ABA receptors may influence their function and the difference in expression patterns observed for *PYL7* and *PYL9*.

Upregulation of ABA receptors in response to darkness is observed in receptors from all three clades (A – *PYR1*, B – PYL4, PYL5, C – *PYL7, PYL8*). However, upregulation appears greatest for receptors in clade B, in particular *PYL5*. This is interesting considering *PYL5* has recently been identified as a receptor required for the stomatal movement response to CO_2 [149], and that leaf intercellular CO_2 levels increase when incubated in darkness. Additionally, clade B receptor *PYL6* shows a trend of upregulation in response to darkness, but due to variability in transcript fold change observed across all treatments this cannot be statistically confirmed. The relevance of dark induced ABA receptor upregulation with respect to ABA signalling is unclear. It may provide a way of increasing ABA-independent PP2C inhibition (as has been observed for *PYL5-6*, PYL8-10 [33]) and therefore increase basal levels of ABA signalling in dark conditions. Or alternatively, it may provide a method of increasing the sensitivity to ABA in the dark. This seems likely, when coupled with the general decrease in PP2C phosphatase expression observed in response to darkness (fig. 4.1). However, due to the complex nature of ABA receptor function (with multiple family members and homo and heterodimer formation affecting receptor activity [291,292]) the dark induced upregulation of certain ABA receptors may have a more nuanced affect upon ABA signalling.

The effect of mutations in ABA biosynthesis and signalling genes on the dark induced upregulation of PYL5 were analysed in fig. 4.8. Both *q1124* and *nced3/5* mutants showed increased *PYL5* transcript levels under light conditions, and no significant changes under dark conditions. This suggests that in light, basal ABA signalling may be repressing *PYL5* expression, whereas in darkness this repression is lifted. ABA degradation mutants with increased ABA levels, *cyp707a1* and *cyp707a3,* show slightly reduced *PYL5* levels in both light and dark conditions. This suggests in these mutants increased ABA levels may be increasing the repression of *PYL5* in both light and dark conditions. Overall, these data suggest there is a degree of interaction between light, darkness, and ABA signalling over the regulation of *PYL5* expression.

4.4.3 Exploring a physiological role for the dark induced upregulation of ABA receptors

To explore whether there is a physiological role for the upregulation of ABA receptors in dark conditions the densities of epidermal cells (stomata and pavement cells) were analysed in plants grown under different day lengths. Under different daylengths plants would experience different amounts of darkness and it was hypothesised that this could allow dark induced effects of ABA signalling to have an effect on stomatal development. In order to measure plants at the same developmental stage, leaves were analysed upon plant bolting.

Here, pavement cell density decreases and stomatal index increases with increasing daylength while stomatal density remains the same. This suggests more cells are entering the stomatal lineage and pavement cells are larger under long day conditions (fig. 4.9). In both short and long day conditions the ABA degradation and activation mutants, *cyp707a1* and *bglu18-1*, show no differences to wildtype. The strong ABA biosynthesis and signalling mutants *nced3/5* and *s112458* show increased stomatal and pavement cell density when compared to wildtype, with no difference in stomatal index. This is similar to what has been observed for strong ABA biosynthesis mutants before and suggests strong mutations in ABA signalling and biosynthesis negatively affect pavement cell enlargement [209]. However, the quadruple receptor mutant *q1124* shows no difference of stomatal density, pavement cell density, or stomatal index with wildtype under long day conditions, but an increased pavement cell density and decreased stomatal index under short day conditions. This suggests under short day conditions pavement cells are smaller and/or fewer cells are entering the stomatal lineage in *q1124* mutants. This in turn suggests the change in daylength could be inhibiting pavement cell expansion and/or entrance into the stomatal lineage through one or more of the ABA receptors affected in the *q1124* mutant (*PYR1, PYL1, PYL2, PYL4*). However, the addition of mutations in *PYL5* and/or *PYL8* appear to rescue this.

Further work is required in order to determine whether these day length dependent differences in the *q1124* are due directly to the extended night period experienced by plants under short day conditions, or through other indirect differences between the short and long day conditions. These indirect daylength differences include circadian regulation differences (which have been shown to regulate stomatal aperture [293]), differences in sugar production, the absolute age of the plants at bolting, among others.

4.5 Conclusion

This study has shown that in Arabidopsis a specific set of ABA receptors are upregulated by dark treatment in leaf tissue. Focusing on the *PYL5* ABA receptor, the receptor most upregulated by darkness, it is shown that the upregulation of *PYL5* is likely mediated in part by the lifting of ABA signalling mediated *PYL5* expression inhibition (or transcript degradation) that occurs under light conditions. However, the physiological relevance for *PYL5* upregulation in darkness remains unclear, analysing stomatal development for plants grown at different day lengths there could be a role for *PYL5* in regulating pavement cell expansion and/or entry of cells into the stomatal lineage, however more work is required.

CHAPTER 5: EXPLORING THE ROLES OF AN ARABIDOPSIS CGMP ACTIVATED KINASE IN CONTROLLING STOMATAL MOVEMENTS

5.1 Introduction

cGMP is a second messenger signalling molecule that has been linked to the regulation of a number of physiological and developmental processes in plants. These processes include root growth [294–296], seed germination [297,298], defence against pathogens [299,300], and stomatal movements [301–304]. cGMP was originally identified and isolated from rat urine in 1963 [305] but it wasn't until the 1980s that a function for the signalling molecule was determined, when cGMP levels in smooth muscle cells were found to be increased by a factor that was eventually identified as nitric oxide (NO) [306], as well as the atrial natriuretic peptide [307]. This increase in cGMP levels was found to be required for smooth muscle cell relaxation [308]. By the 1980s key components of cGMP signalling had been identified in mammals including phosphodiesterases, guanylyl cyclases , and a cGMP activated kinase (protein kinase G – PKG) as reviewed here [308,309].

5.1.1 Key components of cGMP signalling have only recently been discovered in plants

In comparison to metazoans the physiological relevance of cGMP signalling in plants has been contentious until relatively recently [310]. One reason for this is because of the low levels of cellular

cGMP. Whereas animals and other eukaryotes have cellular cGMP levels in the nano-micro molar range, in plants cGMP levels are firmly in the nano molar range [311]. Another reason is due to the lack of identification of key cGMP metabolism proteins. A guanylyl cyclase (GC) candidate wasn't identified until 2003. Here, GUANYLYL CYCLASE 1 (GC1) was identified in Arabidopsis and shown to possess GC activity forming a new class of GCs [312]. Since the discovery of GC1, a number of leucine rich repeats receptor like kinase (LRR-RLK) proteins have been identified as potentially harbouring a GC domain within their kinase domains (including the brassinosteroid receptor BRASSINOSTEROID INSENSITIVE 1 - BRI1 [313,314]). Interestingly, for the LRR-RLK PHYTOSULFOKINE RECEPTOR 1 (PSKR1), which has also been shown to possess GC activity within its kinase domain [315], Ca^{2+} has been demonstrated to be the switch between kinase and GC catalytic activity [316]. Additionally, a NO dependent guanylyl cyclase has been identified in Arabidopsis [317], however compared to mammalian NO dependent cyclases, this protein shows a much lower rate of cGMP synthesis [318].

The identities of plant cGMP phosphodiesterases and cGMP activated kinases (the plant equivalents of PKGs) have only been identified in the past 3 years [298,303]. In the case of plant of phosphodiesterases, although plant extracts had been shown to possess phosphodiesterase activity, studies were unsuccessful in their attempts to purify and isolate proteins with phosphodiesterase activity [318]. A protein with phosphodiesterase activity was discovered in Marchantia [319], however no homologues of this protein could be found in vascular plants. Recently a novel plant phosphodiesterase (PHOSPHODIESTERASE 1 - PDE1) was identified in Arabidopsis through the use of extensive cross species sequence analysis and an initial screen using the cGMP fluorescence reporter δ-FlincG. PDE1 was shown to be involved in stomatal responses to ultraviolet A (UVA) light [303]. Similarly to plant phosphodiesterases, the search for plant cGMP activated kinases has been unsuccessful [320] until recently with the discovery of a protein with a cGMP binding domain coupled with both kinase and phosphatase domains in rice (*Oryza sativa*) [298]. This protein was shown to act as a phosphatase, until binding to cGMP, upon which its phosphatase activity was inhibited and its kinase activity was promoted, thus it was identified as a plant PKG. In both cases the plant PKG and PDE show distinct features when compared to their metazoan counterparts, which suggests there has been a significant degree of divergence between the evolution of cGMP signalling in plants and animals. This leaves the possibility for novel cGMP signalling dynamics to be discovered in plant systems.

5.1.2 The role of cGMP signalling in stomatal movements

cGMP signalling was first linked to stomatal movements when it was implicated in the stomatal opening response to plant natriuretic peptides [321,322]. Here through the use of a membrane permeable cGMP analogue (8-Br-cGMP) studies suggest cGMP opens stomata through the stimulation of inward rectifying K^+ channels. Intriguingly, they found that cGMP inhibits the activity of the main driver of stomatal opening, the H^+ATPase. Additionally, cGMP was linked to the auxin induced stomatal opening response, via similar pharmacological experiments [323–325]. However, these pharmacological studies should be interpreted with caution due to the assumptions that plant cGMP signalling is analogous to metazoan cGMP signalling when using pharmacological treatments.

In contrast with the work suggesting cGMP is involved in stomatal opening, a study also linked cGMP signalling to ABA and NO induced stomatal closure. The study found that, although 8-Br-cGMP treatment of epidermal peels from pea plants (*Pisum sativum*) did not induce closure on its own, it could rescue NO and ABA induced stomatal closure phenotypes when they were coupled with a guanylyl cyclase inhibitor [304]. Additionally, Arabidopsis seedling cGMP levels were found to increase in response to salt and osmotic stress [326]. Further work, measuring cGMP concentrations, using guanylyl cyclase inhibitors, and 8-Br-cGMP, linked cGMP to ABA induced stomatal closure. Here they placed cGMP production downstream of H_2O_2 and NO, and upstream of Ca^{2+} in the ABA signalling pathway [327]. This leads to a potential situation in which cGMP signalling may be inducing Ca^{2+} oscillations in guard cells. This is partially supported by the fact cyclic nucleotide gated channels (CNGCs) CNGC5 and CNGC6 were shown to mediate inward guard cell Ca^{2+} currents in response to 8-Br-cGMP [328]. However, it was also shown using *cngc5/6* double mutants that these channels were not required for ABA induced Ca^{2+} currents or stomatal closure, but it does not rule out other CNGC channels or redundancy between many CNGCs being responsible for ABA induced Ca^{2+} currents.

An explanation for the seemingly dual role nature of cGMP was explored in a study that identified a nitrated cGMP derivative in Arabidopsis guard cells. This study proposed that during stress responses (such as an ABA response) reactive nitrogen species (generated by the reaction of NO and reactive oxygen species) react with cGMP to form 8-nitro-cGMP, which is then responsible for triggering cytoplasmic Ca^{2+} elevations and ultimately stomatal closure. However non-nitrated cGMP (represented by treatment with the cell permeable 8-Br-cGMP) is able to

induce stomatal opening in darkness, potentially explaining the seemingly contradictory roles of cGMP [301]. A further cGMP derivative 8-mercapto-cGMP has also been identified and proposed to function in H_2S induced stomatal closure [302].

In addition to ABA, NO, and H_2S induced stomatal closure, as previously mentioned, cGMP signalling has also been linked to UVA-induced stomatal closure with the discovery of a plant specific phosphodiesterase PDE1 [303]. This suggests wide ranging roles for cGMP with respect to regulating stomatal movements.

This current investigation set out to explore the function of a predicted cGMP binding protein in Arabidopsis. Specifically, the study aimed to determine whether this protein was involved in plant responses to drought using whole plant gravimetric transpiration measurements and thermal imaging. Additionally, stomatal movements in response to ABA, Ca^{2+}, and darkness were analysed. Midway through the study this protein was identified as a plant specific PKG in rice (*Oryza sativa*) [298], therefore in this study the protein in question is referred to as PKG. Using homozygous T-DNA insertion mutants of *PKG* this study finds no obvious role in plant drought responses, or ABA and Ca^{2+}-induced stomatal movements. However, this study does observe defective dark-induced stomatal closure in *pkg* mutants, suggesting a potential role for cGMP signalling (or at least the protein identified as PKG) in this process.

5.2 Specific methods

5.2.1 Controlled drought experiment

Experimental Set up: 71 individual pots were cut out from 4x6 plastic pot insert trays. Each individual pot was numbered and its weight was recorded. Pots were filled with a 3:1 all purpose compost (Sinclair): silver sand (Melcourt) mixture. After each pot was filled the weight was recorded. Additionally, after every 10 pots, a soil sample was taken and placed in a pre-weighed container and weighed. After every individual pot was filled, the soil samples were placed in a 90˚C oven to determine the soil water content (SWC – g H_2O g^{-1} soil) of the soil mixture used to fill the pots. The SWC was assessed over the potting period and found to remain relatively constant. The average SWC content value was used to determine the amount of dry soil (ie the dry weight DW) in each individual pot. Individual pots were watered with the amount of water required to generate an SWC of 0.8 g H_2O g^{-1} soil. An SWC of 0.8 g H_2O g^{-1} soil was chosen as the SWC at which point the soil mixture was saturated was determined to be 0.903 ± 0.009 g H_2O g^{-1} soil, therefore an SWC of 0.8 g H2O g^{-1} soil would allow the soil to be close to saturation point. The SWC of each pot can be determined by (FW – DW)/DW. Where FW is the fresh weight of the pot ie, the current weight of the pot including soil, plant and water.

Plant growth pre-experimental week: Plants were sown and stratified as described in the general methods. After 1 week of growth seedlings were transplanted individually into pots with a SWC of 0.8 g H_2O g^{-1} soil. Care was taken to transfer as little soil as possible during the transplantation. The location of each pot in the growth chamber was recorded. Plants were grown until 4 weeks of age (28 days). Every day each pot was weighed and watered in order to bring the SWC back to 0.8 g H_2O g^{-1} soil. The location of every pot was randomised every day to account for potential positional effects. Every week, images were taken of each plant rosette against a black background. ImageJ was used to calculate rosette area by thresholding images to generate masks. The area of each mask was measured and converted from pixels to mm^2. This value represented plant rosette area.

Experimental week: Fig. 5.2 shows a simple plan for thermal imaging and gravimetric transpiration measurements over the course of the 5^{th} week (days 27 – 35). At the start of this week plants were either kept at a SWC 0.8 g H_2O g^{-1} soil (well-watered) or left to reach and then maintain a SWC of 0.4 g H_2O g^{-1} soil (drought). Throughout this week the rosette area of each plant was measured daily.

Thermal imaging was carried out using an asc655 camera (FLIR) placed within the plant growth cabinet and analysed using the FLIR ResearcherIR software. Images were captured every minute over the dusk dawn transition periods of days 27/28, 29/30, 31/32, and 33/34. For each individual plant, a mean temperature value was determined from the average of 3 5x5 pixel areas on leaves at similar developmental stages. The mean temperature of each individual plant was used as one data point in subsequent analysis. Data was statistically analysed at specific timepoints using 2-way ANOVAs with TukeyHSD multiple comparison tests in R.

Gravimetric transpiration measurements were carried out to determine the transpiration rates for each plant. In addition to the pots containing Arabidopsis plants, 10 pots containing soil but no Arabidopsis plants were used as controls. 5 were kept at well-watered conditions, and 5 were placed under drought conditions. These empty pots were covered with paper replicas of Arabidopsis rosettes designed from rosette area pictures of the experimental plants. These pots acted as a control for the rate of soil water evaporation unrelated to Arabidopsis transpiration. The paper Arabidopsis replicas covered areas of the pot similar to that of true plants, but unlike the true plants, did not transpire. Plant weights were recorded either at dawn, 2, 4, and 6 hours post dawn, or at 4, 6, and 8 hours post dawn depending on the experimental day.

Transpiration was calculated by determining the loss of water per second in g s^{-1} since the previous weight measurement. This value was converted to mmol s^{-1}. The mean value for the control pots of each treatment were subtracted from the experimental plants at each time point. This value was then divided by the rosette area to determine transpiration rate (mmol m^{-2} s^{-1}). Data were statistically analysed at specific time points using 2-way ANOVAs with TukeyHSD multiple comparison tests in R.

5.2.2 Stomatal movement experiments

ABA inhibition of opening: 5-week-old plants were grown under standard conditions. Leaf discs were harvested pre-dawn as described in general methods. Leaf discs were incubated in 10/50 buffer in darkness (50 mm petri dishes covered in black electrical tape) for 2 hours at 22 °C before transfer to 50 mm petri dishes containing 10/50 buffer supplemented with 0, 0.1, 1.0, or 10.0 μM ABA (0.05% v/v final EtOH) under 120 μmol m^{-2} s^{-1} white light. Leaf discs were

incubated for a further 2 hours before stomatal apertures were measured as described in general methods.

Ca^{2+} induced stomatal closure: 5-week-old plants were grown under standard conditions. Epidermal peels were harvested 2 hours after dawn and transferred to 50 mm petri dishes containing 10/50 buffer. The epidermal peels were incubated under 120 μmol m^{-2} s^{-1} white light for 2 hours at 22 ˚C before transfer to petri dishes containing 10/50 buffer supplemented with 0, 0.1, 1.0, or 10.0 mM $CaCl_2$. Stomatal apertures were measured as described in general methods.

Dark induced stomatal closure: 5-week-old plants were grown under standard conditions. Leaf discs were harvested 2 hours after dawn and transferred to 50 mm petri dishes containing 10/50 buffer. The petri dishes were incubated under 120 μmol m^{-2} s^{-1} white light for 2 hours at 22 ˚C. Leaf discs were transferred to dark petri dishes. Stomatal apertures were measured over a 2 hour timecourse at 0, 30, 60, and 120 mins after transfer to darkness. An additional set of leaf discs were left in light conditions over the 2 hour timecourse to act as a control. Stomatal apertures were measured as described in general methods.

5.3 Results

5.3.1 Identification of a potential cGMP binding protein kinase

In order to identity potential proteins involved in cGMP signalling a search was carried out for proteins containing the cyclic nucleotide binding CAP ED conserved domain (conserved domain id: cd00038/IPR000595). This domain was initially identified in the *Escherichia coli* transcription factor Catabolite Activator Protein (CAP) and functions as a cAMP binding domain altering the activity of CAP transcription factor [329]. This domain was later found to be homologous to domains within mammalian cAMP, cGMP dependent protein kinases, and cyclic nucleotide gated channels (CNGCs) [330,331]. When CNGCs were identified in plants, they were found also to contain this domain [332], including *Arabidopsis thaliana CGNC5* and *CGNC6* which have been shown to participate in guard cell cGMP induced Ca^{2+} influx [328]. However, other than CNGCs there are few known proteins that contain known cyclic nucleotide binding domains in plants. Until recently, with the characterisation of a plant cGMP activated kinase [298], no cyclic nucleotide activated kinases had been identified in plants [320,333].

This search was carried out using the conserved domains database (CDD) on the National Center for Biotechology Information (NCBI). Other than ion transport proteins, only one potential target was identified, AT2G20050 (formally known as AT2G20040). This protein has been mentioned previously [320,333], but until very recently no data have been published regarding it's functional roles [298]. Online Arabidopsis microarray data suggests AT2G20050 is expressed in a variety of cell types (including guard cells) in both root and shoot tissue [334]. Intriguingly, this protein is predicted to contain an N terminal phosphatase domain (serine/threonine phosphatase type 2C, cd00143/IPR001932) and a C terminal protein kinase domain (protein kinase catalytic domain like, cl21453) separated by 2 tandem regions in the middle of the peptide sequence that have homology to the CAP ED domain. This gene has been found to exist as a single copy in Arabidopsis and rice (*Oryza sativa*) and shown to function in rice gibberellin signalling, regulating seed germination, internode elongation, pollen viability, and salt stress developmental responses. It was shown that in the absence of cAMP or cGMP, this protein exhibits phosphatase activity, however in the presence of cAMP or cGMP it can bind to the cyclic nucleotide via one of its CAP ED cyclic nucleotide binding domains (with a 10 fold higher affinity for cGMP over cAMP) which inhibits phosphatase activity and activates kinase activity. It is thought that this protein functions in the gibberellin signalling pathway after gibberellin-induced NO activates cGMP production. This in turn binds and activates the kinase activity of

this protein. Thus cGMP acts as a molecular switch changing the protein's role from de-phosphorylation to that of phosphorylation, leading the study to identify this protein as the plant Protein Kinase G (PKG) [298].

5.3.2 Controlled drought experiment

Two independent homozygous mutant alleles of *PKG* were obtained, *pkg-1* (SALK 108016) and *pkg-2* (SALK 000828). A schematic of the AT2G20050 gene encoding PKG is shown in fig. 5.1. As cGMP signalling has been linked to the control of stomatal apertures in response to various signals [301–304,328,335], the current study set out to explore potential roles for PKG in plant drought responses. A controlled drought experiment was undertaken using thermal imaging and gravimetric transpiration analysis (outlined in fig. 5.2a).

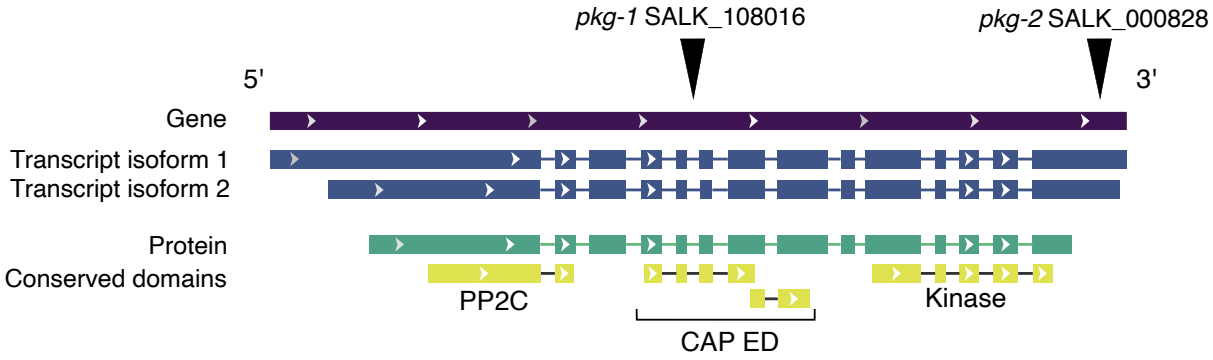

Figure 5.1 AT2G20050 encodes PKG in *Arabidopsis thaliana*

A schematic illustrating the AT2G20050 gene is shown. There are 2 transcript isoforms predicted for the AT2G20050 gene. Both predicted transcript isoforms encode a protein with 3 conserved domains. There is an N terminal phosphatase PP2C domain, a central region containing a CAP ED domain, and a C terminal kinase domain. The two T-DNA insertion mutants isolated for AT2G20050 are *pkg-1* (SALK 108016) and *pkg-2* (SALK 000828). *pkg-1* is located within the centre of the gene in an intron. *pkg-2* is located in the last 300 bp of the gene within the 3' UTR.

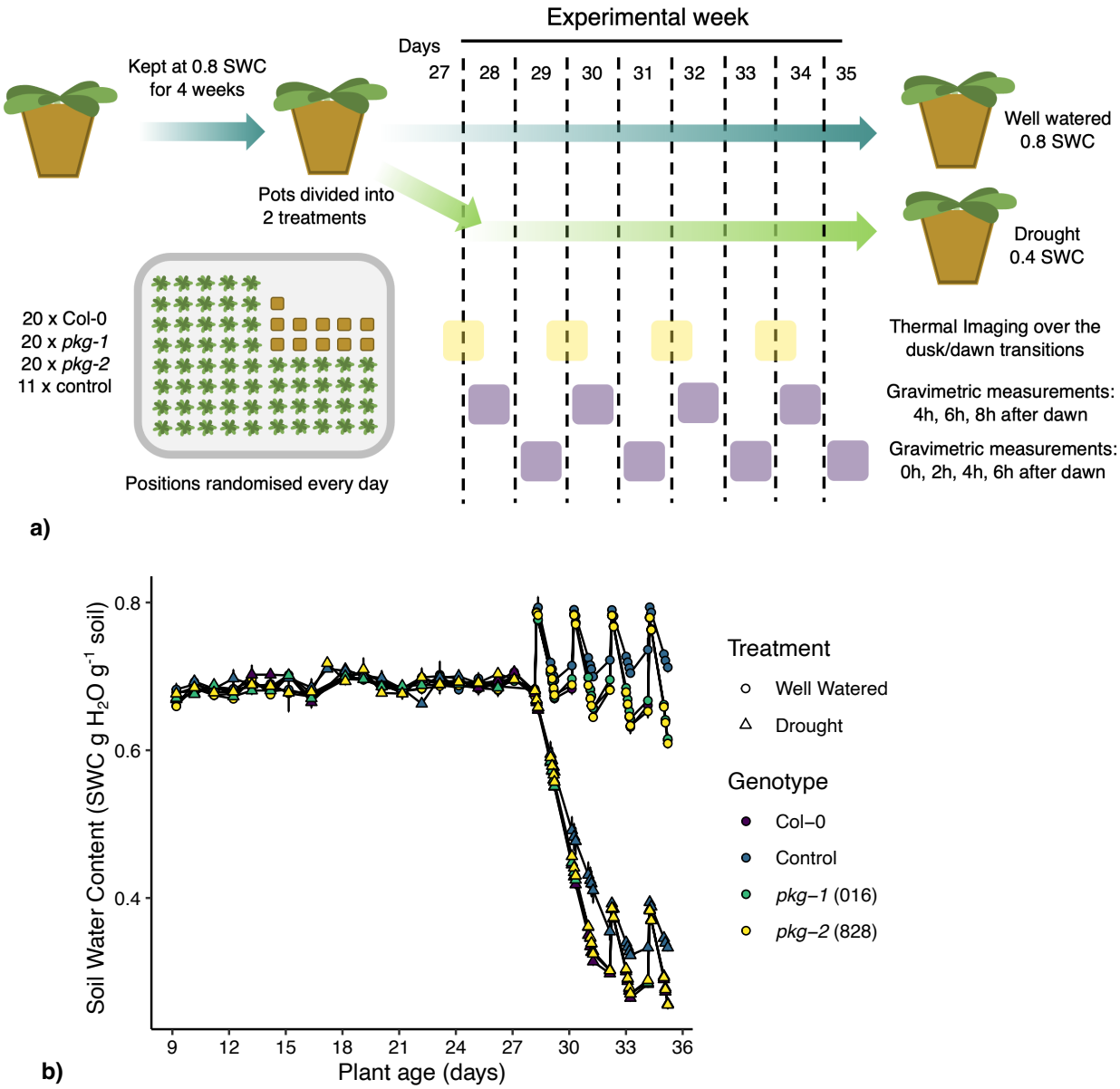

Figure 5.2 Controlled drought experiment overview

a) Graphical overview of controlled drought experiment. Arabidopsis plants, 20 of each genotype and 11 empty control pots, were placed in well-watered conditions (soil water content, SWC = 0.8 g H_2O g^{-1} soil) for 4 weeks. Every day, pot positions were randomised and SWC restored to 0.8 g H_2O g^{-1} soil. On day 28, half of each genotype and 5 control pots were moved to drought conditions (SWC = 0.4 g H_2O g^{-1} soil). Over days 27-35 pots were analysed using thermal imaging and gravimetric transpiration measurements. **b)** Average SWC values for each genotype under well-watered (circles) and drought conditions (triangles) over the course of the experiment. n =10 for treatments involving Col-0, *pkg-1,* and *pkg-2*. n =5-6 for treatments involving control pots. Data is presented as mean ± s.e.m.

5.3.3 Gravimetric transpiration analysis

The SWC for each genotype over days 10-28, prior to the onset of drought is shown in fig. 5.3a. There are no major differences in the SWC experienced between genotypes. At day 16 of the experiment there is a notable dip in SWC for all genotypes, this was due to a delay in the watering of pots for that day, allowing the SWC of each pot to decrease more than usual. However, a difference in SWC of 0.025 g H_2O g^{-1} soil for one day is unlikely to have had a major effect on plant growth. An ANOVA was performed looking at how the mean SWC calculated over days 10-28 correlates with genotype and pot dry soil weight. The mean SWC from days 10-28 for each genotype is shown in fig. 5.3b. There are no significant differences between the SWCs for pots of different genotypes ($F_{3,63} = 2.335$, $p = 0.082$). It was thought that the amount of soil that was initially packed into each pot may affect the changes in SWC. Therefore, the average SWC over days 10-28 was plotted for different pot dry soil weights (fig. 5.3c). Similarly, there are no significant differences in SWC for pots with different soil dry weights ($F_{4,63} = 2.003$, $p = 0.105$). When analysing the SWC values over days 10-28 with respect to pot position (fig. 3d), it is clear there are positional effects in the cabinet, with pots with x coordinates between 7-8 and y coordinates between 2-5 showing slightly lower SWCs than most other pots. However, these differences in SWC are very low ~ 0.01 g H_2O g^{-1} soil. Additionally, this positional effect was accounted for by the random repositioning of pots every day throughout the experiment.

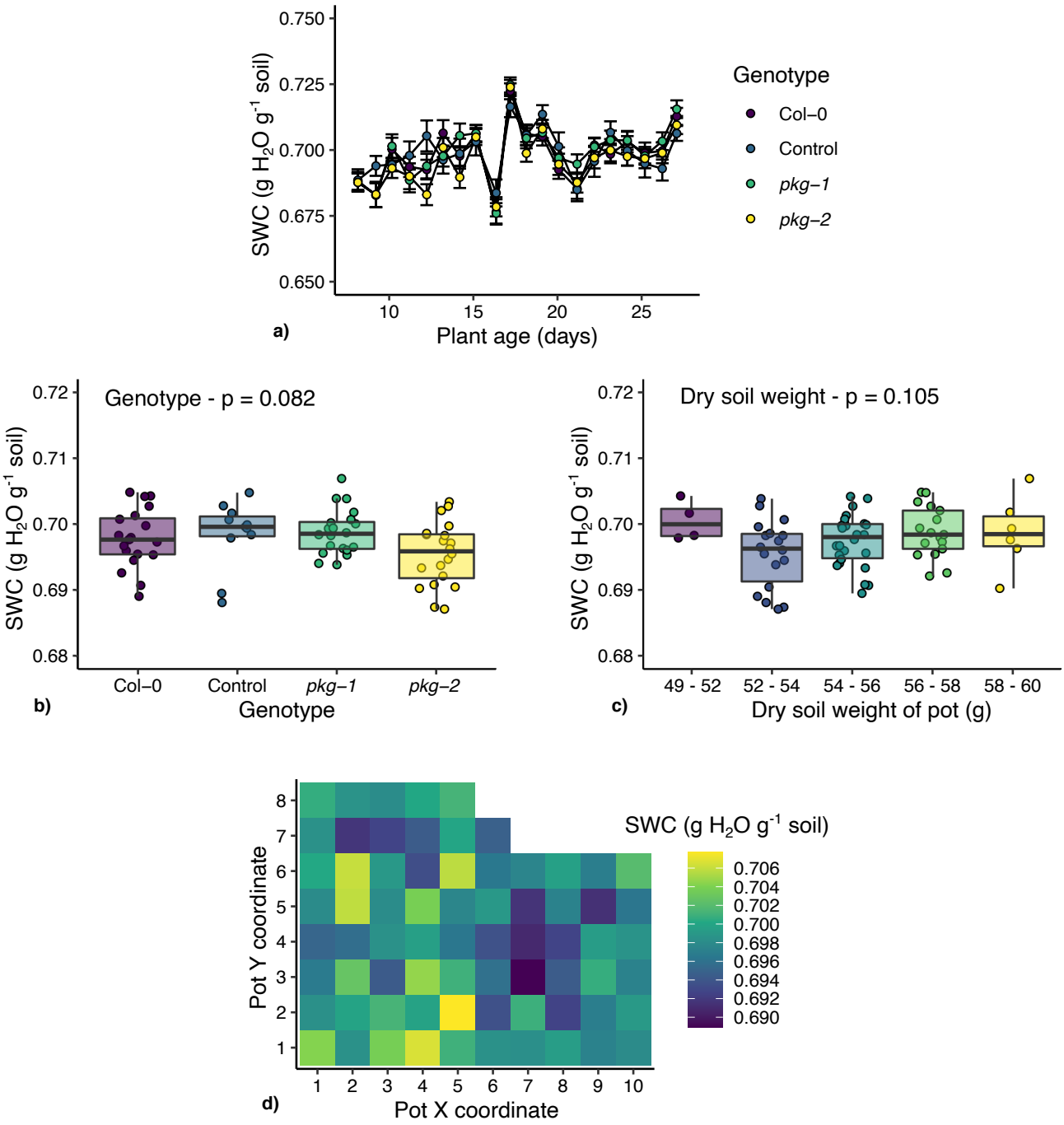

Figure 5.3 The effect of genotype, pot dry weight, and position on SWC

a) Soil water content (SWC) for each genotype over course of the experiment prior to drought treatment (days 10–28). Data is presented as mean ± s.e.m. for each genotype. n = 20 for Col-0, *pkg-1*, and *pkg-2*. **b)** and **c)** Average SWC over days 10-28 for each pot grouped by genotype and pot dry soil weight categories respectively. Data is presented as boxplots showing the median and interquartile range (IQR), whiskers show maximum and minimum data points within 1.5 * IQR. All data are represented by points. For **b)** n = 20 for Col-0, *pkg-1*, and *pkg-2* and n = 11 for control pots. For **c)** n = 4-26. Data was analysed using a 2-way ANOVA. **d)** mean SWC for each pot_position over days 10-28. SWC values are represented by fill gradient.

The SWC data for each genotype over the experimental week (days 27–35) are shown in fig. 5.4a. The spikes in SWC observed after 28 days (fig. 5.2b and fig 5.4a) are due to the weighing of plants 3-4 times daily in order to gravimetrically determine transpiration. On day 28 pots were split into two treatment groups: a well-watered group (maintaining a SWC of 0.8 g H_2O g^{-1} soil) and a drought group (with a decreased SWC of 0.4 g H_2O g^{-1} soil). It took until day 31 for pots to reach an SWC of 0.4 g H_2O g^{-1} soil. As expected, control pots showed the slowest decrease in SWC likely due to the fact that they contained no transpiring Arabidopsis material. The water loss per gram of dry soil (μmol s^{-1} g^{-1}) was determined for every pot from day 31 onwards (fig. 5.4b). By subtracting the mean water loss rates of the control pots (which represent water loss from soil evaporation for each treatment) from the pots containing Arabidopsis and multiplying by the dry soil weight and area covered by each Arabidopsis rosette, the transpiration rates of each pot could be measured in mmol m^{-2} s^{-1} (fig. 5.4c). Each transpiration value represents the average transpiration rate since the previous weighing. Therefore, the initial values for each day represent the average transpiration rate since 8 hours post dawn for days 31, 33, 35 and 6 hours post dawn for days 32 and 34. As these initial values for each day encompass the previous night, they are expectedly lower than other values recorded in the day due to stomatal closure at night.

The difference in transpiration rates between plants under well-watered and drought conditions increases through the experimental week (fig. 5.4c). This appears to be due to an increase in the transpiration rates of well-watered plants as the experimental week continues. The final transpiration measurements of day 35 are shown in fig. 5.4d. There is a significant effect of drought treatment on transpiration ($F_{1,51} = 35.476$, $p < 0.0001$), where plants exposed to drought show reduced transpiration values. No significant differences in transpiration measurements are observed between the different genotypes ($F_{2,51} = 1.373$, $p = 0.263$), suggesting no strong mutant phenotypes with respect to transpiration. Due to the low precision of the experiment, this doesn't rule out weaker phenotypes.

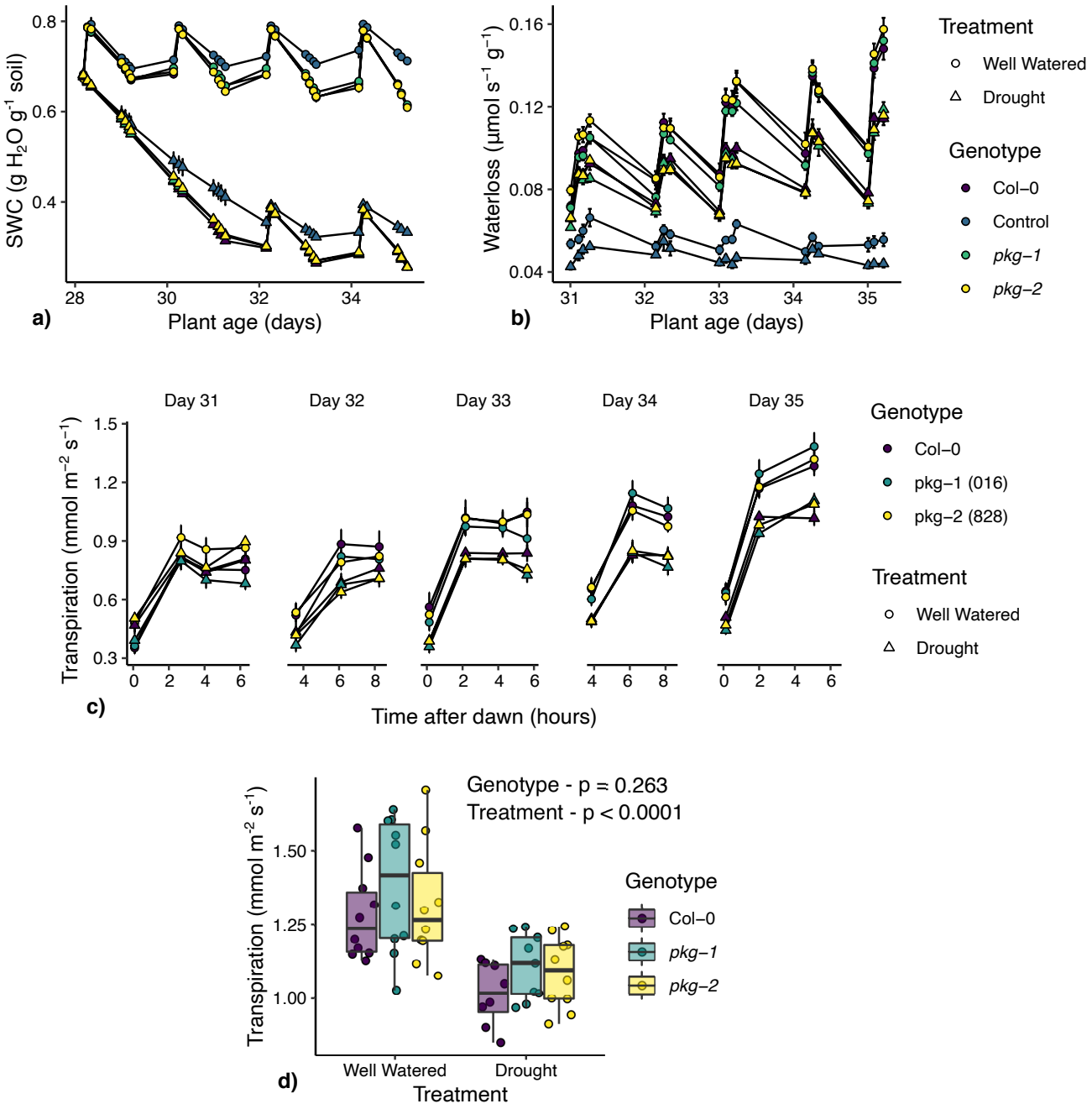

Figure 5.4 Gravimetric Transpiration Analysis over experimental week

a) soil water content (SWC) values for each genotype and treatment combination over the experimental week (days 28-35). n = 10 for Col-0, *pkg-1*, and *pkg-2* treatment, and n = 5 for each control treatment. **b)** waterloss per gram of pot dry soil per second for each genotype and treatment combination over days 31-35. n = 9-10 for Col-0, *pkg-1*, and *pkg-2* treatments, and n = 4-5 for control treatments. **c)** transpiration values over days 31-35 for each genotype treatment combination, n =9-10. Data is presented as mean ± s.e.m. for **a)**, **b)**, and **c)**. **d)** transpiration values of the last recording of day 35. Data is presented in boxplots showing median and interquartile range, with whiskers showing maximum and minimum datapoints within 1.5 * IQR. n = 9-10, all data are represented by data points. Data statistically analysed using a 2-way ANOVA.

5.3.4 Thermal Imaging Analysis

Arabidopsis leaf temperatures were analysed using thermal imaging over the dusk and dawn transition periods. Initially, to determine whether there were position, genotype, treatment, or day effects on leaf temperature, the average temperatures were analysed directly on the onset of dusk and dawn (figs 5.5 and 5.6 respectively). For dusk, an ANOVA analysing how leaf temperature correlates with pot position, genotype, treatment, and day of experiment, shows day of recording ($F_{3,63} = 159.750$, $p < 0.0001$) and treatment ($F_{1,63} = 35.221$, $p < 0.0001$) have significant effects on leaf temperature, whereas genotype ($F_{2,63} = 0.596$, $p = 0.554$) and pot position ($F_{23,63} = 1.266$, $p = 0.228$) do not. Similarly, for the dawn transition day of recording ($F_{3,63} = 150.792$, $p < 0.0001$) and treatment ($F_{1,63} = 50.230$, $p < 0.0001$) show significant effects on leaf temperature. However, position also has a significant (but small) effect on leaf temperature ($F_{23,63} = 3.431$, $p < 0.0001$) whereas genotype does not ($F_{2,63} = 1.943$, $p = 0.151$).

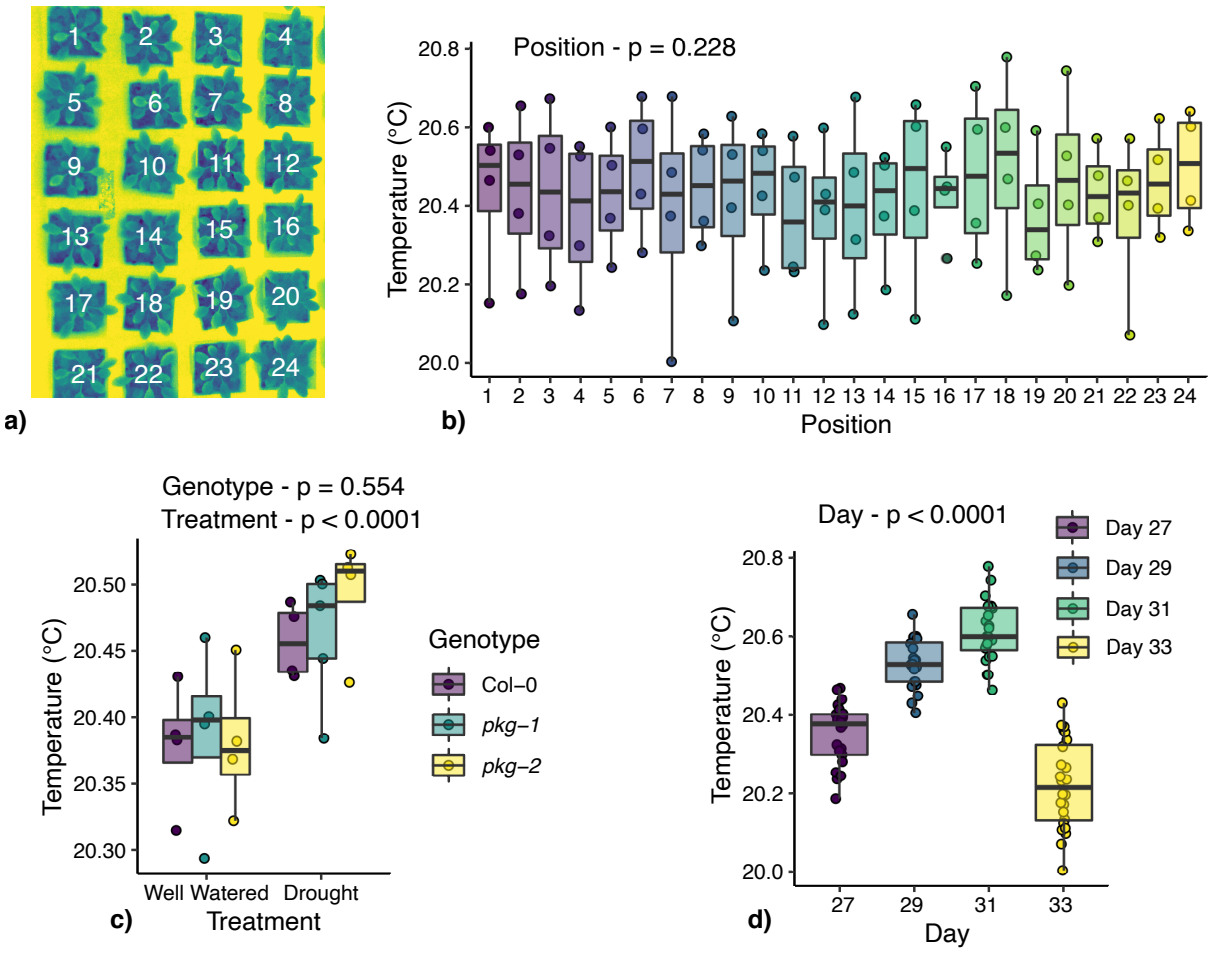

Figure 5.5 Factors affecting thermal imaging at the dusk transition

a) a thermal image representing the positions of pots during the imaging analysis. **b)** average leaf temperature at the onset of dusk for each pot position, n = 4. **c)** leaf temperatures for each genotype and treatment combination (average for each pot over 4 thermal imaging runs), n = 4. **d)** average leaf temperature at the onset of dusk for each pot categorised by the day of thermal imaging, n = 24. Data from **b)**, **c)**, and **d)** are represented by boxplots showing median, interquartile range (IQR) with whiskers showing minimum and maximum datapoints within 1.5 * IQR, all data are represented by data points. Data were analysed using an ANOVA.

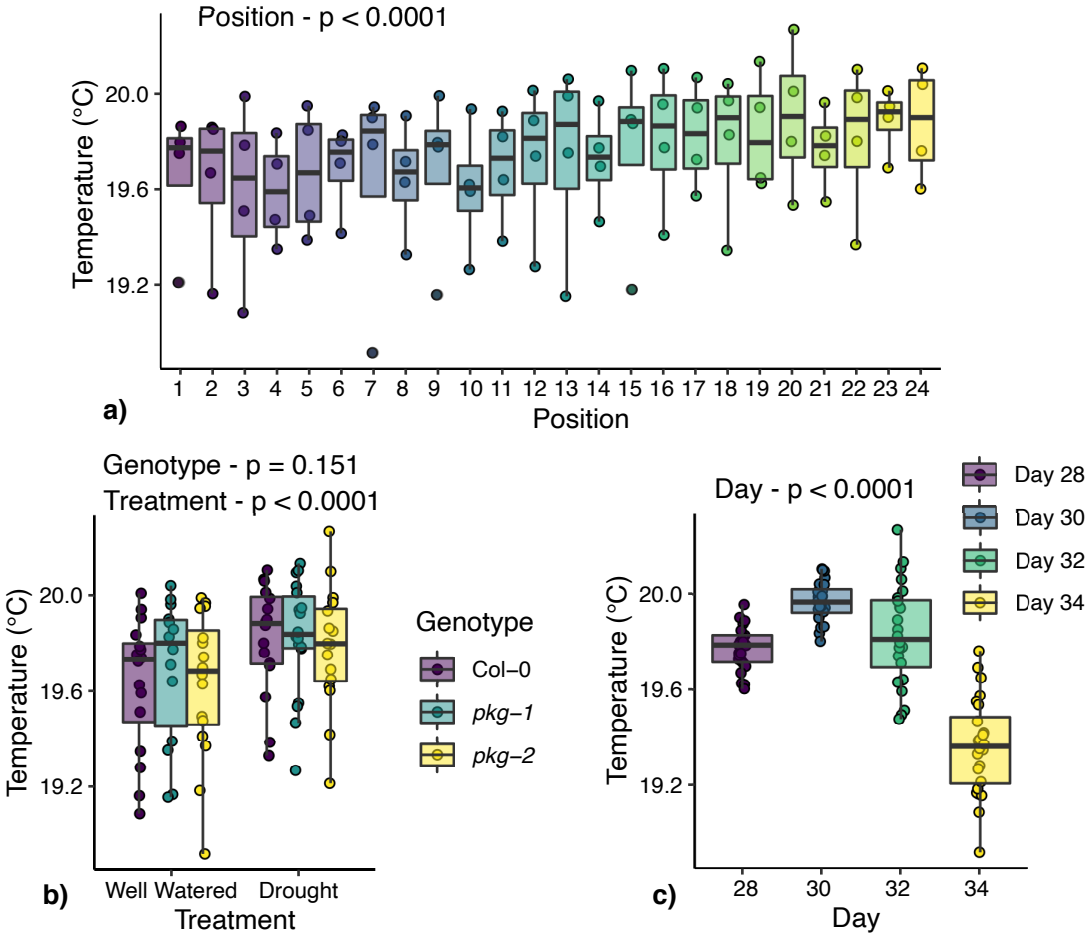

Figure 5.6 Factors affecting thermal imaging at the dawn transition

a) average leaf temperature at the onset of dawn for each pot position, n = 4. **b)** leaf temperatures for each genotype and treatment combination (average for each pot over 4 thermal imaging runs), n = 4. **c)** average leaf temperature at the onset of dawn for each pot categorised by the day of thermal imaging, n = 24. Data from **a)**, **b)**, and **c)** are represented by boxplots showing median, interquartile range (IQR) with whiskers showing minimum and maximum datapoints within 1.5 * IQR, all data are represented by data points. Data were analysed using an ANOVA.

The absolute leaf temperatures of *pkg* mutants and WT over the dusk transition period are shown in fig. 5.7a. On all days, leaves show a reduction of temperature in response to dusk. This is likely due to turning off the cabinet lights, and thus less light energy is warming the leaf tissue. Initially on days 27 and 29 there are no obvious differences between the well-watered and drought treatments. At days 31 and 33 differences start to appear between the two treatments. The temperature of leaves 2 hours after the onset of dusk on day 33 are shown in fig. 5.7b. There is no significant effect of genotype on leaf temperature ($F_{2,18} = 0.039$, $p = 0.962$), but drought treated plants show significantly higher temperatures ($F_{1,18} = 14.014$, $p = 0.001$). The higher temperature leaves of the droughted plants suggest that stomata may be more closed. However, similar to the gravimetric transpiration data (fig. 5.4) there are no clear and consistent differences between the different genotypes.

Absolute leaf temperatures over the dawn transition period are shown in fig 5.8a. Here, the inverse to what is seen at dusk is observed. Upon, the onset of dawn there is an increase in leaf temperature, likely caused by the turning on of cabinet lights. Similarly to dusk, differences between well-watered and drought treated plants do not appear until days 32 and 34. Fig. 5.8b shows leaf temperatures 2 hours after the onset of dawn on day 34. Increased leaf temperatures are observed in drought treated plants ($F_{1,18} = 17.355$, $p < 0.001$) , and there are no clear significant differences between genotypes ($F_{2,18} = 0.135$, $p = 0.874$) .

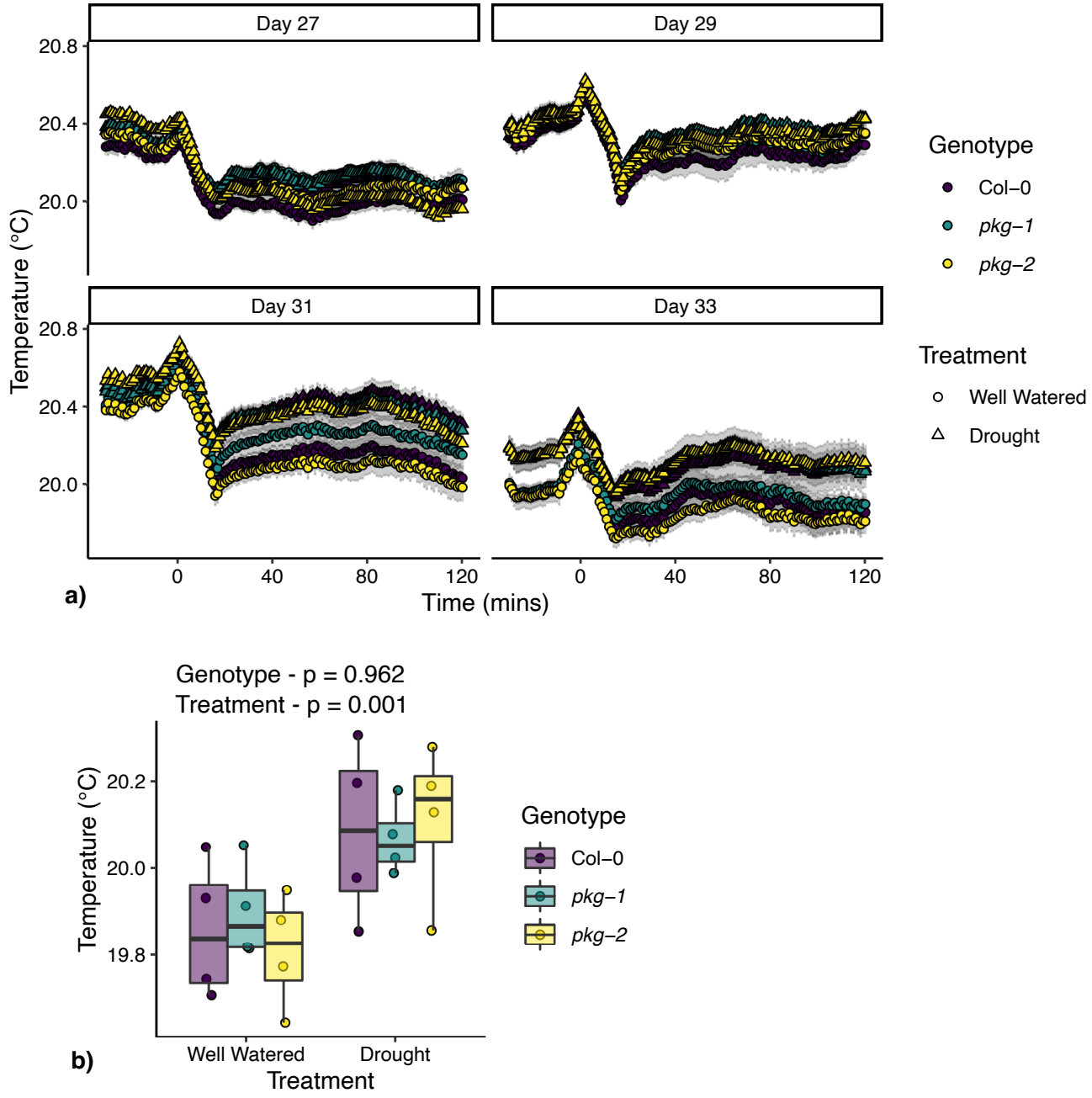

Figure 5.7 Leaf temperature over the dusk transition

a) Leaf temperature over the dusk transition period for all genotype and treatment combinations. Data are presented as mean ± s.e.m. n = 4. **b)** Leaf temperatures 120 mins after the onset of dusk on day 33. Boxplots represent the median and interquartile range (IQR), and whiskers represent the minimum and maximum datapoints within 1.5 * IQR for each genotype treatment combination, n = 4. Data was analysed using a 2 way ANOVA.

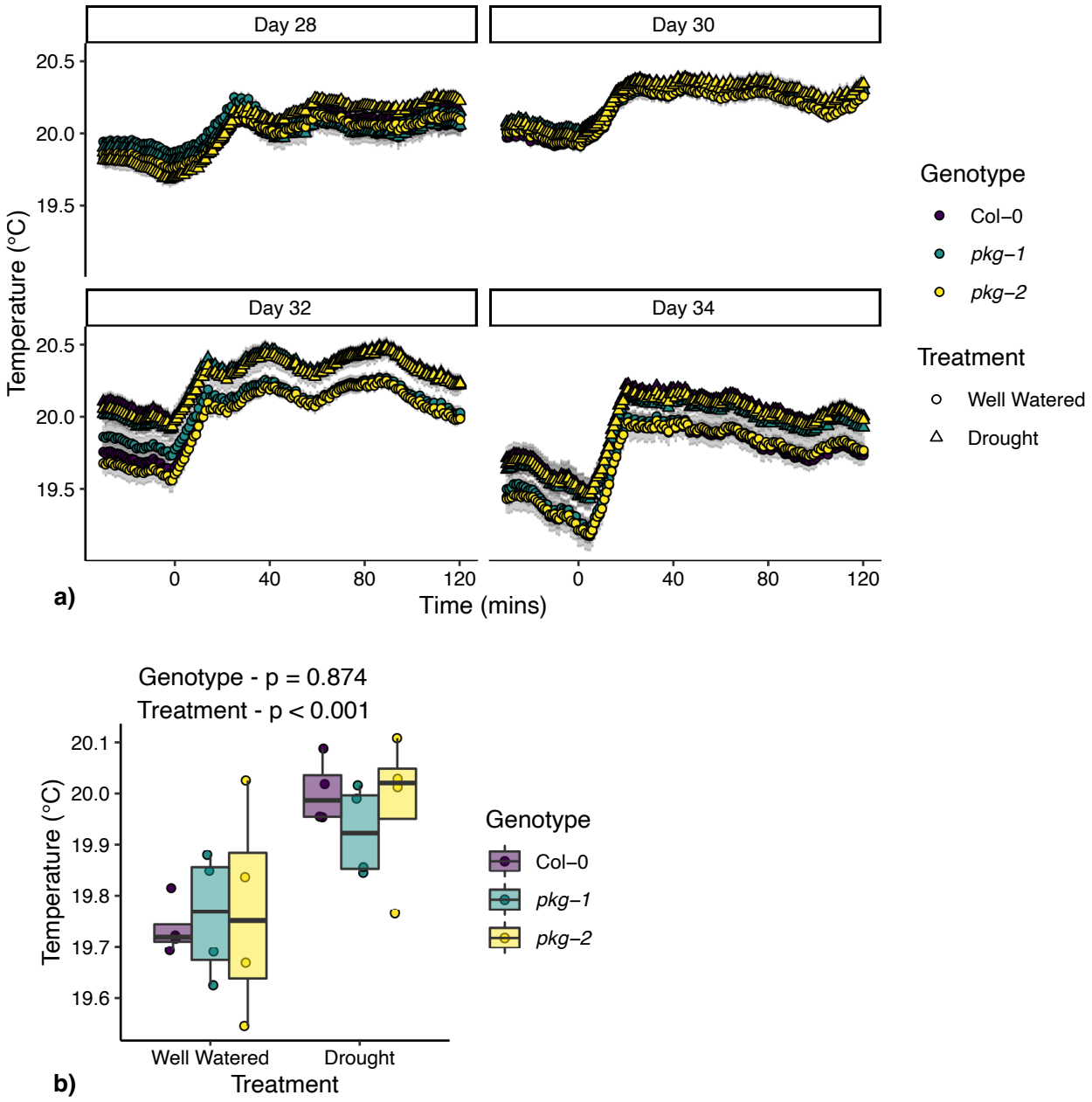

Figure 5.8 Leaf temperature over the dawn transition

a) Leaf temperature over the dawn transition period for all genotype and treatment combinations. Data are presented as mean ± s.e.m. n = 4. **b)** Leaf temperatures 120 mins after the onset of dawn on day 34. Boxplots represent the median and interquartile range (IQR), and whiskers represent the minimum and maximum datapoints within 1.5 * IQR for each genotype treatment combination, n = 4. Data was analysed using a 2 way ANOVA.

5.3.5 Mutations within PKG do not affect ABA inhibition of stomatal opening

The ability of ABA to inhibit stomatal opening in the *pkg* mutants was tested. Here, leaf discs of *pkg-1* and *pkg-2* mutants were harvested pre-dawn, incubated in darkness for 2 hours before being transferred into light in the presence of 0, 0.1, 1, and 10 μM ABA. Apertures were measured after 2 hours in light. Fig. 5.9 shows that there are no significant differences between the stomatal responses of Col-0 and *pkg* mutants when placed in light in the presence of ABA. An ANOVA looking at the effect of genotype and treatment on aperture shows the ABA treatment had a large effect on aperture ($F_{3,1048} = 100.302$, $p < 0.0001$), whereas the effect of genotype was much smaller ($F_{2,1048} = 4.542$, $p = 0.011$). However, there was also a significant interaction between the two variables ($F_{6,1048} = 3.130$, $p = 0.005$), which likely stems from the slightly decreased stomatal aperture observed for the *pkg-2* mutant at 10 μM ABA. Regardless these data suggest PKG is not involved in directly mediating ABA-induced inhibition of stomatal opening in leaf discs, supporting the absence of a drought phenotype observed in the controlled drought experiment.

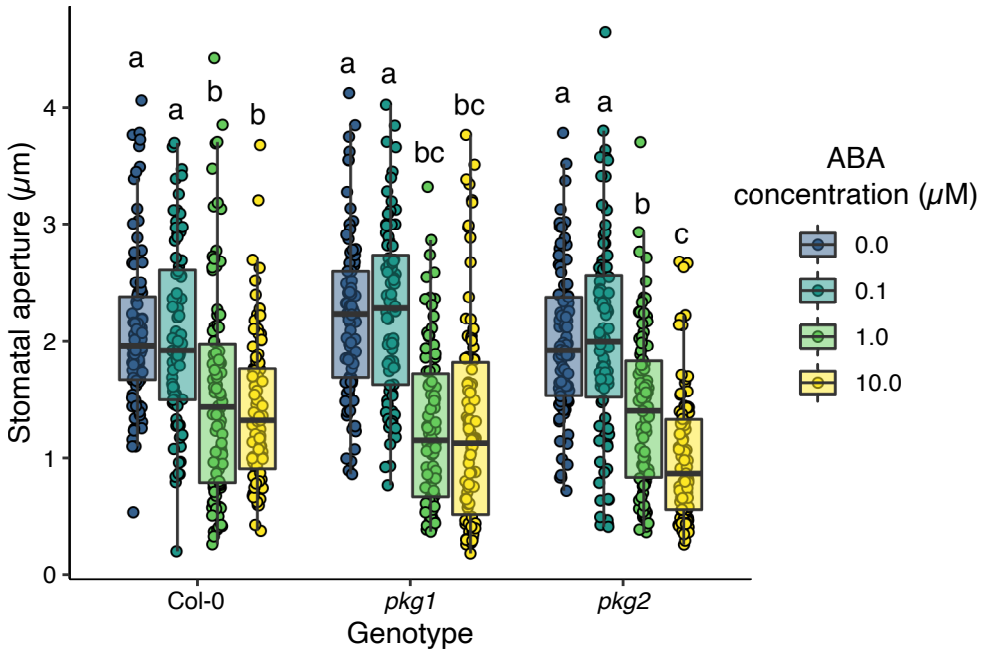

Figure 5.9 *pkg* shows WT ABA inhibition of light-induced stomatal opening

Stomatal apertures were recorded from leaf discs of Col-0 and *pkg* mutants, harvested pre-dawn, incubated in darkness for 2 hours before being transferred to light in the presence of a range of ABA concentrations. Boxplots represent median and interquartile range (IQR) of data, whiskers show the maximum and minimum data points within 1.5 * IQR. All data are shown as points in the figure. n = 80-90 from 8-9 individual plants over 3 independent experiments. Data was statistically analysed using 2-way ANOVA with Tukey post hoc multiple comparison tests, samples indicated with the same letter cannot be distinguished at $p < 0.05$.

5.3.6 Exploring the role of PKG in response to extracellular calcium

As cGMP signalling has been linked to calcium signalling through the function of CNGCs as Ca^{2+} permeable ion channels [328], the effect of extracellular calcium on stomatal aperture was explored in the *pkg-1* and *pkg-2* mutants. Here, an epidermal peel stomatal bioassay was performed in order to test whether guard cells in the absence of functional epidermal cells and mesophyll, respond as WT to $CaCl_2$. Epidermal peels were harvested 2 hours after dawn, incubated under light for a further 2 hours before transfer to a buffer containing various concentrations of $CaCl_2$. Fig. 5.10a and b show the responses of the *pkg-1* and *pkg-2* mutant stomata respectively. As in fig. 5.9, the *pkg* stomata show wild type responses. A 2-way ANOVA performed on the data for *pkg-1* shows there is a weak effect of genotype ($F_{1,712} = 5.636$, $p = 0.018$) but a strong effect of $CaCl_2$ treatment ($F_{3,712} = 100.038$, $p < 0.0001$). The effect of genotype is likely due to the slight increase in stomatal aperture observed across all treatments for *pkg-1*. Similarly, for *pkg-2* there is a weak effect of genotype on stomatal aperture ($F_{1,712} = 10.449$, $p = 0.001$) and a strong effect of $CaCl_2$ treatment ($F_{3,712} = 89.768$, $p < 0.0001$). Like, *pkg-1* there is a slight increase in stomatal aperture across all treatments that is likely behind the significant genotype effect. However, for both *pkg-1* and *pkg-2*, when TukeyHSD multiple comparison tests are performed comparing to them to wild type, no significant differences are observed for comparisons between any treatment. Overall, this suggests extracellular Ca^{2+}-induced closure is not affected by mutations within PKG.

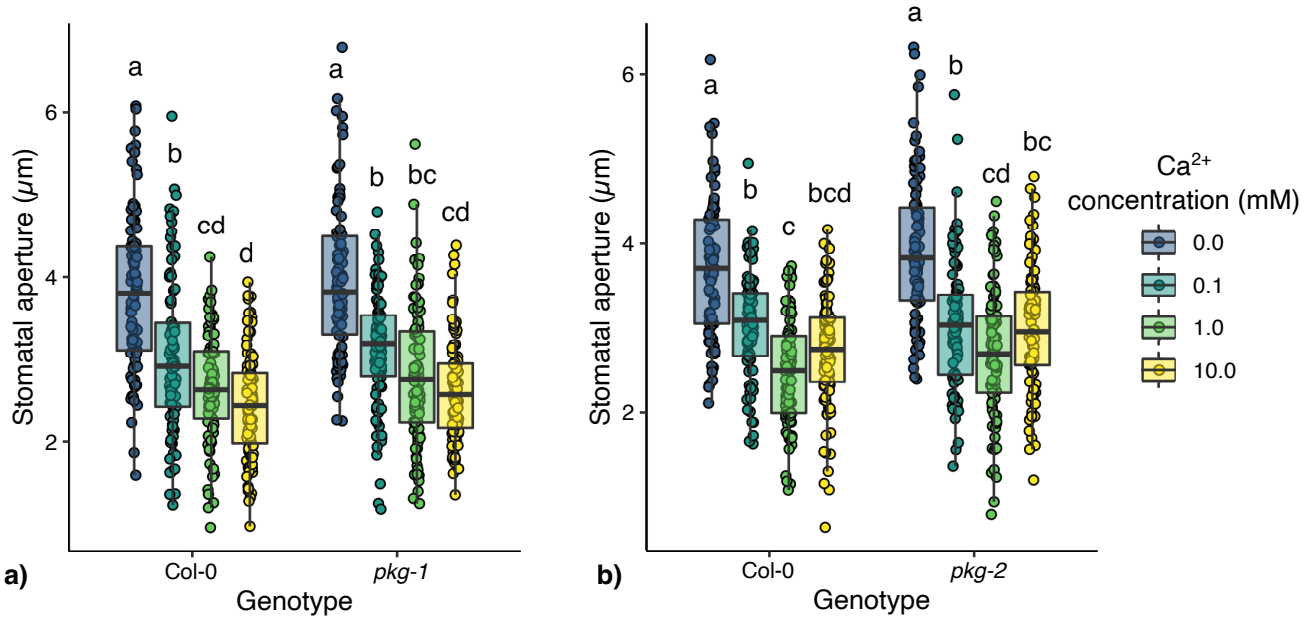

Figure 5.10 Extracellular Ca^{2+} induced closure responses in *pkg-1* and *pkg-2* mutants

Stomatal apertures from leaf discs of **a)** *pkg-1* and **b)** *pkg-2* mutants in response to various to extracellular Ca^{2+}. Epidermal peels were harvested 2 hours post dawn, incubated under light for 2 hours, before transfer to buffer containing various concentrations of $CaCl_2$. Epidermal peels were incubated under light in various $CaCl_2$ concentrations for a further 2 hours before stomatal aperture measurement. Boxplots represent median and interquartile range (IQR), whiskers represent the minimum and maximum data points within 1.5 * IQR. All data are represented by points, n = 90 apertures from 9 plants over 3 independent experiments. Data was statistically analysed using 2-way ANOVAs with Tukey post hoc multiple comparison tests, samples indicated with the same letter cannot be distinguished at $p < 0.05$.

5.3.7 Exploring the role of PKG in the stomatal response to darkness

In addition to exploring the stomatal movement phenotypes of the *pkg* mutants in response to ABA and extracellular Ca^{2+}, the dark-induced closure phenotype of the *pkg* mutant was also investigated. Here leaf discs were harvested 2 hours after dawn, incubated under light for 2 hours, before apertures were monitored over a 2 hour time course in response to darkness. Fig. 5.11 shows the stomatal responses of the *pkg-1* and *pkg-2* mutants to darkness. Unlike the ABA inhibition of stomatal opening and the extracellular Ca^{2+} induced stomatal closure responses, there are clear dark induced stomatal closure defects for the *pkg* mutants. A 2-way ANOVA shows there is a significant effect of genotype and treatment ($F_{2,1396} = 32.014$, $p < 0.0001$) and ($F_{4,1396} = 94.373$, $p < 0.0001$). However, there is also a significant effect of the interaction between genotype and treatment ($F_{8,1396} = 5.851$, $p < 0.0001$). This suggests there is a significant difference between the stomatal apertures of Col-0 and *pkg* mutants in response to darkness. Whereas Col-0 is able to continue decreasing stomatal apertures from of 2.82 ± 0.07 μm at 0 mins to 1.68 ± 0.06 μm at 120 mins, for *pkg-1* and *pkg-2* stomatal apertures finish significantly decreasing after 30 mins. Over the experiment the mean aperture of *pkg-1* and *pkg-2* decrease from 2.76 ± 0.07 μm and 2.75 ± 0.06 μm at 0 mins to 2.28 ± 0.07 μm and 2.18 ± 0.06 μm at 120 mins respectively. Overall, this suggests a role for the PKG protein in the stomatal dark induced closure response.

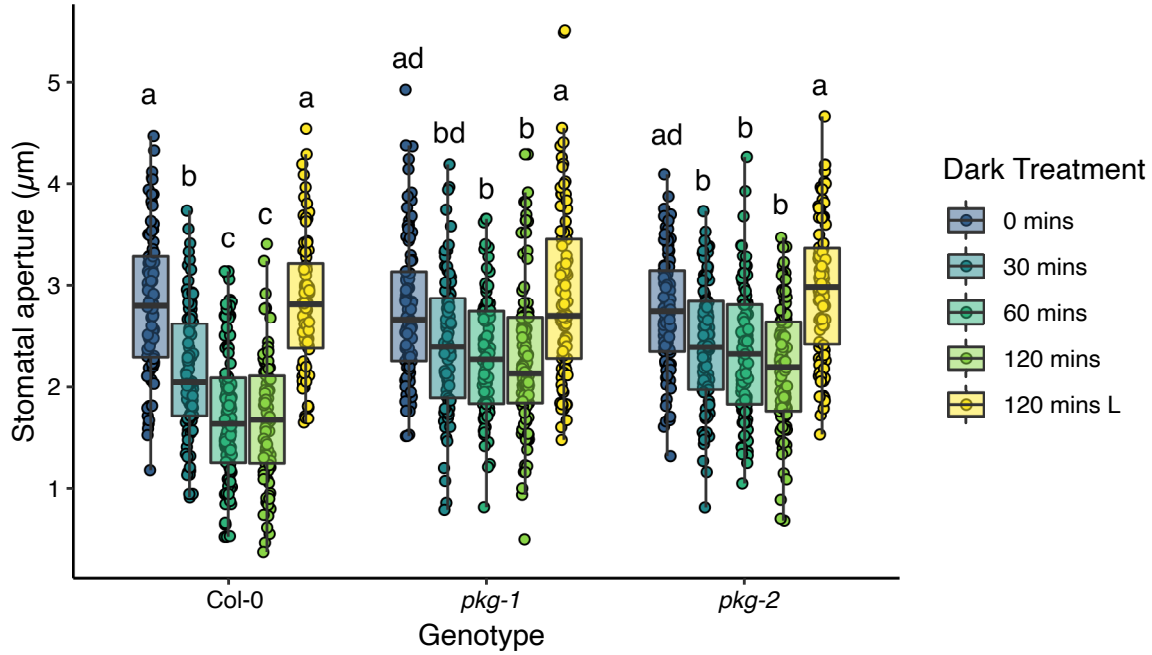

Figure 5.11 Dark induced stomatal closure responses of the *pkg* mutants

Stomatal apertures from leaf discs of *pkg-1* and *pkg-2* in response to dark induced stomatal closure. Leaf discs were harvested 2 hours post dawn, incubated under light for 2 hours before transfer to darkness. Apertures were measured over a 2 hour dark time course, 120 mins L refer to leaf discs that were kept in light over the 2 hour dark timecourse as a control. Boxplots represent the median and interquartile range of the data, whiskers represent the minimum and maximum data points that are within 1.5 * IQR. All data are represented as points in the figure. n = 90 stomata from 9 individual plants over 3 independent experiments. Data was statistically analysed using a 2-way ANOVA with Tukey multiple comparison post hoc tests, samples indicated with the same letter cannot be distinguished at $p < 0.05$.

5.4 Discussion

Until recently, with the identification of a plant specific cyclic nucleotide phosphodiesterase [303] and a plant homologue of PKG [298], the identity of these key cGMP signalling components were unknown in plants [333,336]. Although it is accepted that cGMP is playing a cellular signalling role in plants, the precise mechanisms and roles of cGMP signalling are unclear. cGMP (and various cGMP analogues) have been implicated multiple times in the regulation of stomatal aperture [301–304]. Here, this study uses homozygous mutants within the recently identified PKG gene in Arabidopsis to explore whether PKG plays a role in plant drought responses and stomatal movements.

The water usage of *pkg-1* and *pkg-2* mutants was tracked over a period of 5 weeks, culminating in a week of controlled drought treatment, the experiment is outlined in fig. 5.2. Here, the soil water content (SWC) for each pot was monitored in order to ensure each plant received the same water availability conditions. Gravimetric transpiration measurements have previously been used to track the whole plant responses of various species, including Arabidopsis, in many situations [303,337–340]. The majority of these studies use automated weighing, either through continual use of multiple electronic scales, or through the use of automated weighing systems. Here, due to limited access to balances, pots were manually weighed. It is likely this increased the error of pot weight measurements and as a result the resolution at which plant transpiration could be determined. Fig 5.4 shows that, like wild-type, the transpiration levels of both *pkg* mutants under drought conditions were reduced relative to well-watered plants, suggesting no major roles for PKG in the plant drought response. Due to the reduced resolution of transpiration measurements in this study, smaller differences between wild type and *pkg* mutant transpiration cannot be ruled out. However, thermal imaging of plants over the drought period (figs. 5.7 and 5.8) show no significant differences between wild-type and *pkg* mutant plant leaf temperature also supporting no major role of PKG in plant drought responses.

It is possible that the plants in the controlled drought experiment experienced a mild form of drought treatment. In this experiment no wilting of leaves was observed for any plant genotype, which leads to the conclusion that the drought treatment may not have been sufficiently severe enough to induce a stress response. If the drought treatment had started earlier in the experiment, had been more severe (with an SWC of less than 0.4 g H_2O g^{-1} soil), or carried on

for longer this could have produced a stronger plant drought stress response. If this is the case a role for PKG in the plant drought response cannot be ruled out.

As well as whole plant drought responses, the movement of stomata were also analysed in more detail. The responses of *pkg* mutants to the ABA-induced inhibition of light-induced stomatal opening, extracellular Ca^{2+}-induced stomatal closure, and dark-induced stomatal closure were tested (figs. 5.9, 5.10, and 5.11 respectively). *pkg* mutants displayed wild-type responses to ABA-induced inhibition of opening and extracellular Ca^{2+}-induced closure, however, the dark-induced closure response of *pkg* mutants was defective, suggesting a role for PKG in dark-induced closure. The lack of an ABA-induced inhibition of stomatal opening phenotype is surprising considering cGMP signalling has been suggested to play a role within ABA signalling [304], downstream of H_2O_2 [327]. However, these results only suggest that PKG is not playing a major role in the ABA signalling pathway (in the context of inhibition of stomatal opening). cGMP may be targeting other downstream components such as CNGCs and not PKG in this context. Also, this study focused on the inhibition of light-induced stomatal opening by ABA and although there are similarities between the ABA induced closure and ABA inhibition of opening, these are distinguishable processes [174,341], and thus this study cannot rule out a role for PKG in ABA-induced closure. The lack of an extracellular Ca^{2+} induced closure phenotype is less surprising, as studies have often placed cGMP signalling upstream of Ca^{2+} [327,335], as cGMP signalling activates CNGCs which have been shown to mediate cytosolic Ca^{2+} influxes [328].

The dark-induced closure phenotype exhibited by the *pkg* mutants is more surprising. It is rare to come across mutants that show strong defects within dark induced stomatal closure that aren't also linked to the regulation of photoreceptors, H^+ATPases, or the cytoskeleton [56,156,180,181]. Recently the LRR-RLK pseudokinase GHR1 has been linked to dark induced closure [115], as well as a signalling module involving AtRBOHD/F dependent H_2O_2, NIA1 dependent NO, and a MEK1/MPK6 kinase cascade [182]. This information could lead to a potential signalling pathway outlined in fig. 5.12 involving RBOHD/F, GHR1, MEK1/MPK6, NIA1, and PKG. However, more work would be required to test whether this is true. This would include identifying whether the *pkg-1* and *pkg-2* mutants are knock out or knock down mutants, analysing whether similar dark induced closure phenotypes are observed when leaf transpiration is monitored using gas exchange equipment, and measuring cGMP levels in response to dark treatment.

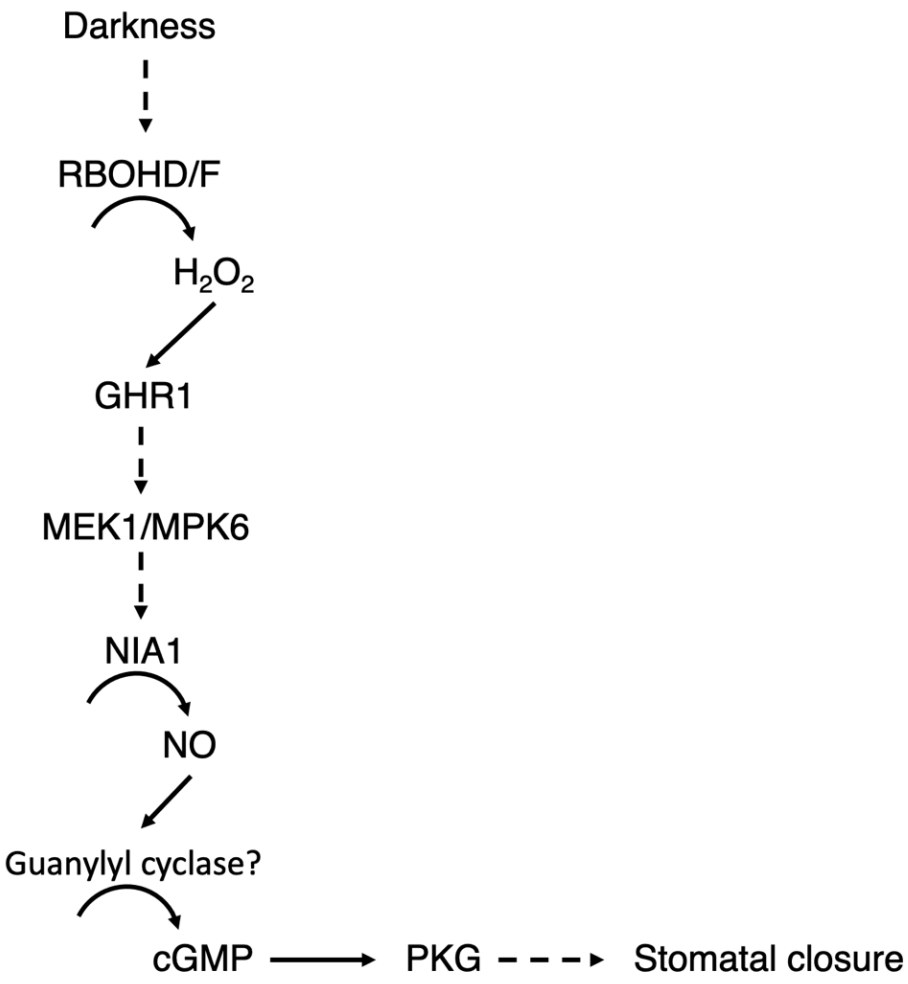

Figure 5.12 Potential mechanism for dark induced stomatal closure

A potential mechanism for dark induced stomatal closure devised from this study as well as studies showing that RBOHD/F, GHR1, MEK1/MPK6, and NIA1 are required for dark induced closure [115,182]. Darkness activates RBOHD/F via unknown mechanisms, the H_2O_2 produced is recognised by GHR1 which either directly or indirectly leads to the activation of the MEK1/MPK6 kinase cascade. The kinase cascade leads to activation of NIA1, producing NO. Here this study predicts this may activate a NO dependent guanylyl cyclase (potentially NOGC1), leading to cGMP production. cGMP binds to PKG which can then phosphorylate further downstream targets leading to stomatal closure.

5.5 Conclusion

In summary, this study used mutants in an Arabidopsis predicted cGMP binding protein that was independently identified a homologue of a plant specific PKG in rice [298]. The drought response of the *pkg* mutants were tested and no evidence was observed for a role of PKG in the plant drought response. Additionally, stomatal movements in response to ABA, extracellular Ca^{2+}, and darkness were analysed in the *pkg* mutants, where wild type stomatal responses were observed for all signals other than darkness. This suggests the Arabidopsis homologue of the plant specific PKG plays a role in stomatal responses to darkness, and potentially links cGMP signalling to the stomatal dark-induced closure.

CHAPTER 6: GENERAL DISCUSSION

The first occurrences of stomata are found in fossil records dating back 400 million years. Stomata were an early adaptation of land plants that facilitated their spread by helping enable them to occupy more extreme environments with more changeable or dry conditions [342]. Correct stomatal function is key for plant success, allowing plants to rapidly regulate gas exchange in accordance with changes in their environment. Through controlling the movement of CO_2 and H_2O into and out of leaf tissue, stomata are able to balance fuelling photosynthesis with restricting water loss [3]. However, as well as acting on an individual plant level, the combined action of vast numbers of stomata found on terrestrial vegetation allow them to play key roles in global carbon and water cycles [1,2].

Stomatal movements and densities are regulated by a host of environmental and internal signals. These include light quality and quantity, water availability, temperature and atmospheric CO_2 concentrations among others. Due to the multitude of signals acting upon stomata, plants have evolved complex signalling pathways that allow the integration of many of these signals (which at times oppose one another) onto the core machinery regulating stomatal movements and development. Using guard cell abscisic acid (ABA) signalling as an example, high degrees of redundancy (such as the 14 member PYL receptor family) and the activation of parallel downstream signalling cascades (such as Ca^{2+} dependent and independent cascades) leads to a robust signalling network with the potential for regulation at multiple points [343].

ABA signalling is best known for its role in the plant drought response where it acts as a potent promoter of stomatal closure and inhibitor of light induced stomatal opening, thereby reducing waterloss under drought conditions [80]. ABA has also been implicated in dark-induced stomatal closure [214]. In Merilo et al., 2013, both ABA receptor, PP2C phosphatase, and ABA biosynthesis mutants have been shown to exhibit increased stomatal conductances in both light and dark conditions. However, all receptor mutants studied except *pyr1pyl1pyl2pyl4pyl5pyl8* are able to reduce their stomatal conductance in response to darkness, suggesting that ABA signalling generally affects stomatal conductance regardless of light condition. The lack of response in

pyr1pyl1pyl2pyl4pyl5pyl8 and reduced response in biosynthesis mutant *aba1*-3 suggests ABA signalling may still be making a contribution to dark induced stomatal closure, however as mutants can be isolated that show defective dark-induced closure but functional ABA responses its role in this process is unclear [180]. There are further links between darkness and ABA as darkness has also been shown to activate ABA signalling during seedling development, through interactions between ABA receptors, PIFs, and the ABA signalling induced transcription factor ABI5 [246]. In chapter 3 the contribution of ABA signalling to stomatal responses to darkness and light is explored.

Chapter 3 presents data that supports a non-essential role for ABA signalling in dark-induced stomatal closure. Measuring the stomatal apertures of ABA receptor mutants *pyr1pyl1pyl2pyl4* and *pyr1pyl1pyl2pyl4pyl5pyl8,* ABA biosynthesis mutant *nced3/5*, ABA activation mutant *bg1* and *bg2*, and ABA degradation mutants *cyp707a1* and *cyp707a3* in response to darkness, the chapter shows that all mutants analysed were able to respond to darkness, similarly to previously reported stomatal conductance data (except *pyr1pyl1pyl2pyl4pyl5pyl8* which had previously been reported to be unresponsive to darkness) [214]. Additionally, the chapter presents further evidence that mutations that affect ABA signalling and metabolism affect stomatal apertures regardless of light or dark treatment, suggesting a potential role for ABA in regulating steady state stomatal apertures. A non-stress role for basal ABA signalling has been discussed recently [232], and is supported by the fact *in vitro* studies have shown certain ABA receptor/PP2C complexes are able to initiate ABA signalling under basal ABA concentrations [233] and that functional ABA signalling is required for normal development under non stress, well-watered conditions [235,344,345].

Although all ABA signalling and metabolism mutants were able to respond to darkness, chapter 3 presents evidence that the speed of stomatal responses to both darkness and light are affected. Other studies have also observed altered stomatal conductance kinetics in ABA signalling and metabolism mutants in response to other signals [150]. The importance of the rapidity of stomatal movements has received renewed interest as a potential target for improving crop water use efficiency [241]. Due to the time difference between changes in photosynthetic activity and stomatal conductance, where stomatal conductance changes an order of magnitude slower than photosynthetic activity, when a plant moves from high to low light, there is a period of time where the photosynthetic activity has adjusted to the new light level but stomatal conductance hasn't (photosynthetic activity and stomatal conductance become temporarily uncoupled). This leads to a period of excessive waterloss. Similarly, when a plant moves from low light to high

light, photosynthetic activity and stomatal conductance also become uncoupled, leading to a period of reduced CO_2 gain [346]. Recently, the genetic manipulation of stomatal kinetics was shown to improve both waterloss and carbon assimilation, leading to increased biomass production in Arabidopsis [240]. This proved particularly effective when plants were grown under fluctuating light conditions, which more closely mirror outdoor conditions than constant light/dark cycles. The data from chapter 3 highlights ABA signalling components as potential targets for manipulating stomatal response speeds.

In chapter 4, the longer-term responses of ABA signalling to darkness are explored. Previous studies have shown that ABA signalling in guard cells is affected on a transcriptional level in response to dark treatment [149] and on both transcriptional and post-translational levels in developing seedlings [246]. Through analysis of microarray and QPCR data, chapter 4 shows a subset of ABA receptors are upregulated in response to darkness. Interestingly the expression levels of the majority of other ABA signalling components (PP2C phosphatases, SnRK2 kinases, and ABA induced transcription factors) show the opposite, downregulation, in response to darkness. The impact this has on net ABA signalling is unclear, however, it is possible that upregulation of ABA receptors and downregulation of the PP2C phosphatases (negative regulators of ABA signalling [103,347,348]) overall could actively promote or increase the sensitivity of ABA signalling. Despite that, in situations in which ABA signalling is actively promoted, negative feedback on a transcriptional level is often observed [349]. In these cases, the downregulation of positive ABA signalling components (such as the ABA receptors) and upregulation of PP2C phosphatases occurs in order to prevent overresponses [149,349]. Overall, this suggests the longer-term responses of darkness do not directly promote ABA signalling but increase the sensitivity of the signalling pathway.

Chapter 4 also investigates the physiological relevance of the upregulation of ABA receptors in response to darkness. As changes observed on a transcriptional level 2 hours after treatment are unlikely to be mediating immediate responses to a signal, it was thought that the upregulation of ABA receptors would be affecting processes that occur on a longer timescale [350]. A potential role could be altering the sensitivity of stomata to future signals. The priming of stomata to signals has been shown in developing leaves, where as new leaves develop and experience lower relative humidities they become more sensitive to ABA [239]. Another process that may be affected by upregulation of ABA receptors in response to darkness is stomatal development. ABA is known to inhibit entry of cells into the stomatal lineage and promote the expansion of pavement cells

[209]. Chapter 4 provides information regarding the effect of daylength and defects within ABA signalling and metabolism on stomatal development. Here, the effect of mutations within ABA signalling and metabolism genes agree with previous reports; where ABA signalling and metabolism mutants show increased stomatal densities. Daylength is also shown to have a small effect epidermal cell development, where under longer daylengths the ratio of mature stomata to epidermal cells increases (suggesting more cells are entering into the stomatal lineage). Additionally, the chapter presents evidence that suggests certain ABA receptors may be involved in regulating stomatal development differently under different daylength conditions, however further work is required to verify this.

As well as investigating the role of ABA signalling in plant responses to darkness, this study also aimed to identify new stomatal signalling components. cGMP signalling has been well documented in mammalian systems [308,309], however, until recently the identity of key cGMP signalling components in plants, including phosphodiesterase enzymes that break down cGMP, and cGMP activated protein kinases (also known as protein kinase Gs) that transmit cGMP signalling were unknown [310]. A plant specific phosphodiesterase was discovered recently and found to be involved in the UV-B mediated inhibition of stomatal opening [303]. Additionally, during this study a plant specific protein kinase G (PKG) was identified in rice and found to be involved in various developmental processes as well as the salt stress response [298]. Chapter 5 describes the isolation of two homozygous mutant lines of the Arabidopsis homologue of this gene (*pkg-1* and *pkg-2*). Data is presented showing this gene doesn't appear to be involved in the plant drought response, stomatal responses to ABA or extracellular Ca^{2+}. However, evidence is found for a role of the Arabidopsis PKG in dark-induced stomatal closure.

A role for cGMP signalling in the regulation of stomatal movements in darkness has previously been suggested, but in this case cGMP was proposed to promote stomatal opening in the dark [301]. Seemingly conflicting reports of the role of cGMP signalling have been described previously as cGMP signalling has been linked to both the promotion of stomatal opening by auxin and plant natriuretic peptides [321–325], the inhibition of opening by UVA [303], and the promotion of stomatal closure by ABA and NO [304,326,327]. Reasons for these conflicting roles may be due to differentially modified cGMP molecules with different functions, leading to complex roles for cGMP in the regulation of stomatal movements. Nitrated cGMP has been observed to function in the ABA response, while non-nitrated cGMP treatment was shown to promote opening in darkness [301]. Alternatively, many of these studies rely on pharmacological treatment using cGMP

analogues and inhibitors of cGMP metabolic enzymes, which may not be functioning as intended. Consequently, the results from these experiments may need to be interpreted with caution.

Regardless, recently a signalling module composed of ROS generating enzymes RBOHD/F, a MEK1/MPK6 kinase cascade, and NO generating NIA1, was suggested to be involved in mediating dark-induced stomatal closure [182]. Due to the links between cGMP within NO induced signalling pathways [301,304,317], where cGMP is thought to function downstream of NO production, cGMP signalling could be placed downstream of NO production in this signalling module. However, further work would be required to explore whether this is the case.

6.1 Conclusions

This thesis set out to explore the role of ABA signalling in stomatal responses to darkness (fig. 6.1). Evidence for a non-essential role for ABA signalling in the promotion of dark-induced closure is presented. However, data also suggest that defects within ABA signalling and metabolism affect the speed of stomatal movements in both light-induced opening and dark-induced closure responses. The speed of stomatal movements is a trait that has recently been shown to be a potential target to increase plant water use efficiency under variable light conditions and as such could be a valuable breeding trait for crop engineering. Evidence from this thesis points to components in ABA signalling and metabolism as genetic targets that could be used to manipulate stomatal response speed. This thesis also explores the longer-term effect of darkness on ABA signalling and finds darkness upregulates a specific subset of ABA receptor transcripts. This may act to increase the sensitivity of the ABA signalling pathway under dark conditions. The physiological relevance for the upregulation of ABA receptors in darkness is explored with respect to stomatal development, where plants were grown under different day length cycles. Data suggest different daylengths have a small effect on stomatal development and specific ABA receptors may be involved in regulating these differences, however further experimentation is required to investigate the role of ABA signalling in this response. Furthermore, this thesis also identifies a role for a plant specific protein kinase G in dark-induced stomatal closure, implicating cGMP signalling in this response. A potential mechanism for dark induced closure involving ROS production, a MEK1/MAPK6 kinase cascade, NO production, and cGMP signalling is proposed.

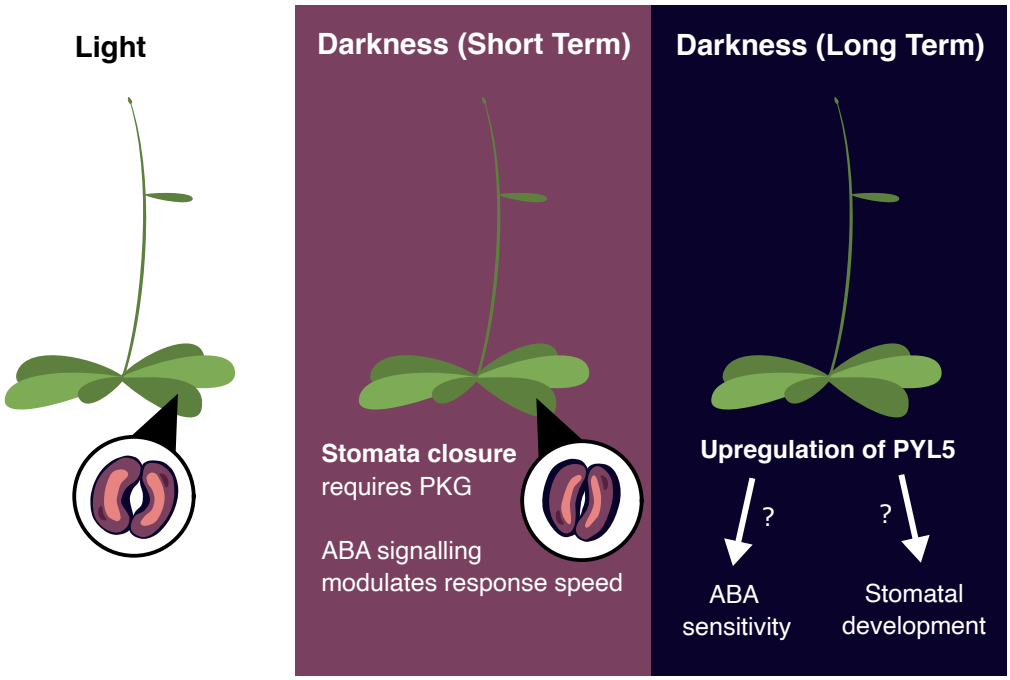

Figure 6.1 Thesis graphic summary

This thesis investigates stomatal responses to darkness on a short-term level, where evidence is presented supporting a role for plant protein kinase G (PKG) in dark-induced stomatal closure. ABA signalling and metabolism are found not to be essential for dark induced closure, however, they are shown to modulate stomatal movement speeds to darkness and light. On a longer-term basis darkness is found to upregulate a subset of ABA receptors including PYL5. It is hypothesised that this may affect stomatal ABA signalling sensitivity and/or stomatal development. The physiological relevance of this upregulation is explored with respect to stomatal development.

CHAPTER 7: BIBLIOGRAPHY

1. Hetherington, A. M. & Woodward, F. I. The role of stomata in sensing and driving environmental change. *Nature* **424**, 901–908 (2003).
2. Keenan, T. F. *et al.* Increase in forest water-use efficiency as atmospheric carbon dioxide concentrations rise. *Nature* **499**, 324–327 (2013).
3. Lawson, T. & Matthews, J. Guard Cell Metabolism and Stomatal Function. *Annu. Rev. Plant Biol.* **71**, 273–302 (2020).
4. Nunes, T. D. G., Zhang, D. & Raissig, M. T. Form, development and function of grass stomata. *Plant J.* **101**, 780–799 (2020).
5. Mohl, H. von. Welche Ursachen bewirken die Erweiterung und Verengung der Spaltoffnungen? *Bot. Ztg.* 697–704 (1856).
6. Jezek, M. & Blatt, M. R. The Membrane Transport System of the Guard Cell and Its Integration for Stomatal Dynamics. *Plant Physiol.* **174**, 487–519 (2017).
7. Wille, A. C. & Lucas, W. J. Ultrastructural and histochemical studies on guard cells. *Planta* **160**, 129–142 (1984).
8. LLoyd, F. E. *The physiology of stomata.* (Carnegie Institution of Washington, 1908).
9. Imamura, S. Untersuchungen uber den Mechanismus der Turgorschwandung der Spaltoffnungesschliesszellen. *Jpn J Bot* 82–88 (1943).
10. Fujino, M. Stomatal movement and active migration of potassium. *Kagaku* 660–661 (1959).
11. Fischer, R. A. Stomatal opening: role of potassium uptake by guard cells. *Science* **160**, 784–785 (1968).
12. Allaway, W. G. Accumulation of malate in guard cells of Vicia faba during stomatal opening. *Planta* **110**, 63–70 (1973).

13. Pearson, C. Daily Changes in Stomatal Aperture and in Carbohydrates and Malate Within Epidermis and Mesophyll of leaves of Commelina Cyanea and Vicia Faba. *Aust. J. Biol. Sci.* **26**, 1035 (1973).

14. MacRobbie, E. A. C. & Lettau, J. Potassium content and aperture in "intact" stomatal and epidermal cells of Commelina communis L. *J. Membr. Biol.* **56**, 249–256 (1980).

15. Granot, D. & Kelly, G. Evolution of Guard-Cell Theories: The Story of Sugars. *Trends Plant Sci.* **24**, 507–518 (2019).

16. Schnabl, H. & Raschke, K. Potassium Chloride as Stomatal Osmoticum in Allium cepa L., a Species Devoid of Starch in Guard Cells. *Plant Physiol.* **65**, 88–93 (1980).

17. Wege, S. *et al.* Phosphorylation of the vacuolar anion exchanger AtCLCa is required for the stomatal response to abscisic acid. *Sci. Signal.* **7**, ra65 (2014).

18. Amodeo, G., Talbott, L. D. & Zeiger, E. Use of Potassium and Sucrose by Onion Guard Cells during a Daily Cycle of Osmoregulation. *Plant Cell Physiol.* **37**, 575–579 (1996).

19. Talbott, L. D. & Zeiger, E. Central Roles for Potassium and Sucrose in Guard-Cell Osmoregulation. *Plant Physiol.* **111**, 1051–1057 (1996).

20. Scheibe, R., Reckmann, U., Hedrich, R. & Raschke, K. Malate Dehydrogenases in Guard Cells of *Pisum sativum*. *Plant Physiol.* **93**, 1358–1364 (1990).

21. Tcherkez, G., Cornic, G., Bligny, R., Gout, E. & Ghashghaie, J. In Vivo Respiratory Metabolism of Illuminated Leaves. *Plant Physiol.* **138**, 1596–1606 (2005).

22. Dong, H. *et al.* Modulation of Guard Cell Turgor and Drought Tolerance by a Peroxisomal Acetate–Malate Shunt. *Mol. Plant* **11**, 1278–1291 (2018).

23. Flütsch, S. *et al.* Guard Cell Starch Degradation Yields Glucose for Rapid Stomatal Opening in Arabidopsis. *Plant Cell* **32**, 2325–2344 (2020).

24. Daloso, D. M. *et al.* Tobacco guard cells fix CO_2 by both Rubisco and PEPcase while sucrose acts as a substrate during light-induced stomatal opening: Isotope labelling kinetics in guard cells. *Plant Cell Environ.* **38**, 2353–2371 (2015).

25. Daloso, D. M. *et al.* Guard cell-specific upregulation of *sucrose synthase 3* reveals that the role of sucrose in stomatal function is primarily energetic. *New Phytol.* **209**, 1470–1483 (2016).

26. McLachlan, D. H. *et al.* The Breakdown of Stored Triacylglycerols Is Required during Light-Induced Stomatal Opening. *Curr. Biol.* **26**, 707–712 (2016).

27. Kinoshita, T. Blue light activates the plasma membrane H+-ATPase by phosphorylation of the C-terminus in stomatal guard cells. *EMBO J.* **18**, 5548–5558 (1999).

28. Schroeder, J. I., Raschke, K. & Neher, E. Voltage dependence of K+ channels in guard-cell protoplasts. *Proc. Natl. Acad. Sci.* **84**, 4108–4112 (1987).

29. Nakamura, R. L. *et al.* Expression of an Arabidopsis Potassium Channel Gene in Guard Cells. *Plant Physiol.* **109**, 371–374 (1995).

30. Pilot, G. *et al.* Guard Cell Inward K+ Channel Activity inArabidopsis Involves Expression of the Twin Channel Subunits KAT1 and KAT2. *J. Biol. Chem.* **276**, 3215–3221 (2001).

31. Lebaudy, A. *et al.* Plant adaptation to fluctuating environment and biomass production are strongly dependent on guard cell potassium channels. *Proc. Natl. Acad. Sci.* **105**, 5271–5276 (2008).

32. Eisenach, C. & De Angeli, A. Ion Transport at the Vacuole during Stomatal Movements. *Plant Physiol.* **174**, 520–530 (2017).

33. Andrés, Z. *et al.* Control of vacuolar dynamics and regulation of stomatal aperture by tonoplast potassium uptake. *Proc. Natl. Acad. Sci. U. S. A.* **111**, E1806-1814 (2014).

34. Gao, X.-Q. *et al.* The Dynamic Changes of Tonoplasts in Guard Cells Are Important for Stomatal Movement in *Vicia faba*. *Plant Physiol.* **139**, 1207–1216 (2005).

35. Grabov, A. & Blatt, M. R. Membrane voltage initiates Ca2+ waves and potentiates Ca2+ increases with abscisic acid in stomatal guard cells. *Proc. Natl. Acad. Sci.* **95**, 4778–4783 (1998).

36. Merlot, S. *et al.* Constitutive activation of a plasma membrane H+-ATPase prevents abscisic acid-mediated stomatal closure. *EMBO J.* **26**, 3216–3226 (2007).

37. Grabov, A. & Blatt, M. R. Parallel control of the inward-rectifier K+ channel by cytosolic free Ca2+ and pH inVicia guard cells. *Planta* **201**, 84–95 (1997).

38. Grabov, A. & Blatt, M. R. A Steep Dependence of Inward-Rectifying Potassium Channels on Cytosolic Free Calcium Concentration Increase Evoked by Hyperpolarization in Guard Cells. *Plant Physiol.* **119**, 277–288 (1999).

39. Schmidt, C., Schelle, I., Liao, Y. J. & Schroeder, J. I. Strong regulation of slow anion channels and abscisic acid signaling in guard cells by phosphorylation and dephosphorylation events. *Proc. Natl. Acad. Sci.* **92**, 9535–9539 (1995).

40. Grabov, A., Leung, J., Giraudat, J. & Blatt, M. R. Alteration of anion channel kinetics in wild-type and abi1-1 transgenic Nicotiana benthamiana guard cells by abscisic acid. *Plant J.* **12**, 203–213 (1997).

41. Geiger, D. *et al.* Activity of guard cell anion channel SLAC1 is controlled by drought-stress signaling kinase-phosphatase pair. *Proc. Natl. Acad. Sci. U. S. A.* **106**, 21425–21430 (2009).

42. Meyer, S. *et al.* AtALMT12 represents an R-type anion channel required for stomatal movement in Arabidopsis guard cells: AtALMT12-mediated release of anions in guard cells. *Plant J.* **63**, 1054–1062 (2010).

43. Blatt, MichaelR. & Armstrong, F. K+ channels of stomatal guard cells: Abscisic-acid-evoked control of the outward rectifier mediated by cytoplasmic pH. *Planta* **191**, (1993).

44. Blatt, MichaelR. Potassium channel currents in intact stomatal guard cells: rapid enhancement by abscisic acid. *Planta* **180**, (1990).

45. Suhita, D., Raghavendra, A. S., Kwak, J. M. & Vavasseur, A. Cytoplasmic Alkalization Precedes Reactive Oxygen Species Production during Methyl Jasmonate- and Abscisic Acid-Induced Stomatal Closure. *Plant Physiol.* **134**, 1536–1545 (2004).

46. Peiter, E. The plant vacuole: Emitter and receiver of calcium signals. *Cell Calcium* **50**, 120–128 (2011).

47. Ranf, S. *et al.* Loss of the vacuolar cation channel, AtTPC1, does not impair Ca2+ signals induced by abiotic and biotic stresses. *Plant J.* **53**, 287–299 (2007).

48. Islam, M. M. *et al.* Roles of AtTPC1, Vacuolar Two Pore Channel 1, in Arabidopsis Stomatal Closure. *Plant Cell Physiol.* **51**, 302–311 (2010).

49. Bak, G. *et al.* Rapid Structural Changes and Acidification of Guard Cell Vacuoles during Stomatal Closure Require Phosphatidylinositol 3,5-Bisphosphate. *Plant Cell Online* **25**, (2013).

50. Latz, A. *et al.* TPK1, a Ca2+-regulated Arabidopsis vacuole two-pore K+ channel is activated by 14-3-3 proteins: TPK1 activation by 14-3-3. *Plant J.* **52**, 449–459 (2007).

51. Latz, A. *et al.* Salt Stress Triggers Phosphorylation of the Arabidopsis Vacuolar K+ Channel TPK1 by Calcium-Dependent Protein Kinases (CDPKs). *Mol. Plant* **6**, 1274–1289 (2013).

52. Gobert, A., Isayenkov, S., Voelker, C., Czempinski, K. & Maathuis, F. J. M. The two-pore channel TPK1 gene encodes the vacuolar K+ conductance and plays a role in K+ homeostasis. *Proc. Natl. Acad. Sci.* **104**, 10726–10731 (2007).

53. Eun, S. O. & Lee, Y. Actin Filaments of Guard Cells Are Reorganized in Response to Light and Abscisic Acid. *Plant Physiol.* **115**, 1491–1498 (1997).

54. Gao, X.-Q. *et al.* Array and distribution of actin filaments in guard cells contribute to the determination of stomatal aperture. *Plant Cell Rep.* **27**, 1655–1665 (2008).

55. Shimono, M. *et al.* Quantitative Evaluation of Stomatal Cytoskeletal Patterns during the Activation of Immune Signaling in Arabidopsis thaliana. *PLOS ONE* **11**, e0159291 (2016).

56. Isner, J.-C. *et al.* Actin filament reorganisation controlled by the SCAR/WAVE complex mediates stomatal response to darkness. *New Phytol.* **215**, 1059–1067 (2017).

57. Kim, M., Hepler, P. K., Eun, S. O., Ha, K. S. & Lee, Y. Actin Filaments in Mature Guard Cells Are Radially Distributed and Involved in Stomatal Movement. *Plant Physiol.* **109**, 1077–1084 (1995).

58. Meckel, T., Gall, L., Semrau, S., Homann, U. & Thiel, G. Guard Cells Elongate: Relationship of Volume and Surface Area during Stomatal Movement. *Biophys. J.* **92**, 1072–1080 (2007).

59. Shope, J. C., DeWald, D. B. & Mott, K. A. Changes in Surface Area of Intact Guard Cells Are Correlated with Membrane Internalization. *Plant Physiol.* **133**, 1314–1321 (2003).

60. Bourdais, G. *et al.* The use of quantitative imaging to investigate regulators of membrane trafficking in Arabidopsis stomatal closure. *Traffic* **20**, 168–180 (2019).

61. Yu, F. *et al.* ESCRT-I Component VPS23A Affects ABA Signaling by Recognizing ABA Receptors for Endosomal Degradation. *Mol. Plant* **9**, 1570–1582 (2016).

62. Belda-Palazon, B. *et al.* FYVE1/FREE1 Interacts with the PYL4 ABA Receptor and Mediates Its Delivery to the Vacuolar Degradation Pathway. *Plant Cell* **28**, 2291–2311 (2016).

63. Sutter, J.-U. *et al.* Abscisic Acid Triggers the Endocytosis of the Arabidopsis KAT1 K+ Channel and Its Recycling to the Plasma Membrane. *Curr. Biol.* **17**, 1396–1402 (2007).

64. Eisenach, C., Chen, Z.-H., Grefen, C. & Blatt, M. R. The trafficking protein SYP121 of Arabidopsis connects programmed stomatal closure and K+ channel activity with vegetative growth. *Plant J.* **69**, 241–251 (2012).

65. Himschoot, E., Pleskot, R., Van Damme, D. & Vanneste, S. The ins and outs of Ca2+ in plant endomembrane trafficking. *Curr. Opin. Plant Biol.* **40**, 131–137 (2017).

66. Woolfenden, H. C. *et al.* Models and Mechanisms of Stomatal Mechanics. *Trends Plant Sci.* **23**, 822–832 (2018).

67. Rui, Y. *et al.* Balancing Strength and Flexibility: How the Synthesis, Organization, and Modification of Guard Cell Walls Govern Stomatal Development and Dynamics. *Front. Plant Sci.* **9**, 1202 (2018).

68. Amsbury, S. *et al.* Stomatal Function Requires Pectin De-methyl-esterification of the Guard Cell Wall. *Curr. Biol.* **26**, 2899–2906 (2016).

69. Giannoutsou, E., Apostolakos, P. & Galatis, B. Spatio-temporal diversification of the cell wall matrix materials in the developing stomatal complexes of Zea mays. *Planta* **244**, 1125–1143 (2016).

70. Rui, Y. & Anderson, C. T. Functional Analysis of Cellulose and Xyloglucan in the Walls of Stomatal Guard Cells of Arabidopsis. *Plant Physiol.* **170**, 1398–1419 (2016).

71. Zhang, X.-Q. *et al.* Overexpression of the Arabidopsis α-expansin gene AtEXPA1 accelerates stomatal opening by decreasing the volumetric elastic modulus. *Plant Cell Rep.* **30**, 27–36 (2011).

72. Stebbins, G. L. & Shah, S. S. Developmental studies of cell differentiation in the epidermis of monocotyledons. *Dev. Biol.* **2**, 477–500 (1960).

73. Franks, P. J. & Farquhar, G. D. The Mechanical Diversity of Stomata and Its Significance in Gas-Exchange Control. *Plant Physiol.* **143**, 78–87 (2007).

74. Chen, Z.-H. *et al.* Molecular Evolution of Grass Stomata. *Trends Plant Sci.* **22**, 124–139 (2017).

75. Raissig, M. T. *et al.* Mobile MUTE specifies subsidiary cells to build physiologically improved grass stomata. *Science* **355**, 1215–1218 (2017).

76. FAO Statistical Pocketbook. *World Food and Agriculture (2015)*. (Rome: Food and Agriculture Organization of the United Nations., 2015).

77. Mittelheuser, C. J. & Steveninck, R. F. M. V. Stomatal Closure and Inhibition of Transpiration induced by (RS)-Abscisic Acid. *Nature* **221**, 281–282 (1969).

78. Kriedemann, P. E., Loveys, B. R., Fuller, G. L. & Leopold, A. C. Abscisic Acid and Stomatal Regulation. *Plant Physiol.* **49**, 842–847 (1972).

79. Macrobbie, E. a. C. Effects of ABA in 'Isolated' Guard Cells of Commelina communis L. *J. Exp. Bot.* **32**, 563–572 (1981).

80. Kuromori, T., Seo, M. & Shinozaki, K. ABA Transport and Plant Water Stress Responses. *Trends Plant Sci.* **23**, 513–522 (2018).

81. Holbrook, N. M., Shashidhar, V. R., James, R. A. & Munns, R. Stomatal control in tomato with ABA-deficient roots: Response of grafted plants to soil drying. *J. Exp. Bot.* **53**, 1503–1514 (2002).

82. Christmann, A., Weiler, E. W., Steudle, E. & Grill, E. A hydraulic signal in root-to-shoot signalling of water shortage. *Plant J.* **52**, 167–174 (2007).

83. Audran, C. *et al.* Expression Studies of the Zeaxanthin Epoxidase Gene in Nicotiana plumbaginifolia. *Plant Physiol.* **118**, 1021–1028 (1998).

84. Qin, X. & Zeevaart, J. A. D. The 9-cis-epoxycarotenoid cleavage reaction is the key regulatory step of abscisic acid biosynthesis in water-stressed bean. *Proc. Natl. Acad. Sci.* **96**, 15354–15361 (1999).

85. Ikegami, K., Okamoto, M., Seo, M. & Koshiba, T. Activation of abscisic acid biosynthesis in the leaves of Arabidopsis thaliana in response to water deficit. *J. Plant Res.* **122**, 235 (2008).

86. Ren, H. *et al.* Dynamic analysis of ABA accumulation in relation to the rate of ABA catabolism in maize tissues under water deficit. *J. Exp. Bot.* **58**, 211–219 (2007).

87. Manzi, M., Lado, J., Rodrigo, M. J., Arbona, V. & Gómez-Cadenas, A. ABA accumulation in water-stressed Citrus roots does not rely on carotenoid content in this organ. *Plant Sci.* **252**, 151–161 (2016).

88. Takahashi, F. *et al.* A small peptide modulates stomatal control via abscisic acid in long-distance signalling. *Nature* **556**, 235–238 (2018).

89. McLachlan, D. H., Pridgeon, A. J. & Hetherington, A. M. How Arabidopsis Talks to Itself about Its Water Supply. *Mol. Cell* **70**, 991–992 (2018).

90. Chater, C. *et al.* Elevated CO2-Induced Responses in Stomata Require ABA and ABA Signaling. *Curr. Biol. CB* **25**, 2709–16 (2015).

91. Nambara, E. *et al.* Abscisic acid and the control of seed dormancy and germination. *Seed Sci. Res.* **20**, 55–67 (2010).

92. Cao, F. Y., Yoshioka, K. & Desveaux, D. The roles of ABA in plant–pathogen interactions. *J. Plant Res.* **124**, 489–499 (2011).

93. Galvez-Valdivieso, G. *et al.* The High Light Response in Arabidopsis Involves ABA Signaling between Vascular and Bundle Sheath Cells. *Plant Cell* **21**, 2143–2162 (2009).

94. Lorrai, R. *et al.* Abscisic acid inhibits hypocotyl elongation acting on gibberellins, DELLA proteins and auxin. *AoB Plants* **10**, (2018).

95. Vishwakarma, K. *et al.* Abscisic Acid Signaling and Abiotic Stress Tolerance in Plants: A Review on Current Knowledge and Future Prospects. *Front. Plant Sci.* **8**, (2017).

96. Nambara, E. & Marion-Poll, A. Abscisic acid biosynthesis and catabolism. *Annu. Rev. Plant Biol.* **56**, 165–185 (2005).

97. Xiong, L. & Zhu, J.-K. Regulation of Abscisic Acid Biosynthesis. *Plant Physiol.* **133**, 29–36 (2003).

98. Lee, K. H. *et al.* Activation of Glucosidase via Stress-Induced Polymerization Rapidly Increases Active Pools of Abscisic Acid. *Cell* **126**, 1109–1120 (2006).

99. Xu, Z.-Y. *et al.* A Vacuolar β-Glucosidase Homolog That Possesses Glucose-Conjugated Abscisic Acid Hydrolyzing Activity Plays an Important Role in Osmotic Stress Responses in Arabidopsis. *Plant Cell* **24**, 2184–2199 (2012).

100. Park, S.-Y. *et al.* Abscisic acid inhibits PP2Cs via the PYR/PYL family of ABA- binding START proteins. *Science* **324**, 1068–1071 (2010).

101. Santiago, J. *et al.* The abscisic acid receptor PYR1 in complex with abscisic acid. *Nature* **462**, 665–668 (2009).

102. Ma, Y. *et al.* Regulators of PP2C phosphatase activity function as abscisic acid sensors. *Science* **324**, 1064–8 (2009).

103. Umezawa, T. *et al.* Type 2C protein phosphatases directly regulate abscisic acid-activated protein kinases in Arabidopsis. *Proc. Natl. Acad. Sci. U. S. A.* **106**, 17588–17593 (2009).

104. Takahashi, Y. *et al.* MAP3Kinase-dependent SnRK2-kinase activation is required for abscisic acid signal transduction and rapid osmotic stress response. *Nat. Commun.* **11**, 12 (2020).

105. Lee, S. C., Lan, W., Buchanan, B. B. & Luan, S. A protein kinase-phosphatase pair interacts with an ion channel to regulate ABA signaling in plant guard cells. *Proc. Natl. Acad. Sci. U. S. A.* **106**, 21419–21424 (2009).

106. Brandt, B. *et al.* Reconstitution of abscisic acid activation of SLAC1 anion channel by CPK6 and OST1 kinases and branched ABI1 PP2C phosphatase action. *Proc. Natl. Acad. Sci.* **109**, 10593–10598 (2012).

107. Bensmihen, S., Giraudat, J. & Parcy, F. Characterization of three homologous basic leucine zipper transcription factors (bZIP) of the ABI5 family during Arabidopsis thaliana embryo maturation. *J. Exp. Bot.* **56**, 597–603 (2005).

108. Yoshida, T. *et al.* AREB1, AREB2, and ABF3 are master transcription factors that cooperatively regulate ABRE-dependent ABA signaling involved in drought stress tolerance and require ABA for full activation. *Plant J.* **61**, 672–685 (2010).

109. Laxalt, A. M., García-Mata, C. & Lamattina, L. The Dual Role of Nitric Oxide in Guard Cells: Promoting and Attenuating the ABA and Phospholipid-Derived Signals Leading to the Stomatal Closure. *Front. Plant Sci.* **7**, (2016).

110. Munemasa, S. *et al.* Mechanisms of abscisic acid-mediated control of stomatal aperture. *Curr. Opin. Plant Biol.* **28**, 154–162 (2015).

111. Sierla, M., Waszczak, C., Vahisalu, T. & Kangasjärvi, J. Reactive Oxygen Species in the Regulation of Stomatal Movements. *Plant Physiol.* **171**, 1569–1580 (2016).

112. Xia, X.-J. *et al.* Interplay between reactive oxygen species and hormones in the control of plant development and stress tolerance. *J. Exp. Bot.* **66**, 2839–56 (2015).

113. Pei, Z.-M. *et al.* Calcium channels activated by hydrogen peroxide mediate abscisic acid signalling in guard cells. *Nature* **406**, 731–734 (2000).

114. Sirichandra, C. *et al.* Phosphorylation of the Arabidopsis AtrbohF NADPH oxidase by OST1 protein kinase. *FEBS Lett.* **583**, 2982–6 (2009).

115. Sierla, M. *et al.* The Receptor-like Pseudokinase GHR1 Is Required for Stomatal Closure. *Plant Cell* **30**, 2813–2837 (2018).

116. Klüsener, B. *et al.* Convergence of calcium signaling pathways of pathogenic elicitors and abscisic acid in Arabidopsis guard cells. *Plant Physiol.* **130**, 2152–63 (2002).

117. Allen, G. J. *et al.* Cameleon calcium indicator reports cytoplasmic calcium dynamics in Arabidopsis guard cells. *Plant J.* **19**, 735–747 (1999).

118. Staxen, I. *et al.* Abscisic acid induces oscillations in guard-cell cytosolic free calcium that involve phosphoinositide-specific phospholipase C. *Proc. Natl. Acad. Sci. U. S. A.* **96**, 1779–84 (1999).

119. McAinsh, M. R., Brownlee, C. & Hetherington, A. M. Abscisic acid-induced elevation of guard cell cytosolic Ca2+ precedes stomatal closure. *Nature* **343**, 186–188 (1990).

120. Gilroy, S., Fricker, M. D., Read, N. D. & Trewavas, A. J. Role of Calcium in Signal Transduction of Commelina Guard Cells. *Plant Cell* **3**, 333–344 (1991).

121. Huang, S. *et al.* Calcium signals in guard cells enhance the efficiency by which abscisic acid triggers stomatal closure. *New Phytol.* **224**, 177–187 (2019).

122. Hubbard, K. E., Siegel, R. S., Valerio, G., Brandt, B. & Schroeder, J. I. Abscisic acid and CO2 signalling via calcium sensitivity priming in guard cells, new CDPK mutant phenotypes and a method for improved resolution of stomatal stimulus-response analyses. *Ann. Bot.* **109**, 5–17 (2012).

123. Sheen, J. Ca2+-Dependent Protein Kinases and Stress Signal Transduction in Plants. *Science* **274**, 1900–1902 (1996).

124. Cheng, S.-H., Willmann, M. R., Chen, H.-C. & Sheen, J. Calcium Signaling through Protein Kinases. The Arabidopsis Calcium-Dependent Protein Kinase Gene Family. *Plant Physiol.* **129**, 469–485 (2002).

125. Kudla, J., Xu, Q., Harter, K., Gruissem, W. & Luan, S. Genes for calcineurin B-like proteins in Arabidopsis are differentially regulated by stress signals. *Proc. Natl. Acad. Sci.* **96**, 4718–4723 (1999).

126. Shi, J. *et al.* Novel Protein Kinases Associated with Calcineurin B–like Calcium Sensors in Arabidopsis. *Plant Cell* **11**, 2393–2405 (1999).

127. Luan, S., Kudla, J., Rodriguez-Concepcion, M., Yalovsky, S. & Gruissem, W. Calmodulins and Calcineurin B–like Proteins: Calcium Sensors for Specific Signal Response Coupling in Plants. *Plant Cell* **14**, S389–S400 (2002).

128. Day, I. S., Reddy, V. S., Shad Ali, G. & Reddy, A. S. N. Analysis of EF-hand-containing proteins in Arabidopsis. *Genome Biol.* **3**, RESEARCH0056 (2002).

129. Domingos, P., Prado, A. M., Wong, A., Gehring, C. & Feijo, J. A. Nitric Oxide: A Multitasked Signaling Gas in Plants. *Mol. Plant* **8**, 506–520 (2015).

130. Gayatri, G., Agurla, S. & Raghavendra, A. S. Nitric oxide in guard cells as an important secondary messenger during stomatal closure. *Front. Plant Sci.* **4**, (2013).

131. Sun, L. R., Yue, C. M. & Hao, F. S. Update on roles of nitric oxide in regulating stomatal closure. *Plant Signal. Behav.* **14**, e1649569 (2019).

132. Desikan, R., Griffiths, R., Hancock, J. & Neill, S. A new role for an old enzyme: Nitrate reductase-mediated nitric oxide generation is required for abscisic acid-induced stomatal closure in Arabidopsis thaliana. *Proc. Natl. Acad. Sci.* **99**, 16314–16318 (2002).

133. Bright, J., Desikan, R., Hancock, J. T., Weir, I. S. & Neill, S. J. ABA-induced NO generation and stomatal closure in Arabidopsis are dependent on H2O2 synthesis. *Plant J. Cell Mol. Biol.* **45**, 113–22 (2006).

134. Garcia-Mata, C. *et al.* Nitric oxide regulates K+ and Cl- channels in guard cells through a subset of abscisic acid-evoked signaling pathways. *Proc. Natl. Acad. Sci.* **100**, 11116–11121 (2003).

135. Distéfano, A. M., García-Mata, C., Lamattina, L. & Laxalt, A. M. Nitric oxide-induced phosphatidic acid accumulation: a role for phospholipases C and D in stomatal closure: NO induces phosphatidic acid accumulation in guard cells. *Plant Cell Environ.* **31**, 187–194 (2007).

136. Zhang, Y. *et al.* Phospholipase dalpha1 and phosphatidic acid regulate NADPH oxidase activity and production of reactive oxygen species in ABA-mediated stomatal closure in Arabidopsis. *Plant Cell* **21**, 2357–77 (2009).

137. Wang, P. *et al.* Nitric oxide negatively regulates abscisic acid signaling in guard cells by S-nitrosylation of OST1. *Proc. Natl. Acad. Sci. U. S. A.* **112**, 613–618 (2015).

138. Song, S.-J. *et al.* A Tonoplast-Associated Calcium-Signaling Module Dampens ABA Signaling during Stomatal Movement. *Plant Physiol.* **177**, 1666–1678 (2018).

139. Ali, A., Pardo, J. M. & Yun, D.-J. Desensitization of ABA-Signaling: The Swing From Activation to Degradation. *Front. Plant Sci.* **11**, 379 (2020).

140. Hu, H. *et al.* Carbonic anhydrases are upstream regulators of CO2-controlled stomatal movements in guard cells. *Nat. Cell Biol.* **12**, 87–93 (2010).

141. Tian, W. *et al.* A molecular pathway for CO2 response in Arabidopsis guard cells. *Nat. Commun.* **6**, 6057 (2015).

142. Hõrak, H. *et al.* A Dominant Mutation in the HT1 Kinase Uncovers Roles of MAP Kinases and GHR1 in CO2-Induced Stomatal Closure. *Plant Cell* **28**, 2493–2509 (2016).

143. Hashimoto, M. *et al.* Arabidopsis HT1 kinase controls stomatal movements in response to CO2. *Nat. Cell Biol.* **8**, 391–397 (2006).

144. Vahisalu, T. *et al.* SLAC1 is required for plant guard cell S-type anion channel function in stomatal signalling. *Nature* **452**, 487–491 (2008).

145. Webb, A. A. R., McAinsh, M. R., Mansfield, T. A. & Hetherington, A. M. Carbon dioxide induces increases in guard cell cytosolic free calcium. *Plant J.* **9**, 297–304 (1996).

146. Schulze, S. *et al.* A role for calcium-dependent protein kinases in differential CO_2 - and ABA-controlled stomatal closing and low CO_2 -induced stomatal opening in Arabidopsis. *New Phytol.* **229**, 2765–2779 (2021).

147. Webb, Aar. & Hetherington, A. M. Convergence of the Abscisic Acid, CO2, and Extracellular Calcium Signal Transduction Pathways in Stomatal Guard Cells. *Plant Physiol.* **114**, 1557–1560 (1997).

148. Movahedi, M. *et al.* Stomatal responses to carbon dioxide in light require abscisic acid catabolism in Arabidopsis. *Interface Focus* **20200036**, (2021).

149. Dittrich, M. *et al.* The role of Arabidopsis ABA receptors from the PYR/PYL/RCAR family in stomatal acclimation and closure signal integration. *Nat. Plants* **5**, 1002–1011 (2019).

150. Hsu, P.-K. *et al.* Abscisic acid-independent stomatal CO_2 signal transduction pathway and convergence of CO_2 and ABA signaling downstream of OST1 kinase. *Proc. Natl. Acad. Sci.* **115**, E9971–E9980 (2018).

151. Zhang, L. *et al.* FRET kinase sensor development reveals SnRK2/OST1 activation by ABA but not by MeJA and high CO2 during stomatal closure. *eLife* **9**, e56351 (2020).

152. Xue, S. *et al.* Central functions of bicarbonate in S-type anion channel activation and OST1 protein kinase in CO_2 signal transduction in guard cell: CO_2 signalling in guard cells. *EMBO J.* **30**, 1645–1658 (2011).

153. Yamamoto, Y. *et al.* The Transmembrane Region of Guard Cell SLAC1 Channels Perceives CO_2 Signals via an ABA-Independent Pathway in Arabidopsis. *Plant Cell* **28**, 557–567 (2016).

154. Zhang, J. *et al.* Identification of SLAC1 anion channel residues required for CO_2 /bicarbonate sensing and regulation of stomatal movements. *Proc. Natl. Acad. Sci.* **115**, 11129–11137 (2018).

155. Kinoshita, T. *et al.* phot1 and phot2 mediate blue light regulation of stomatal opening. *Nature* **414**, 656–660 (2001).

156. Mao, J., Zhang, Y.-C., Sang, Y., Li, Q.-H. & Yang, H.-Q. A role for Arabidopsis cryptochromes and COP1 in the regulation of stomatal opening. *Proc. Natl. Acad. Sci.* **102**, 12270–12275 (2005).

157. Takemiya, A., Kinoshita, T., Asanuma, M. & Shimazaki, K.-I. Protein phosphatase 1 positively regulates stomatal opening in response to blue light in Vicia faba. *Proc. Natl. Acad. Sci. U. S. A.* **103**, 13549–13554 (2006).

158. Takemiya, A. *et al.* Phosphorylation of BLUS1 kinase by phototropins is a primary step in stomatal opening. *Nat. Commun.* **4**, 2094 (2013).

159. Hiyama, A. *et al.* Blue light and CO2 signals converge to regulate light-induced stomatal opening. *Nat. Commun.* **8**, 1284 (2017).

160. Hayashi, M. *et al.* Raf-like kinases CBC1 and CBC2 negatively regulate stomatal opening by negatively regulating plasma membrane H^+-ATPase phosphorylation in *Arabidopsis*. *Photochem. Photobiol. Sci.* **19**, 88–98 (2020).

161. Wang, F.-F., Lian, H.-L., Kang, C.-Y. & Yang, H.-Q. Phytochrome B Is Involved in Mediating Red Light-Induced Stomatal Opening in Arabidopsis thaliana. *Mol. Plant* **3**, 246–259 (2010).

162. Sharkey, T. D. & Raschke, K. Effect of Light Quality on Stomatal Opening in Leaves of *Xanthium strumarium* L. *Plant Physiol.* **68**, 1170–1174 (1981).

163. Schwartz, A. & Zeiger, E. Metabolic energy for stomatal opening. Roles of photophosphorylation and oxidative phosphorylation. *Planta* **161**, 129–136 (1984).

164. Mott, K. A. Do Stomata Respond to CO_2 Concentrations Other than Intercellular? *Plant Physiol.* **86**, 200–203 (1988).

165. Lawson, T., Lefebvre, S., Baker, N. R., Morison, J. I. L. & Raines, C. A. Reductions in mesophyll and guard cell photosynthesis impact on the control of stomatal responses to light and CO2. *J. Exp. Bot.* **59**, 3609–3619 (2008).

166. Messinger, S. M., Buckley, T. N. & Mott, K. A. Evidence for Involvement of Photosynthetic Processes in the Stomatal Response to CO_2. *Plant Physiol.* **140**, 771–778 (2006).

167. Matrosova, A. *et al.* The HT1 protein kinase is essential for red light-induced stomatal opening and genetically interacts with OST1 in red light and CO2 -induced stomatal movement responses. *New Phytol.* **208**, 1126–1137 (2015).

168. Ando, E. & Kinoshita, T. Red Light-Induced Phosphorylation of Plasma Membrane H+-ATPase in Stomatal Guard Cells. *Plant Physiol.* **178**, 838–849 (2018).

169. Goh, C. H., Kinoshita, T., Oku, T. & Shimazaki, Ki. Inhibition of Blue Light-Dependent H+ Pumping by Abscisic Acid in Vicia Guard-Cell Protoplasts. *Plant Physiol.* **111**, 433–440 (1996).

170. Roelfsema, M. R. G., Staal, M. & Prins, H. B. A. Blue light-induced apoplastic acidification of *Arabidopsis thaliana* guard cells: Inhibition by ABA is mediated through protein phosphatases. *Physiol. Plant.* **103**, 466–474 (1998).

171. Hayashi, M., Inoue, S., Takahashi, K. & Kinoshita, T. Immunohistochemical Detection of Blue Light-Induced Phosphorylation of the Plasma Membrane H+-ATPase in Stomatal Guard Cells. *Plant Cell Physiol.* **52**, 1238–1248 (2011).

172. Garcia-Mata, C. & Lamattina, L. Abscisic acid (ABA) inhibits light-induced stomatal opening through calcium- and nitric oxide-mediated signaling pathways. *Nitric Oxide* **17**, 143–151 (2007).

173. Yan, J., Tsuichihara, N., Etoh, T. & Iwai, S. Reactive oxygen species and nitric oxide are involved in ABA inhibition of stomatal opening. *Plant Cell Environ.* **30**, 1320–1325 (2007).

174. Wang, X.-Q. G Protein Regulation of Ion Channels and Abscisic Acid Signaling in Arabidopsis Guard Cells. *Science* **292**, 2070–2072 (2001).

175. Mills, L. N. *et al.* The effects of manipulating phospholipase C on guard cell ABA-signalling. *J. Exp. Bot.* **55**, 199–204 (2003).

176. Worrall, D. *et al.* Involvement of sphingosine kinase in plant cell signalling. *Plant J. Cell Mol. Biol.* **56**, 64–72 (2008).

177. Yin, Y. *et al.* Difference in Abscisic Acid Perception Mechanisms between Closure Induction and Opening Inhibition of Stomata. *PLANT Physiol.* **163**, 600–610 (2013).

178. He, J. *et al.* The BIG protein distinguishes the process of CO2 -induced stomatal closure from the inhibition of stomatal opening by CO2. *New Phytol.* **218**, 232–241 (2018).

179. Hashimoto-Sugimoto, M. *et al.* Dominant and recessive mutations in the Raf-like kinase HT1 gene completely disrupt stomatal responses to CO2 in Arabidopsis. *J. Exp. Bot.* **67**, 3251–3261 (2016).

180. Costa, J. M. *et al. OPEN ALL NIGHT LONG* : The Dark Side of Stomatal Control. *Plant Physiol.* **167**, 289–294 (2015).

181. Jiang, K. *et al.* The ARP2/3 Complex Mediates Guard Cell Actin Reorganization and Stomatal Movement in *Arabidopsis*. *Plant Cell* **24**, 2031–2040 (2012).

182. Zhang, T.-Y. *et al.* Role and interrelationship of MEK1-MPK6 cascade, hydrogen peroxide and nitric oxide in darkness-induced stomatal closure. *Plant Sci.* **262**, 190–199 (2017).

183. Dow, G. J. & Bergmann, D. C. Patterning and processes: how stomatal development defines physiological potential. *Curr. Opin. Plant Biol.* **21**, 67–74 (2014).

184. Franks, P. J., Drake, P. L. & Beerling, D. J. Plasticity in maximum stomatal conductance constrained by negative correlation between stomatal size and density: an analysis using Eucalyptus globulus. *Plant Cell Environ.* **32**, 1737–1748 (2009).

185. Zoulias, N., Harrison, E. L., Casson, S. A. & Gray, J. E. Molecular control of stomatal development. *Biochem. J.* **475**, 441–454 (2018).

186. MacAlister, C. A., Ohashi-Ito, K. & Bergmann, D. C. Transcription factor control of asymmetric cell divisions that establish the stomatal lineage. *Nature* **445**, 537–540 (2007).

187. Pillitteri, L. J., Sloan, D. B., Bogenschutz, N. L. & Torii, K. U. Termination of asymmetric cell division and differentiation of stomata. *Nature* **445**, 501–505 (2007).

188. Pillitteri, L. J., Bogenschutz, N. L. & Torii, K. U. The bHLH protein, MUTE, controls differentiation of stomata and the hydathode pore in Arabidopsis. *Plant Cell Physiol.* **49**, 934–943 (2008).

189. Ohashi-Ito, K. & Bergmann, D. C. Arabidopsis FAMA controls the final proliferation/differentiation switch during stomatal development. *Plant Cell* **18**, 2493–2505 (2006).

190. Qi, X. & Torii, K. U. Hormonal and environmental signals guiding stomatal development. *BMC Biol.* **16**, 21 (2018).

191. Wang, H. *et al.* BZU2/ZmMUTE controls symmetrical division of guard mother cell and specifies neighbor cell fate in maize. *PLOS Genet.* **15**, e1008377 (2019).

192. Ohki, S., Takeuchi, M. & Mori, M. The NMR structure of stomagen reveals the basis of stomatal density regulation by plant peptide hormones. *Nat. Commun.* **2**, 512 (2011).

193. Lin, G. *et al.* A receptor-like protein acts as a specificity switch for the regulation of stomatal development. *Genes Dev.* **31**, 927–938 (2017).

194. Lee, J. S. *et al.* Competitive binding of antagonistic peptides fine-tunes stomatal patterning. *Nature* **522**, 439–443 (2015).

195. Lampard, G. R., MacAlister, C. A. & Bergmann, D. C. Arabidopsis Stomatal Initiation Is Controlled by MAPK-Mediated Regulation of the bHLH SPEECHLESS. *Science* **322**, 1113–1116 (2008).

196. Bergmann, D. C., Lukowitz, W. & Somerville, C. R. Stomatal development and pattern controlled by a MAPKK kinase. *Science* **304**, 1494–1497 (2004).

197. Wang, H., Ngwenyama, N., Liu, Y., Walker, J. C. & Zhang, S. Stomatal development and patterning are regulated by environmentally responsive mitogen-activated protein kinases in Arabidopsis. *Plant Cell* **19**, 63–73 (2007).

198. Hara, K., Kajita, R., Torii, K. U., Bergmann, D. C. & Kakimoto, T. The secretory peptide gene EPF1 enforces the stomatal one-cell-spacing rule. *Genes Dev.* **21**, 1720–1725 (2007).

199. Dong, J., MacAlister, C. A. & Bergmann, D. C. BASL controls asymmetric cell division in Arabidopsis. *Cell* **137**, 1320–1330 (2009).

200. Qi, X. *et al.* Autocrine regulation of stomatal differentiation potential by EPF1 and ERECTA-LIKE1 ligand-receptor signaling. *eLife* **6**, e24102 (2017).

201. Hunt, L. & Gray, J. E. The signaling peptide EPF2 controls asymmetric cell divisions during stomatal development. *Curr. Biol. CB* **19**, 864–869 (2009).

202. Hara, K. *et al.* Epidermal cell density is autoregulated via a secretory peptide, EPIDERMAL PATTERNING FACTOR 2 in Arabidopsis leaves. *Plant Cell Physiol.* **50**, 1019–1031 (2009).

203. Hunt, L., Bailey, K. J. & Gray, J. E. The signalling peptide EPFL9 is a positive regulator of stomatal development. *New Phytol.* **186**, 609–614 (2010).

204. Sugano, S. S. *et al.* Stomagen positively regulates stomatal density in Arabidopsis. *Nature* **463**, 241–244 (2010).

205. Kang, C.-Y., Lian, H.-L., Wang, F.-F., Huang, J.-R. & Yang, H.-Q. Cryptochromes, Phytochromes, and COP1 Regulate Light-Controlled Stomatal Development in *Arabidopsis*. *Plant Cell* **21**, 2624–2641 (2009).

206. Lee, J.-H., Jung, J.-H. & Park, C.-M. Light Inhibits COP1-Mediated Degradation of ICE Transcription Factors to Induce Stomatal Development in Arabidopsis. *Plant Cell* **29**, 2817–2830 (2017).

207. Klermund, C. *et al.* LLM-Domain B-GATA Transcription Factors Promote Stomatal Development Downstream of Light Signaling Pathways in *Arabidopsis thaliana* Hypocotyls. *Plant Cell* **28**, 646–660 (2016).

208. Quarrie, S. A. & Jones, H. G. Effects of Abscisic Acid and Water Stress on Development and Morphology of Wheat. *J. Exp. Bot.* **28**, 192–203 (1977).

209. Tanaka, Y., Nose, T., Jikumaru, Y. & Kamiya, Y. ABA inhibits entry into stomatal-lineage development in Arabidopsis leaves. *Plant J.* **74**, 448–457 (2013).

210. Iida, S. *et al.* Loss of heterophylly in aquatic plants: not ABA-mediated stress but exogenous ABA treatment induces stomatal leaves in Potamogeton perfoliatus. *J. Plant Res.* **129**, 853–862 (2016).

211. Allen, J., Guo, K., Zhang, D., Ince, M. & Jammes, F. ABA-glucose ester hydrolyzing enzyme ATBG1 and PHYB antagonistically regulate stomatal development. *PLOS ONE* **14**, e0218605 (2019).

212. Woodward, F. I. & Kelly, C. K. The influence of CO2 concentration on stomatal density. *New Phytol.* **131**, 311–327 (1995).

213. Engineer, C. B. *et al.* Carbonic anhydrases, EPF2 and a novel protease mediate CO2 control of stomatal development. *Nature* **513**, 246–250 (2014).

214. Merilo, E. *et al.* PYR/RCAR Receptors Contribute to Ozone-, Reduced Air Humidity-, Darkness-, and CO2-Induced Stomatal Regulation. *Plant Physiol.* **162**, 1652–1668 (2013).

215. Okamoto, M. *et al.* Activation of dimeric ABA receptors elicits guard cell closure, ABA-regulated gene expression, and drought tolerance. *Proc. Natl. Acad. Sci.* **110**, 12132–12137 (2013).

216. Gonzalez-Guzman, M. *et al.* Arabidopsis PYR/PYL/RCAR Receptors Play a Major Role in Quantitative Regulation of Stomatal Aperture and Transcriptional Response to Abscisic Acid. *Plant Cell* **24**, 2483–2496 (2012).

217. Frey, A. *et al.* Epoxycarotenoid cleavage by NCED5 fine-tunes ABA accumulation and affects seed dormancy and drought tolerance with other NCED family members: Functional analysis of the NCED5 gene. *Plant J.* **70**, 501–512 (2012).

218. Okamoto, M. *et al.* CYP707A1 and CYP707A2, Which Encode Abscisic Acid 8'-Hydroxylases, Are Indispensable for Proper Control of Seed Dormancy and Germination in Arabidopsis. *Plant Physiol.* **141**, 97–107 (2006).

219. Okamoto, M. *et al.* High Humidity Induces Abscisic Acid 8'-Hydroxylase in Stomata and Vasculature to Regulate Local and Systemic Abscisic Acid Responses in Arabidopsis. *Plant Physiol.* **149**, 825–834 (2009).

220. Ondzighi-Assoume, C. A., Chakraborty, S. & Harris, J. M. Environmental Nitrate Stimulates Abscisic Acid Accumulation in Arabidopsis Root Tips by Releasing It from Inactive Stores. *Plant Cell* **28**, 729–745 (2016).

221. Ogasawara, K. *et al.* Constitutive and Inducible ER Bodies of Arabidopsis thaliana Accumulate Distinct β-Glucosidases. *Plant Cell Physiol.* **50**, 480–488 (2009).

222. Wickham, H. *ggplot2*. (Springer New York, 2009). doi:10.1007/978-0-387-98141-3.

223. Liang, Y.-K. *et al.* AtMYB61, an R2R3-MYB Transcription Factor Controlling Stomatal Aperture in Arabidopsis thaliana. *Curr. Biol.* **15**, 1201–1206 (2005).

224. Leymarie, J., Lascève, G. & Vavasseur, A. Interaction of stomatal responses to ABA and CO2 in Arabidopsis thaliana. *Funct. Plant Biol.* **25**, 785 (1998).

225. Park, S.-Y. *et al.* Abscisic acid inhibits type 2C protein phosphatases via the PYR/PYL family of START proteins. *Science* **324**, 1068–1071 (2009).

226. Iuchi, S. *et al.* Regulation of drought tolerance by gene manipulation of 9-cis-epoxycarotenoid dioxygenase, a key enzyme in abscisic acid biosynthesis in Arabidopsis: Regulation of drought tolerance by AtNCED3. *Plant J.* **27**, 325–333 (2001).

227. Tan, B. C., Schwartz, S. H., Zeevaart, J. A. D. & McCarty, D. R. Genetic control of abscisic acid biosynthesis in maize. *Proc. Natl. Acad. Sci.* **94**, 12235–12240 (1997).

228. Umezawa, T. *et al.* CYP707A3, a major ABA 8'-hydroxylase involved in dehydration and rehydration response in *Arabidopsis thaliana*. *Plant J.* **46**, 171–182 (2006).

229. Rui, Y. *et al.* POLYGALACTURONASE INVOLVED IN EXPANSION3 Functions in Seedling Development, Rosette Growth, and Stomatal Dynamics in Arabidopsis thaliana. *Plant Cell* **29**, 2413–2432 (2017).

230. Mustilli, A.-C., Merlot, S., Vavasseur, A., Fenzi, F. & Giraudat, J. Arabidopsis OST1 protein kinase mediates the regulation of stomatal aperture by abscisic acid and acts upstream of reactive oxygen species production. *Plant Cell* **14**, 3089–99 (2002).

231. Chen, K. *et al.* Abscisic acid dynamics, signaling, and functions in plants. *J. Integr. Plant Biol.* **62**, 25–54 (2020).

232. Yoshida, T., Christmann, A., Yamaguchi-Shinozaki, K., Grill, E. & Fernie, A. R. Revisiting the Basal Role of ABA – Roles Outside of Stress. *Trends Plant Sci.* **24**, 625–635 (2019).

233. Tischer, S. V. *et al.* Combinatorial interaction network of abscisic acid receptors and coreceptors from *Arabidopsis thaliana*. *Proc. Natl. Acad. Sci.* **114**, 10280–10285 (2017).

234. Fujita, Y. *et al.* Three SnRK2 Protein Kinases are the Main Positive Regulators of Abscisic Acid Signaling in Response to Water Stress in Arabidopsis. *Plant Cell Physiol.* **50**, 2123–2132 (2009).

235. Miao, C. *et al.* Mutations in a subfamily of abscisic acid receptor genes promote rice growth and productivity. *Proc. Natl. Acad. Sci.* **115**, 6058–6063 (2018).

236. Inoue, S.-I. & Kinoshita, T. Blue Light Regulation of Stomatal Opening and the Plasma Membrane H+-ATPase. *Plant Physiol.* **174**, 531–538 (2017).

237. Tominaga, M., Kinoshita, T. & Shimazaki, K. Guard-Cell Chloroplasts Provide ATP Required for H+ Pumping in the Plasma Membrane and Stomatal Opening. *Plant Cell Physiol.* **42**, 795–802 (2001).

238. Kollist, H., Nuhkat, M. & Roelfsema, M. R. G. Closing gaps: linking elements that control stomatal movement. *New Phytol.* **203**, 44–62 (2014).

239. Pantin, F. *et al.* Developmental Priming of Stomatal Sensitivity to Abscisic Acid by Leaf Microclimate. *Curr. Biol.* **23**, 1805–1811 (2013).

240. Papanatsiou, M. *et al.* Optogenetic manipulation of stomatal kinetics improves carbon assimilation, water use, and growth. *Science* **363**, 1456–1459 (2019).

241. Lawson, T. & Vialet-Chabrand, S. Speedy stomata, photosynthesis and plant water use efficiency. *New Phytol.* **221**, 93–98 (2019).

242. Grantz, D. A., Linscheid, B. S. & Grulke, N. E. Differential responses of stomatal kinetics and steady-state conductance to abscisic acid in a fern: comparison with a gymnosperm and an angiosperm. *New Phytol.* **222**, 1883–1892 (2019).

243. Oh, E. *et al.* PIL5, a Phytochrome-Interacting bHLH Protein, Regulates Gibberellin Responsiveness by Binding Directly to the *GAI* and *RGA* Promoters in *Arabidopsis* Seeds. *Plant Cell* **19**, 1192–1208 (2007).

244. Oh, E. *et al.* Genome-Wide Analysis of Genes Targeted by PHYTOCHROME INTERACTING FACTOR 3-LIKE5 during Seed Germination in *Arabidopsis*. *Plant Cell* **21**, 403–419 (2009).

245. Park, J., Lee, N., Kim, W., Lim, S. & Choi, G. ABI3 and PIL5 Collaboratively Activate the Expression of *SOMNUS* by Directly Binding to Its Promoter in Imbibed *Arabidopsis* Seeds. *Plant Cell* **23**, 1404–1415 (2011).

246. Qi, L. *et al.* PHYTOCHROME-INTERACTING FACTORS Interact with the ABA Receptors PYL8 and PYL9 to Orchestrate ABA Signaling in Darkness. *Mol. Plant* **13**, 414–430 (2020).

247. Demir, F. *et al.* Arabidopsis nanodomain-delimited ABA signaling pathway regulates the anion channel SLAH3. *Proc. Natl. Acad. Sci.* **110**, 8296–8301 (2013).

248. García-León, M. *et al.* Arabidopsis ALIX Regulates Stomatal Aperture and Turnover of Abscisic Acid Receptors. *Plant Cell* **31**, 2411–2429 (2019).

249. Creux, N. & Harmer, S. Circadian Rhythms in Plants. *Cold Spring Harb. Perspect. Biol.* **11**, a034611 (2019).

250. Nozue, K. *et al.* Rhythmic growth explained by coincidence between internal and external cues. *Nature* **448**, 358–361 (2007).

251. Seluzicki, A., Burko, Y. & Chory, J. Dancing in the dark: darkness as a signal in plants: Dark signaling in plants. *Plant Cell Environ.* **40**, 2487–2501 (2017).

252. Paik, I. & Huq, E. Plant photoreceptors: Multi-functional sensory proteins and their signaling networks. *Semin. Cell Dev. Biol.* **92**, 114–121 (2019).

253. Kim, J. *et al.* PIF1-Interacting Transcription Factors and Their Binding Sequence Elements Determine the in Vivo Targeting Sites of PIF1. *Plant Cell* **28**, 1388–1405 (2016).

254. Hayes, S. *et al.* Soil Salinity Limits Plant Shade Avoidance. *Curr. Biol.* **29**, 1669-1676.e4 (2019).

255. Boccalandro, H. E. *et al.* Phytochrome B Enhances Photosynthesis at the Expense of Water-Use Efficiency in Arabidopsis. *Plant Physiol.* **150**, 1083–1092 (2009).

256. Casson, S. A. *et al.* phytochrome B and PIF4 Regulate Stomatal Development in Response to Light Quantity. *Curr. Biol.* **19**, 229–234 (2009).

257. Hazen, S. P. *et al.* LUX ARRHYTHMO encodes a Myb domain protein essential for circadian rhythms. *Proc. Natl. Acad. Sci.* **102**, 10387–10392 (2005).

258. Michael, T. P. *et al.* A Morning-Specific Phytohormone Gene Expression Program underlying Rhythmic Plant Growth. *PLoS Biol.* **6**, e225 (2008).

259. Smith, S. M. *et al.* Diurnal Changes in the Transcriptome Encoding Enzymes of Starch Metabolism Provide Evidence for Both Transcriptional and Posttranscriptional Regulation of Starch Metabolism in Arabidopsis Leaves. *Plant Physiol.* **136**, 2687–2699 (2004).

260. Bläsing, O. E. *et al.* Sugars and Circadian Regulation Make Major Contributions to the Global Regulation of Diurnal Gene Expression in *Arabidopsis*. *Plant Cell* **17**, 3257–3281 (2005).

261. Harmer, S. L. *et al.* Orchestrated Transcription of Key Pathways in Arabidopsis by the Circadian Clock. *Science* **290**, (2000).

262. Edwards, K. D. *et al. FLOWERING LOCUS C* Mediates Natural Variation in the High-Temperature Response of the *Arabidopsis* Circadian Clock. *Plant Cell* **18**, 639–650 (2006).

263. Bauer, H. *et al.* The Stomatal Response to Reduced Relative Humidity Requires Guard Cell-Autonomous ABA Synthesis. *Curr. Biol.* **23**, 53–57 (2013).

264. Ritchie, M. E. *et al.* limma powers differential expression analyses for RNA-sequencing and microarray studies. *Nucleic Acids Res.* **43**, e47–e47 (2015).

265. Schweighofer, A., Hirt, H. & Meskiene, I. Plant PP2C phosphatases: emerging functions in stress signaling. *Trends Plant Sci.* **9**, 236–243 (2004).

266. Yoshida, T. *et al.* Four Arabidopsis AREB/ABF transcription factors function predominantly in gene expression downstream of SnRK2 kinases in abscisic acid signalling in response to osmotic stress. *Plant Cell Environ.* **38**, 35–49 (2015).

267. Giraudat, J. *et al.* Isolation of the Arabidopsis ABI3 gene by positional cloning. *Plant Cell* **4**, 1251–1261 (1992).

268. Finkelstein, R. R., Li Wang, M., Lynch, T. J., Rao, S. & Goodman, H. M. The Arabidopsis Abscisic Acid Response Locus *ABI4* Encodes an APETALA2 Domain Protein. *Plant Cell* **10**, 1043–1054 (1998).

269. Carles, C. *et al.* Regulation of Arabidopsis thaliana Em genes: role of ABI5. *Plant J.* **30**, 373–383 (2002).

270. Yamaguchi-Shinozaki, K. & Shinozaki, K. Characterization of the expression of a desiccation-responsive rd29 gene of Arabidopsis thaliana and analysis of its promoter in transgenic plants. *Mol. Gen. Genet. MGG* **236**, 331–340 (1993).

271. Liu, Z. *et al.* UDP-glucosyltransferase71c5, a major glucosyltransferase, mediates abscisic acid homeostasis in Arabidopsis. *Plant Physiol.* **167**, 1659–1670 (2015).

272. Priest, D. M., Jackson, R. G., Ashford, D. A., Abrams, S. R. & Bowles, D. J. The use of abscisic acid analogues to analyse the substrate selectivity of UGT71B6, a UDP-glycosyltransferase of *Arabidopsis thaliana*. *FEBS Lett.* **579**, 4454–4458 (2005).

273. Zhang, G.-Z. *et al.* Ectopic expression of UGT75D1, a glycosyltransferase preferring indole-3-butyric acid, modulates cotyledon development and stress tolerance in seed germination of Arabidopsis thaliana. *Plant Mol. Biol.* **90**, 77–93 (2016).

274. Rehman, H. M. *et al.* Comparative genomic and transcriptomic analyses of Family-1 UDP glycosyltransferase in three Brassica species and Arabidopsis indicates stress-responsive regulation. *Sci. Rep.* **8**, 1875 (2018).

275. Mockler, T. C. *et al.* The Diurnal Project: Diurnal and Circadian Expression Profiling, Model-based Pattern Matching, and Promoter Analysis. *Cold Spring Harb. Symp. Quant. Biol.* **72**, 353–363 (2007).

276. Kim, H., Kim, Y., Yeom, M., Lim, J. & Nam, H. G. Age-associated circadian period changes in Arabidopsis leaves. *J. Exp. Bot.* **67**, 2665–2673 (2016).

277. Endo, M., Shimizu, H., Nohales, M. A., Araki, T. & Kay, S. A. Tissue-specific clocks in Arabidopsis show asymmetric coupling. *Nature* **515**, 419–422 (2014).

278. Niwa, Y., Yamashino, T. & Mizuno, T. The Circadian Clock Regulates the Photoperiodic Response of Hypocotyl Elongation through a Coincidence Mechanism in Arabidopsis thaliana. *Plant Cell Physiol.* **50**, 838–854 (2009).

279. Jeong, Y. Y. & Seo, P. J. Bidirectional regulation between circadian clock and ABA signaling. *Commun. Integr. Biol.* **10**, e1296999 (2017).

280. Adams, S. *et al.* Circadian control of abscisic acid biosynthesis and signalling pathways revealed by genome-wide analysis of LHY binding targets. *New Phytol.* **220**, 893–907 (2018).

281. Hanano, S., Domagalska, M. A., Nagy, F. & Davis, S. J. Multiple phytohormones influence distinct parameters of the plant circadian clock. *Genes Cells* **11**, 1381–1392 (2006).

282. Lee, H. G., Mas, P. & Seo, P. J. MYB96 shapes the circadian gating of ABA signaling in Arabidopsis. *Sci. Rep.* **6**, 17754 (2016).

283. Legnaioli, T., Cuevas, J. & Mas, P. TOC1 functions as a molecular switch connecting the circadian clock with plant responses to drought. *EMBO J.* **28**, 3745–3757 (2009).

284. Shen, Y.-Y. *et al.* The Mg-chelatase H subunit is an abscisic acid receptor. *Nature* **443**, 823–826 (2006).

285. Hubbard, K. E., Nishimura, N., Hitomi, K., Getzoff, E. D. & Schroeder, J. I. Early abscisic acid signal transduction mechanisms: newly discovered components and newly emerging questions. *Genes Dev.* **24**, 1695–1708 (2010).

286. Müller, A. H. & Hansson, M. The Barley Magnesium Chelatase 150-kD Subunit Is Not an Abscisic Acid Receptor. *Plant Physiol.* **150**, 157–166 (2009).

287. Yang, J.-F., Chen, M.-X., Zhang, J.-H., Hao, G.-F. & Yang, G.-F. Genome-wide phylogenetic and structural analysis reveals the molecular evolution of the ABA receptor gene family. *J. Exp. Bot.* **71**, 1322–1336 (2020).

288. Chan, Z. Expression profiling of ABA pathway transcripts indicates crosstalk between abiotic and biotic stress responses in Arabidopsis. *Genomics* **100**, 110–115 (2012).

289. Zhao, Y. *et al.* The ABA Receptor PYL8 Promotes Lateral Root Growth by Enhancing MYB77-Dependent Transcription of Auxin-Responsive Genes. *Sci. Signal.* **7**, ra53–ra53 (2014).

290. Xing, L., Zhao, Y., Gao, J., Xiang, C. & Zhu, J.-K. The ABA receptor PYL9 together with PYL8 plays an important role in regulating lateral root growth. *Sci. Rep.* **6**, 27177 (2016).

291. Zhao, Y. *et al.* The unique mode of action of a divergent member of the ABA-receptor protein family in ABA and stress signaling. *Cell Res.* **23**, 1380–1395 (2013).

292. Hao, Q. *et al.* The Molecular Basis of ABA-Independent Inhibition of PP2Cs by a Subclass of PYL Proteins. *Mol. Cell* **42**, 662–672 (2011).

293. Hassidim, M. *et al.* CIRCADIAN CLOCK ASSOCIATED1 (CCA1) and the Circadian Control of Stomatal Aperture. *Plant Physiol.* **175**, 1864–1877 (2017).

294. Pagnussat, G. C., Lanteri, M. L. & Lamattina, L. Nitric Oxide and Cyclic GMP Are Messengers in the Indole Acetic Acid-Induced Adventitious Rooting Process. *Plant Physiol.* **132**, 1241–1248 (2003).

295. Bai, X., Todd, C. D., Desikan, R., Yang, Y. & Hu, X. N -3-Oxo-Decanoyl-l-Homoserine-Lactone Activates Auxin-Induced Adventitious Root Formation via Hydrogen Peroxide- and Nitric Oxide-Dependent Cyclic GMP Signaling in Mung Bean. *Plant Physiol.* **158**, 725–736 (2012).

296. Nan, W. *et al.* Cyclic GMP is involved in auxin signalling during Arabidopsis root growth and development. *J. Exp. Bot.* **65**, 1571–1583 (2014).

297. Teng, Y., Xu, W. & Ma, M. cGMP is required for seed germination in Arabidopsis thaliana. *J. Plant Physiol.* **167**, 885–889 (2010).

298. Shen, Q. *et al.* Dual Activities of Plant cGMP-Dependent Protein Kinase and Its Roles in Gibberellin Signaling and Salt Stress. *Plant Cell* **31**, 3073–3091 (2019).

299. Durner, J., Wendehenne, D. & Klessig, D. F. Defense gene induction in tobacco by nitric oxide, cyclic GMP, and cyclic ADP-ribose. *Proc. Natl. Acad. Sci.* **95**, 10328–10333 (1998).

300. Klessig, D. F. *et al.* Nitric oxide and salicylic acid signaling in plant defense. *Proc. Natl. Acad. Sci.* **97**, 8849–8855 (2000).

301. Joudoi, T. *et al.* Nitrated Cyclic GMP Modulates Guard Cell Signaling in *Arabidopsis*. *Plant Cell* **25**, 558–571 (2013).

302. Honda, K. *et al.* 8-Mercapto-Cyclic GMP Mediates Hydrogen Sulfide-Induced Stomatal Closure in Arabidopsis. *Plant Cell Physiol.* **56**, 1481–1489 (2015).

303. Isner, J.-C. *et al.* Short- and Long-Term Effects of UVA on Arabidopsis Are Mediated by a Novel cGMP Phosphodiesterase. *Curr. Biol.* **29**, 2580-2585.e4 (2019).

304. Neill, S. J., Desikan, R., Clarke, A. & Hancock, J. T. Nitric Oxide Is a Novel Component of Abscisic Acid Signaling in Stomatal Guard Cells. *Plant Physiol.* **128**, 13–16 (2002).

305. Ashman, D. F., Lipton, R., Melicow, M. M. & Price, T. D. Isolation of adenosine 3',5'-monophosphate and guanosine 3',5'-monophosphate from rat urine. *Biochem. Biophys. Res. Commun.* **11**, 330–334 (1963).

306. Ignarro, L. J., Buga, G. M., Wood, K. S., Byrns, R. E. & Chaudhuri, G. Endothelium-derived relaxing factor produced and released from artery and vein is nitric oxide. *Proc. Natl. Acad. Sci.* **84**, 9265–9269 (1987).

307. Waldman, S. A., Rapoport, R. M. & Murad, F. Atrial natriuretic factor selectively activates particulate guanylate cyclase and elevates cyclic GMP in rat tissues. *J. Biol. Chem.* **259**, 14332–14334 (1984).

308. Beavo, J. A. & Brunton, L. L. Cyclic nucleotide research — still expanding after half a century. *Nat. Rev. Mol. Cell Biol.* **3**, 710–717 (2002).

309. Kots, A. Y., Martin, E., Sharina, I. G. & Murad, F. A Short History of cGMP, Guanylyl Cyclases, and cGMP-Dependent Protein Kinases. *CGMP Gener. Eff. Ther. Implic.* **191**, 1–14 (2009).

310. Newton, R. P. & Smith, C. J. Cyclic nucleotides. *Phytochemistry* **65**, 2423–2437 (2004).

311. Gehring, C. & Turek, I. S. Cyclic Nucleotide Monophosphates and Their Cyclases in Plant Signaling. *Front. Plant Sci.* **8**, 1704 (2017).

312. Ludidi, N. & Gehring, C. Identification of a Novel Protein with Guanylyl Cyclase Activity in *Arabidopsis thaliana*. *J. Biol. Chem.* **278**, 6490–6494 (2003).

313. Kwezi, L. *et al.* The Arabidopsis thaliana Brassinosteroid Receptor (AtBRI1) Contains a Domain that Functions as a Guanylyl Cyclase In Vitro. *PLoS ONE* **2**, e449 (2007).

314. Wheeler, J. I. *et al.* The brassinosteroid receptor BRI1 can generate cGMP enabling cGMP-dependent downstream signaling. *Plant J.* **91**, 590–600 (2017).

315. Kwezi, L. *et al.* The Phytosulfokine (PSK) Receptor Is Capable of Guanylate Cyclase Activity and Enabling Cyclic GMP-dependent Signaling in Plants. *J. Biol. Chem.* **286**, 22580–22588 (2011).

316. Muleya, V. *et al.* Calcium is the switch in the moonlighting dual function of the ligand-activated receptor kinase phytosulfokine receptor 1. *Cell Commun. Signal.* **12**, 60 (2014).

317. Mulaudzi, T. *et al.* Identification of a novel *Arabidopsis thaliana* nitric oxide-binding molecule with guanylate cyclase activity *in vitro*. *FEBS Lett.* **585**, 2693–2697 (2011).

318. Gross, I. & Durner, J. In Search of Enzymes with a Role in 3', 5'-Cyclic Guanosine Monophosphate Metabolism in Plants. *Front. Plant Sci.* **7**, (2016).

319. Kasahara, M. *et al.* An adenylyl cyclase with a phosphodiesterase domain in basal plants with a motile sperm system. *Sci. Rep.* **6**, 39232 (2016).

320. Świeżawska, B., Duszyn, M., Jaworski, K. & Szmidt-Jaworska, A. Downstream Targets of Cyclic Nucleotides in Plants. *Front. Plant Sci.* **9**, 1428 (2018).

321. Pharmawati, M., Billington, T. & Gehring, C. A. Stomatal guard cell responses to kinetin and natriuretic peptides are cGMP-dependent. *Cell. Mol. Life Sci. CMLS* **54**, 272–276 (1998).

322. Pharmawati, M., Maryani, M. M., Nikolakopoulos, T., Gehring, C. A. & Irving, H. R. Cyclic GMP modulates stomatal opening induced by natriuretic peptides and immunoreactive analogues. *Plant Physiol. Biochem.* **39**, 385–394 (2001).

323. Cousson, A. & Vavasseur, A. Putative involvement of cytosolic Ca 2+ and GTP-binding proteins in cyclic-GMP-mediated induction of stomatal opening by auxin in Commelina communis L. *Planta* **206**, 308–314 (1998).

324. Cousson, A. Pharmacological evidence for the implication of both cyclic GMP-dependent and -independent transduction pathways within auxin-induced stomatal opening in Commelina communis (L.). *Plant Sci.* **161**, 249–258 (2001).

325. Cousson, A. Pharmacological evidence for a positive influence of the cyclic GMP-independent transduction on the cyclic GMP-mediated Ca2+-dependent pathway within Arabidopsis stomatal opening in response to auxin. *Plant Sci.* **164**, 759–767 (2003).

326. Donaldson, L., Ludidi, N., Knight, M. R., Gehring, C. & Denby, K. Salt and osmotic stress cause rapid increases in *Arabidopsis thaliana* cGMP levels. *FEBS Lett.* **569**, 317–320 (2004).

327. Dubovskaya, L. V. *et al.* cGMP-dependent ABA-induced stomatal closure in the ABA-insensitive Arabidopsis mutant abi1-1. *New Phytol.* **191**, 57–69 (2011).

328. Wang, Y.-F. *et al.* Identification of Cyclic GMP-Activated Nonselective Ca2+-Permeable Cation Channels and Associated CNGC5 and CNGC6 Genes in Arabidopsis Guard Cells. *PLANT Physiol.* **163**, 578–590 (2013).

329. Busby, S. & Ebright, R. H. Transcription activation by catabolite activator protein (CAP). *J. Mol. Biol.* **293**, 199–213 (1999).

330. Francis, S., H. Molecular properties of mammalian proteins that interact with cGMP: protein kinases, cation channels, phosphodiesterases, and multi-drug anion transporters. *Front. Biosci.* **10**, 2097 (2005).

331. Weber, I. T., Shabb, J. B. & Corbin, J. D. Predicted structures of the cGMP binding domains of the cGMP-dependent protein kinase: a key alanine/threonine difference in evolutionary divergence of cAMP and cGMP binding sites. *Biochemistry* **28**, 6122–6127 (1989).

332. Leng, Q., Mercier, R. W., Yao, W. & Berkowitz, G. A. Cloning and First Functional Characterization of a Plant Cyclic Nucleotide-Gated Cation Channel. *Plant Physiol.* **121**, 753–761 (1999).

333. Martinez-Atienza, J., Van Ingelgem, C., Roef, L. & Maathuis, F. J. M. Plant Cyclic Nucleotide Signalling: Facts and Fiction. *Plant Signal. Behav.* **2**, 540–543 (2007).

334. Winter, D. *et al.* An "Electronic Fluorescent Pictograph" Browser for Exploring and Analyzing Large-Scale Biological Data Sets. *PLoS ONE* **2**, e718 (2007).

335. Isner, J.-C. & Maathuis, F. J. M. cGMP signalling in plants: from enigma to main stream. *Funct. Plant Biol.* **45**, 93 (2018).

336. Donaldson, L., Meier, S. & Gehring, C. The arabidopsis cyclic nucleotide interactome. *Cell Commun. Signal.* **14**, 10 (2016).

337. Kostaki, K.-I. *et al.* Guard Cells Integrate Light and Temperature Signals to Control Stomatal Aperture. *Plant Physiol.* **182**, 1404–1419 (2020).

338. Ryan, A. C. *et al.* Gravimetric phenotyping of whole plant transpiration responses to atmospheric vapour pressure deficit identifies genotypic variation in water use efficiency. *Plant Sci.* **251**, 101–109 (2016).

339. Even, M. *et al.* Night-time transpiration in barley (Hordeum vulgare) facilitates respiratory carbon dioxide release and is regulated during salt stress. *Ann. Bot.* **122**, 569–582 (2018).

340. Coupel-Ledru, A. *et al.* Reduced nighttime transpiration is a relevant breeding target for high water-use efficiency in grapevine. *Proc. Natl. Acad. Sci.* **113**, 8963–8968 (2016).

341. Mishra, G. A Bifurcating Pathway Directs Abscisic Acid Effects on Stomatal Closure and Opening in Arabidopsis. *Science* **312**, 264–266 (2006).

342. Pires, N. D. & Dolan, L. Morphological evolution in land plants: new designs with old genes. *Philos. Trans. R. Soc. B Biol. Sci.* **367**, 508–518 (2012).

343. Chen, K. *et al.* Abscisic acid dynamics, signaling, and functions in plants. *J. Integr. Plant Biol.* **62**, 25–54 (2020).

344. Sharp, R. E., LeNoble, M. E., Else, M. A., Thorne, E. T. & Gherardi, F. Endogenous ABA maintains shoot growth in tomato independently of effects on plant water balance: evidence for an interaction with ethylene. *J. Exp. Bot.* **51**, 1575–1584 (2000).

345. LeNoble, M. E. Maintenance of shoot growth by endogenous ABA: genetic assessment of the involvement of ethylene suppression. *J. Exp. Bot.* **55**, 237–245 (2003).

346. McAusland, L. *et al.* Effects of kinetics of light-induced stomatal responses on photosynthesis and water-use efficiency. *New Phytol.* **211**, 1209–1220 (2016).

347. Kuhn, J. M., Boisson-Dernier, A., Dizon, M. B., Maktabi, M. H. & Schroeder, J. I. The Protein Phosphatase *AtPP2CA* Negatively Regulates Abscisic Acid Signal Transduction in Arabidopsis, and Effects of *abh1* on *AtPP2CA* mRNA. *Plant Physiol.* **140**, 127–139 (2006).

348. Saez, A. *et al.* Enhancement of Abscisic Acid Sensitivity and Reduction of Water Consumption in Arabidopsis by Combined Inactivation of the Protein Phosphatases Type 2C ABI1 and HAB1. *Plant Physiol.* **141**, 1389–1399 (2006).

349. Wang, X. *et al.* ABRE-BINDING FACTORS play a role in the feedback regulation of ABA signaling by mediating rapid ABA induction of ABA co-receptor genes. *New Phytol.* **221**, 341–355 (2019).

350. Kollist, H. *et al.* Rapid Responses to Abiotic Stress: Priming the Landscape for the Signal Transduction Network. *Trends Plant Sci.* **24**, 25–37 (2019).

CHAPTER 8: APPENDIX

www.nature.com/scientificreports

scientific reports

Check for updates

OPEN

ABA signalling and metabolism are not essential for dark-induced stomatal closure but affect response speed

Ashley J. Pridgeon & Alistair M. Hetherington✉

Stomata are microscopic pores that open and close, acting to balance CO_2 uptake with water loss. Stomata close in response to various signals including the drought hormone abscisic acid (ABA), microbe-associated-molecular-patterns, high CO_2 levels, and darkness. The signalling pathways underlying ABA-induced stomatal closure are well known, however, the mechanism for dark-induced stomatal closure is less clear. ABA signalling has been suggested to play a role in dark-induced stomatal closure, but it is unclear how this occurs. Here we investigate the role of ABA in promoting dark-induced stomatal closure. Tracking stomatal movements on the surface of leaf discs we find, although steady state stomatal apertures are affected by mutations in ABA signalling and metabolism genes, all mutants investigated close in response to darkness. However, we observed a delayed response to darkness for certain ABA signalling and metabolism mutants. Investigating this further in the quadruple ABA receptor mutant (*pyr1pyl1pyl2pyl4*), compared with wild-type, we found reduced stomatal conductance kinetics. Although our results suggest a non-essential role for ABA in dark-induced stomatal closure, we show that ABA modulates the speed of the dark-induced closure response. These results highlight the role of ABA signalling and metabolic pathways as potential targets for enhancing stomatal movement kinetics.

Plants are able to rapidly respond to environmental stimuli by regulating gas exchange through changes in the aperture of stomata on leaf surfaces. Stomata are composed of two guard cells surrounding a central pore. Changes in guard cell turgor pressure bring about changes in the aperture of the stomatal pore. The regulation of gas exchange allows plants to balance the uptake of carbon dioxide (CO_2) with the loss of water[1]. Much work has focused on the underlying mechanisms of stomatal movements, especially on how ion transport across guard cell membranes helps to mediate changes in guard cell turgor pressure, the mechanisms behind blue and red light induced stomatal opening, and how the drought hormone abscisic acid (ABA) leads to stomatal closure and the inhibition of stomatal opening[2]. However, the process underlying dark-induced stomatal closure is unclear. It is unknown whether darkness actively accesses stomatal closure machinery or whether it is a passive response to the absence of light. In addition, as there is an increase in leaf intercellular CO_2 concentration (Ci) during dark treatment it is possible that CO_2 also has a contribution to make towards dark-induced closure. However, the contribution of Ci to dark-induced closure has not been investigated in the present study.

Few mutants have been identified that show strongly defective dark-induced stomatal closure responses. Those that do are often involved in regulating stomatal opening; such as mutants in COP1, an E3 ubiquitin ligase that functions downstream of the cryptochrome and phototropin photoreceptors[3], or the dominant mutation, *ost2-2D,* causing constitutive activation of the H^+ ATPase AHA1 (a proton pump that hyperpolarises guard cell membranes, inducing ion transport and ultimately stomatal opening)[4]. Additionally, reorganisation of the actin cytoskeleton has been shown to be crucial for stomatal dark-induced closure, as mutations within the Arp2/3 and SCAR/WAVE complexes that control actin cytoskeleton dynamics show lack of dark-induced closure[5,6]. Weaker phenotypes have also been observed, such as in the *myb61* transcription factor mutant, where stomatal apertures are increased in dark conditions, however here, stomatal apertures are also increased in light conditions and there is a noticeable but reduced response to darkness[7]. More recently additional signalling components required for dark-induced closure have been identified. The pseudokinase GHR1, involved in activating the downstream ion channel SLAC1, has been shown to be required for stomatal closure in response to a number of signals, including

School of Biological Sciences, Life Sciences Building, University of Bristol, 24 Tyndall Avenue, Bristol BS8 1TQ, UK. ✉email: Alistair.Hetherington@bristol.ac.uk

darkness[8]. A MEK1/MPK6 signalling cascade activated by H_2O_2 (produced by RBOHD and RBOHF) and culminating in the production of NO (by NIA1) has also been shown to be required for dark-induced closure[9].

Studies have linked ABA signalling to dark-induced closure, but the precise way in which it is involved in regulating dark-induced closure is unclear. Microarray data have shown components of the ABA signalling pathway undergo transcriptional regulation in response to darkness, however these changes are likely to reflect longer term adaptation rather than the short term closure[10]. Additionally, another study has shown that a selection of ABA receptor mutants (*pyr1pyl1pyl2pyl4*, *pyr1pyl4pyl5pyl8*, *pyr1pyl2pyl4pyl5pyl8*, *pyr1pyl1pyl2pyl4pyl5pyl8*) all show increased stomatal conductance under light and dark conditions. However, when comparing the change in stomatal conductance from light to dark conditions all of the previously mentioned ABA receptor mutants (except the strongest mutant, *pyr1pyl1pyl2pyl4pyl5pyl8*) show changes in stomatal conductance similar to wild type. Similarly, mutations within PP2C phosphatases (downstream negative regulators of ABA signalling) and ABA degradation mutants, affect stomatal conductance without preventing responses to darkness. In the ABA biosynthesis mutants, *aba1-1* and *aba3-1,* stomatal conductance is also increased, however both mutants still respond to a dark (although this appears weakened in *aba3-1*)[11]. In addition, stomatal aperture changes in the PP2C mutants *abi1* and *abi2* show reduced responses to darkness[12]. This suggests a situation where ABA signalling may make a contribution to dark-induced stomatal closure, however, it also suggests that ABA has more general effects on stomatal apertures regardless of light or dark conditions.

Here we investigate how defects in ABA signalling and metabolism affect stomatal response to darkness and light. We analyse the movement of stomata through direct measurements on leaf discs and through monitoring changes in stomatal conductance. We find evidence that ABA signalling is not essential for dark-induced closure. However, we provide additional evidence that defects in ABA signalling and metabolism affect the timing of stomatal responses to both light and darkness. Overall, we conclude that ABA signalling does not play a major role in mediating dark-induced closure but does play a role in modulating the speed of closure.

Results

ABA signalling and biosynthesis mutant responses to darkness. To explore whether mutations in ABA biosynthesis, degradation or signalling genes affect stomatal responses to darkness, stomatal movements were measured in leaf discs from ABA metabolism and signalling mutants. Aperture measurements taken over a 2 h dark treatment time course, with independent leaf disc measurements at each timepoint, allowed for detection of trends in stomatal responses. Of the 14 member ABA receptor family, quadruple and sextuple ABA receptor mutants (*pyr1pyl1pyl2pyl4*[13]—*q1124* and *pyr1pyl1pyl2pyl4pyl5pyl8* [14]—*s112458*) were used. The ABA biosynthesis double mutant *nced3nced5*[15] (*nced3/5*—a double mutant in the *NCED3* and *5* genes which catalyse the first committal step in ABA biosynthesis, thought to be the rate limiting step under drought conditions[15–17]) and mutants within 2 genes involved in rapid ABA activation from inactive glucose esters (*bg1* and *bg2*[18]) were used. Additionally mutants in ABA hydroxylation genes (*cyp707a1* and *cyp707a3*[19]) involved in ABA catabolism were used (exact mutant accession codes are shown in the methods section).

Delays in stomatal closure following dark treatment were observed for the ABA receptor mutants *q1124* and *s112458*, the ABA biosynthesis mutant *nced3/5*, and the ABA activation mutant *bg1,* which all show no significant change in stomatal aperture, compared with wild type, after 30 mins dark treatment (Fig. 1a–c). No delays in dark-induced stomatal closure were observed in the ABA activation mutant *bg2* or the ABA catabolism mutants *cyp707a1* or *cyp707a3* (Fig. 1c,d). Absolute changes in stomatal aperture for each mutant are shown in Fig. S1. The absence of a delay phenotype in the *bg2* mutant could be due to the difference in subcellular location and/or reduced activity of the BG2 protein compared with BG1[18]. Additionally, mutations in *CYP707A1 and 3* genes lead to increased levels of ABA[19,20] and increased ABA signalling activity (the opposite of what occurs in ABA biosynthesis and signalling mutants), explaining the lower starting apertures (as observed previously[19]) and potentially the absence of delay.

In addition to delays in dark-induced stomatal closure, changes to stomatal apertures regardless of treatment are observed for many of the mutants analysed. The ABA receptor and biosynthesis mutants (*q1124*, *s112458* and *nced3/5*) show significantly increased stomatal apertures before (*q1124*—$p = 0.00003$, *s112458*—$p < 0.00001$, *nced3/5*—$p < 0.00001$) and after 2 h of dark treatment compared with Col-0 (*q1124*—$p < 0.00001$, *s112458*—$p < 0.00001$, *nced3/5*—$p < 0.0001$). Conversely, the ABA catabolism mutants (*cyp707a1* and *cyp707a3*) show reduced stomatal apertures prior to dark treatment (*cyp707a1*—$p = 0.00268$, *cyp707a3*—$p = 0.02927$) and similar apertures after 2 h dark treatment. The ABA biosynthesis mutants *bg1* and *bg2* show no difference when compared with Col-0 before or 2 h after dark treatment.

Stomatal conductance responses to darkness. The stomatal conductance responses to darkness applied at midday were also measured in the following genotypes; Col-0, *q1124*, *bg1*, *cyp707a1*, and *cyp707a3*. Due to the greatly reduced leaf size phenotype of the *s112458* and *nced3/5* mutants, stomatal conductance could not be recorded. Focusing on dark-induced decreases in stomatal conductance, it is evident this response occurs much faster than dark-induced closure in leaf discs (Fig. 1). The absolute and relative stomatal conductance values are shown for the mutants in Fig. 2a, c, e and b, d, f respectively. Here, delayed responses are only noticeable for the *q1124* receptor mutant (Fig. 2a,b). All mutants appear to decrease their stomatal conductance by around 50% in response to darkness. The difference in the periods of delays observed in leaf discs and in measurements of stomatal conductance may reflect that stomatal conductance responses are faster than changes in stomatal aperture measured on leaf discs, similar to observed differences in stomatal movement when comparing responses to red light in epidermal peels and intact leaves[21]. Stomatal conductance responses generally reach their maximum by 25 mins (Figs. 2, 4, 5, 6) whereas leaf disc stomatal aperture responses reach their maximum by 120 mins (Figs. 1, 7). The slower movements on leaf discs may allow for more subtle mutant phenotypes to

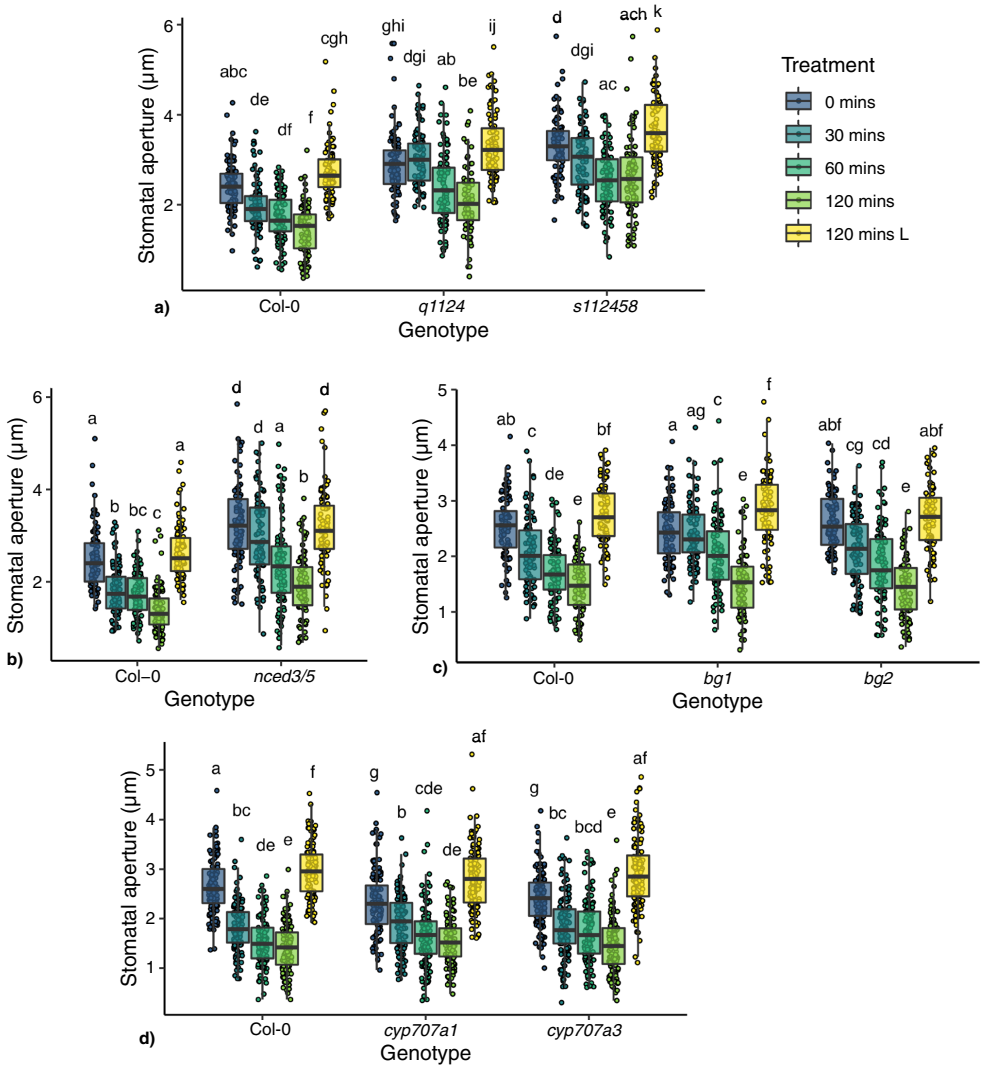

Figure 1. Stomatal responses of ABA signalling, biosynthesis and degradation mutants to darkness. Stomatal responses to darkness over a 120 min time course were tracked in leaf discs harvested from (**a**) ABA receptor mutants (*q1124* and *s112458*), (**b**) *nced3/5*, (**c**) ABA activation mutants (*bg1* and *bg2*) and (**d**) ABA degradation mutants (*cyp707a1* and *cyp707a3*). Leaf discs were incubated under light for 120 mins before transfer to darkness. 120 mins L represent aperture data from leaf discs left under light for 120 mins. n = 90 from 9 individual plants over 3 independent experiments. Data is presented in boxplots showing the median and interquartile range of each group. The upper and lower whiskers represent data within 1.5 * the interquartile range. All data values are represented by points. Data statistically analysed using 2-way ANOVA with Tukey multiple comparison tests, letters denote significant differences at $p < 0.05$.

be identified. Additionally, when tracking the intercellular leaf CO_2 concentration (C_i) over the course of the experiments a rapid increase is seen upon dark treatment, that then rapidly decreases upon reintroduction to

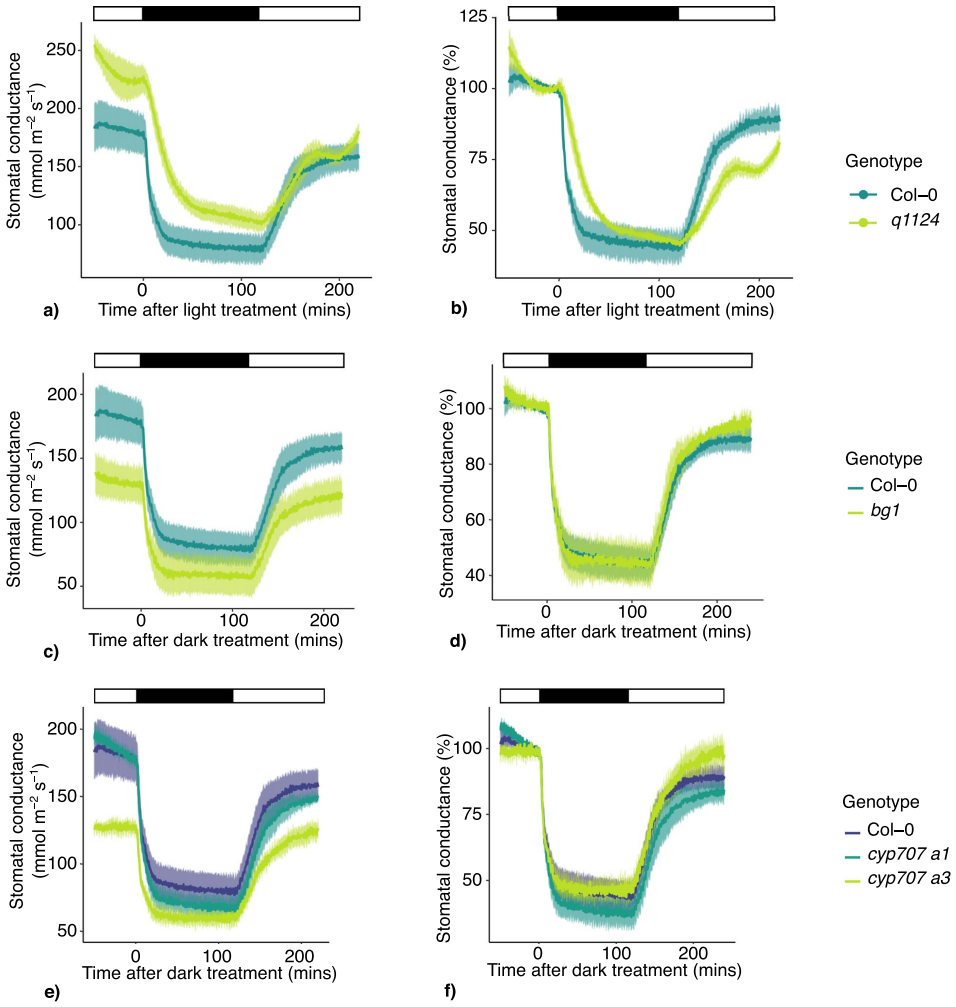

Figure 2. Stomatal conductance responses to darkness for ABA signalling, activation, and degradation mutants. Stomatal conductance of ABA signalling and metabolism mutants were measured in response to 120 mins darkness, followed by a further 120 mins light. Absolute and relative stomatal conductance values for (**a**, **b**) *q1124*, (**c**, **d**) *bg1* and (**e**, **f**) *cyp707a1* and *cyp707a3* are shown. Lines represent the mean ± s.e.m. 3–4 plants were measured per genotype. Light treatment is represented above each plot, with black boxes representing darkness and white boxes representing light.

light, before returning to levels comparable to those before the initial dark treatment (Fig. 3). This build-up of C_i may contribute to the stomatal conductance response, however this requires further investigation.

Further analysis of *q1124* stomatal conductance responses to darkness. For Col-0 and *q1124*, the stomatal conductance responses were measured when whole plants were placed in darkness 4–5 h after dawn. Leaves were clamped into the gas analyser leaf cuvette, 2 h prior to the onset of darkness. After 1 h of darkness plants were reintroduced to light for a further hour. *q1124* shows higher stomatal conductance (at time 0—$p = 0.00231$) and stomatal conductance is reduced to a lesser extent than wild type in darkness. This is true in absolute (Fig. 4a) and relative (Fig. 4b) terms. The time taken for *q1124* to reach half of its total stomatal conductance response to darkness (darkness half response time—Fig. 4c) and to light (light half response time—

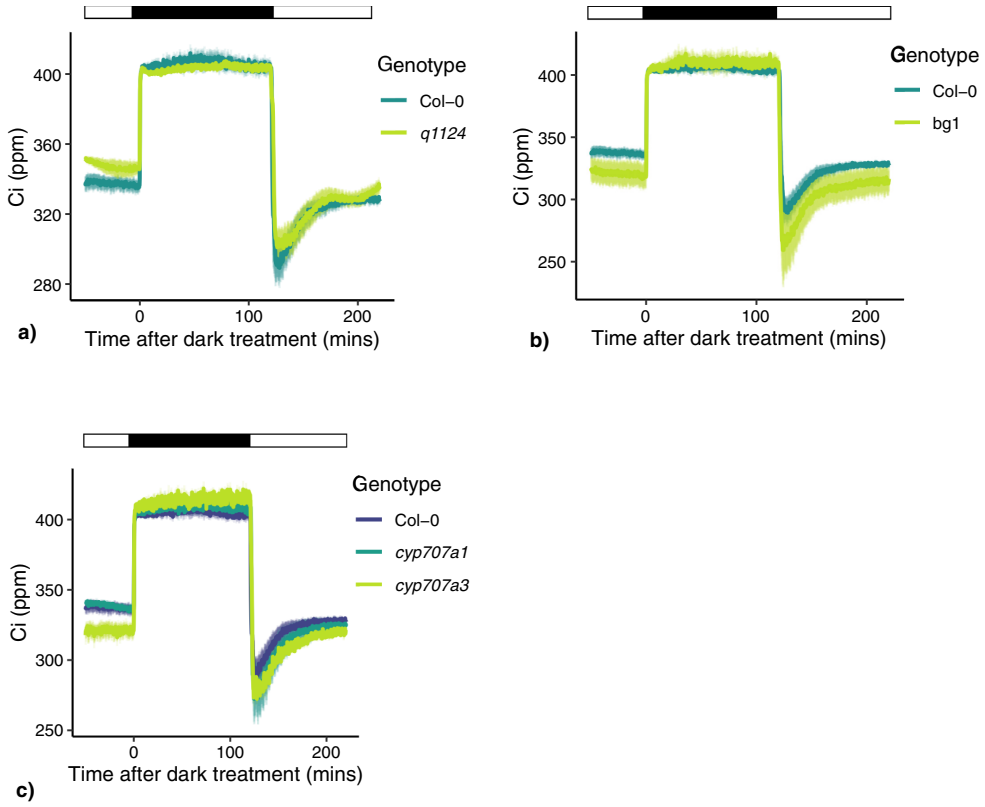

Figure 3. Intercellular CO_2 concentration in response to darkness applied at midday. Intercellular CO_2 concentration (C_i) of leaves of (**a**) ABA receptor mutant (*q1124*), (**b**) ABA activation mutant (*bg1*), (**c**) ABA degradation mutants (*cyp707a1* and *cyp707a3*) in response to darkness applied at midday. Lines represent the mean ± s.e.m. 3–4 plants were measured per genotype. Light treatment is represented above each plot, with black boxes representing darkness and white boxes representing light.

Fig. 4d) shows greater variability when compared with Col-0, and the q1124 half response time in response to darkness is significantly increased (p = 0.0148). However, there do appear to be differences in the response of *q1124* to darkness when comparing Figs. 2a, b and 4a, b suggesting a degree of biological variation in the *q1124* dark response phenotype.

Stomatal conductance in Col-0 and *q1124* was also measured at dusk. Unlike the response to darkness measured at midday, where plants were plunged into darkness, the onset of dusk was marked with a 15 min transition from light to dark. The absolute stomatal conductance of Col-0 and *q1124* is shown in Fig. 5a. It is clear that both genotypes respond to dusk. Because of the differences in absolute initial stomatal conductance, relative stomatal conductance were calculated. The data in Fig. 5b suggest that the speed of stomatal conductance change in the *q1124* ABA quadruple receptor mutant is reduced compared with Col-0. The difference between Col-0 and *q1124* is less pronounced than that observed in Fig. 4, yet measurement of dusk half response times supports a slower stomatal conductance response of *q1124* to darkness (p = 0.00607).

The effect of mutations in ABA biosynthesis, signalling and activation on stomatal responses to light. In addition to the delay in dark-induced stomatal closure and slower stomatal conductance responses observed in *q1124*, the data in Figs. 2 and 4 suggest that there might also be defects in the light-induced opening response of the quadruple receptor mutant. Stomatal conductance of *q1124* was measured over the dawn period. Here, similarly to dusk, the onset of dawn was marked with a 15 min transition period from dark to light. Absolute and relative stomatal conductance values are presented in Fig. 6a, b respectively. Similar to the response observed at dusk, in comparison to wild type, the *q1124* mutant shows increased absolute stomatal conduct-

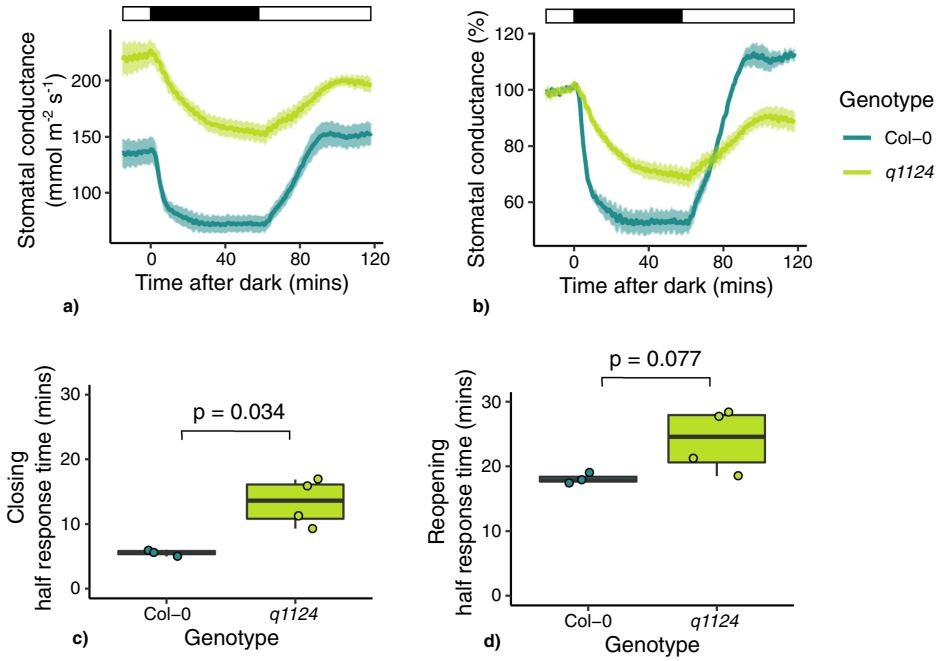

Figure 4. *q1124* stomatal conductance responses to darkness at midday. Stomatal conductance of *q1124* ABA quadruple receptor mutant was measured in response to darkness applied 4–5 h post dawn. (**a**) Absolute and (**b**) relative stomatal conductane values are presented as the mean ± s.e.m. The time taken to reach half of the maximum stomatal conductance change (half response times) in response to (**c**) darkness and (**d**) light are presented in boxplots showing the median and interquartile ranges. 3–4 plants measured per genotype. Light treatment is represented above each stomatal conductance plot, with black boxes representing darkness and white boxes representing light.

ance values and an increased half stomatal conductance response time, suggesting this response also occurs at a slower rate (Fig. 6c) ($p = 0.000239$).

The stomatal movements of *q1124*, *nced3/5* and *bg1* mutants were also analysed in leaf discs. Here, leaf discs were harvested pre-dawn under green light, incubated in the dark for 2 h, before being transferred to light. The apertures were monitored over a 2 h time course. Figure 7 shows both the absolute and relative change in stomatal aperture for the three mutants. It is evident that both *q1124* and *nced3/5* have significantly increased stomatal apertures at 0 mins ($p < 0.0001$, $p < 0.0001$ respectively), whereas *bg1* is similar to Col-0. This makes comparisons between the absolute stomatal apertures of Col-0, *q1124* and *nced3/5* more difficult to interpret. However, when analysing the absolute change in stomatal aperture for both *q1124* and *nced3/5* there are no initial significant differences at 30 mins, but by 120 mins there are significantly reduced responses ($p < 0.005$, $p < 0.0001$ respectively).

Unlike *q1124* and *nced3/5*, the *bg1* mutant shows a response analogous to that observed when plants are placed in darkness (except instead of an initial delay in dark-induced stomatal closure, here a delay in light-induced stomatal opening is observed). *bg1* shows a significantly weakened response at 30 mins ($p < 0.0005$), before the *bg1* mutant eventually catches up to Col-0 by 60 and 120 mins.

Discussion

ABA is well known as a regulator of seed dormancy and plant responses to drought including reductions in stomatal aperture and inhibition of light-induced opening[22]. Additionally, evidence is emerging supporting roles for basal ABA signalling under non-stress situations[23]. On a molecular level, a subset of ABA receptor family members (subfamily 1) are known to activate downstream signalling under basal amounts of ABA[24] and mutation of ABA signalling and metabolism components alters plant growth and development under non stress conditions[25,26]. Here we explore the role of ABA and ABA signalling in stomatal responses to the onset of light and darkness.

The mechanisms behind light-induced stomatal opening are relatively well understood. Stomatal opening in response to light is driven by the activity of plasma membrane H^+ATPases. This generates a proton gradient across the guard cell plasma membranes, resulting in membrane hyperpolarization leading to the influx of cations and

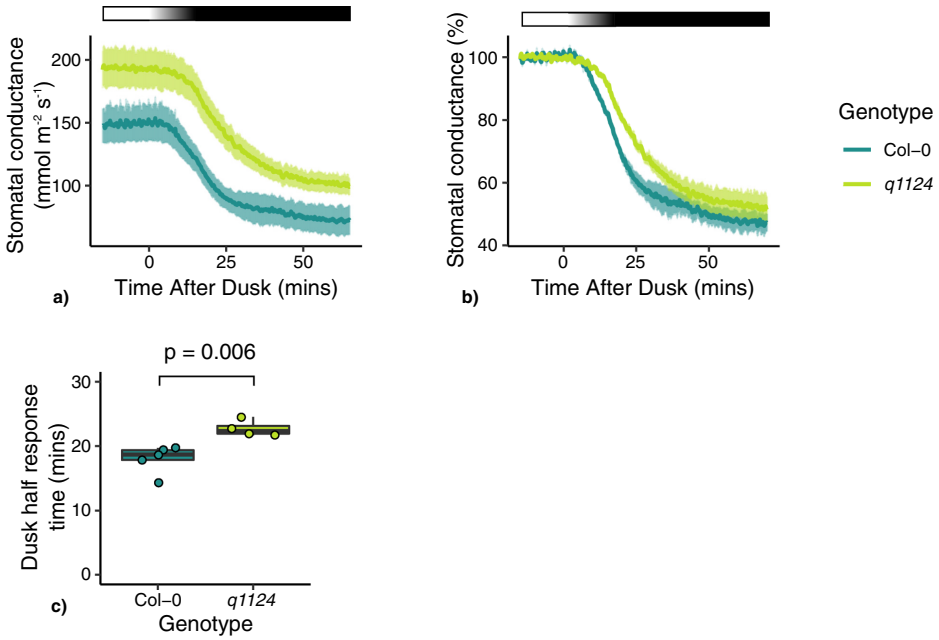

Figure 5. *q1124* stomatal conductance response at dusk. Stomatal conductance of the *q1124* quadruple ABA receptor over the dusk transition period. On the onset of dusk, the lights were dimmed over a 15 min period until completely turned off. (**a**) Absolute and (**b**) relative stomatal conductance values are presented as the mean ± s.e.m. (**c**) The time taken to reach half of the maximum stomatal conductance change (half response times) upon dusk are presented in boxplots showing the median and interquartile ranges. 4–5 plants measured per genotype. Light treatment is represented above each stomatal conductance plot, with black boxes representing darkness and white boxes representing light. A gradient represents the 15 min transition from light to darkness.

anions, changes in guard cell turgor pressure, and ultimately the opening of stomata. Blue and red light promote stomatal opening via independent pathways. Blue light-induced opening is predominantly initiated via activation of phototropin photoreceptors within the guard cell[27], whereas red light-induced opening is dependent on photosynthetic electron transport[28,29]. When Arabidopsis plants are moved from light to dark their stomata close, however, the mechanisms behind dark-induced stomatal closure are less clear[30]. Studies have linked ABA signalling to dark-induced closure, but it is unclear to what extent ABA signalling is required for this process[4,10–12].

Here, we present evidence that supports a non-central role for ABA metabolism and ABA signalling in dark-induced stomatal closure. In leaf discs we observe that all ABA signalling and metabolism mutants analysed were able to respond to darkness (Fig. 1). Compared with wild type, ABA receptor mutants (*q1124* and *s112458*) and the ABA biosynthesis mutant (*nced3/5*) showed increased stomatal apertures before treatment whereas ABA degradation mutants (*cyp707a1* and *cyp707a3*) showed decreased stomatal apertures. This is in line with previous reports, namely that, defects in ABA signalling and production lead to increases in steady state stomatal apertures and transpiration, whereas defects in ABA degradation lead to the opposite[11,14,15,20]. This shows links between ABA, ABA signalling and the regulation of stomatal apertures under non stress conditions. However, following dark treatment *cyp707a1* and *cyp707a3* mutants close to the same extent as wild type. On the other hand, the stomata of *q1124, s112458,* and *nced3/5* mutants all remain more open than wild type. These results are similar to those observed for stomatal conductance in ABA receptor mutants (*q1124*/*pyr1pyl1pyl2pyl4, pyr1pyl4pyl5pyl8, pyr1pyl2pyl4pyl5pyl8*) in Merilo et al. 2013 with one exception. Whereas Merilo et al. 2013 report no response to darkness, here we report that the stomata of *s112458* mutant are still able to respond to darkness, but to a lesser extent than wild type. The strong ABA biosynthesis mutant *nced3/5* also behaves similarly to the *aba1-1* and *aba3-1* biosynthesis mutants in Merilo et al. 2013. *nced3/5* shows significantly more open stomata throughout the experiment and responds to darkness, although to a lesser extent than wild type. Additionally, we report ABA signalling (*q1124* and *s112458*) and biosynthesis mutants (*nced3/5* and *bg1*) show a delay in closure, with no significant change in stomatal aperture following 30 min of dark treatment, when measured in leaf discs. In Merilo et al. 2013, T-DNA insertion mutants in the downstream ABA signalling component OST1 (*ost1-3*) and the ion channel SLAC1 (*slac1-3*) show similar dark-induced transpiration changes to those of ABA biosynthesis

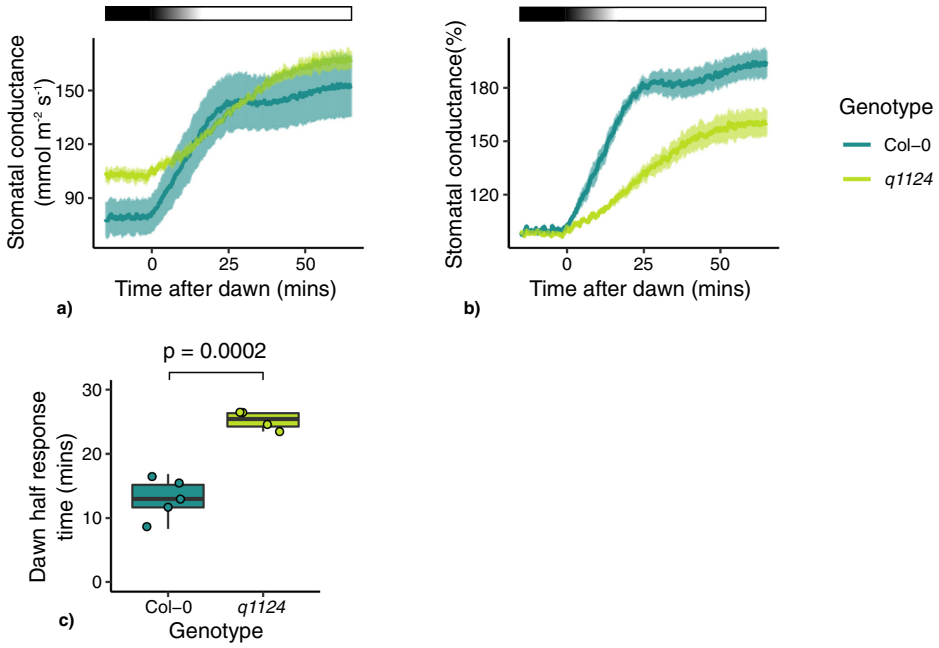

Figure 6. *q1124* stomatal conductance responses at dawn. Stomatal conductance of the *q1124* quadruple ABA receptor over the dawn transition period. On the onset of dawn, the lights were turned on over a 15 min period until reaching full brightness. (**a**) Absolute and (**b**) relative stomatal conductance values are presented as the mean ± s.e.m. (**c**) The time taken to reach half of the maximum stomatal conductance change (half response times) upon dusk are presented in boxplots showing the median and interquartile ranges. 4–5 plants measured per genotype. Light treatment is represented above each plot, with black boxes representing darkness and white boxes representing light. A gradient represents the 15 min transition from darkness to light.

mutants (*aba1-1* and *aba3-1*), where stomatal conductances are increased but still show responses to darkness. This suggests a non-central role for ABA and ABA signalling in dark-induced closure.

Exploring this further we find that the time taken for *q1124* mutant to reach its maximum stomatal conductance response is increased compared to Col-0 (Figs. 2, 4, 5, 6). This is observed when darkness and light are applied during the middle of the day and also at the dawn and dusk transition periods. This suggests that although ABA signalling is not essential for dark-induced closure, it appears to be involved in increasing the speed of stomatal responses to darkness and light. It should be noted there is a difference between the time taken for stomatal apertures to show maximum responses (Fig. 1) and stomatal conductance responses to reach their maximum (Figs. 2, 4, 5, 6), with stomatal movement on leaf discs appearing slower than that of changes in conductance. The reasons for this are unclear but likely due to differences between the systems of a leaf disc and an attached leaf.

Manipulating the speed of stomatal responses has been shown to increase biomass accumulation[31] and may improve key plant processes such as photosynthetic carbon assimilation and water use efficiency[32], suggesting it could be a key target for plant breeders. How defects within ABA metabolism and signalling are affecting the speed of stomatal responses is currently unclear but may stem from altered amounts or activities of further signalling components and/or ion channels within plant cells. Additionally, exogenous ABA application has been reported to alter stomatal kinetic responses to changes in light conditions in gymnosperms, suggesting roles for ABA in modulating stomatal kinetics across taxa[33].

At the onset of darkness there is a rapid increase in CO_2 within the leaf (C_i), which rapidly decreases upon the re-introduction of light (Fig. 3). As photosynthetic CO_2 fixation ceases in darkness an increase in C_i is not surprising. However, the role of C_i in driving stomatal responses is unclear. Some studies suggest that under changing light conditions C_i allows interaction between photosynthetic assimilation rate (A) and stomatal conductance, making C_i a potential candidate for coordinating mesophyll and stomatal responses to light[34]. However, other studies show that stomatal conductance responses to changes in light still occur when C_i is kept constant and in mutants where C_i is increased[28,35]. This has led to the suggestion that other signals, not C_i, are involved in coordinating stomatal responses with photosynthetic activity[1]. Regardless, the increase of C_i in response to darkness is highlighted here (Fig. 3) but its contribution to stomatal responses to changes in light is beyond the scope of this study.

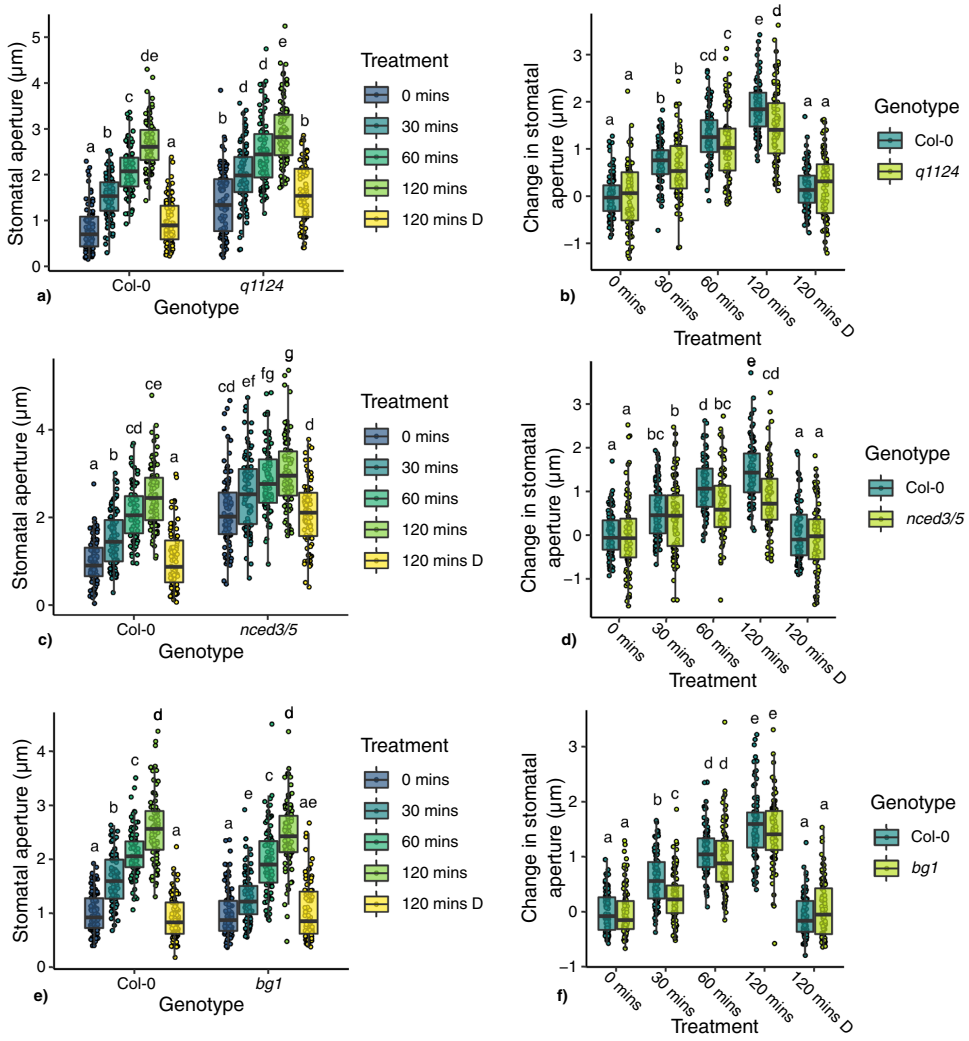

Figure 7. Stomatal responses of ABA biosynthesis and signalling mutants to light. (**a**, **c**, **e**) show absolute stomatal apertures and (**b**, **d**, **f**) show absolute change in stomatal aperture for *q1124*, *nced3/5*, and *bg1* respectively. Leaf discs were harvested under green light before dawn and incubated in darkness for 2 h before treatment. Treatment times refer to time in light (other than 120 mins D—which refers to 120 mins in darkness). Data is presented in boxplots showing the median and interquartile range of each group. The upper and lower whiskers represent data within 1.5 × the interquartile range. All data values are represented by points. Data was analysed using a 2-way ANOVA with Tukey HSD multiple comparison test, letters denote significant differences at $p < 0.05$.

Similar to our conclusions regarding the role of ABA in guard cell dark signalling, it has been reported that CO_2-induced stomatal closure proceeds through an ABA-independent pathway downstream of OST1 and that basal ABA signalling enhances CO_2-induced closure[36,37]. However, there is disagreement as to the precise role of ABA in stomatal responses to CO_2, as other studies suggest that ABA and ABA signalling are required for elevated CO_2 induced stomatal closure[38]. Most recently, a study has shown ABA catabolism plays a role in regulating stomatal responses to changes in CO_2 concentration both on a physiological and developmental scale[39].

In conclusion, our results using ABA signalling and metabolism mutants show that stomatal conductance and stomatal apertures decrease in response to darkness. The differences between the mutants and the wild type were reflected in the slower rates of closure and stomatal conductance changes found in the mutants. While our results do not support a primary role for ABA in the events underlying dark-induced stomatal closure, we find a role for this hormone in modulating the speed of reaction. This highlights the role of ABA in regulating stomatal aperture/transpiration under non-stress conditions.

Methods

Plant material and growth conditions. *Arabidopsis thaliana* was grown in a 3:1 all purpose compost (Sinclair): silver sand (Melcourt) mixture. Seeds were stratified in the dark for 48 h at 4 °C. Plants were grown under 120 µmol m^{-2} s^{-1} white light in short day conditions with a 10 h photoperiod, 22/20 °C day/night temperatures, and 70% relative humidity in a Snjider Labs Micro Clima-Series High Specs Plant Growth Chamber.

All genotypes were in a Col-0 background. ABA receptor mutants *q1124* (*pyr1pyl1pyl2pyl4*[13]) and *s112458* (*pyr1pyl1pyl2pyl4pyl5pyl8*[14]) and ABA biosynthesis mutant *nced3/5* have been previously described[13–15]. The *s112458* mutant was kindly provided by Prof Pedro Rodriguez (IBMCP), the *q1124* mutant was kindly provided by Dr Sean Cutler (University of California), the *nced3/5* mutant was kindly provided by Dr Annie Marion-Poll (INRA). Remaining mutants were obtained from the Nottingham Arabidopsis Stock Centre (NASC). *bg1* (SALK_024344/*bg1-3*[40]), *bg2* (SALK_047384/*bg2-3*[18]), *cyp707a1* (SALK_069127/*cyp707a1-1*[41]), *cyp707a3* (SALK_078173[19]). All genotypes were confirmed homozygous populations using PCR. Primers are detailed in Supplementary Table S1. The collection of the plant material used in this study complied with relevant institutional, national, and international guidelines and legislation, and the collection of plant seed was carried out in accordance with national regulations.

Stomatal aperture bioassays. Experiments were performed on 5 week old plants. Stomatal apertures were measured using leaf discs (4 mm in diameter). For dark-induced closure leaf discs were harvested 2 h after dawn, and incubated in petri dishes containing 10/50 buffer (10 mM MES/KOH, 50 mM KCl, pH 6.2) at 22 °C and illuminated with 120 µmol m^{-2} s^{-1} white light (Crompton Lamps 13 W white) for a further 2 h. Leaf discs were transferred to 10/50 buffer at 22 °C in darkness. Stomatal apertures were measured over a 2 h time course, at 0, 30, 60 and 120 min of dark treatment. A set of control leaf discs were kept in the light for 120 min over the same period (120 min L). For light-induced opening leaf discs were harvested prior to dawn under green light. Leaf discs were incubated in 10/50 buffer at 22 °C in darkness for 2 h before transfer to 120 mmol m^{-2} s^{-1} light. Stomatal apertures were measured over a 2 h time course at 0, 30, 60 and 120 min of light treatment. A set of control leaf discs were kept in the dark for 120 min over the same period (120 min D). For measurement of stomatal aperture leaf discs were imaged using a Leica DMI6000 B inverted microscope and apertures measured using ImageJ (FIJI). For each experimental repeat 30 apertures (over three individual plants) were measured for each treatment, in total over all repeats this amounts to 90 apertures per treatment per genotype. Data was statistically analysed using 2-way ANOVA with Tukey multiple comparison tests.

Stomatal conductance measurements. Experiments were performed on 6–8 week old plants. A GFS3000 IR gas analyser (Walz) fitted with a 2.5 cm^2 leaf cuvette was used to measure transpiration. The leaf cuvette was set to 16,000 ppm H_2O, 400 ppm CO_2, 22 °C. Flow was set to 750 µmol s^{-1} and impeller speed was set to 7. For darkness applied at midday mature leaves were placed in the cuvette and left to equilibrate for 2 h in a plant growth cabinet under 120 µmol m^{-2} s^{-1} white light. Darkness was imposed for 60/120 min (Figs. 4 and 2 respectively), before reintroduction to 120 µmol m^{-2} s^{-1} white light. For dusk/dawn measurements mature leaves were placed in the cuvette at least 2 h prior to the onset of dusk. Plants were left in the cuvette throughout the night until 2 h post dawn the following day. Stomatal conductance half response times were determined by identifying the time required for transpiration to reach half of the total response over the experiment. Data was analysed using 1-way ANOVAs.

R (version: 4.0.2, url: https://www.r-project.org/) was used to perform statistics and the package ggplot2 used to generate figures[42].

Received: 23 October 2020; Accepted: 17 February 2021
Published online: 11 March 2021

References

1. Lawson, T. & Matthews, J. Guard cell metabolism and stomatal function. *Annu. Rev. Plant Biol.* **71**, 273–302 (2020).
2. Jezek, M. & Blatt, M. R. The membrane transport system of the guard cell and its integration for stomatal dynamics. *Plant Physiol.* **174**, 487–519 (2017).
3. Mao, J., Zhang, Y.-C., Sang, Y., Li, Q.-H. & Yang, H.-Q. A role for Arabidopsis cryptochromes and COP1 in the regulation of stomatal opening. *Proc. Natl. Acad. Sci.* **102**, 12270–12275 (2005).
4. Costa, J. M. *et al. OPEN ALL NIGHT LONG*: The dark side of stomatal control. *Plant Physiol.* **167**, 289–294 (2015).
5. Jiang, K. *et al.* The ARP2/3 complex mediates guard cell actin reorganization and stomatal movement in *Arabidopsis*. *Plant Cell* **24**, 2031–2040 (2012).
6. Isner, J.-C. *et al.* Actin filament reorganisation controlled by the SCAR/WAVE complex mediates stomatal response to darkness. *New Phytol.* **215**, 1059–1067 (2017).
7. Liang, Y.-K. *et al.* AtMYB61, an R2R3-MYB transcription factor controlling stomatal aperture in *Arabidopsis thaliana*. *Curr. Biol.* **15**, 1201–1206 (2005).
8. Sierla, M. *et al.* The receptor-like pseudokinase GHR1 is required for stomatal closure. *Plant Cell* **30**, 2813–2837 (2018).

9. Zhang, T.-Y. *et al.* Role and interrelationship of MEK1-MPK6 cascade, hydrogen peroxide and nitric oxide in darkness-induced stomatal closure. *Plant Sci.* **262**, 190–199 (2017).
10. Dittrich, M. *et al.* The role of Arabidopsis ABA receptors from the PYR/PYL/RCAR family in stomatal acclimation and closure signal integration. *Nat. Plants* **5**, 1002–1011 (2019).
11. Merilo, E. *et al.* PYR/RCAR receptors contribute to ozone-, reduced air humidity-, darkness-, and CO_2-induced stomatal regulation. *Plant Physiol.* **162**, 1652–1668 (2013).
12. Leymarie, J., Lascève, G. & Vavasseur, A. Interaction of stomatal responses to ABA and CO_2 in *Arabidopsisthaliana*. *Funct. Plant Biol.* **25**, 785 (1998).
13. Park, S.-Y. *et al.* Abscisic acid inhibits type 2C protein phosphatases via the PYR/PYL family of START proteins. *Science* **324**, 1068–1071 (2009).
14. Gonzalez-Guzman, M. *et al.* Arabidopsis PYR/PYL/RCAR receptors play a major role in quantitative regulation of stomatal aperture and transcriptional response to abscisic acid. *Plant Cell* **24**, 2483–2496 (2012).
15. Frey, A. *et al.* Epoxycarotenoid cleavage by NCED5 fine-tunes ABA accumulation and affects seed dormancy and drought tolerance with other NCED family members: Functional analysis of the NCED5 gene. *Plant J.* **70**, 501–512 (2012).
16. Iuchi, S. *et al.* Regulation of drought tolerance by gene manipulation of 9-cis-epoxycarotenoid dioxygenase, a key enzyme in abscisic acid biosynthesis in Arabidopsis: Regulation of drought tolerance by AtNCED3. *Plant J.* **27**, 325–333 (2001).
17. Tan, B. C., Schwartz, S. H., Zeevaart, J. A. D. & McCarty, D. R. Genetic control of abscisic acid biosynthesis in maize. *Proc. Natl. Acad. Sci.* **94**, 12235–12240 (1997).
18. Xu, Z.-Y. *et al.* A vacuolar β-glucosidase homolog that possesses glucose-conjugated abscisic acid hydrolyzing activity plays an important role in osmotic stress responses in Arabidopsis. *Plant Cell* **24**, 2184–2199 (2012).
19. Okamoto, M. *et al.* High humidity induces abscisic acid 8′-hydroxylase in stomata and vasculature to regulate local and systemic abscisic acid responses in arabidopsis. *Plant Physiol.* **149**, 825–834 (2009).
20. Umezawa, T. *et al.* CYP707A3, a major ABA 8′-hydroxylase involved in dehydration and rehydration response in *Arabidopsis thaliana*. *Plant J.* **46**, 171–182 (2006).
21. Roelfsema, M. R. G. & Hedrich, R. Studying guard cells in the intact plant: Modulation of stomatal movement by apoplastic factors. *New Phytol.* **153**, 425–431 (2002).
22. Chen, K. *et al.* Abscisic acid dynamics, signaling, and functions in plants. *J. Integr. Plant Biol.* **62**, 25–54 (2020).
23. Yoshida, T., Christmann, A., Yamaguchi-Shinozaki, K., Grill, E. & Fernie, A. R. Revisiting the basal role of ABA—Roles outside of stress. *Trends Plant Sci.* **24**, 625–635 (2019).
24. Tischer, S. V. *et al.* Combinatorial interaction network of abscisic acid receptors and coreceptors from *Arabidopsis thaliana*. *Proc. Natl. Acad. Sci.* **114**, 10280–10285 (2017).
25. Fujita, Y. *et al.* Three SnRK2 protein kinases are the main positive regulators of abscisic acid signaling in response to water stress in *Arabidopsis*. *Plant Cell Physiol.* **50**, 2123–2132 (2009).
26. Miao, C. *et al.* Mutations in a subfamily of abscisic acid receptor genes promote rice growth and productivity. *Proc. Natl. Acad. Sci.* **115**, 6058–6063 (2018).
27. Inoue, S.-I. & Kinoshita, T. Blue light regulation of stomatal opening and the plasma membrane H^+-ATPase. *Plant Physiol.* **174**, 531–538 (2017).
28. Lawson, T., Lefebvre, S., Baker, N. R., Morison, J. I. L. & Raines, C. A. Reductions in mesophyll and guard cell photosynthesis impact on the control of stomatal responses to light and CO_2. *J. Exp. Bot.* **59**, 3609–3619 (2008).
29. Tominaga, M., Kinoshita, T. & Shimazaki, K. Guard-cell chloroplasts provide ATP required for H+ pumping in the plasma membrane and stomatal opening. *Plant Cell Physiol.* **42**, 795–802 (2001).
30. Kollist, H., Nuhkat, M. & Roelfsema, M. R. G. Closing gaps: Linking elements that control stomatal movement. *New Phytol.* **203**, 44–62 (2014).
31. Papanatsiou, M. *et al.* Optogenetic manipulation of stomatal kinetics improves carbon assimilation, water use, and growth. *Science* **363**, 1456–1459 (2019).
32. Lawson, T. & Vialet-Chabrand, S. Speedy stomata, photosynthesis and plant water use efficiency. *New Phytol.* **221**, 93–98 (2019).
33. Grantz, D. A., Linscheid, B. S. & Grulke, N. E. Differential responses of stomatal kinetics and steady-state conductance to abscisic acid in a fern: Comparison with a gymnosperm and an angiosperm. *New Phytol.* **222**, 1883–1892 (2019).
34. Mott, K. A. Do stomata respond to CO_2 concentrations other than intercellular?. *Plant Physiol.* **86**, 200–203 (1988).
35. von Caemmerer, S. *et al.* Stomatal conductance does not correlate with photosynthetic capacity in transgenic tobacco with reduced amounts of Rubisco. *J. Exp. Bot.* **55**, 1157–1166 (2004).
36. Hsu, P.-K. *et al.* Abscisic acid-independent stomatal CO_2 signal transduction pathway and convergence of CO_2 and ABA signaling downstream of OST1 kinase. *Proc. Natl. Acad. Sci.* **115**, E9971–E9980 (2018).
37. Xue, S. *et al.* Central functions of bicarbonate in S-type anion channel activation and OST1 protein kinase in CO_2 signal transduction in guard cell: CO_2 signalling in guard cells. *EMBO J.* **30**, 1645–1658 (2011).
38. Chater, C. *et al.* Elevated CO_2-induced responses in stomata require ABA and ABA signaling. *Curr. Biol.* **25**, 2709–2716 (2015).
39. Movahedi, M. *et al.* Stomatal responses to carbon dioxide in light require abscisic acid catabolism in Arabidopsis. *Interface Focus* https://doi.org/10.1098/rsfs.2020.0036 (2021).
40. Ondzighi-Assoume, C. A., Chakraborty, S. & Harris, J. M. Environmental nitrate stimulates abscisic acid accumulation in Arabidopsis root tips by releasing it from inactive stores. *Plant Cell* **28**, 729–745 (2016).
41. Okamoto, M. *et al.* CYP707A1 and CYP707A2, which encode abscisic acid 8′-hydroxylases, are indispensable for proper control of seed dormancy and germination in arabidopsis. *Plant Physiol.* **141**, 97–107 (2006).
42. Wickham, H. *ggplot2* (Springer, New York, 2009). https://doi.org/10.1007/978-0-387-98141-3.

Acknowledgements
This work was supported by the Biotechnology and Biological Sciences Research Council-funded South West Biosciences Doctoral Training Partnership [training grant reference: BB/M009122/1]. The authors would like to thank Prof Pedro Rodriguez for the gift of the *s112458* (*pyr1pyl1pyl2pyl4pyl5pyl8*) sextuple mutant, Dr Sean Cutler for the *q1124* (*pyr1pyl1pyl2pyl4*) mutant, and Dr Annie Marion-Poll for the gift of the *nced3/5* mutant.

Author contributions
A.J.P. and A.M.H designed the study. The experimental work was carried out by A.J.P. The manuscript written by A.J.P. and A.M.H.

Competing interests
The authors declare no competing interests.

Additional information

Supplementary Information The online version contains supplementary material available at https://doi.org/10.1038/s41598-021-84911-5.

Correspondence and requests for materials should be addressed to A.M.H.

Reprints and permissions information is available at www.nature.com/reprints.

Publisher's note Springer Nature remains neutral with regard to jurisdictional claims in published maps and institutional affiliations.